UNIWERSYTET ŚLĄSKI
INSTYTUT FIZYKI
IM. AUGUSTA CHEŁKOWSKIEGO

Uniwersytet Śląski w Katowicach
Wydział Nauk Ścisłych i Technicznych
Instytut Fizyki im. Augusta Chełkowskiego

ROZPRAWA DOKTORSKA

Wpływ różnic w budowie molekularnej i warunków termodynamicznych na architekturę supramolekularną i właściwości dielektryczne wybranych halogenopochodnych alkoholi monohydroksylowych.

mgr KINGA ŁUCAK

Promotor: prof. dr hab. Sebastian Pawlus
Promotor pomocniczy: dr inż. Anna Szeremeta, prof. UŚ

UNIWERSYTET ŚLĄSKI
W KATOWICACH

Chorzów, 2025

Spis treści

Podziękowania

Chciałabym podziękować mojemu Promotorowi, Profesorowi Sebastianowi Pawlusowi, za ogromne zaangażowanie, nieocenione wsparcie merytoryczne, konstruktywne uwagi oraz cierpliwość, które towarzyszyły mi na każdym etapie realizacji niniejszej rozprawy doktorskiej. Dziękuję za inspirujące rozmowy, zaufanie oraz możliwość rozwijania się we współpracy z Profesorem.

Podziękowania kieruję również do mojej Promotor Pomocniczej, Profesor Anny Szeremety, za życzliwość, opiekę naukową, motywację, dzielenie się wiedzą i doświadczeniem, a także nieustające wsparcie przy realizacji badań i pracy nad publikacjami.

Dziękuję Profesorowi Romanowi Wrzalikowi za inspirującą współpracę, pomoc przy interpretacji wyników oraz cenne wskazówki naukowe, które pozwoliły mi lepiej zrozumieć analizowane zjawiska.

Dziękuję także Profesorowi Kamilowi Kamińskiemu za życzliwość oraz naukowe sugestie, wzbogacające interpretację wyników i poszerzające moje spojrzenie na badany problem.

Składam również podziękowania wszystkim współautorom publikacji naukowych wchodzących w skład niniejszej rozprawy.

Słowa wdzięczności kieruję także do osób, które towarzyszyły mi podczas codziennej pracy w laboratorium. Dziękuję Alfredowi za wszelką pomoc techniczną i za to, że zawsze mogłam liczyć na jego doświadczenie i spokój. Podziękowania do dziewczyn z działu chemii (pokój E/14) – za każdą przeprowadzoną rozmowę, dzielenie się wiedzą oraz miłą atmosferę.

Nie byłoby tej pracy bez moich najbliższych. Dziękuję moim Rodzicom za zrozumienie, cierpliwość i nieustające wsparcie, a mojej siostrze Karolinie – za wiarę we mnie, otuchę i dobre słowo w najtrudniejszych chwilach. Dziękuję również mojemu chłopakowi Olkowi za wyrozumiałość i motywację, gdy sama jej już nie miałam.

Tę pracę doktorską dedykuję mojemu kochanemu Bratu, Krystianowi.
Wierzę, że z dumą patrzysz na mnie z góry. Ta praca jest dowodem na to, że Twoja siła i wrażliwość są nadal obecne w moim życiu – każdego dnia

Streszczenie

Struktury supramolekularne to uporządkowane układy powstające w wyniku oddziaływań międzycząsteczkowych, takich jak wiązania wodorowe czy halogenowe. Ich obecność zmienia właściwości cieczy, wpływając między innymi na dynamikę molekularną, temperatury przejść fazowych i odpowiedź elektryczną. Badania nad tego rodzaju układami umożliwiają zrozumienie organizacji cząsteczek w cieczach przez nie tworzonych oraz ich reorganizacji pod wpływem zmiennych warunków termodynamicznych. W niniejszej rozprawie doktorskiej podjęto systematyczne badania halogenowych alkoholi monohydroksylowych jako modelowych układów cieczy asocjujących, ze względu na prostą budowę molekularną oraz zdolność do tworzenia wiązań wodorowych. Analizowane związki różniły się długością łańcucha węglowego, rodzajem podstawionego atomu halogenu (chlor, brom, jod) oraz położeniem grupy hydroksylowej. Celem pracy było określenie wpływu budowy molekularnej oraz zmieniających się, temperatury i ciśnienia na architekturę struktur supramolekularnych oraz ich dynamikę. W badaniach zastosowano szerokopasmową spektroskopię dielektryczną, która pozwala na detekcję dwóch głównych procesów: relaksacji Debye'a – związanej z kolektywnym ruchem molekuł tworzących łańcuchowe struktury supramolekularne stabilizowane wiązaniami wodorowymi, oraz relaksacji strukturalnej (α) – wynikającej z ruchów łańcuchów alkilowych. Eksperymenty przeprowadzono w szerokim zakresie temperatur i ciśnień, co pozwoliło na analizę wpływu warunków termodynamicznych na badane procesy. Badania metodą spektroskopii dielektrycznej uzupełniono o różnicową kalorymetrię skaningową, dyfrakcję rentgenowską, spektroskopię w podczerwieni z transformacją Fouriera, a także symulacje dynamiki molekularnej oraz obliczenia z zakresu teorii funkcjonału gęstości. Wykazano, że podstawienie grupy metylowej w łańcuchu węglowym atomem halogenu prowadzi do ograniczenia zdolności cząsteczek alkoholu do tworzenia dużych struktur łańcuchowych, co z kolei prowadzi do obniżenia amplitudy relaksacji Debye'a. Efekt ten nasila się wraz ze wzrostem masy atomowej halogenu. Jednocześnie stwierdzono, że obecność atomów halogenu w cząsteczkach alkoholi prowadzi do formowania nie tylko typowych dla alkoholi klastrów stabilizowanych wiązaniami wodorowymi typu OH···O, lecz również agregatów stabilizowanych przez oddziaływania typu halogen···halogen oraz OH···halogen. Oddziaływania te współistnieją z wiązaniami wodorowymi i modyfikują topologię agregatów supramolekularnych, prowadząc do heterogeniczności układu, wynikającej z tworzenia się nowych typów klastrów. Dodatkowo, zmiana położenia grupy hydroksylowej w cząsteczce wpływa na preferowaną architekturę

klastrów – układy z grupą –OH umieszczoną centralnie w łańcuchu węglowym wykazują tendencję do tworzenia struktur pierścieniowych, podczas gdy lokalizacja tej grupy na końcu sprzyja formowaniu układów o architekturze liniowej. Obserwowano także reorganizację tych struktur pod wpływem zwiększonego ciśnienia. W zakresie długości łańcucha węglowego wykazano, że krótsze alkohole (z dwoma atomami węgla) tworzą klastry charakteryzujące się mniejszymi odległościami między cząsteczkami oraz większym stopniem uporządkowania przestrzennego, skutkujące większą amplitudą relaksacji Debye'a niż w przypadku dłuższych związków. Rezultaty omawianych badań zawarte zostały w trzech publikacjach naukowych będących podstawą niniejszej rozprawy doktorskiej. Otrzymane wyniki i ich interpretacja stanowią istotny wkład w rozwój wiedzy na temat zależności między budową cząsteczek a architekturą i dynamiką struktur supramolekularnych w cieczach asocjujących.

1. Wstęp

1.1 Znaczenie badań nad strukturami supramolekularnymi

Zrozumienie mechanizmów organizacji molekuł w fazie skondensowanej stanowi jedno z kluczowych wyzwań współczesnej fizykochemii. Szczególne zainteresowanie budzi w tym kontekście chemia supramolekularna – dziedzina badająca zespoły cząsteczek, które spontanicznie tworzą uporządkowane struktury wskutek wzajemnych oddziaływań [1, 2, 3]. Wśród oddziaływań prowadzących do takiej organizacji szczególne znaczenie mają wiązania wodorowe, siły van der Waalsa, interakcje elektrostatyczne (np. między jonami a dipolami), a także rzadsze, lecz istotne oddziaływania halogenowe, typowe dla atomów takich jak chlor, brom czy jod [4–9]. W literaturze uporządkowane układy molekuł powstałe na skutek ich wzajemnych oddziaływań określa się często mianem struktur supramolekularnych, ze względu na ich charakterystyczną architekturę przestrzenną lub po prostu asocjatami, podkreślając ich pochodzenie od oddziaływań międzycząsteczkowych [2, 4]. Układy supramolekularne mogą przyjmować różne formy – od prostych dimerów czy trimerycznych klastrów, przez łańcuchy lub pierścienie, aż po bardziej złożone sieci przestrzenne [1, 10]. Co istotne, ich powstawanie wpływa na modyfikację właściwości materiałowych, które nie są obserwowane w przypadku pojedynczych, nieoddziałujących cząsteczek. Przykładowo, zmieniają się takie parametry jak lepkość, przewodnictwo elektryczne, rozpuszczalność czy odpowiedź elektryczna na przyłożone pole elektryczne [2, 11]. W układach biologicznych zorganizowane asocjaty pełnią funkcje kluczowe: stabilizują strukturę drugorzędową i trzeciorzędową białek, umożliwiają specyficzne rozpoznawanie międzycząsteczkowe, a także warunkują procesy takie jak replikacja DNA czy transport przez błony lipidowe. W obszarze chemii materiałów struktury supramolekularne stanowią podstawę do projektowania inteligentnych materiałów**,** takich jak ciekłe kryształy czy polimery supramolekularne o właściwościach adaptacyjnych. Dzięki dynamicznym oddziaływaniom niekowalencyjnym, materiały te potrafią reagować na zmiany warunków otoczenia – takich jak temperatura, pH czy działanie promieniowania elektromagnetycznego (np. UV lub światła widzialnego) i odwracalnie zmieniać swoją strukturę oraz funkcjonalność [1, 6–8].

1.2 Modelowe układy badawcze – alkohole monohydroksylowe

Od ponad stu lat alkohole monohydroksylowe pozostają w centrum zainteresowania badaczy, stanowiąc przedmiot intensywnych analiz eksperymentalnych i obliczeniowych [3, 12–15]. Swoje wyjątkowe właściwości fizyczne i chemiczne alkohole monohydroksylowe zawdzięczają kilku fundamentalnym cechom strukturalnym: z jednej strony są to cząsteczki o stosunkowo prostej budowie – zawierają tylko jedną grupę hydroksylową –OH, z drugiej zaś wykazują silną tendencję do tworzenia struktur supramolekularnych poprzez wiązania wodorowe [12–14]. Dodatkowym atutem wielu monoalkoholi, jako układów modelowych, jest ich zdolność do łatwego przechładzania do stanu szklistego, co umożliwia badanie ich dynamiki relaksacyjnej w bardzo szerokim zakresie czasowym [3, 13, 14]. Ich właściwości były i są intensywnie badane przy użyciu różnorodnych metod badawczych, takich jak spektroskopia dielektryczna, spektroskopia Ramana (IR), magnetyczny rezonans jądrowy (NMR) czy symulacje dynamiki molekularnej (MDS) [3, 12–15]. Szczególną uwagę monoalkohole przyciągają ze względu na obecność dominującego procesu relaksacji Debye'a (D), który wyróżnia je na tle innych cieczy asocjujących. Proces ten, obserwowany szczególnie wyraźnie w widmach dielektrycznych licznych alkoholi z tej grupy, związany jest z kolektywnym ruchem cząsteczek tworzących supramolekularne łańcuchy stabilizowane wiązaniami wodorowymi [3, 12, 14, 16, 23, 24], co zilustrowano porównawczo na **rysunku 1**. Pomimo licznych badań, molekularne źródło relaksacji Debye'a nie zostało jednoznacznie wyjaśnione i wciąż pozostaje przedmiotem dyskusji [8, 13, 16–25]. Z jednej strony alkohole te są dobrze poznane, z drugiej jednak nadal dostarczają nowych pytań badawczych, szczególnie w kontekście ich zachowania w warunkach zmiennej temperatury czy ciśnienia.

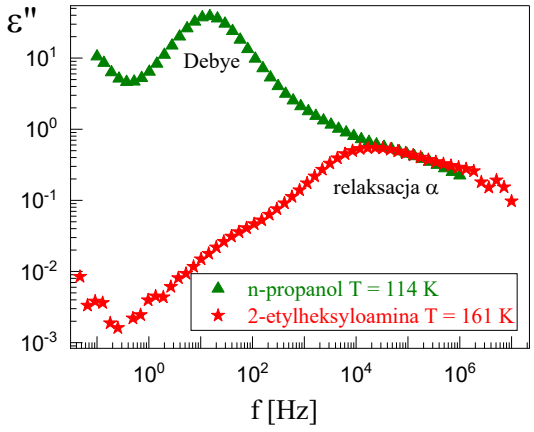

Rysunek 1. Porównanie widm strat elektrycznych (ε″) dla n-propanolu i 2-etylheksyloaminy, dobranych tak, aby odpowiadały podobnym czasom relaksacji strukturalnej (relaksacja α). Dane dla 2-etylheksyloaminy zaczerpnięto z pracy [15].

Aby skutecznie badać naturę struktur supramolekularnych oraz zrozumieć mechanizmy ich powstawania i reorganizacji w zmiennych warunkach termodynamicznych, niezbędne jest zastosowanie układów modelowych, które pozwalają w sposób kontrolowany śledzić, jak zmieniają się właściwości molekularne badanych związków w wyniku modyfikacji struktury molekuł [23, 24]. Kluczowe znaczenie mają w tym przypadku związki o dobrze poznanej strukturze, wykazujące tendencję do samoorganizacji, a jednocześnie podatne na systematyczne zmiany geometrii i charakteru oddziaływań międzycząsteczkowych. Do grupy takich modelowych układów idealnie wpisują się właśnie alkohole monohydroksylowe [26, 27, 28]. Ich prostota strukturalna w połączeniu z dużą różnorodnością możliwych modyfikacji, np. poprzez systematyczne wydłużanie łańcucha alkilowego, zmianę położenia grupy hydroksylowej, dodawanie grup bocznych czy też wprowadzenie dodatkowych podstawników – na przykład atomów halogenowych – sprawia, że alkohole te stanowią bardzo atrakcyjny obiekt badań nad zależnością między strukturą molekularną a dynamiką molekularną układu [3, 15, 19, 23–30]. Szczególną cechą wyróżniającą monoalkohole jest sposób, w jaki cząsteczki te tworzą uporządkowane struktury supramolekularne [18, 26]. W odróżnieniu od wody, która buduje rozgałęzione, trójwymiarowe sieci wiązań wodorowych, alkohole te, zawierając pojedynczą grupę hydroksylową mają tendencję do formowania bardziej przewidywalnych, prostszych asocjatów – najczęściej liniowych lub pierścieniowych [19]. Takie właściwości strukturalne sprzyjają dokładnej analizie oddziaływań międzycząsteczkowych i czynią te związki cennymi układami modelowymi w badaniach nad dynamiką molekularną i procesami relaksacyjnymi [13].

1.3 Asocjaty w zmiennych warunkach termodynamicznych

Właściwości struktur supramolekularnych mogą się istotnie zmieniać w zależności od warunków termodynamicznych. Badania prowadzone pod zmieniającym się ciśnieniem umożliwiają śledzenie wpływu kompresji na organizację molekuł – w warunkach izotermicznych (czyli przy stałej temperaturze) zwiększenie ciśnienia prowadzi do zmniejszenia odległości między cząsteczkami, przy niezmiennej energii termicznej. Natomiast w warunkach izobarycznych (czyli pod stałym ciśnieniem), badanie wpływu zmian temperatury na badane związki pozwala prześledzić, w jaki sposób energia termiczna oraz związana z nią zmiana gęstości wpływają na mobilność cząsteczek oraz dynamikę procesów relaksacyjnych, a tym samym na stopień i charakter asocjacji w cieczach supramolekularnych. Dzięki prowadzeniu badań zarówno w warunkach izotermicznych, jak i izobarycznych,

możliwe jest oddzielenie efektów temperaturowych od efektów wynikających ze wzrostu upakowania cząsteczek co pozwala na zrozumienie roli temperatury, ciśnienia oraz parametrów molekularnych (takich jak długość łańcucha czy obecność podstawników) w kształtowaniu struktury supramolekularnej i dynamiki molekularnej badanych układów [24, 31–36]. Asocjacyjne struktury molekularne mogą być analizowane za pomocą różnych metod eksperymentalnych i obliczeniowych. W badaniach będących przedmiotem niniejszej rozprawy zastosowałam szerokopasmową spektroskopię dielektryczną (ang. Broadband Dielectric Spectroscopy, BDS) jako główną technikę badawczą. Technika ta umożliwiła mi analizę dipolowych procesów relaksacyjnych zachodzących w cieczach asocjujących, w szerokim zakresie częstotliwości i temperatur, a także ciśnień [30–32]. Spośród wielu procesów, które mogą być identyfikowane za pomocą tej metody, w niniejszej pracy skupiono się na dwóch procesach relaksacyjnych: relaksacji D, charakterystycznej dla monoalkoholi oraz relaksacji strukturalnej (α), która związana jest z ruchami łańcuchów alkilowych [14, 23, 24, 31, 37].

2. Relaksacja dielektryczna – mechanizmy i modele

2.1 Mechanizmy relaksacji dielektrycznej

Szerokopasmowa spektroskopia dielektryczna opiera się na badaniu odpowiedzi układów dipolowych na zmienne pole elektryczne. Molekuły z trwałym momentem dipolowym, będące podstawą badanych cieczy polarnych, w stanie bez pola ulegają przypadkowej orientacji, co wynika z fluktuacji termicznych i braku preferencji kierunkowej (**rysunek 2a**). Dopiero przyłożenie zewnętrznego pola elektrycznego prowadzi do częściowego uporządkowania orientacji dipoli, co skutkuje powstaniem makroskopowej polaryzacji (**rysunek 2b**) [38–40].

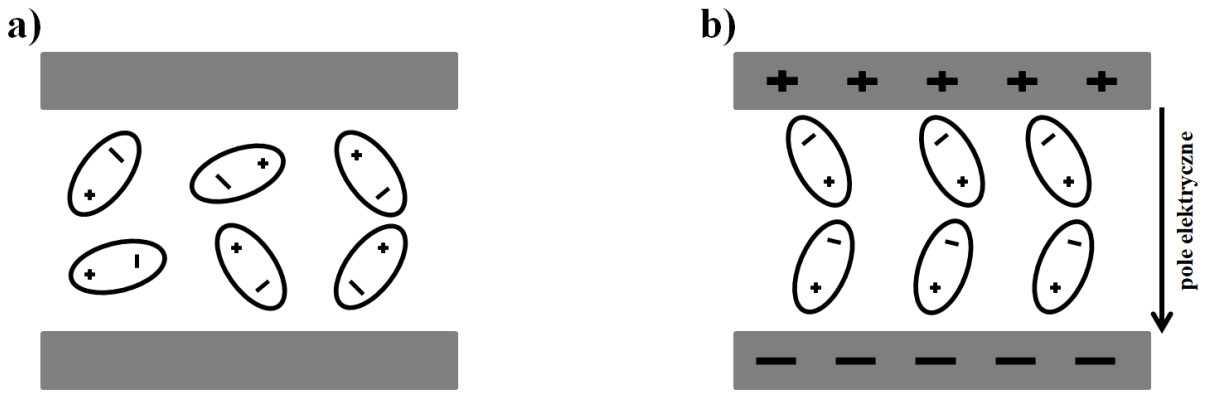

Rysunek 2. (a) Losowa orientacja dipoli w braku zewnętrznego pola elektrycznego. (b) Uporządkowana orientacja dipoli w obecności przyłożonego pola elektrycznego. Adaptacja na podstawie: [38].

Odpowiedź dielektryka na zewnętrzne pole elektryczne zawiera dwie składowe: polaryzację orientacyjną ($P_{or,}$) związaną z orientowaniem się trwałych dipoli wzdłuż pola elektrycznego oraz polaryzację indukowaną (P_∞), często określaną jako deformacyjna, pochodzącą z deformacji powłok elektronowych i przesunięć jąder atomowych. Proces osiągania równowagi przez polaryzację po włączeniu lub wyłączeniu pola nie następuje natychmiastowo, lecz wymaga czasu (**rysunek 3a**). Natychmiast po włączeniu pola pojawia się polaryzacja indukowana P_∞. Jest ona sumą dwóch składowych: polaryzacji elektronowej P_e, wynikającej z deformacji chmur elektronowych względem jąder atomowych oraz polaryzacji atomowej P_a, będącej efektem deformacji wiązań chemicznych pomiędzy atomami. Sumarycznie polaryzację indukowaną można zapisać jako [38–40]:

$$P_\infty = P_e + P_a = \varepsilon_0 (\varepsilon_\infty - 1) E, \quad (1)$$

gdzie: $\varepsilon_0 = 8.854 \cdot 10^{-12} \frac{F}{m}$ – przenikalność elektryczna próżni, ε_∞ – wysokoczęstotliwościowa przenikalność elektryczna substancji, E – natężenie pola elektrycznego.

Polaryzacja orientacyjna P_{or} nie osiąga natychmiastowo wartości równowagowej, ponieważ związana jest z powolniejszą reorientacją cząsteczek pod wpływem pola elektrycznego, tłumioną przez siły tarcia obecne w układzie. Podobnie zachowuje się układ po nagłym wyłączeniu pola elektrycznego – szybka polaryzacja indukowana P_∞ zanika natychmiast, natomiast polaryzacja orientacyjna P_{or} wymaga pewnego czasu, aby stopniowo zmniejszyć

się do zera. W rezultacie, po osiągnięciu stanu równowagi przez układ obserwuje się dodatkowy wkład związany z uporządkowaniem orientacyjnym cząsteczek [38, 39]:

$$P_{or} = P_0 - P_\infty = \varepsilon_0 (\varepsilon_s - \varepsilon_\infty) E, \quad (2)$$

gdzie: ε_s – statyczna przenikalność elektryczna materiału. Przebieg zmian polaryzacji w czasie, wywołany prostokątnym impulsem pola elektrycznego E, zilustrowano schematycznie na **rysunku 3**.

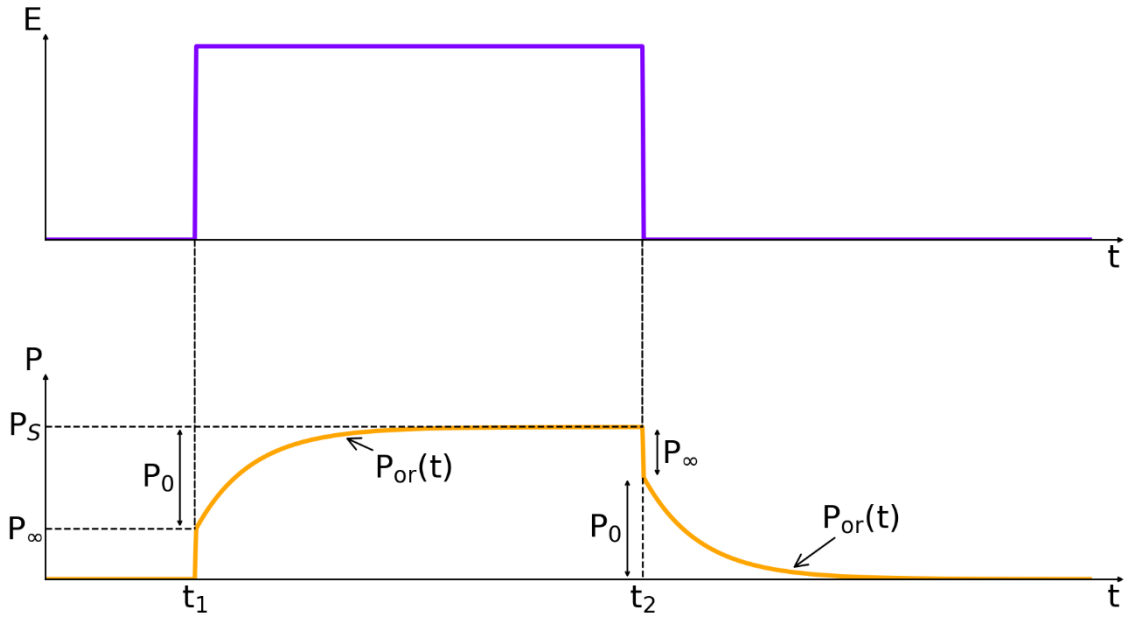

Rysunek 3. Przebieg zmian polaryzacji dielektryka w czasie w odpowiedzi na prostokątny impuls pola elektrycznego E. Symbol P_∞ – polaryzacja indukowaną, P_{or} – polaryzacja orientacyjna, P_0 – maksymalna wartość polaryzacji orientacyjnej P_{or}, P_s – maksymalna wartość polaryzacji całkowitej. Adaptacja na podstawie: [38, 39]

Do ilościowego opisu zmian polaryzacji orientacyjnej w czasie stosuje się funkcję relaksacyjną φ (t), której typowy przebieg – ma charakter wykładniczy [38, 40]:

$$\varphi(t) = \exp\left(\frac{-t}{\tau_{diel}}\right), \quad (3)$$

gdzie: τ_{diel} oznacza czas relaksacji dielektrycznej, będący parametrem charakterystycznym dla procesu reorientacji dipoli. Przebieg narastania polaryzacji orientacyjnej w czasie można przedstawić za pomocą zależności [38, 40]:

$$P_{or}(t) = (P_s - P_\infty)\,[1 - \exp(-\frac{t}{\tau_{diel}})]. \quad (4)$$

Funkcję opisującą narastanie i zanik polaryzacji orientacyjnej można również przedstawić w formie równania różniczkowego [38, 39]:

$$\tau_{diel}\frac{dP_{or}(t)}{dt} = P_s - P_\infty - P_{or}(t). \quad (5)$$

Dla przypadku, w którym pole elektryczne zmienia się harmonicznie w czasie, jego przebieg można opisać równaniem [40]:

$$E(t) = E_0 \cdot \exp(-i\omega t), \quad (6)$$

gdzie: ω to częstość kołowa (kątowa). Aby rozwiązać równanie różniczkowe (5) dla przypadku harmonicznego pola elektrycznego, konieczne jest wyrażenie prawej strony tego równania jako funkcji pola elektrycznego. W tym celu wykorzystuje się zależność [38, 40]:

$$P_s - P_\infty = \varepsilon_0\,(\varepsilon_s - \varepsilon_\infty)\,E(t). \quad (7)$$

Podstawiając wyrażenie (6) do równania (7), otrzymujemy końcową postać równania różniczkowego [38]:

$$\tau_{diel}\frac{dP_{or}(t)}{dt} = \varepsilon_0\,(\varepsilon_s - \varepsilon_\infty)\,E_0 \cdot \exp(-i\omega t) - P_{or}(t). \quad (8)$$

Rozwiązanie powyższego równania prowadzi do [40]:

$$P_{or}(t) = \frac{\varepsilon_0\,(\varepsilon_s - \varepsilon_\infty)}{1 + i\omega\tau_{diel}}\,E_0 \exp(-i\omega t). \quad (9)$$

Wektor indukcji elektrycznej D(t) związany jest z zespoloną przenikalnością wyrażeniem [38–40]:

$$D(t) = \varepsilon_0\,\varepsilon^*(\omega)\,E(t), \quad (10)$$

gdzie: $\varepsilon^*(\omega)$ to zespolona przenikalność elektryczna, w postaci:

$$\varepsilon^*(\omega)=\varepsilon'(\omega)-i\varepsilon''(\omega). \quad (11)$$

Część rzeczywista ε′(ω) określa dyspersję dielektryczną, natomiast część urojona ε″(ω) opisuje straty elektryczne wynikające z opóźnienia w odpowiedzi układu na przyłożone pole elektryczne. Zjawisko to związane jest z reorientacją cząsteczek posiadających moment dipolowy oraz z ich dynamiką relaksacyjną, czyli sposobem i szybkością powrotu układu do stanu równowagi po ustaniu działania pola zewnętrznego [38–40].

Obie te składowe opisują odpowiednio zjawiska dyspersji i strat elektrycznych w funkcji częstości kołowej ω.

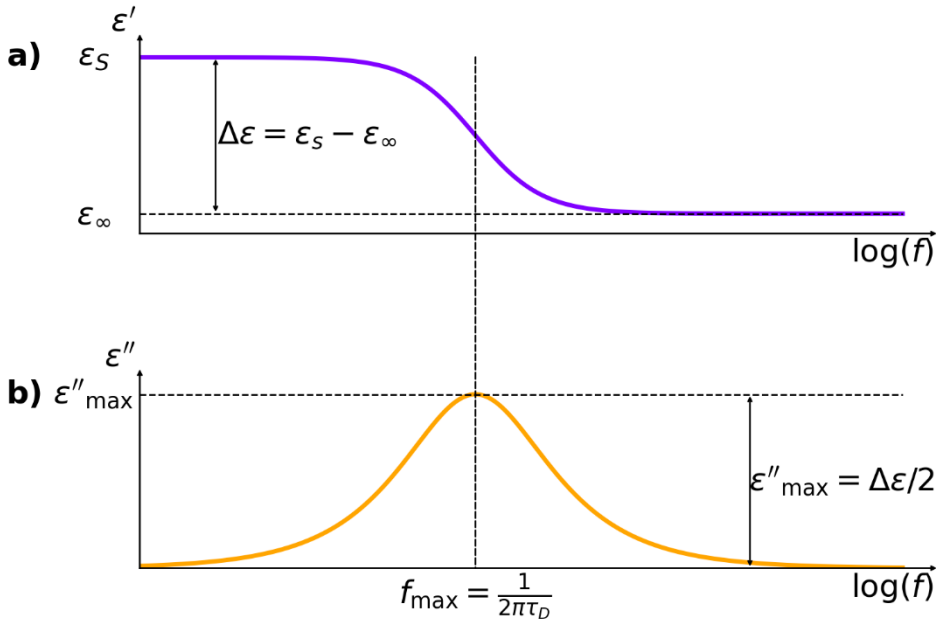

Rysunek 4. Przykładowe wykresy zależności (a) dyspersji (ε′) i (b) absorpcji (ε″) dla procesu relaksacyjnego opisanego równaniem Debye'a. Adaptacja na podstawie: [40]

W miarę wzrostu częstotliwości przyłożonego pola elektrycznego obserwuje się stopniowy spadek wartości części rzeczywistej przenikalności elektrycznej, co manifestuje się jako schodkowy charakter dyspersji (**rysunek 4a**). Jednocześnie część urojona, odpowiadająca za straty elektryczne, wykazuje wyraźne maksimum, przyjmujące kształt funkcji dzwonowej (**rysunek 4b**). Warto podkreślić, że położenie tego maksimum jest bezpośrednio związane z czasem relaksacji τ, opisującym reorientację dipoli w badanym materiale i wyraża się zależnością: $\tau = \frac{1}{2\pi f_{max}}$ [39–40].

2.2 Modele relaksacyjne

W celu ilościowego opisu obserwowanych właściwości widm dielektrycznych szeroko stosuje się różnorodne modele teoretyczne, które pozwalają uwzględnić zarówno symetryczne, jak i asymetryczne poszerzenie, a także rozkład czasów relaksacji w badanych układach. Klasycznym podejściem w analizach pozostaje model Debye'a, który zakłada, że oddziaływania pomiędzy dipolami można pominąć, a cząsteczki zanurzone są w jednorodnym środowisku. Zespolona przenikalność elektryczna w tym modelu wyraża się wzorem [38–40]:

$$\varepsilon^*(\omega) = \varepsilon_\infty + \frac{\varepsilon_s - \varepsilon_\infty}{1 + i\omega t_D}. \tag{12}$$

Rozdzielając rzeczywistą i urojoną część zespolonej przenikalności dielektrycznej $\varepsilon^*(\omega)$, otrzymuje się wyrażenia opisujące odpowiednio dyspersję oraz straty elektryczne [40]:

$$\varepsilon'(\omega) = \varepsilon_\infty + \frac{\varepsilon_s - \varepsilon_\infty}{1 + (\omega t_D)^2}, \tag{13}$$

$$\varepsilon''(\omega) = \frac{(\varepsilon_s - \varepsilon_\infty)\,\omega t t_D}{1 + (\omega t_D)^2}. \tag{14}$$

Model Debye'a opisuje proste, jednorodne układy, w których maksimum $\varepsilon''(\omega)$, obserwowane na krzywej strat elektrycznych, jest symetryczne i wąskie, bez oznak poszerzenia. Jednak rzeczywiste substancje, w tym również badane w niniejszej pracy halogenowane alkohole monohydroksylowe, wykazują znacznie bardziej złożone zachowanie odpowiedzi dielektrycznej. W eksperymentalnych widmach zespolonej przenikalności elektrycznej często obserwuje się poszerzenie oraz asymetrię maksimum $\varepsilon''(\omega)$, wynikające z niejednorodności lokalnego otoczenia cząsteczek oraz z występowania oddziaływań między nimi. W celu ich poprawnego opisu stosuje się rozszerzenia modelu Debye'a, które uwzględniają rozkład czasów relaksacji [38–40].

Jednym z nich jest model Cole–Cole'a (CC), w którym wprowadzony zostaje parametr α, opisujący symetryczne poszerzenie funkcji relaksacyjnej [40, 41]:

$$\varepsilon^*(\omega) = \varepsilon_\infty + \frac{\varepsilon_s - \varepsilon_\infty}{1 + (i\omega\tau_{diel})^{1-\alpha}}. \tag{15}$$

Dla α = 0 model sprowadza się do funkcji Debye'a, natomiast α > 0 pozwala na odwzorowanie symetrycznego poszerzenia krzywej relaksacyjnej, obserwowanego w widmach ε″(ω).

Kolejnym modelem jest model Davidson–Cole'a (DC), w którym wprowadza się parametr β parametryzujący asymetrię procesu relaksacyjnego [40, 42, 43]:

$$\varepsilon^*(\omega) = \varepsilon_\infty + \frac{\varepsilon_S - \varepsilon_\infty}{(1+ i\omega\tau_{diel})^\beta} \ . \tag{16}$$

Połączenie dwóch przedstawionych powyżej rozszerzeń modelu Debye'a – modelu CC (dla symetrycznego poszerzenia maksimum) oraz modelu DC (dla poszerzenia asymetrycznego) – stanowi model Havriliaka i Negamiego (HN) [40, 44].

$$\varepsilon^*(\omega) = \varepsilon_\infty + \frac{\varepsilon_S - \varepsilon_\infty}{[1+ (i\omega\tau_{diel})^{1-\alpha}]^\beta} \ . \tag{17}$$

Model ten umożliwia jednoczesne uwzględnienie zarówno symetrycznego poszerzenia (parametr α), jak i asymetrii (parametr β). Przyjęcie tego modelu pozwala na opis rzeczywistych danych, szczególnie dla cieczy wykazujących złożoną dynamikę relaksacyjną [40, 44].

Tabela 1. Podsumowanie modeli relaksacyjnych stosowanych w analizie wyników BDS. Adaptacja na podstawie: [40].

Model	Równanie	Parametry	Redukcja do modelu Debye'a
Debye	$\varepsilon^*(\omega) = \varepsilon_\infty + \frac{\varepsilon_S - \varepsilon_\infty}{1 + i\omega t_D}$	τ_D	Model bazowy
Cole–Cole	$\varepsilon^*(\omega) = \varepsilon_\infty + \frac{\varepsilon_S - \varepsilon_\infty}{1+ (i\omega\tau_{diel})^{1-\alpha}}$	$0 \leq \alpha < 1$	$\alpha = 0 \rightarrow$ Debye
Davidson–Cole	$\varepsilon^*(\omega) = \varepsilon_\infty + \frac{\varepsilon_S - \varepsilon_\infty}{(1+ i\omega\tau_{diel})^\beta}$	$0 < \beta \leq 1$	$\beta = 1 \rightarrow$ Debye
Havriliak–Negami	$\varepsilon^*(\omega) = \varepsilon_\infty + \frac{\varepsilon_S - \varepsilon_\infty}{[1+ (i\omega\tau_{diel})^{1-\alpha}]^\beta}$	$0 \leq \alpha < 1$, $0 < \beta \leq 1$	$\alpha=0$, $\beta=1 \rightarrow$ Debye

3. Motywacja

Zastosowanie szerokopasmowej spektroskopii dielektrycznej stwarza wyjątkową możliwość śledzenia dynamiki molekularnej i zjawisk asocjacyjnych w cieczach w szerokim zakresie warunków termodynamicznych. Technika ta umożliwia pomiary w zakresie częstotliwości sięgającym 12–13 dekad, jak wykazano m.in. w badaniach glicerolu, propylenu karbonylowego [45, 46] – co znacznie przewyższa możliwości wielu innych metod, takich jak DSC, NMR czy IR. BDS umożliwia nie tylko detekcję poszczególnych relaksacji, ale również, określenie ich molekularnego źródła, czyli rodzaju ruchów odpowiedzialnych za obserwowaną odpowiedź elektryczną oraz ewolucji tych procesów w funkcji temperatury i ciśnienia, co czyni tę metodę szczególnie użyteczną w badaniach nad reorganizacją struktur supramolekularnych w układach ulegających przechłodzeniu do stanu szklistego należących do rodziny monoalkoholi [45, 46]. W niniejszej rozprawie wykorzystano BDS ze względu na wysoką skuteczność w śledzeniu zmian w dynamice molekularnej i strukturze asocjacyjnej, nawet w przypadku niewielkich modyfikacji chemicznych badanych układów, do badań halogenowych alkoholi monohydroksylowych – związków, które z racji swojej struktury molekularnej mogą tworzyć różnorodne układy asocjacyjne. Wprowadzenie atomu halogenowego (Cl, Br, I) wpływa na elektroujemność i polaryzowalność molekuły, a w konsekwencji na moment dipolowy i typ występujących oddziaływań międzycząsteczkowych. Oprócz klasycznych wiązań wodorowych typu O–H···O, mogą pojawiać się interakcje O–H···X oraz X···X (gdzie X to halogen), w wyniku których tworzą się nowe typy asocjatów i w konsekwencji zwiększeniu ulega heterogeniczność układu [47–50]. Dotychczasowe badania dielektryczne alkoholi monohydroksylowych koncentrowały się głównie na prostych alkilowych cząsteczkach lub układach aromatycznych [3, 8, 26, 27], natomiast monoalkohole zawierające atomy halogenowe nie były dotąd przedmiotem systematycznych badań dielektrycznych, mimo potencjalnych różnic w ich dynamice relaksacyjnej w porównaniu do innych alkoholi. W szczególności, brakowało systematycznych badań uwzględniających wpływ takich czynników jak: rodzaj podstawionego atomu halogenowego, położenie grupy hydroksylowej w szkielecie cząsteczki oraz długość łańcucha alkilowego. W prezentowanej pracy dobrano zestaw halogenowych alkoholi monohydroksylowych w taki sposób, aby umożliwić zbadanie powyższych czynników z wykorzystaniem unikatowego zakresu częstotliwości dostępnego w BDS oraz z wykorzystaniem innych technik pomiarowych oraz obliczeniowych. Dzięki temu możliwa była charakterystyka typów klastrów supramolekularnych, sposobu ich reorganizacji

oraz intensywności i charakteru temperaturowo-ciśnieniowego obserwowanych procesów relaksacyjnych.

4. Cel pracy

Celem niniejszej rozprawy doktorskiej było określenie:

— wpływu podstawienia końcowej grupy metylowej atomem halogenu: chloru (Cl), bromu (Br), jodu (I) na obecność i właściwości procesu relaksacyjnego Debye'a.

— wpływu obecności atomu halogenu dla momentu dipolowego cząsteczki, dynamiki molekularnej oraz architektury klastrów supramolekularnych.

— wpływu geometrii cząsteczki (położenia grupy –OH i atomu halogenu oraz długości łańcucha alkilowego) na sposób organizacji cząsteczek w strukturach supramolekularnych (takich jak łańcuchy, pierścienie, agregaty rozgałęzione) oraz na wynikające z tego zmiany właściwości dielektrycznych badanych układów.

— reorganizacji struktur supramolekularnych pod wpływem zmieniającego się ciśnienia.

5. Publikacje i aktywność naukowa

Wyniki przedstawione w rozprawie zostały opublikowane w następujących artykułach z listy filadelfijskiej:

P1. K. Łucak, A.Z. Szeremeta, R. Wrzalik, J. Grelska, K. Jurkiewicz, N. Soszka, B. Hachuła, D. Kramarczyk, K. Grzybowska, B. Yao, K. Kamiński, S. Pawlus. Experimental and computational approach to studying supramolecular structures in propanol and its halogen derivatives. *The Journal of Physical Chemistry B*, *127*(42), 9102–9110, (2023).
IF: 2.8, Punkty MNiSW: 140

P2. K. Łucak, A. Z. Szeremeta, J. Grelska, K. Jurkiewicz, S. Kołodziej, R. Wrzalik, K. Kamiński, S. Pawlus. Effect of high pressure on the molecular dynamics of halogen monoalcohols. *Journal of Molecular Liquids*, *423*, 127045, (2025).
IF: 5.3, Punkty MNiSW: 100

P3. K. Łucak, A. Z. Szeremeta, A. Janowska, K. Jurkiewicz, K. Grzybowska, K. Kamiński, S. Pawlus. Influence of molecular structure and thermodynamic conditions on the dynamics, halogen bonding, and self–assembly of halogenated monoalcohols. *Journal of Molecular Liquids*, 433, 127787, (2025).
IF: 5.3, Punkty MNiSW: 100

Ponadto jestem autorką i współautorką poniższych publikacji naukowych:

R1. K. Łucak, D. Kramarczyk, O. Janus, S. Pawlus. How differences in the molecular structure of monohydroxy alcohols affect the tendency to crystallization. *European Physical Journal E*, 45(8), 64 (2022).

R2. A. Nowok, J. Grelska, M. Dulski, A. Z. Szeremeta, K. Łucak, K. Jurkiewicz, H. Hellwig, S. Pawlus. Normal–to–supercooled liquid transition in molecular glass–formers: A hidden structural transformation fuelled by conformational interconversion. The Journal of Physical Chemistry B, 128(20), 5055–5063, (2024).

R3. K. Grzybowska, M. Rams–Baron, K. Łucak, A. Grzybowski, M. Paluch. Study of thermal properties, molecular dynamics, and physical stability of etoricoxib mixtures with octaacetylmaltose near the glass transition. *International Journal of Molecular Sciences*, 23, 9794, (2022).

Rezultaty moich badań zaprezentowałam na międzynarodowych konferencjach naukowych:

- K. Łucak, A. Z. Szeremeta, D. Kramarczyk, O. Janus, S. Pawlus, Structure modification of alcohols and its effect on the Debye relaxation, *Diffusion Fundamentals IX* (21–24/09/2022), Kraków, Polska (prezentacja plakatu).

- K. Łucak, A. Z. Szeremeta, S. Pawlus, The supramolecular structures in propanol and its halogen derivatives, *Young Multis – Multiscale Phenomena in Condensed Matter Conference for young researchers*, online (03–05/07/2023) (wystąpienie ustne).

- K. Łucak, A. Z. Szeremeta, J. Grelska, K. Jurkiewicz, S. Pawlus, Molecular dynamics of halogen monoalcohols at different thermodynamic conditions, *12th Conference*

on Broadband Dielectric Spectroscopy and its Applications, Lizbona, Portugalia (01–09/09/2025) (wystąpienie ustne).

Badania, których wyniki zawarte są w pracy doktorskiej były finansowane przez Narodowe Centrum Nauki w ramach projektu OPUS „*Wysokociśnieniowe badania spektroskopowe i dyfrakcyjne jako klucz do zrozumienia osobliwego zachowania asocjujących cieczy z wiązaniami wodorowymi i oddziaływaniami van der Waalsa”* (no. UMO–2019/35/B/ST3/02670), którego kierownikiem był prof. dr hab. Sebastian Pawlus.

6. Przedmiot badań

W niniejszej pracy badawczej analizowano monohydroksylowe alkohole alifatyczne, zawierające pojedynczą grupę hydroksylową –OH oraz różniące się typem podstawionego atomu halogenu: Cl, Br, I, długością łańcucha węglowego oraz pozycją grup funkcyjnych w cząsteczce.

Badane alkohole można podzielić na następujące grupy:

- Pochodne halogenowane propanolu (z trójwęglowym łańcuchem):
  • 3–chloro–1–propanol (3Cl1P),
  • 3–bromo–1–propanol (3Br1P),
  • 3–jodo–1–propanol (3I1P),
  • 1–chloro–2–propanol (1Cl2P),
  • 1–bromo–2–propanol (1Br2P).
  Związki te tworzą pary izomerów (np. 3Br1P vs. 1Br2P), co umożliwiło analizę wpływu wzajemnego położenia grupy –OH i atomu halogenu na ich właściwości.
- Pochodne halogenowane etanolu (z dwuwęglowym łańcuchem):
  • 2–chloro–1–etanol (2Cl1E),
  • 2–bromo–1–etanol (2Br1E),
  • 2–jodo–1–etanol (2I1E).
  Związki te różnią się długością łańcucha węglowego w stosunku do pochodnych propanolu, co pozwoliło na rozpoznanie jaki wpływ ma długość łańcucha alkilowego na architekturę struktur asocjacyjnych.

Związkiem referencyjnym był n–propanol (nP) – prosty, nasycony alkohol z trójwęglowym łańcuchem.

Struktury chemiczne badanych alkoholi przedstawiono na **rysunku 5**. Ich nazwy podano w języku angielskim – zgodnie z nomenklaturą stosowaną w literaturze naukowej – a tam, gdzie była ona odmienna, również w języku polskim. Dodatkowo uwzględniono akronimy przyjęte w publikacjach.

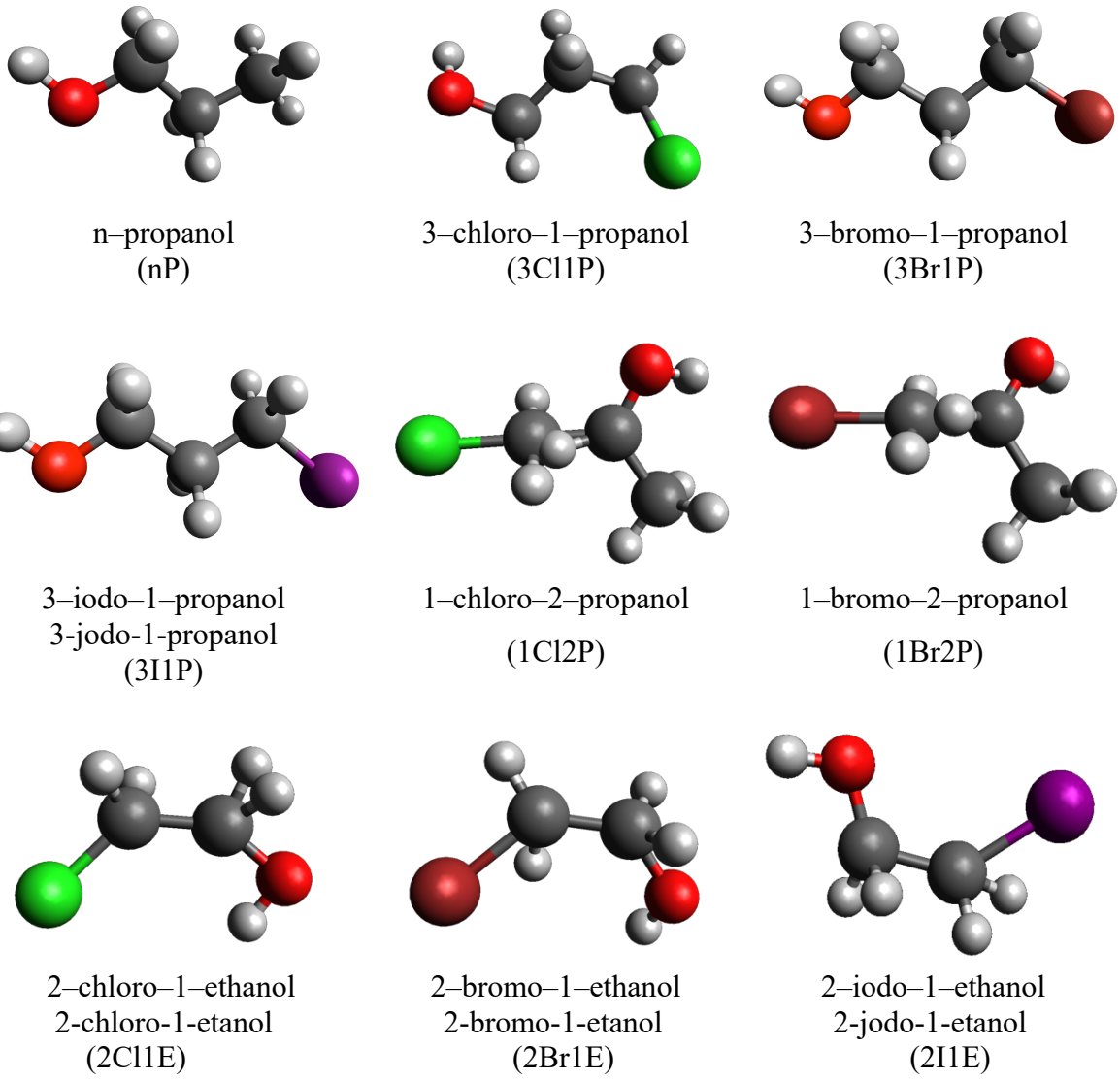

Rysunek 5. Modele cząsteczek badanych alkoholi monohydroksylowych.

7. Metodologia - Szerokopasmowa spektroskopia dielektryczna (BDS)

Szerokopasmowa spektroskopia dielektryczna jest narzędziem służącym do badania odpowiedzi materiału na zmienne pole elektryczne. W trakcie pomiarów rejestruje się zespoloną impedancję próbki, której składowymi są pojemność i przewodnictwo, co następnie pozwala na wyznaczenie zespolonej przenikalności elektrycznej $\varepsilon^*(\omega)$ [40]. Typowy układ pomiarowy składa się z kondensatora, w którym próbka umieszczona jest pomiędzy dwiema elektrodami, a odległość między nimi ustalana jest za pomocą cienkiej przekładki dystansowej z włókna szklanego. Do takiego układu przykładane jest zmienne napięcie $U^*(\omega)$, którego sygnał analizowany jest przy użyciu analizatora impedancji. Pozwala to na wyznaczenie zespolonej impedancji badanego materiału $Z^*(\omega) = U^*(\omega) / I^*(\omega)$, będącej ilorazem zmierzonego napięcia i natężenia prądu przepływającego przez próbkę [38– 40]. Schematyczny obraz takiego układu pomiarowego przedstawiono na **rysunku 6**. Znając zespoloną impedancję $Z^*(\omega)$, można bezpośrednio wyznaczyć zespoloną przenikalność elektryczną badanego materiału, korzystając z poniższego wzoru [38, 39]:

$$\varepsilon^*(\omega) = -\frac{i}{\omega Z^*(\omega) C_0}, \tag{18}$$

gdzie: C_0 - pojemność pustego kondensatora bez badanego materiału, zależy jedynie od geometrii układu. Wyraża się wzorem $C_0 = \varepsilon_0 A/d$, gdzie: A jest powierzchnią elektrod, d jest odległością między nimi [39, 40].

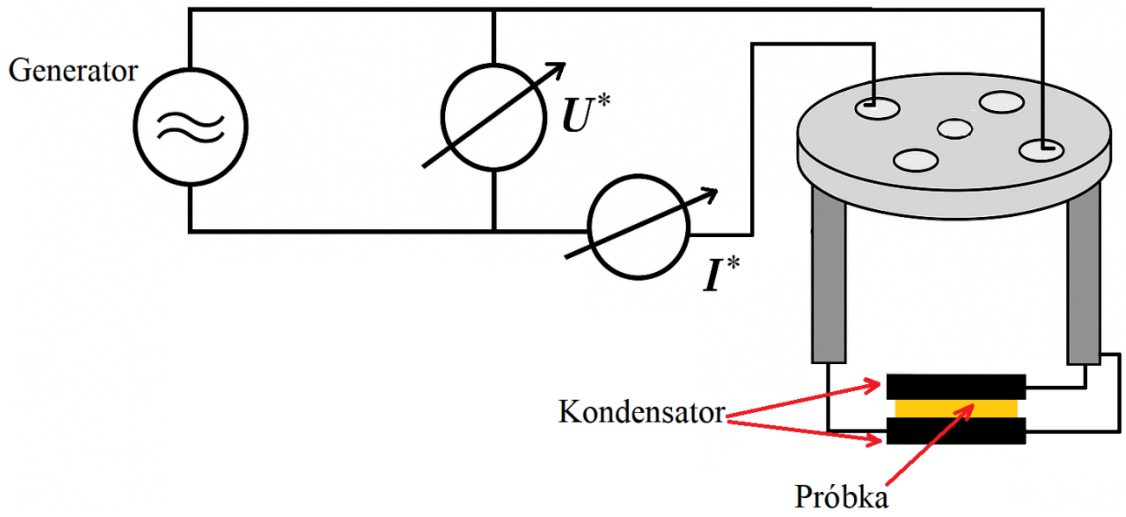

Rysunek 6. Uproszczony schemat pomiaru impedancji próbki za pomocą spektrometru dielektrycznego w domenie częstotliwościowej. Adaptacja na podstawie: [38, 40]

7.1 Przygotowanie próbek

Wszystkie związki chemiczne wykorzystane w badaniach zostały zakupione w firmach Sigma–Aldrich oraz TCI Chemicals. Przed pomiarem każda z próbek była suszona przy użyciu strumienia ciekłego azotu, co pozwalało na usunięcie ewentualnych śladów wody.

7.2 Pomiary temperaturowe BDS pod ciśnieniem atmosferycznym

W ramach prowadzonych badań, których rezultatem jest niniejsza rozprawa przeprowadzono pomiary dielektryczne halogenowych alkoholi monohydroksylowych w warunkach ciśnienia atmosferycznego korzystając z szerokopasmowego spektrometru dielektrycznego firmy Novocontrol. Aparatura była wyposażona w analizator impedancji Alpha oraz układ chłodzenia Quatro [23, 24]. Do pomiarów zastosowano kondensator płasko–równoległy, którego elektrody wykonane były ze stali nierdzewnej i miały średnicę 10 mm. Odległość między elektrodami ustalono za pomocą dwóch włókien szklanych o średnicy 100 μm, a dodatkowe uszczelnienie zapewniał pierścień wykonany z teflonu [23]. Rejestrowane widma zespolonej przenikalności elektrycznej obejmowały zakres częstotliwości 10^{-1} – 10^{6} Hz. Pomiary wykonywano w warunkach quasi–statycznych, zapewniając stabilizację temperatury na poziomie około 0.2 K, przy pomocy ciekłego azotu. Po każdej stabilizacji warunków utrzymywano temperaturę na zadanym poziomie przez minimum 3 minuty przed rozpoczęciem rejestracji widma. Pomiarów zależności temperaturowych dokonano z krokiem $\Delta T = 2$ K. Schemat głowicy pomiarowej oraz kondensatora przedstawiono na **rysunku 7**. Do akwizycji danych pomiarowych wykorzystano oprogramowanie WinDATA (Novocontrol).

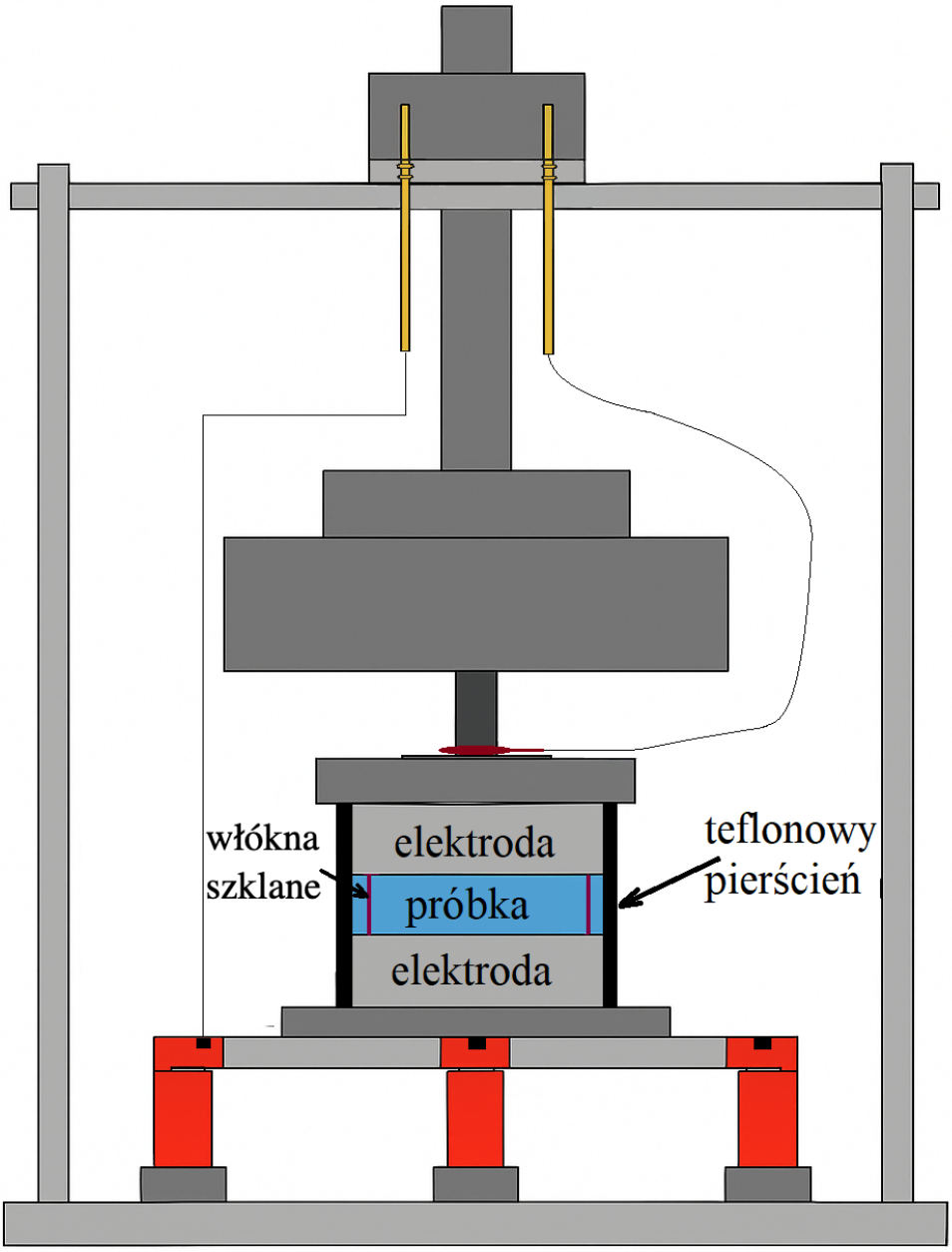

Rysunek 7. Schemat układu pomiarowego wykorzystywanego w badaniach dielektrycznych.

7.3 Pomiary w warunkach ciśnieniowych do 1.8 GPa

W pomiarach ciśnieniowych, sięgających do 1.8 GPa, wykorzystano system ciśnieniowy UNIPRESS (Instytut Wysokich Ciśnień PAN, Warszawa, Polska). Celę pomiarową używaną w tych badaniach przedstawiono na **rysunku 8.** Przygotowanie układu polegało na umieszczeniu cieczy badanej w teflonowej kapsułce, którą następnie zamykano korkiem pomiarowym z wbudowanym układem dwóch elektrod tworzących kondensator.

Elektrody te wykonane były ze stali nierdzewnej, a przewody pomiarowe prowadzono na zewnątrz układu i łączono z analizatorem impedancji Alpha–A (Novocontrol). Kondensator z kapsułką teflonową i elektrodami był umieszczany wewnątrz komory ciśnieniowej (UNIPRESS), która z kolei była otoczona płaszczem grzewczo–chłodzącym, umożliwiającym regulację temperatury za pomocą termostatu cieczowego (Julabo). Stabilność temperatury w trakcie eksperymentu utrzymywano z dokładnością do 0.5 K, a jej odczyt zapewniał cyfrowy termometr termoparowy HD 2328.0. Ciśnienie w układzie generowano za pomocą prasy hydraulicznej, która przekazywała siłę na tłok, kompresując badaną próbkę umieszczoną w kapsułce teflonowej. Do akwizycji danych pomiarowych wykorzystano oprogramowanie WinDATA (Novocontrol).

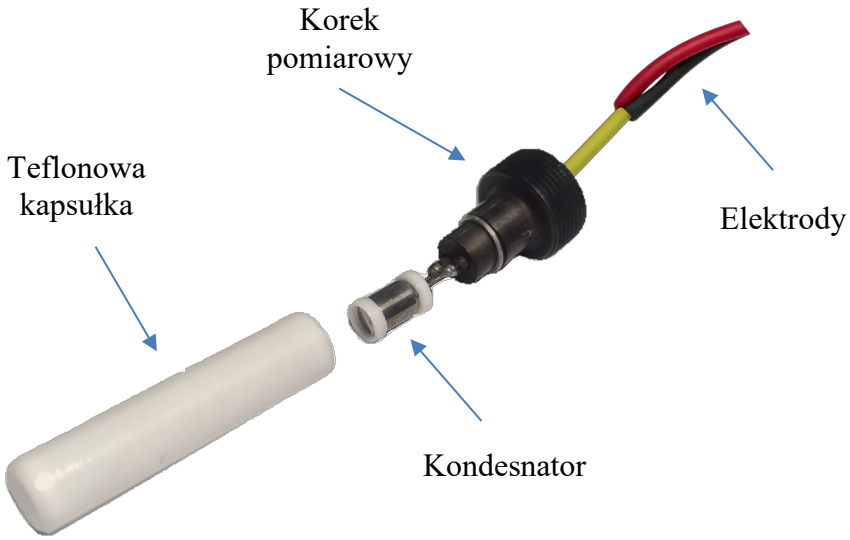

Rysunek 8. Kondensator pomiarowy do badań dielektrycznych w warunkach ciśnieniowych do 1.8 GPa.

7.4 Pomiary w warunkach ciśnieniowych do 600 MPa

Pomiarów w zakresie ciśnienia do 600 MPa dokonano przy użyciu systemu ciśnieniowego wyposażonego w mikropompę MP5 oraz jednostkę sterującą, również dostarczonych przez Instytut Wysokich Ciśnień PAN. Ciśnienie przekazywano do komory pomiarowej za pomocą oleju silikonowego Julabo HL90 i systemu kapilar (Nova Swiss). W celu uniknięcia bezpośredniego kontaktu oleju z próbką, kondensator pomiarowy, o identycznej geometrii jak stosowany w pomiarach w ciśnieniu atmosferycznym, został szczelnie owinięty taśmą teflonową jak pokazano na **rysunku 9** oraz schematycznie zilustrowano w przekroju na **rysunku 10.** Stabilizację temperatury realizowano za pomocą tego samego systemu termostatycznego (Julabo) co w przypadku układu do badań ciśnieniowych do 1.8 GPa. Dokładność regulacji temperatury wynosiła ±0.5 K, a pomiar temperatury realizowano przy pomocy cyfrowego termometru termoparowego HD 2328.0. Zakres częstotliwości stosowany w tych pomiarach był zgodny z tym wykorzystanym dla badań w ciśnieniu atmosferycznym. Do akwizycji danych pomiarowych wykorzystano oprogramowanie WinDATA (Novocontrol).

Rysunek 9. Kondensator pomiarowy do badań dielektrycznych w warunkach ciśnieniowych do 600 MPa.

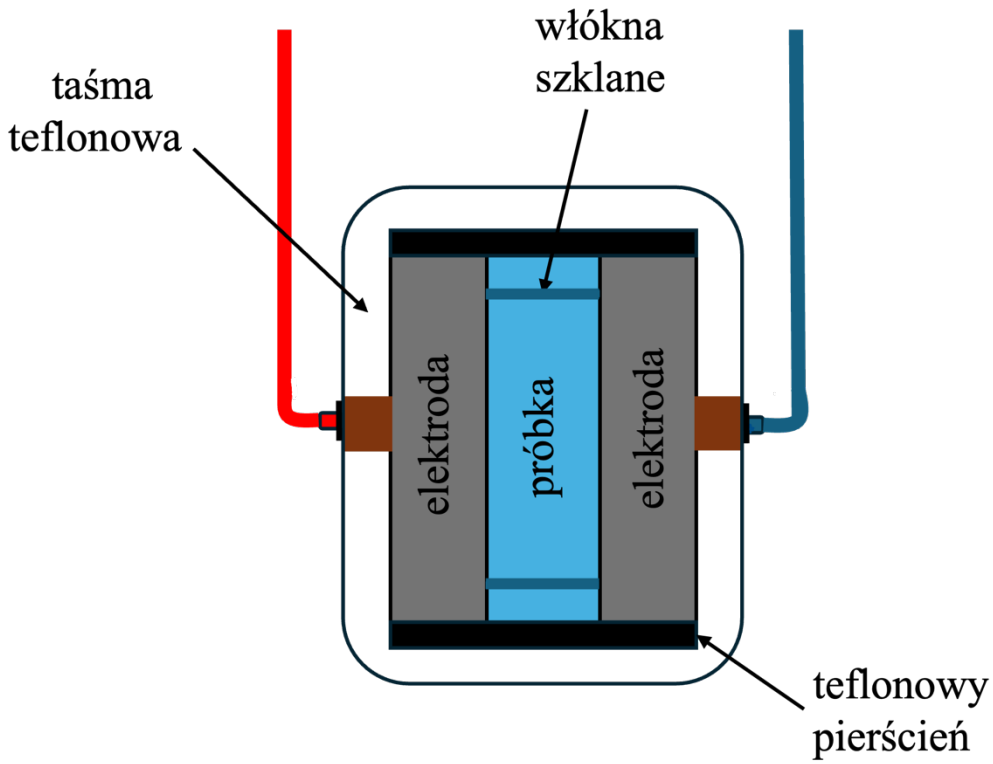

Rysunek 10. Schemat kondensatora pomiarowego w przekroju do badań dielektrycznych w warunkach ciśnieniowych do 600 MPa.

7.5 Analiza danych BDS i uzupełniające techniki badawcze

Analizę zarejestrowanych widm zespolonej przenikalności elektrycznej, obejmującą dopasowanie odpowiednich funkcji relaksacyjnych oraz wyznaczenie czasów relaksacji, przeprowadzono przy użyciu programu WinFit (Novocontrol). Ostateczne opracowanie wyników – w tym przygotowanie wykresów i zestawień przedstawionych w niniejszej rozprawie – wykonano w programie Origin (OriginLab).

Dla pełniejszego opisu właściwości badanych układów oraz pogłębienia interpretacji wyników przeprowadzonej przeze mnie spektroskopii dielektrycznej, analizę wzbogaciłam o dodatkowe techniki badawcze, zrealizowane we współpracy z innymi członkami zespołu. Wykorzystano: DSC, spektroskopię w podczerwieni z transformacją Fouriera (FTIR), dyfrakcję rentgenowską (XRD), a także MDS oraz obliczenia z zakresu teorii funkcjonalnej gęstości (DFT).

8. Wyniki i dyskusja

8.1 Wpływ podstawienia grupy metylowej –(CH_3) atomem halogenu na intensywność procesu Debye'a i relaksacji strukturalnej.

W pierwszej publikacji [P1] szczegółowej analizie poddano wpływ podstawienia grupy metylowej atomem halogenu (chloru, bromu lub jodu) w cząsteczce n–propanolu na obecność i intensywność relaksacji strukturalnej (proces α) oraz procesu Debye'a. Badania objęły cztery związki: n–propanol oraz jego trzy halogenowe pochodne: 3–chloro–1–propanol, 3–bromo–1–propanol i 3–jodo–1–propanol. Już podstawowe właściwości termiczne badanych alkoholi sugerują istotne różnice w charakterze ich dynamiki molekularnej. Temperatura zeszklenia (T_g) dla pochodnych halogenowych, jest istotnie wyższa niż w przypadku n–propanolu (tabela 2), co wskazuje na silniejsze ograniczenie ruchliwości segmentalnej i inny mechanizm asocjacji cząsteczek zawierających atom halogenu. Taka obserwacja stanowiła motywację do dalszej analizy wpływu podstawienia halogenowego na organizację supramolekularną i procesy relaksacyjne, ze szczególnym uwzględnieniem amplitudy i obecności procesu Debye'a. Pomiary metodą spektroskopii dielektrycznej wykonane w szerokim zakresie temperatur jednoznacznie potwierdziły obecność procesu Debye'a dla wszystkich analizowanych związków. W przypadku n–propanolu proces ten wykazuje, charakterystyczną dla monoalkoholi z terminalnie położoną grupą OH, dużą amplitudę, co wiąże się z silną asocjacją molekuł poprzez wiązania wodorowe i powstawaniem uporządkowanych klastrów. Jednakże dla pochodnych halogenowych zaobserwowano wyraźne osłabienie intensywności tego procesu oraz wzmocnienie relaksacji strukturalnej, co zilustrowano na rysunku 1e w pracy [P1]. Stosunek amplitud relaksacji Debye'a do relaksacji strukturalnej znacząco maleje w serii halogenowych pochodnych w porównaniu z n–propanolem (tabela 2). Dowodzi to, że obecność atomu halogenu ogranicza zdolność cząsteczek do tworzenia uporządkowanych agregatów łańcuchowych, będących źródłem relaksacji typu Debye'a. Dodatkowo, analiza widm strat elektrycznych wykazała, że w związku zawierającym atom chloru relaksacja strukturalna charakteryzuje się wyraźniejszym maksimum i większą względną amplitudą w porównaniu do odpowiednich pochodnych bromowej i jodowej. Wartości czynnika Kirkwooda–Fröhlicha (g_k) wyznaczone w temperaturze około 169 K i przedstawione na rysunku 2a w pracy [P1], wskazują, że n-propanol osiąga największą wartość g_k, a tym samym charakteryzuje się najwyższym stopniem uporządkowania orientacyjnego dipoli. W przypadku alkoholi halogenowych obserwuje się wyraźne niższą wartości g_k co przedstawiono w tabeli 2.

Tabela 2. Zestawienie wybranych parametrów fizykochemicznych dla n–propanolu i jego halogenowych pochodnych

Związek chemiczny	T_g (K)	Amplituda Debye/α	współczynnik Kirkwooda (g_k)	Wolne grupy OH [%]
n–propanol	98 ± 2	19.65	≈ 4.7	—
3–chloro–1–propanol	142 ± 2	1.57	≈ 2.5	2.15
3–bromo–1–propanol	150 ± 2	1.87	≈ 1.8	2.36
3–jodo–1–propanol	157 ± 2	2.89	≈ 1.8	3.13

Niższe wartości g_k wskazują na osłabienie uporządkowania orientacyjnego dipoli, co jest konsekwencją mniejszej zdolności cząsteczek do tworzenia trwałych agregatów supramolekularnych o łańcuchowej strukturze. Średnią liczbę cząsteczek tworzących łańcuchy asocjacyjne wyznaczono w oparciu o model łańcucha przejściowego (TCM, transient chain model), zaproponowany przez Gainaru i współpracowników [P1, ref. 26]. Model ten zakłada, że relaksacja Debye'a wynika z fluktuacji momentu dipolowego, związanych z dynamicznym dołączaniem i odłączaniem cząsteczek do końców supramolekularnych łańcuchów utworzonych przez molekuły połączone przez wiązania wodorowe. Liczbę cząsteczek N w takich łańcuchach oszacowano zgodnie z modelem TCM, na podstawie wartości składowych momentów dipolowych oraz wyznaczonych parametrów dielektrycznych ($\Delta\varepsilon_{Debye}$, $\Delta\varepsilon_{\alpha}$), opisanych w [P1, Supplementary Information]. Dla n-propanolu średnia liczba cząsteczek w klastrze wynosiła 7–8, natomiast dla pochodnych halogenowych spadała do 1–3 cząsteczek. Oznacza to, że podstawienie grupy $–CH_3$ atomem halogenu prowadzi do znaczącego skrócenia długości łańcuchów asocjacyjnych i osłabienia ich uporządkowania. Uzupełniające pomiary w podczerwieni [P1, rys. 3a, 3b] ujawniają istotne różnice w zakresie pasma O–H···O. Dla pochodnych halogenowych w temperaturze pokojowej obserwuje się obecność charakterystycznego pasma ok. 3560 cm^{-1}, odpowiadającego wolnym, niezaangażowanym w wiązania wodorowe grupom hydroksylowym. Pasmo to nie występuje w widmie n-propanolu ani w temperaturze pokojowej, ani w T_g, co świadczy o pełnej asocjacji cząsteczek poprzez wiązania wodorowe. Natomiast w pochodnych halogenowych obecność tego pasma obserwuje się w temperaturze pokojowej, co potwierdza niższy stopień asocjacji w porównaniu do n-propanolu. Ilościowy udział tych grup wzrasta wraz z masą atomową halogenu (tabela 2), co świadczy o malejącym stopniu asocjacji cząsteczek wraz ze wzrostem masy atomowej halogenu.

Symulacje dynamiki molekularnej potwierdzają wyniki eksperymentalne. Zgodnie z nimi n–propanol formuje największe supramolekularne agregaty (średnio 13 cząsteczek), podczas gdy dla związków halogenowych wartości te spadają do 5–7, [P1, rys. 4b]. Symulacje dynamiki molekularnej wykazały również, że w alkoholach halogenowych możliwe jest tworzenie dodatkowych typów klastrów molekularnych, wynikających z obecności oddziaływań halogenowych. Zidentyfikowano dwa nowe typy agregatów: klastry O–H···X oraz klastry halogenowe (X···X). Oddziaływania te konkurują z klasycznymi wiązaniami O–H···O, a ich obecność może wprowadzać lokalne zaburzenia i heterogeniczność do architektury supramolekularnej. Wizualizacja struktur klastrowych, z wyraźną segregacją grup OH oraz atomów halogenu, pokazała, że taki układ przestrzenny utrudnia równoległe ustawienie momentów dipolowych poszczególnych cząsteczek, co prowadzi do osłabienia ich skorelowanego ruchu i w rezultacie zmniejszenia intensywności procesu Debye'a. [P1, rys. 4c]. Wyniki pomiarów eksperymentalnych zostały wzbogacone obliczeniami teorii funkcjonału gęstości, które posłużyły do oceny energii oddziaływań w dimerach cząsteczek. Analiza geometrii oraz energii oddziaływań wskazała, że w badanych alkoholach dominują klasyczne, silne wiązania wodorowe typu O–H···O o energii oddziaływań $E \geq 5$ kcal/mol. Oddziaływania typu H–O···X są słabsze ($E < 4$ kcal/mol), a najsłabsze są siły X···X pomiędzy atomami halogenu ($E < 2$ kcal/mol). Co więcej, otrzymane długości wiązań O···O w klastrach (2.9 Å) są zgodne z wynikami symulacji dynamiki molekularnej (2.8 Å), co potwierdza zgodność między podejściem teoretycznym a obserwacjami eksperymentalnymi. Powstałe różnice w strukturze lokalnej i supramolekularnej – takie jak skrócenie długości klastrów, zmniejszenie ich uporządkowania oraz obecność dodatkowych oddziaływań O–H···X i X···X – wpływają na ograniczenie zdolności cząsteczek do koherentnego ustawienia momentów dipolowych. Na poziomie molekularnym oznacza to, że cząsteczki nie tworzą już stabilnych, długich łańcuchów powiązanych wiązaniami wodorowymi z równolegle zorientowanymi momentami dipolowymi, które są odpowiedzialne za pojawienie się intensywnego procesu Debye'a. Zamiast tego obserwuje się bardziej rozproszone i mniej uporządkowane agregaty, co prowadzi do osłabienia relaksacji Debye'a i jednocześnie do wzmocnienia relaksacji strukturalnej, związanej z ruchem łańcuchów alkilowych. Zatem to zmieniona geometria i rodzaj oddziaływań międzycząsteczkowych stanowią molekularną przyczynę obserwowanych zmian intensywności i charakterystyki obu procesów relaksacyjnych.

8.2 Wpływ izomerii i rodzaju atomu halogenu na dynamikę molekularną oraz reorganizację struktur supramolekularnych w zmiennych warunkach termodynamicznych.

W drugiej publikacji [P2] zaprezentowano wyniki badań wpływu izomerii, rodzaju podstawionego atomu halogenu jakim był chlor (Cl) i brom (Br) oraz zmiennych warunków termodynamicznych (temperatury i ciśnienia) na dynamikę molekularną oraz formowanie struktur supramolekularnych w halogenowych monoalkoholach. Analizie poddano cztery związki: 3–chloro–1–propanol, 1–chloro–2–propanol, 3–bromo–1–propanol oraz 1–bromo–2–propanol, które tworzą dwie pary izomerów różniących się położeniem grupy hydroksylowej oraz rodzajem atomu halogenu. Temperatury T_g, wyznaczone metodą DSC, potwierdzają różnice w dynamice molekularnej tych układów (tabela 3). Wyższe wartości T_g dla alkoholi, w których grupa hydroksylowa znajduje się w środku łańcucha węglowego, wskazują na bardziej zwartą i sztywną strukturę supramolekularną tych układów. Pomiary temperaturowe BDS pod ciśnieniem atmosferycznym (0.1 MPa) wykazały obecność dwóch procesów relaksacyjnych: strukturalnego (α) oraz typu Debye'a, choć obserwuje się także relaksacje drugorzędową o mniejszej intensywności. W alkoholach zawierających atom chloru, proces relaksacji strukturalnej α charakteryzuje się wyższą względną amplitudą i jest bardziej wyraźny w stosunku do maksimum relaksacji typu Debye'a, niż w analogicznych związkach zawierających atom bromu. W szczególności, relaksacja α w 3–chloro–1–propanolu i 1–chloro–2–propanolu cechuje się wyraźnie zaznaczonym maksimum, co świadczy o bardziej wyraźnym udziale relaksacji strukturalnej w odpowiedzi elektrycznej układu [P2, rys. 1b, 1c, 1d]. Wyznaczone wartości współczynnika g_k, przedstawione na rysunku 2c w pracy [P2], są znacznie wyższe od jedności dla wszystkich badanych układów, co wskazuje na tendencję cząsteczek do tworzenia agregatów łańcuchowych. Szczególnie wysoka – w porównaniu do innych alkoholi halogenowych – wartość g_k cechuje 1–chloro–2–propanol, co sugeruje, że alkohol ten charakteryzuje się największą liczbą klastrów z wiązaniami wodorowymi lub liczba cząsteczek w takich asocjatach jest największa (tabela 3).

Tabela 3. Wartości czynnika Kirkwooda dla wybranych halogenowych propanoli

Związek chemiczny	T_g (K)	współczynnik Kirkwooda (g_k)
3–chloro–1–propanol	142 ± 2	≈ 2.5
1–chloro–2–propanol	155 ± 2	≈ 3.2
3–bromo–1–propanol	150 ± 2	≈ 1.8
1–bromo–2–propanol	164 ± 2	≈ 2.7

Różnice w wartościach g_k pomiędzy izomerami i typami halogenu sugerują, że położenie grupy –OH i rodzaj atomu halogenu wpływają na architekturę agregatów supramolekularnych. W badaniach wysokociśnieniowych zaobserwowano, że przy izotermicznym wzroście ciśnienia zmniejsza się separacja czasowa między procesami relaksacyjnymi Debye'a i α, co prowadzi do tego, że oba procesy stają się trudne do rozróżnienia i na widmie zespolonej przenikalności elektrycznej ε*(f) obserwowany jest pojedynczy dominujący proces relaksacyjny**,** opisywany jako proces typu Debye'a-like, ponieważ jego główną składową stanowi relaksacja Debye'a [P2, rys. 3a]. Zależność czasów relaksacji procesu Debye'a–like od ciśnienia opisano za pomocą ciśnieniowego odpowiednika funkcji Vogel–Fulcher–Tamman–Hesse (pVFTH) w postaci:

$$\tau = \tau_0 exp\left(\frac{D_p P}{P_0 - P}\right), \tag{18}$$

co pozwoliło na dopasowanie danych τ(p) i dalsze obliczenie objętości aktywacji (ΔV), która określa, w jakim stopniu ciśnienie wpływa na dynamikę badanego układu i stanowi miarę objętościowej reorganizacji towarzyszącej procesowi relaksacyjnemu. W pracy wartość ΔV wyznaczono ze wzoru:

$$\Delta V = RT\left(\frac{dln\tau_{D_{like}}}{dp}\right)_T, \tag{19}$$

1–bromo–2–propanol i 1–chloro–2–propanol charakteryzują się większymi wartościami ΔV niż 3–bromo–1–propanol [P2, rys. 3b], co wskazuje na różną architekturę klastrów oraz ich wrażliwość na ściskanie. Szczególnie 1–bromo–2–propanol wymaga większych wartości ΔV dla reorganizacji molekuł. Obecność grupy hydroksylowej w pozycji nieterminalnej sprzyja tworzeniu układów supramolekularnych o strukturze pierścieniowej. Zarejestrowana dla 1–bromo–2–propanolu najwyższa wartość objętości aktywacji ΔV spośród badanych związków wskazuje, że reorganizacja takiej architektury wymaga większej objętości niż w przypadku struktur łańcuchowych. Jest to zrozumiałe – do przeorganizowania pierścieni potrzeba więcej przestrzeni niż w przypadku łańcuchów, które łatwiej ulegają upakowaniu pod wpływem kompresji. W miarę wzrostu ciśnienia może dochodzić do pękania pierścieni i ich przechodzenia w formy łańcuchowe, co skutkuje wzrostem intensywności procesu Debye'a. Zaobserwowano również istotne różnice w zakresie zmian temperatury przejścia szklistego (T_g) pod wpływem ciśnienia. Jednak ze względu na nakładanie się procesów α i Debye'a wraz z rosnącym ciśnieniem oraz brak wyraźnej separacji ich czasów relaksacji, wprowadzono temperaturę referencyjną T_r, przy której czas relaksacji procesu typu Debye'a–like (będącego superpozycją tych procesów) osiąga 1 sekundę. Podejście to, choć odbiega

od klasycznego sposobu definicji temperatury zeszklenia, opartego na procesie α, umożliwiło spójną analizę trendów ewolucji T_r, w funkcji ciśnienia i zostało szczegółowo uzasadnione w pracy [P2]. Najwyższą wartość współczynnika (dT_r/dp), określającego szybkość wzrostu T_g w funkcji przyłożonego ciśnienia, odnotowano dla 1–bromo–2–propanolu, a niższe – dla 1–chloro–2–propanolu oraz 3–bromo–1–propanolu [P2, rys. 4b]. Wartości te korelują z obliczonymi wartościami ΔV oraz wyznaczonymi współczynnikami kruchości (m_p) dla procesów Debye'a, α i Debye'a–like [P2, rys. 5a–d, tabela 1]. Dalsza analiza zmian amplitudy procesu Debye'a (Debye-like) [P2, rys. 6b–d] pod wpływem ciśnienia ukazuje odmienne mechanizmy reorganizacji struktur supramolekularnych. Dla 3-bromo-1-propanolu obserwuje się obniżenie amplitudy procesu Debye'a pod wpływem ciśnienia, co jest interpretowane jako wynik częściowego załamania uporządkowanych struktur łańcuchowych i przechodzenia układu w bardziej zwarte, rozgałęzione lub pierścieniowe formy agregatów. Natomiast w przypadku 1-bromo-2-propanolu i 1-chloro-2-propanolu ciśnienie indukuje reorganizację odwrotną – układy pierścieniowe przechodzą w bardziej liniowe struktury, co prowadzi do zwiększenia amplitudy procesu Debye'a. Należy nadmienić, że dynamika relaksacyjna 3–chloro–1–propanol nie mogła zostać poddana analizie w warunkach wysokiego ciśnienia, ze względu na obserwowaną krystalizację tego alkoholu w trakcie kompresji. Obliczenia teorii funkcjonału gęstości zawarte w Supplementary Information w pracy [P2] ujawniają istnienie dimerów cyklicznych i liniowych w 1–bromo–2–propanolu i 1–chloru–2–propanolu, natomiast w 3–bromo–1–propanolu dominują dimery liniowe z uwagi na terminalne położenie grupy –OH. Potwierdzają to także wyniki MDS, zgodne z wynikami dla podobnych układów, np. 2–etylo–1–heksanolu i 2–metylo–1–heksaanolu. Analiza wyników MDS wykazała również, że w warunkach podwyższonego ciśnienia możliwe jest tworzenie agregatów typu Br···Br, co potwierdza istnienie klastrów halogenowych. Średni rozmiar klastrów O···O i Br···Br rośnie wraz z ciśnieniem, przy czym w 1–bromo–2–propanolu są one mniejsze niż w 3–bromo–1–propanolu z powodu większych przeszkód sterycznych [P2, rys. 8c]. Do ~2–2.5 GPa dominują klastry O···O, jednak powyżej tej granicy agregaty halogenowe rosną szybciej, co może ograniczać rozwój układu wiązań wodorowych tworzących łańcuchowe struktury supramolekularne i prowadzić do osłabienia sygnału procesu Debye'a.

8.3 Rola długości łańcucha węglowego w kształtowaniu struktury i dynamiki układów alkoholi halogenowych w funkcji temperatury i ciśnienia.

W trzecim artykule [P3] skupiono się na szczegółowym zbadaniu wpływu długości łańcucha węglowego na właściwości dynamiczne i strukturalne halogenowych alkoholi monohydroksylowych w funkcji temperatury i ciśnienia, oraz dla różnych atomów halogenowych. Analizie poddano sześć związków chemicznych: 3–jodo–1–propanol, 2–jodo–1–etanol, 3–chloro–1–propanol, 2–chloro–1–etanol, 3–bromo–1–propanol oraz 2–bromo–1–etanol. Temperatury zeszklenia dla badanych alkoholi halogenowych zostały wyznaczone metodą kalorymetrii skaningowej z modulacją temperatury TMDSC i przedstawione w tabeli 4. Dla każdego z podstawionych halogenów (Cl, Br, I) związki o krótszym łańcuchu węglowym (etanolowe) wykazują wyższe wartości T_g niż ich analogi o dłuższych łańcuchach węglowych (propanolowe), co świadczy o większej sztywności i ograniczonej mobilności supramolekularnych struktur w tych układach. Widma strat elektrycznych ε"(f), zarejestrowane w warunkach ciśnienia atmosferycznego (0.1 MPa), wykazały obecność dwóch dominujących procesów relaksacyjnych – strukturalnego oraz typu Debye'a [P3, rys. 1c]. Dodatkowo, widoczna była również relaksacja drugorzędowa o mniejszej intensywności, która nie była analizowana w ramach przedstawionych badań. W przypadku krótszych alkoholi etanolowych proces Debye'a charakteryzował się maksimum strat elektrycznych o wyższej amplitudzie, co wskazuje na większą tendencję do tworzenia uporządkowanych i bardziej zwartych łańcuchowych struktur supramolekularnych. Z kolei dla alkoholi propanolowych widoczne były wyraźnie rozdzielone sygnały obu procesów. Dłuższy łańcuch węglowy w badanych alkoholach propanolowych nie sprzyjał tworzeniu dłuższych i lepiej uporządkowanych łańcuchów asocjacyjnych, lecz prowadził do powstawania bardziej rozproszonych agregatów, co tłumaczy obniżoną amplitudę procesu Debye'a. Analiza g_k potwierdziła istnienie uporządkowania orientacyjnego wynikającego z obecności sieci wiązań wodorowych. Wartości tego parametru były największe dla 2–chloro–1–etanolu (tabela 4), co sugeruje występowanie dobrze uporządkowanych klastrów z wiązaniami wodorowymi lub największą liczbę cząsteczek w agregatach spośród wszystkich analizowanych związków [P3, rys. 2c].

Tabela 4. Wartości czynnika Kirkwooda dla wybranych monoalkohooli halogenowych

Związek chemiczny	T_g (K)	współczynnik Kirkwooda (g_k)
2–chloro–1–etanol	146 ± 2	≈ 3.2
2–jodo–1–etanol	161 ± 2	≈ 2.9
2–bromo–1–etanol	154 ± 2	≈ 2.6
3–chloro–1–propanol	142 ± 2	≈ 2.5

3–bromo–1–propanol	150 ± 2	≈ 1.8
3 –jodo–1–propanol	157 ± 2	≈ 1.8

Porównanie czasów relaksacji strukturalnej wyznaczonych metodą spektroskopii dielektrycznej oraz TMDSC pokazało bardzo dobrą zgodność obu podejść – dla każdego badanego związku różnice nie przekraczały 0.8 dekady, co mieści się w granicach niepewności wynikających z ekstrapolacji danych TMDSC i potwierdziło słuszność przyporządkowania szybszego procesu relaksacyjnego jako relaksacji strukturalnej na podstawie odpowiedzi elektrycznej. [P3, rys. 3]. W przypadku alkoholi zawierających atom chloru krystalizacja uniemożliwiła przeprowadzenie pomiarów pod ciśnieniem, natomiast w przypadku alkoholi z atomem jodu silna tendencja do krystalizacji ograniczyła zakres możliwych pomiarów w warunkach wysokiego ciśnienia. Warto zauważyć, że 2-jodo-1-etanol ma tendencję do krystalizacji już pod ciśnieniem atmosferycznym powyżej T_g (około 190 K). Krystalizację w warunkach atmosferycznych zaobserwowano również w pomiarach BDS w przypadku 2–chloro–1–etanol (około 169 K). Dla związków z atomem bromu możliwe było przeprowadzenie pomiarów w szerokim zakresie ciśnień. Wraz ze wzrostem ciśnienia zaobserwowano stopniowe zbliżanie się skal czasowych procesów Debye'a i strukturalnego (α), co prowadziło do ich nakładania się i pojawienia się jednego, niesymetrycznego procesu relaksacyjnego typu Debye'a–like. Ilustruje to reorganizację układów supramolekularnych w kierunku bardziej jednorodnych warunków dynamicznych, charakteryzujących się spójną odpowiedzią relaksacyjną i mniejszym zróżnicowaniem czasów relaksacji poszczególnych cząsteczek w układzie, co było szczególnie widoczne w przypadku alkoholu 2–bromo–1–etanolu [P3, rys. 5a]. Zależność pomiędzy strukturą cząsteczek a właściwościami dynamicznymi w pobliżu zeszklenia została opisana z wykorzystaniem parametru stromości *(*ang. *steepeness index)* oznaczonego m_α – dla relaksacji strukturalnej α – oraz analogicznie wyznaczanego parametru m_D, przypisanego procesowi Debye'a. Oba parametry wyznaczono przy założeniu, że odpowiadają one temperaturze referencyjnej, w której czas relaksacji osiąga wartość 1 s. Wskaźnik m_α, przypisany do relaksacji strukturalnej, pozwala na ilościowe porównanie kruchości cieczy – im wyższa jego wartość, tym silniejsza zależność czasu relaksacji od temperatury w pobliżu T_g. W badanych układach alkohole etanolowe wykazywały wyższe wartości m_α (tabela 5), co wiąże się z większą mobilnością segmentów cząsteczkowych. Odpowiedniki propanolowe charakteryzowały się niższymi wartościami m_α co świadczy o bardziej stabilnych układach supramolekularnych. Analogicznie wyznaczony parametr m_D, dotyczący procesu Debye'a, nie powinien być utożsamiany z kruchością cieczy, ponieważ

odnosi się do dynamiki sieci wiązań wodorowych, a nie do relaksacji strukturalnej. Dla alkoholi z krótszym łańcuchem (2Cl1E, 2Br1E, 2I1E) wartości m_D były wyższe niż dla alkoholi z dłuższym łańcuchem (3Cl1P, 3Br1P, 3I1P), (patrz tabela 5) co sugeruje, że alkohole etanolowe mają bardziej elastyczne struktury niż ich propanolowe odpowiedniki. Aby umożliwić porównanie parametrów m_D i m_{Dlike} w warunkach wysokiego ciśnienia, wartości te zostały wyznaczone dla jednakowego czasu relaksacji $\tau_{Debye\text{-}like}$ = -4s, co odpowiada temperaturze odniesienia T_{ref} w danym ciśnieniu (patrz tabela 6). Analiza wpływu ciśnienia pokazała, że w przypadku 2–bromo–1–etanolu, dla którego parametr m_D wyznaczono przy 500 MPa, wartość ta obniża się z wraz ze wzrostem ciśnienia. Ten znaczny spadek wskazuje, że układ wiązań wodorowych w 2–bromo–1–etanolu jest bardzo wrażliwy na kompresję, ulegając znacznej reorganizacji strukturalnej już przy stosunkowo niskim ciśnieniu. Z kolei w przypadku 3-bromo-1-propanolu, dla którego parametr m_D wyznaczono przy 1400 MPa, ciśnienie prowadzi do wzrostu wartości m_D dla procesu Debye'a, co wskazuje na odmienny charakter reorganizacji strukturalnej w porównaniu do 2-bromo-1-etanolu [P3, rys. 7]. Taki przebieg zmian świadczy o większej podatności struktur supramaolekularnych powiązanych wiązaniami wodorowymi w 3-bromo-1-propanolu na odkształcenia strukturalne pod wpływem kompresji.

Tabela 5. Wartości indeksów kruchości dla procesu strukturalnego α (m_α) oraz procesu Debye'a (m_D) dla badanych alkoholi przy 0.1 MPa.

Związek chemiczny	m_α	m_D
2–chloro–1–etanol	54 ± 2	49 ± 2
2–bromo–1–etanol	58 ± 2	52 ± 2
2–jodo–1–etanol	47 ± 2	54 ± 2
3–jodo–1–propanol	45 ± 2	43 ± 2
3–bromo–1–propanol	55 ± 2	43 ± 2
3–chloro–1–propanol	57 ± 2	43 ± 2

Tabela 6. Wartości m_D i m_{Dlike} dla 2–Bromo–1–etanolu i 3 -Bromo–1–propanolu przy τ_{Debye} = -4s.

Związek chemiczny	m_D	m_{Dlike}
2–Bromo–1–Etanol	24 przy 0.1 MPa	15 przy 500 MPa
3–Bromo–1–Propanol	20 przy 0.1 MPa	23 przy1400 MPa

Symulacje dynamiki molekularnej przeprowadzone dla alkoholi 2–bromo–1–etanol oraz 3–bromo–1–propanol wykazały istotne różnice w morfologii tworzących się struktur supramolekularnych. W warunkach wysokiego ciśnienia struktury supramolekularne badanych alkoholi przekształcają się z układów łańcuchowych w bardziej zwarte cykliczne lub rozgałęzione agregaty, w wyniku obserwowanego wzrostu liczby cząsteczek w klastrze. Wysokie ciśnienie powodowało wzrost liczby oddziaływań typu Br···Br, co wskazuje na konkurencję pomiędzy wiązaniami wodorowymi a oddziaływaniami halogenowymi [P3, rys. 9]. Zmianom tym towarzyszył wzrost liczby oddziaływań typu Br···Br, wskazujący na rosnącą rolę oddziaływań halogenowych kosztem wiązań wodorowych. Pomimo ogólnego spadku liczby wiązań wodorowych w warunkach wysokiego ciśnienia, rozmiar przeciętnego klastra wzrastał, co sugeruje przejście do bardziej skomplikowanej, struktury supramolekularnej, obejmującej większą liczbę cząsteczek powiązanych oddziaływaniami halogenowymi i wodorowymi, o zwartym i rozgałęzionym charakterze. Warto jednak podkreślić, że nawet przy wzroście znaczenia oddziaływań halogenowych (Br···Br), to właśnie klastry powiązane klasycznymi wiązaniami wodorowymi (O–H···O) niezmiennie dominują liczebnie w badanych układach.

9. Podsumowanie

W niniejszej rozprawie pokazano wpływ struktury molekularnej oraz warunków termodynamicznych na dynamikę molekularną i proces asocjacji wybranych halogenowych alkoholi monohydroksylowych. Badania prowadzone z wykorzystaniem metod eksperymentalnych i teoretycznych pozwoliły szczegółowo scharakteryzować sposób formowania układów asocjacyjnych. Najważniejsze wyniki przedstawiono schematycznie na rysunku 11. Podstawienie grupy $–CH_3$ atomem halogenu (Cl, Br, I) skutkuje istotnym osłabieniem intensywności procesu Debye'a i równoczesnym wzrostem udziału relaksacji α w odpowiedzi dielektrycznej. Atom halogenu zaburza uporządkowaną korelację dipoli, co potwierdzają obniżone wartości czynnika Kirkwooda w porównaniu do n–propanolu. Obliczenia teorii funkcjonału gęstości wykazały, że głównym typem oddziaływań pozostają klasyczne wiązania wodorowe O–H···O, jednak obecność dodatkowych, słabszych oddziaływań O–H···X oraz X···X wpływa istotnie na lokalną organizację cząsteczek, ograniczając wielkość i regularność powstających agregatów, czyli zwiększają heterogeniczność układu. Analiza izomerów wykazała, że położenie grupy hydroksylowej w cząsteczce odgrywa kluczową rolę w architekturze tworzonych asocjatów. Układy

o terminalnym położeniu grupy –OH formują struktury łańcuchowe, natomiast alkohole z grupą hydroksylową w pozycji środkowej sprzyjają powstawaniu bardziej kompaktowych struktur zamkniętych (o topologii pierścieniowej) i rozgałęzionych. Wzrost ciśnienia prowadzi do reorganizacji tych układów supramolekularnych, zmniejszając separację czasową między relaksacją Debye'a i strukturalną oraz prowadząc do ich częściowego nakładania się (superpozycji), w wyniku, którego obserwowany jest pojedynczy proces relaksacyjny o nie-eksponencjalnym kształcie. Zjawisko to było szczególnie dobrze widoczne w przypadku 1–bromo–2–propanolu i 1–chloro–2–propanolu, a towarzyszący wzrost amplitudy procesu Debye'a-like sugerował przejście od stabilnych struktur pierścieniowych do klastrów łańcuchowych. Jednocześnie, w układach o architekturze łańcuchowej (np. 3–bromo–1–propanol), obserwowano spadek intensywności tego procesu, co interpretowano jako rozpad mniej stabilnych agregatów łańcuchowych. Symulacje dynamiki molekularnej potwierdziły, że pod wpływem kompresji nasilają się oddziaływania halogenowe typu X···X, konkurujące z klasycznymi wiązaniami wodorowymi. Cząsteczki o krótszym łańcuchu węglowym (pochodne etanolu) wykazują większą tendencję do tworzenia gęsto upakowanych, dobrze zorganizowanych klastrów, podczas gdy dłuższe (pochodne propanolu) cechują się większą elastycznością struktur. Przedstawione w pracy wyniki rzucają nowe światło na fundamentalne zagadnienia oddziaływań międzycząsteczkowych, dynamiki molekularnej w halogenowych alkoholach monohydroksylowych, a w szczególności na obecności konkurujących oddziaływań międzycząsteczkowych. Rezultaty opublikowano w trzech czasopismach z listy filadelfijskiej, a ich kompleksowe zestawienie umożliwiło stworzenie spójnego obrazu struktury i dynamiki molekularnej halogenowanych alkoholi monohydroksylowych. Najważniejszym osiągnięciem mojej pracy było wykazanie, że obecność atomów halogenowych prowadzi do wyraźnego wzrostu heterogeniczności organizacji supramolekularnej badanych cieczy, przy jednoczesnym utrzymaniu dominującej roli klasycznych wiązań wodorowych. Pokazano również, że wpływ kompresji nie jest uniwersalny, lecz silnie zależy od geometrii cząsteczki – położenia grupy hydroksylowej czy długości łańcucha węglowego – co determinuje sposób reorganizacji struktur supramolekularnych. Dzięki zastosowaniu komplementarnych metod eksperymentalnych i teoretycznych możliwe było opisanie dynamiki oraz topologii agregatów molekularnych w różnych warunkach termodynamicznych. Wyniki te otwierają drogę do dalszych badań nad bardziej złożonymi układami, w szczególności diolami halogenowymi, w których obecność dwóch grup hydroksylowych oraz atomu halogenu może prowadzić do jeszcze bardziej zróżnicowanych mechanizmów asocjacji i reorganizacji supramolekularnej.

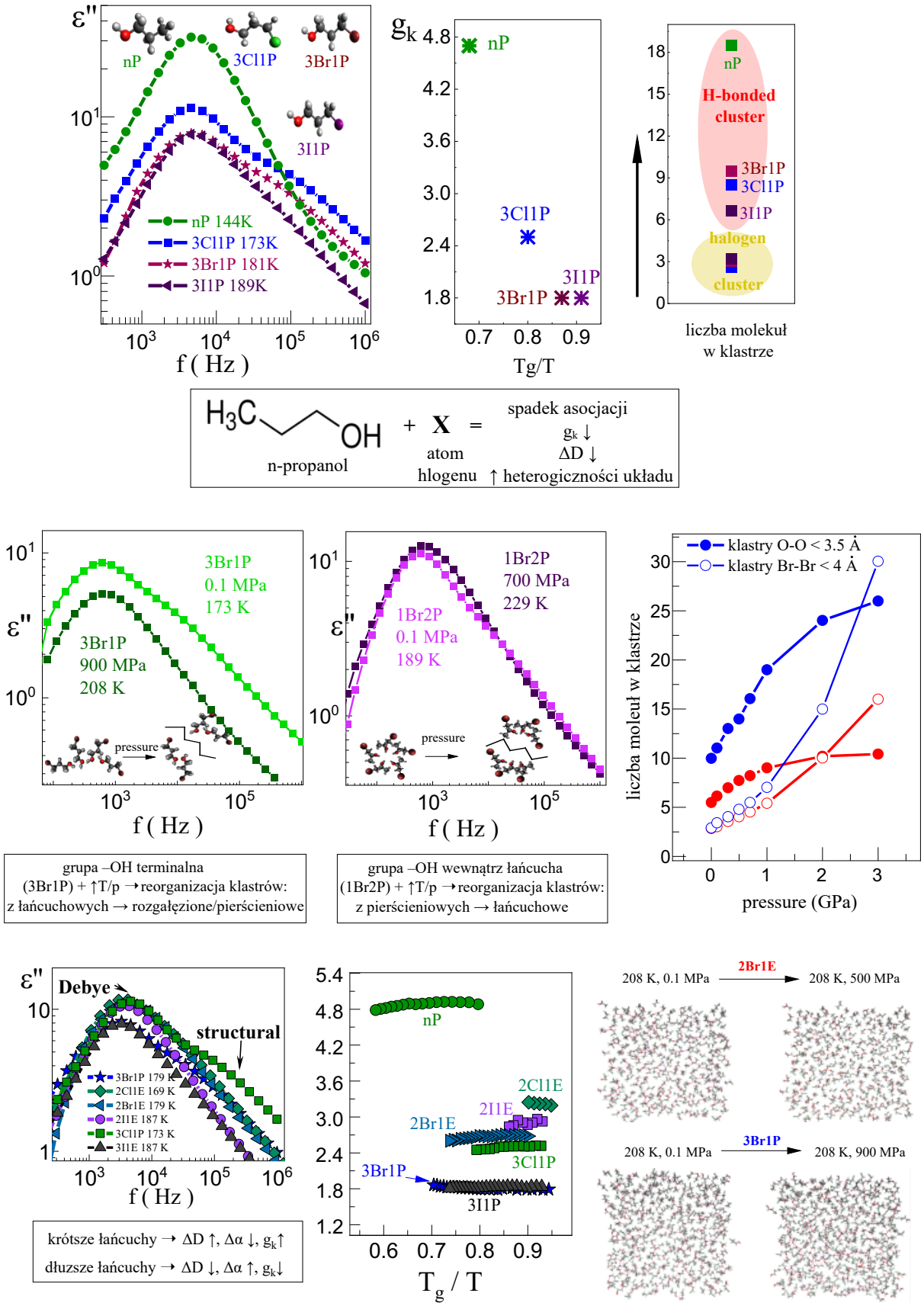

Rysunek 11. Grafika podsumowująca wyniki pracy, na podstawie danych i ilustracji z publikacji [P1 – P3].

10. Publikacje naukowe

10.1 [P1] Experimental and computational approach to studying supramolecular structures in propanol and its halogen derivatives

K. Łucak, A.Z. Szeremeta, R. Wrzalik, J. Grelska, K. Jurkiewicz, N. Soszka, B. Hachuła, D. Kramarczyk, K. Grzybowska, B. Yao, K. Kamiński, S. Pawlus. *The Journal of Physical Chemistry B*, *127*(42), 9102–9110, (2023). DOI: 10.1021/acs.jpcb.3c02092

Punkty MNiSW (2024): 140
Impact Factor (2023): 2.8

Mój wkład w publikację polegał na wykonaniu pomiarów dielektrycznych, uczestniczeniu w pomiarach kalorymetrycznych, analizie wyników i ich dyskusji oraz przygotowaniu artykułu.

THE JOURNAL OF PHYSICAL CHEMISTRY B
A JOURNAL OF THE AMERICAN CHEMICAL SOCIETY

pubs.acs.org/JPCB
Article

Experimental and Computational Approach to Studying Supramolecular Structures in Propanol and Its Halogen Derivatives

Kinga Łucak,* Anna Z. Szeremeta, Roman Wrzalik, Joanna Grelska, Karolina Jurkiewicz, Natalia Soszka, Barbara Hachuła, Daniel Kramarczyk, Katarzyna Grzybowska, Beibei Yao, Kamil Kamiński, and Sebastian Pawlus

Cite This: J. Phys. Chem. B 2023, 127, 9102−9110

Read Online

ACCESS | Metrics & More | Article Recommendations | Supporting Information

ABSTRACT: A series of four alcohols, *n*-propanol and its halogen (Cl, Br, and I) derivatives, were selected to study the effects of variation in polarity and halogen-driven interactions on the hydrogen bonding pattern and supramolecular structure by means of experimental and theoretical methods. It was demonstrated on both grounds that the average strength of H-bonds remains the same but dissociation enthalpy, the size of molecular nanoassemblies, as well as long-range correlations between dipoles vary with the molecular weight of halogen atom. Further molecular dynamics simulations indicated that it is connected to the variation in the molecular order introduced by specific halogen-based hydrogen bonds and halogen−halogen interactions. Our results also provided important experimental evidence supporting the assumption of the transient chain model on the molecular origin of the structural process in self-assembling alcohols.

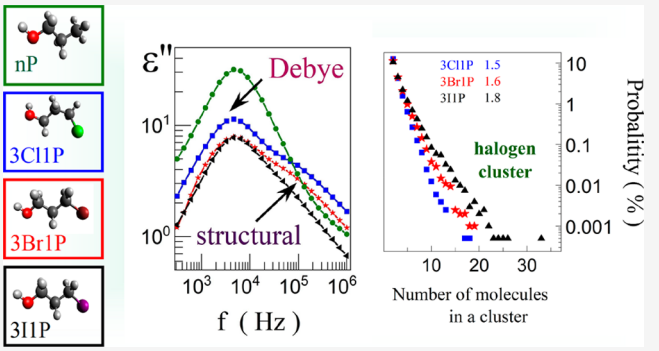

1. INTRODUCTION

Monohydroxy alcohols (MAs), due to their unique physical and chemical properties and close similarity to water, are at the center of attention to many research groups, and industry oriented on the cryogenic applications or development of new solvents.[1−3] One of their most fascinating features is an exponential response function−called Debye (D) relaxation, which is a source of hot debate. It is commonly observed in dielectric measurements of aliphatic MAs, irrespective of the position of hydroxyl units in the molecule.[4−6] According to the current knowledge, the dynamic properties of the D process for associating liquids are an emanation of their complex internal structure driven by the formation of various supramolecular clusters through hydrogen bonds (HBs). However, the exact molecular origin of this characteristic polarization decay is still yet to be addressed.[5,7−18] Herein one can briefly mention that there are several possible explanations for the nature of this process.[19−25] Among them, the transient chain model (TCM) proposed by Gainaru and co-workers[26] provides the most commonly accepted description of the molecular origin of the D relaxation. The model postulates that the D mode appears due to changes in the dipole moment associated with the attachment and detachment of molecules to the ends of the H-bonded chains.

To find a deeper connection between the dynamical properties of the D process and the architecture or size of the supramolecular associates, authors focused their attention on the investigations of the two basic classes of monohydroxy alcohols.[8,9,17,18] The first one obeys alcohols differing in the position of the OH group in the carbon skeleton or in the chain length of the backbone with a constant location of the OH group. These chemical modifications led to different patterns of association. For example, chain-like motifs of HBs are preferred in the primary alcohols where OH group is located at the end of the molecular backbone (e.g., propanol, 2-ethyl-1-hexanol),[13] while in other cases, ring-type or more branched assemblies of HBs, at the expense of chain structures, are preferred.[25] Importantly, variation in the architecture of the supramolecular clusters is reflected in the change of amplitude, relaxation time, and time scale separation from the structural process, characterizing the Debye mode.

The second category of alcohols includes molecules in which the attached functional group is devoid of the dipole moment. For example, a phenyl group added to the alkyl chain behaves as a steric hindrance, preventing the formation of effective

Received: March 29, 2023
Revised: September 28, 2023
Published: October 17, 2023

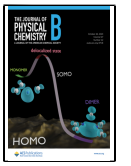

https://doi.org/10.1021/acs.jpcb.3c02092
J. Phys. Chem. B 2023, 127, 9102−9110

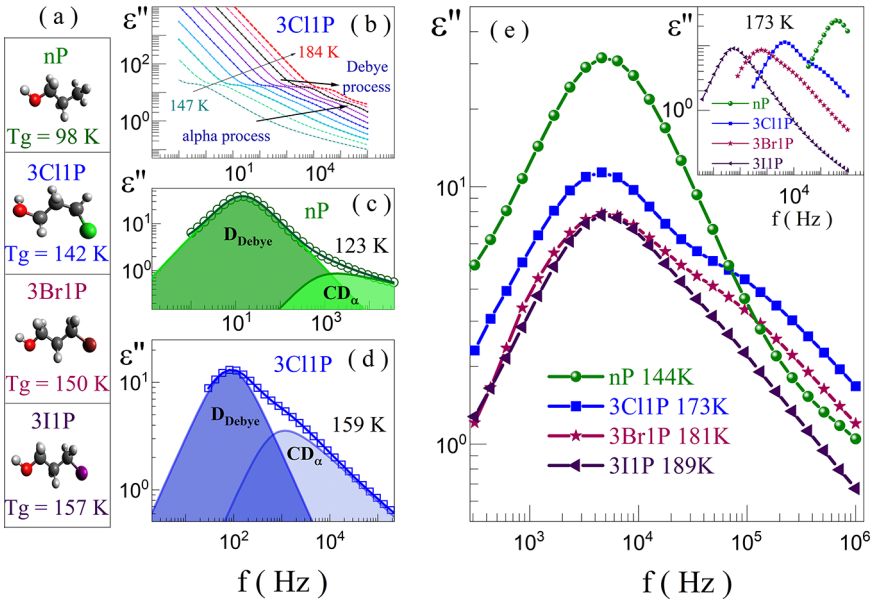

Figure 1. Molecular structure models and glass transition temperatures of the studied alcohols: nP, 3Cl1P, 3Br1P, and 3I1P (a). Dielectric loss spectra for 3Cl1P (b). Dielectric loss spectrum for: nP at 123 K (c) and 3Cl1P (d) at 159 K obtained after subtraction of dc-conductivity. In (c) and (d), the respective solid lines are the results of fitting with the use of the Debye and Cole–Davidson functions (open circles, nP; and open squares, 3Cl1P) show the experiential data. Comparison of the D process characterized by the same relaxation times for all of the studied alcohols (e). The inset shows the dielectric loss spectra after the subtraction of conductivity.

HBs. It leads to the inhibition of the self-association phenomenon and the unification of the time scales of the α- and D processes. As a consequence of that, a single relaxation process in dielectric loss spectra is detected.[27−30]

Surprisingly, much less is done on the systems where an additional dipole moment comparable to the one generated by the hydroxyl moiety is introduced into the structure. The most prominent and simplest examples of such systems are halogen derivatives of MAs, which constitute a new class of MAs. One can expect that introducing an atom of a high electronegativity to the molecule causes additional dipole–dipole halogen–halogen interactions as well as halogen-based HBs that may compete with the "classical" HBs. As a consequence, the association process may be disturbed. Therefore, it is so important to investigate the impact of additional polar units on the size and architecture of the supramolecular structures, local molecular order, driving forces leading to the structuring, etc.

Herein, we chose to study "ordinary alcohol", *n*-propanol (nP), and its halogen derivatives: 3-chloro-1-propanol (3Cl1P), 3-bromo-1-propanol (3Br1P), and 3-iodo-1-propanol (3I1P). Their structures are shown in Figure 1a. Broadband dielectric (BDS) and Fourier transform infrared (FTIR) spectroscopy, differential scanning calorimetry (DSC) supported by the molecular dynamics simulations (MDS), and density functional theory (DFT) calculations were applied to investigate the competition between the additional dipole–dipole halogen–halogen, halogen-based H-bonds, and the classical H-bonds. Consequently, we could construct a thorough picture of the impact of these interactions on the association nature of the halogen alcohols (XAs, where X indicates the halogen atom: Cl, Br, or I).

2. EXPERIMENTAL SECTION

2.1. Broadband Dielectric Spectroscopy (BDS). The dielectric studies were performed by means of a Novocontrol BDS spectrometer equipped with an Alpha Impedance Analyzer and a Quatro Cryosystem. The capacitor used for the dielectric measurements consisted of two parallel plates of 10 mm diameter made of stainless steel, distanced with two glass fibers of 100 μm thickness and sealed with a Teflon ring. The dielectric spectra were collected in the frequency range of 10^{-1}–10^{6} Hz at a quasi-static conditions, that is after stabilization of the temperature for 3 min prior to each measurements using nitrogen gas with a precision better than 0.2 K. The temperature-dependent measurements were performed with a step of ΔT = 2 K for 3Cl1P, 3Br1P, and 3I1P and nP with the step of ΔT = 3 K.

2.2. Fourier Transform Infrared Spectroscopy (FTIR). FTIR experiments were performed by using a Thermo Scientific Nicolet iS50 spectrometer. The spectra were recorded with a resolution of 4 cm^{-1} as an average of 16 scans. The frequency region covered the range of 400–4000 cm^{-1}. Low-temperature FTIR measurements (from 299 to 143 K) were carried out using a Linkam THMS 600 heating/cooling stage (Linkam Scientific Instruments Ltd., Surrey, UK). The spectra were collected every 2 K with the cooling rate of 2 K min^{-1}. The halogenated alcohols (HAs) were placed between CaF_2 windows, and the poly(ethylene terephthalate) (PET) spacers (3.5 μm thick) were used to maintain the desired thickness and constant geometry of the sample. High-temperature FTIR measurements of nP were conducted in the ATR mode using GladiATR (PIKE Technologies) in the temperature range of 300–373 K. An average of 16 scans with the resolution of 4 cm^{-1} was collected in the wavenumber range of 400–4000 cm^{-1}. A transmission solution cell with KBr windows (the path length of 1.04 mm) was used to obtain FTIR spectra of XAs solutions in benzene and cyclohexane (0.1 and 0.01 M). To perform the deconvolution of the OH stretching vibration band, MagicPlot Pro software (version 2.9.3, MagicPlot Systems LLC, Saint Petersburg, Russia) was used. The step-by-step process of the deconvolution procedure is described in Reference.[28]

https://doi.org/10.1021/acs.jpcb.3c02092
J. Phys. Chem. B 2023, 127, 9102−9110

2.3. Raman Spectroscopy. The Raman measurements for 3Cl1P and its 0.1 M solution in cyclohexane were performed using a Horiba Xplora Plus Raman spectrometer with a laser operating at 780 nm (the power 30 mW). The Olympus MPlanN 10× objective was chosen. Every spectrum was recorded with an acquisition time of 2 s and an accumulation of 60 scans.

2.4. Molecular Dynamics Simulations (MDS). Molecular dynamics simulations were carried out using the GROMACS package (version 2020).[31−33] Interactions in the systems were described using the general AMBER force field (GAFF)[34] and topology provided by AmberTool21.[35] The simulation parameters were adopted the same as in our previous paper.[10] Structure factors were calculated based on the optimized models of spatial arrangement of molecules (2000 molecules) using of the TRAVIS software.[36−38]

2.5. Density Functional Theory (DFT) Calculations. DFT calculations using the B3LYP and CAM-B3LYP functionls, combined with the basic set 6-311G(d,p), were performed in the Gaussian09 software package.[39] The second functional was used because it improves long-range interactions, which are important for determining the energy and geometry of the dimers. The single molecule's and dimer's geometries have been optimized using the opt = tight and int = very tight options. The interaction energy was estimated by using the counterpoise method to correct the base set superposition error (BSSE). Initial single molecule and hydrogen bonded dimer structures were prepared using GaussView 5.[40] The dipole moment of each molecule was decomposed into components oriented parallel and perpendicular to the straight line passing through the carbon atom (C1) bound to the hydroxyl group and the farthest atom of the chain (C3 for propanol and X = Cl, Br, or I for molecule containing halogen atoms).

2.6. Density Measurements. The density (ρ) of nP, 3Cl1P, and 3Br1P was determined using a vibrating-tube densimeter DMA 4500 M (Anton Paar, Austria). The apparatus was calibrated directly before measurements with dry air and bidistilled water. The water was always freshly degassed (by boiling) before using its electrolytic conductivity was 1×10^{-12} S·cm^{-1} at T = 298.15 K. Importantly, viscosity-related errors were automatically corrected in full range, which was checked using the oil N100 at 293.15 and 323.15 K. Standard uncertainties of ρ and T are $u(\rho) = 0.002 \cdot \rho$ and u(T) = 0.01 K, respectively. It was taken into account that the directional coefficients of the linear functions for 3Cl1P and 3Br1P are similar, and an analogous nature of the density change for 3I1P was assumed. The estimated density for 3I1P was obtained.

2.7. Refractometry. The refractive index (RI) measurements of the examined liquids were carried out using the Mettler Toledo refractometer RM40 in the temperature range from 303.15 to 353.15 K. The temperature stability controlled with the aid of a built-in Peltier thermostat was better than 0.1 K. The light source is a light-emitting diode (LED), the beam of which passes through a polarization filter, an interference filter (589.3 nm), and various lenses before it reaches the sample via the sapphire prism characterized by a high thermal conductivity. The measurements of RI were performed with a resolution of 0.0001.

2.8. Differential Scanning Calorimetry (DSC). The studied alcohols: 3Cl1P, 3Br1P, and 3I1P were measured calorimetrically with the use of a Mettler-Toledo DSC apparatus equipped with an HSS8 ceramic sensor (heat flux sensor with 120 thermocouples) and a liquid nitrogen-cooling accessory. The temperature-dependent measurements were conducted on the samples previously poured into a sealed aluminum pan of 40 μL volume. The thermograms were collected on cooling and heating in the temperature range of 123−298 K. The cooling and heating rates were 10 K min^{-1}, respectively. The calorimetric measurements were carried out in the atmosphere of nitrogen with a flow of 60 mL min^{-1}. Glass transition temperature of each compound was determined from the heating scans as the midpoint of the glass transition step.

3. RESULTS AND DISCUSSION

As a first step, we performed dielectric measurements in a wide range of temperatures to check whether the D relaxation exists in the halogen derivatives and to what extent its properties are similar to what we observed in *n*-propanol. Representative loss spectra $\varepsilon''(f)$ of nP obtained at selected temperatures above the glass transition temperature (T_g), revealed the presence of two relaxation processes (Figure S1). The dominant D mode and α relaxation (detected as an excess wing on the high frequency (f) flank of the D process) of smaller amplitudes can be distinguished. The secondary relaxation (β) also occurs in nP,[11] but is not described in this publication. In the case of halogen derivatives of nP, the dielectric loss spectra are more affected by the contribution of the direct current (dc) conductivity (σ), which partially covers the dominating D process. Stronger conductivity contributions in the spectra in halogen derivatives of nP can be explained by more ionic impurities that could originate during the obtaining processes of alcohol. This effect is well illustrated in the dielectric loss spectra of 3Cl1P; please see Figure 1b. In order to better visualize the maxima of the detected relaxation processes, we subtracted a conductivity contribution from the raw data. Figures 1c,d show a comparison of $\varepsilon''(f)$ for nP and 3Cl1P, measured at selected temperatures after subtraction of the conductivity, together with the fits utilizing the Debye and Cole−Davidson functions. One can see that for 3Cl1P, the α relaxation process becomes more prominent with respect to nP.

To illustrate this effect, we compared the loss spectra characterized by the same peak frequency of the D relaxation (Figure 1e). This enabled us to demonstrate that the amplitude of the D process decreases, whereas the intensity of the structural relaxation increases in the case of XAs compared to that of nP. Moreover, as the atomic mass of the electronegative X atom decreases, the structural relaxation intensity increases. To parametrize the difference between alcohols we compare the ratios of ε''_{max}. Debye/ε''_{max}. structural and received: nP (19.65), 3Cl1P (1.57), 3Br1P (1.87), and 3I1P (2.89). The work of Gainaru and co-workers[26] has shown that the structural relaxation in alcohols comes from the movements of the alkyl chains. In the case of halogen alcohols, the dipole moment of the chain is larger; this is due to the presence of halogen atoms. Thus, the apparent amplitude of structural relaxation is larger. Hence, the addition of the moiety characterized by varying polarity to the nonpolar part of the molecule should lead to a change in the amplitude of the primary relaxation. In fact, this is what we observed in our experiment. Thus, these experimental data can be treated as additional evidence supporting the TCM and the molecular origin of the D process in the self-assembled clusters.

https://doi.org/10.1021/acs.jpcb.3c02092
J. Phys. Chem. B 2023, 127, 9102−9110

In addition, we detected a change in the glass transition temperature (T_g) as well as in the position of the D process in the studied herein systems (see details in the Supporting Information). These findings can be well visualized by comparison of the dielectric spectra measured at similar temperatures in one chart (inset in Figure 1e). From this figure, one can find that all recorded variations scale up with the size of the X atom. Therefore, the 3I1P with the largest mass shows the greatest shift toward the low frequencies of the D process and the highest T_g.

The variations described above in the T_g and amplitude of the Debye process indicate that the presence of X atoms influences the self-association process in the measured samples. To verify this hypothesis, we decided to calculate the Kirkwood–Fröhlich factor (g_k), which is a useful parameter allowing us to get an insight into the long-range correlation between dipoles induced by the self-association process.[41,42] For the computation of g_k, the following equation was used:

$$g_k = \frac{9k_B\varepsilon_0 MT(\varepsilon_s - \varepsilon_\infty)(2\varepsilon_s + \varepsilon_\infty)}{\rho N_A \mu^2 \varepsilon_s} \quad (1)$$

where ε_s and ε_∞ are the static and high-frequency permittivity, respectively; N_A is Avogadro's number; ρ is the density of the liquid at temperature T; μ_0 is the dipole moment of the isolated molecule; ε_0 is the absolute permittivity of vacuum; M is the molecular weight; and k_B is Boltzmann's constant.[41] As observed in Figure 2a, the determined values of g_k are much

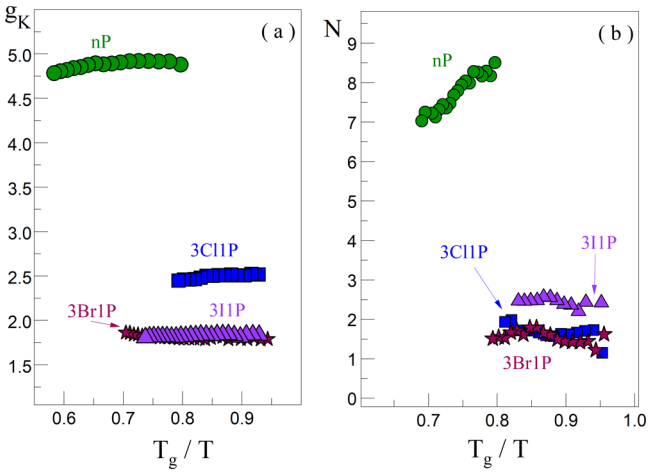

Figure 2. Kirkwood–Fröhlich factor for the studied alcohols (a). The number of molecules creating the transient chains is the source of the Debye relaxation process according to the transient-chain model (b).

higher than 1 for all studied samples, suggesting that rather chain-like structures are formed, irrespective of the sample. In the vicinity of 169 K, the highest g_k coefficient is obtained for nP ($g_k \approx 4.7$), the next for 3Cl1P ($g_k \approx 2.5$), and the lowest one ($g_k \approx 1.8$) is for 3Br1P and 3I1P. Therefore, similar to the change in the T_g or in amplitude of the Debye process, the variation in the g_k scales up with the molecular weight and polarity of the halogen atom. Nevertheless, it should be noted that the highest g_k determined for nP suggests the most prominent long distance correlations between dipoles in this alcohol.[43]

Having in mind the above discussion, we further estimated the average number of molecules involved in the formation of the transient chains (N) based on the formula proposed by Gainaru and co-workers[26] (see details in the Supporting Information). In Figure 2b, N as a function of T was presented. As can be seen, the largest transient chains are formed by nP (N = 7–8 molecules). On the contrary, XAs show lower numbers of the molecules involved in the formation of the H-bonded clusters: 2–3 molecules for 3I1P and 1–2 molecules for 3Br1P as well as for 3Cl1P. Thus, it should be noticed that, according to the TCM, the longest H-bonded oligomers among XAs are created in the alcohol bearing the heaviest X atom in its structure. It is a nonintuitive finding since one could expect that the largest X atom introduces the most serious hindrance preventing clustering. What is even more surprising is that the change in N is at odds with the variation of g_k in halogen derivatives of nP. These unexpected results of the dielectric investigations forced us to perform additional FTIR studies supported by MD simulations to address the observed peculiarities.

The temperature-dependent FTIR spectra obtained for all examined systems are presented in Figure S5. The representative spectra at room temperature around 299 K and at T_g, in the spectral range of 3750–3000 cm^{-1}, are shown in Figure 3a,b. The FTIR spectra at room temperature show two characteristic bands: at ~3330 cm^{-1} and ~3560 cm^{-1}, which are assigned to the stretching vibrations of H-bonded (ν_{OH}^{HB}) and non-H-bonded (free) hydroxyl groups (ν_{OH}^{free}), respectively. The band at 3560 cm^{-1} is absent in the spectrum of nP at room temperature and T_g (compare with Figure 3a,b), indicating its complete association by HBs. On the other hand, 3I1P is characterized by the highest intensity of the ν_{OH}^{free} band, while 3Cl1P is characterized by the lowest one, at 299 K. This fact can be connected with the atomic radius of halogens, i.e., as the size of the X atom (the steric hindrance) increases, the degree of association of XAs via O–H···O bonds decreases. Additionally, the percentage of non-hydrogen-bonded hydroxyl groups in 3Cl1P, 3Br1P, and 3I1P at room temperature, calculated from the analyzed spectra, is equal to 2.15%, 2.36%, and 3.13%, respectively. The presence of ν_{OH}^{free} band was also confirmed through FTIR measurements of the studied alcohols in nonpolar solvents, i.e., cyclohexane and benzene (see Figure S6). As shown in Figure S6, the type of solvent influences the self-assembly process of propanols under investigation, i.e., the different ν_{OH}^{free} band position and intensity ratio of the ν_{OH}^{free} and ν_{OH}^{HB} bands for the same alcohol concentration. Moreover, based on Figure 3c, one can also see that the analyzed alcohols do not differ significantly in the position of the ν_{OH}^{HB} band, which indicates a similar strength of formed HBs at room temperature. During cooling, the red shift of the ν_{OH}^{HB} band occurs, demonstrating the strengthening of H-bonding interactions between XA molecules. The ν_{OH}^{HB} bandwidth (full width at half-maximum, fwhm) reduces when temperature decreases (Figure 3d). Such an effect suggests the formation of a more homogeneous network of HBs at lower temperatures. These temperature-induced spectral variations of the ν_{OH}^{HB} bands are similar to those observed for the other Mas.[44] Interestingly, the ν_{OH}^{HB} bandwidth increases with the increasing weight of the alcohol molecule at both room temperature and T_g (Table S3). Thus, one can state that the increasing steric hindrance due to change in the size of X atom (Cl, Br, and I) in alcohol molecules causes a more heterogeneous distribution of the HBs' strength. Alternatively this effect can be a manifestation of the halogen based H bonding in the derivatives of nP. To address this hypothesis, we also performed Raman measurements for 3Cl1P and its 0.1 M

https://doi.org/10.1021/acs.jpcb.3c02092
J. Phys. Chem. B 2023, 127, 9102–9110

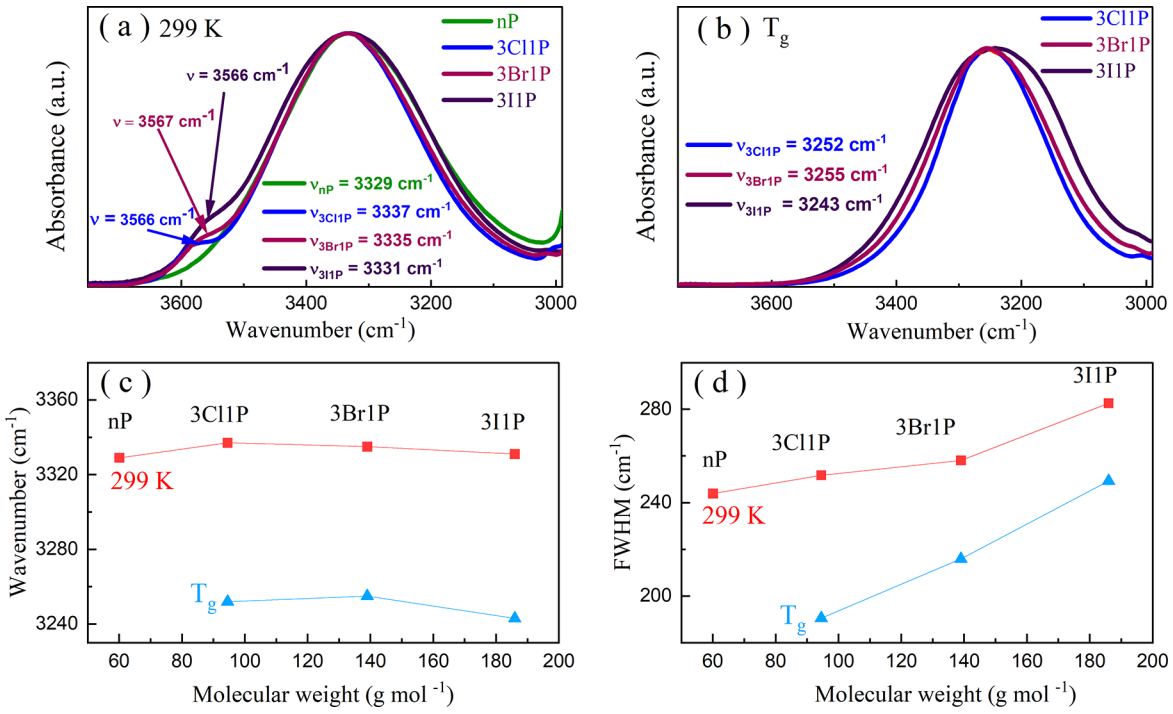

Figure 3. FTIR spectra of alcohols in the frequency range of 3750−3000 cm^{-1} measured at (a) 299 K and (b) glass-transition temperature ($T_{g\text{-}3Cl1P}$ = 142 K, $T_{g\text{-}3Br1P}$ = 150 K, and $T_{g\text{-}3I1P}$ = 157 K). The spectra were normalized to the maximum intensity of the OH stretching vibration band. (c) and (d) Frequency and full width at half-maximum (fwhm) dependencies of the OH stretching vibration band as a function of the molecular weight of XAs, respectively.

solution in cyclohexane and compared them with the IR results (Figure S7). It should be noted that according to DFT calculations, the peak originating from the stretching vibration of free C−Cl group in cyclohexane occurs at 698 cm^{-1}, while the one from the H-bonded C−Cl group in the dimer is located at 682 cm^{-1}. As can be seen in Figure S7, the peak of the C−Cl stretching vibration in diluted 3Cl1P is observed at 662 cm^{-1} (IR) and 661 cm^{-1} (Raman), whereas in bulk, the band's position occurs at 656 cm^{-1} (both for IR and Raman spectra). Thus, the weak shift in these band positions ($\Delta\nu$(IR) = 6 cm^{-1}, $\Delta\nu$(Raman) = 5 cm^{-1} observed for the spectra of bulk and diluted 3Cl1P may indicate that the Cl atoms participate in different intermolecular interactions including halogen−halogen and halogen based H bonds. However, due to their weak strength, the change in C−Cl stretching vibration is very small.

Further, the activation enthalpy (E_a) of the dissociation process of alcohols was calculated based on the van 't Hoff equation, according to the procedure described in our previous paper (see Figure S8).[28,45] The E_a values demonstrate a significant drop for XAs (from 15.2 kJ·mol^{-1} for 3Cl1P to 7 kJ·mol^{-1} for 3I1P) compared to that for nP (33.8 kJ·mol^{-1}). This can be simply explained having in mind that the presence of the X atom prevents the alcohol molecules from linking into larger aggregates by HBs, as deduced from dielectric investigations. As a consequence of that, the effect of cooperativity of these specific interactions gets weaker. Alternatively, one can also suppose that halogen based hydrogen bonds (manifested as growing ν_{OH}^{HB} bandwidth and weak shift in ν_{Cl}) appear in the studied derivatives of nP. Nevertheless, to confirm this hypothesis and gain a much deeper insight into the structure of the studied herein alcohols, further molecular dynamics simulations were performed.

MDS provided a more illustrative description of the supramolecular associates in the investigated compounds. The structural model of each alcohol was optimized based on the system of 2000 molecules at room temperature using a general AMBER force field (GAFF) in the Gromacs package. The model-based structure factors, which give information about the atom−atom spatial correlations, are depicted in Figure 4a. The data are shown in the range of up to 3.0 $Å^{-1}$

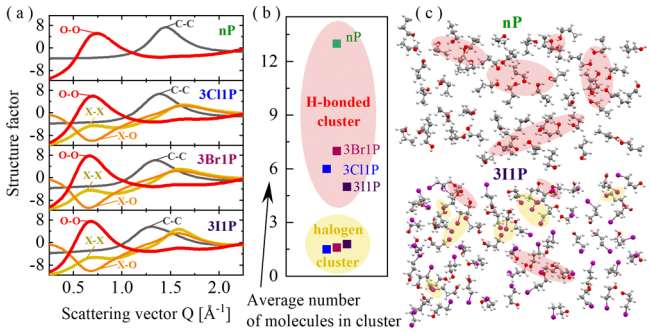

Figure 4. Results obtained from molecular dynamics simulations: partial structure factors (a), the average number of molecules in H-bonded and halogen clusters (b), and 2D fragments of the structural models for nP and 3I1P demonstrating the clusters of OH groups and halogen atoms (marked in red and yellow, respectively) (c).

where the intermolecular interactions play the major role. Only selected partial structure factors are presented for clarity—those having the biggest contribution to the intermolecular correlations (C−C, O−O, and X−X). All partial functions can be seen in Figure S11a. The sum of all partial functions, where C, O, H, and X refer to carbon, oxygen, hydrogen, and halogen elements, respectively, after multiplication by

https://doi.org/10.1021/acs.jpcb.3c02092
J. Phys. Chem. B 2023, 127, 9102−9110

respective atomic form factors and weight fractions, is called the total structure factor $S(Q)$. For nP and 3Cl1P, the total $S(Q)$ was also derived experimentally from the X-ray scattering data ($S(Q)$ for 3Br1P and 3I1P was not possible to determine using the laboratory diffractometer due to high absorption and fluorescence). The experimental and model-based $S(Q)$ values for nP and 3Cl1P show good agreement (see Figure S12), validating the accuracy of the performed simulations and analyzed models.

The main $S(Q)$ peak at scattering vector Q around 1.3−2.0 $Å^{-1}$ arises due to nearest-neighbor spatial correlations between molecules, and the principal contribution to this peak is given by C−C correlations of alkyl tails. Whereas the organization of molecules in bigger associates, which constitute the microstructure of the liquids, yields peaks at Q-values below 1 $Å^{-1}$. The main contribution to this organization for nP and all XAs is given by the O−O correlation at around 0.7 $Å^{-1}$ (Figure 4a). This peak is an evidence for the creation of supramolecular clusters where molecules are organized through OH groups. The O−O distribution function (shown in Figure S11b) induces a large first peak with a maximum at around 2.8 Å, extending up to around 3.5 Å, which is a direct consequence of the structuring of O atoms in O−H···O bonds. Moreover, the pair distribution functions for XAs reveal that there are X-ray-induced O−X distances starting from around 3.0 Å and X−X distances with a clear maximum at around 3.5−4.0 Å (the bigger the halogen atom, the greater the X−X distance). The O−X and X−X oscillations extend up to around 15−20 Å (shown in Figure S11c), which indicates the creation of the medium-range order by these groups. As a consequence of that, X−X correlations also give a maximum in the $S(Q)$ at around 0.7 $Å^{-1}$ (Figure 4a) and suggest that halogen atoms of neighboring molecules may also group into small aggregates; these are called here as "halogen clusters". In turn, the O−X correlations give minima (antipeaks) in the $S(Q)$ at around 0.7 $Å^{-1}$ and indicate that X atoms at one end of the molecular tail are anticorrelated with OH groups at the second end; there is a segregation between these atomic groups. More information on the origin of the $S(Q)$ in alcohols may be found here.[46,47]

Taking into account the structural correlations between atoms and their distances, we distinguished two types of clusters formed in the studied systems: "H-bonded clusters" including the O−O and O−X correlations or "halogen clusters" including the X−X correlations. For both cluster types, we calculated the average number of molecules involved in the aggregates, assuming only a simple condition that a molecule forms a cluster with another one when the distance between the specific atoms is smaller than the cutoff distance of the appropriate radial distribution function: O−O and O−X $\leq$ 3.5 Å for the H-bonded clusters and Cl−Cl $\leq$ 3.8 Å, Br−Br $\leq$ 4 Å, and I−I $\leq$ 4.3 Å for the halogen clusters. The histograms of the cluster sizes are presented in Figure S13a, whereas the average numbers of molecules in such defined clusters are presented in Figure 4b and show that the biggest H-bonded clusters are formed in nP (∼13 molecules). In turn, much smaller nanoassociates connected by HBs exist in halogen compounds (5−7 molecules on average). It is also worth to mention that the derived histograms and the average number of molecules in the H-bonded clusters for nP are very similar to data estimated by other researchers from various computer simulations for nP as well as other simple linear MAs such as *n*-ethanol and *n*-butanol, at room temperature.[46,48−50] However, it should be added that they strongly depend on, e.g., the force field choice and the cluster definition. Here, we used a very broad definition with only distance constraints, so the values of the number of molecules in what we call "clusters" may be overestimated, with respect to the ones obtained from the extrapolation data presented in Figure 2b. Hence, the observed strong discrepancies may be due to a much narrower definition for the transient-chain clusters and assumptions of the model used. Moreover, the data derived from MDS provided systems with a slightly too high structural order compared to experimental data, which may also affect the overestimation of the cluster sizes.

The general organization of molecules in the MD models and the clusters of OH groups are marked on the representative fragments of models for nP and 3I1P in Figure 4c. Moreover, we were able to identify on the models the clusters of halogen atoms. Such aggregates are rather small (dimeric, trimeric) and the average number of molecules associated with such clusters increases with the bigger mass of the halogen atom (1.5 for Cl, 1.6 for Br, and 1.8 for I). The subtle balance between the conventional hydrogen bonding between OH groups and other interactions involving the halogen atoms in the studied relatively simple molecular systems appears to drive very complex heterogeneous microstructure. It is also important to note that we found great agreement of the MDS with the outcomes of the spectroscopic studies exhibiting the lower degree of association of molecules via O−H···O bonds in XAs compared to ordinary nP. The percent of non-H-bonded molecules, determined from the histograms of the cluster sizes derived from MDS, is 1.8% for nP and 3.6, 4.3, 6.4% for 3Cl1P, 3Br1P, and 3I1P, respectively. Thus, it is also in accordance with the FTIR results: The fraction of free molecules increases in the same manner as the intensity of the ν_{OH}^{free} band in IR spectra. One more property of these systems derived from MDS that is consistent with the IR outcomes is a very similar distribution of the O−O lengths in HBs, with the maximum located at around 2.8 Å for all alcohols at room temperature (shown in Figure S13b), suggesting a similar strength of HBs in nP and XAs, despite attaching the halogen atom.

Since experimental and MDS data discussed above indicated that there are different specific interactions including halogen−halogen, halogen-based, and classical H-bonds in the studies systems, additional DFT calculations were applied to evaluate the energy of such interacting systems. Based on the analysis of the geometry of different dimers that were considered, we can conclude that strong hydrogen interactions of the O−H···O type (interaction energy $E \geq 5$ kcal/mol) predominate in the studied alcohols. H−O···X interactions are weaker, but still possible ($E < 4$ kcal/mol), whereas the X···X forces between halogen atoms seem to be the weakest ($E < 2$ kcal/mol). A detailed analysis of the dimeric structures and their interaction energies based on the DFT calculations is included in the Supporting Information. It is worth mentioning that DFT models yield very similar O−O distances in HBs for all studied alcohols (2.9 Å, see Figure S6) to those obtained from MDS (2.8 Å). Also, the O−X and X−X distances are consistent in both theoretical methods, DFT, and MDS, which authenticates the analyzed models of the halogen alcohols.

4. SUMMARY

Summarizing the data discussed in this letter, one can deduce that strongly electronegative halogen atoms: Cl, Br, and I have a significant impact on the molecular association processes.

https://doi.org/10.1021/acs.jpcb.3c02092
J. Phys. Chem. B 2023, 127, 9102−9110

Our studies have shown that molecules in *n*-propanol and its halogen derivatives tend to form clusters via hydrogen bonds during the vitrification process, and the architecture of the HBs in such clusters is rather chain-like. The introduction of halogen atoms into the alkyl chain significantly inhibits the association of molecules by HBs, which is revealed by the greater amount of nonassociated molecules and smaller size of the H-bonded clusters in halogen derivatives compared to pure *n*-propanol. Moreover, based on experimental spectroscopic studies and theoretical calculations we found some strong indications that other types of small molecular associates can be formed due to O−H···X or X···X interactions, where X indicates the halogen atom. They compete with the O−H···O forces and introduce local disorder and heterogeneity into the supramolecular structure. Therefore, these two important findings can be used to explain why the change in the Kirkwood−Frölich factor with respect to the number of molecules in the transient chain model can be an explanation. It is also worth to stress that very weak O−H···X or X···X interactions to contribute to the enormous drop of the dissociation enthalpy of HBs in the investigated halogen derivatives of *n*-propanol, despite of the fact that the position of the stretching vibration of OH group as well as the length of H-bonds remain unaffected by the structure of the molecule differing in the presence and type of the halogen atom. Finally, our data also provide experimental evidence of the molecular origin of the D relaxation process in self-assembling alcohols. Here, we show the relationship between the association of the tested alcohols into chain systems (first degree of association) and, for example, the Kirkwood coefficient and Debye relaxation amplitude. According to them, the largest g_k and Debye process is, in the case of the most associative alcohol, that is, nP. On the other hand, the presence of halogen atoms and the formation of other supramolecular structures (other than those formed through OH−O bonds, among other things) caused by them is the reason for the lower intensity of Debye relaxation in halogen alcohols. We are convinced that the obtained results will contribute to a much better understanding of the self-assembly process in highly viscous systems.

■ ASSOCIATED CONTENT

Supporting Information

The Supporting Information is available free of charge at https://pubs.acs.org/doi/10.1021/acs.jpcb.3c02092.

Details of fitting dielectric spectra with use of Havriliak−Negami functions, calculations of average cluster size of alcohol aggregates, temperature-dependent FTIR spectra and analysis of the studied alcohols, details of the molecular dynamics simulations, dimer interaction energy calculations (PDF)

■ AUTHOR INFORMATION

Corresponding Author

Kinga Łucak − *Institute of Physics, Faculty of Science and Technology, University of Silesia in Katowice, 41-500 Chorzów, Poland;* orcid.org/0000-0001-5510-1157; Email: kinga.lucak@us.edu.pl

Authors

Anna Z. Szeremeta − *Institute of Physics, Faculty of Science and Technology, University of Silesia in Katowice, 41-500 Chorzów, Poland;* orcid.org/0000-0002-6105-4075

Roman Wrzalik − *Institute of Physics, Faculty of Science and Technology, University of Silesia in Katowice, 41-500 Chorzów, Poland*

Joanna Grelska − *Institute of Physics, Faculty of Science and Technology, University of Silesia in Katowice, 41-500 Chorzów, Poland;* orcid.org/0000-0002-7001-4083

Karolina Jurkiewicz − *Institute of Physics, Faculty of Science and Technology, University of Silesia in Katowice, 41-500 Chorzów, Poland;* orcid.org/0000-0002-4289-7827

Natalia Soszka − *Institute of Chemistry, Faculty of Science and Technology, University of Silesia in Katowice, 40-006 Katowice, Poland;* orcid.org/0000-0001-7774-7450

Barbara Hachuła − *Institute of Chemistry, Faculty of Science and Technology, University of Silesia in Katowice, 40-006 Katowice, Poland;* orcid.org/0000-0001-9886-1076

Daniel Kramarczyk − *Institute of Physics, Faculty of Science and Technology, University of Silesia in Katowice, 41-500 Chorzów, Poland;* orcid.org/0000-0003-0783-0122

Katarzyna Grzybowska − *Institute of Physics, Faculty of Science and Technology, University of Silesia in Katowice, 41-500 Chorzów, Poland;* orcid.org/0000-0002-0691-3631

Beibei Yao − *Institute of Physics, Faculty of Science and Technology, University of Silesia in Katowice, 41-500 Chorzów, Poland;* orcid.org/0000-0002-3411-3105

Kamil Kamiński − *Institute of Physics, Faculty of Science and Technology, University of Silesia in Katowice, 41-500 Chorzów, Poland;* orcid.org/0000-0002-5871-0203

Sebastian Pawlus − *Institute of Physics, Faculty of Science and Technology, University of Silesia in Katowice, 41-500 Chorzów, Poland;* orcid.org/0000-0001-9209-4056

Complete contact information is available at: https://pubs.acs.org/10.1021/acs.jpcb.3c02092

Notes

The authors declare no competing financial interest.

■ ACKNOWLEDGMENTS

The authors are grateful for the financial support provided by the National Science Centre within the framework of the OPUS project (dec. no. 2019/35/B/ST3/02670). This research was supported in part by PL-Grid Infrastructure.

■ REFERENCES

(1) Barthel, J.; Bachhuber, K.; Buchner, R.; Hetzenauer, H. Dielectric Spectra of Some Common Solvents in the Microwave Region. Water and Lower Alcohols. *Chem. Phys. Lett.* **1990**, *165* (4), 369−373.

(2) Mashimo, S.; Umehara, T.; Redlin, H. Structures of Water and Primary Alcohol Studied by Microwave Dielectric Analyses. *J. Chem. Phys.* **1991**, *95* (9), 6257−6260.

(3) Desiraju, G.; Steiner, T. Introduction. In *The Weak Hydrogen Bond*; Oxford University Press, 2001; pp 1−28.

(4) Hassion, F. X.; Cole, R. H. Dielectric Properties of Liquid Ethanol and 2-Propanol. *J. Chem. Phys.* **1955**, *23* (10), 1756−1761.

(5) Hansen, C.; Stickel, F.; Berger, T.; Richert, R.; Fischer, E. W. Dynamics of Glass-Forming Liquids. III. Comparing the Dielectric α- and β-Relaxation of 1-Propanol and o-Terphenyl. *J. Chem. Phys.* **1997**, *107* (4), 1086−1093.

(6) Böhmer, R.; Gainaru, C.; Richert, R. Structure and Dynamics of Monohydroxy Alcohols—Milestones towards Their Microscopic

Understanding, 100 Years after Debye. *Phys. Rep.* **2014**, *545* (4), 125−195.
(7) Bauer, S.; Burlafinger, K.; Gainaru, C.; Lunkenheimer, P.; Hiller, W.; Loidl, A.; Böhmer, R. Debye Relaxation and 250 K Anomaly in Glass Forming Monohydroxy Alcohols. *J. Chem. Phys.* **2013**, *138* (9), 094505.
(8) Soszka, N.; Hachuła, B.; Tarnacka, M.; Kaminska, E.; Pawlus, S.; Kaminski, K.; Paluch, M. Is a Dissociation Process Underlying the Molecular Origin of the Debye Process in Monohydroxy Alcohols? *J. Phys. Chem. B* **2021**, *125* (11), 2960−2967.
(9) Bolle, J.; Bierwirth, S. P.; Požar, M.; Perera, A.; Paulus, M.; Münzner, P.; Albers, C.; Dogan, S.; Elbers, M.; Sakrowski, R.; et al. Isomeric Effects in Structure Formation and Dielectric Dynamics of Different Octanols. *Phys. Chem. Chem. Phys.* **2021**, *23* (42), 24211−24221.
(10) Grelska, J.; Jurkiewicz, K.; Burian, A.; Pawlus, S. Supramolecular Structure of Phenyl Derivatives of Butanol Isomers. *J. Phys. Chem. B* **2022**, *126* (19), 3563−3571.
(11) Ngai, K. L.; Wang, L. Relations between the Structural α-Relaxation and the Johari−Goldstein β-Relaxation in Two Monohydroxyl Alcohols: 1-Propanol and 5-Methyl-2-hexanol. *J. Phys. Chem. B* **2019**, *123* (3), 714−719.
(12) Ngai, K. L.; Pawlus, S.; Paluch, M. Explanation of the Difference in Temperature and Pressure Dependences of the Debye Relaxation and the Structural α-Relaxation near T of Monohydroxy Alcohols. *Chem. Phys.* **2020**, *530*, 110617.
(13) Wikarek, M.; Pawlus, S.; Tripathy, S. N.; Szulc, A.; Paluch, M. How Different Molecular Architectures Influence the Dynamics of H-Bonded Structures in Glass-Forming Monohydroxy Alcohols. *J. Phys. Chem. B* **2016**, *120* (25), 5744−5752.
(14) Gainaru, C.; Wikarek, M.; Pawlus, S.; Paluch, M.; Figuli, R.; Wilhelm, M.; Hecksher, T.; Jakobsen, B.; Dyre, J. C.; Böhmer, R. Oscillatory Shear and High-Pressure Dielectric Study of 5-Methyl-3-Heptanol. *Colloid Polym. Sci.* **2014**, *292* (8), 1913−1921.
(15) Gainaru, C.; Figuli, R.; Hecksher, T.; Jakobsen, B.; Dyre, J. C.; Wilhelm, M.; Böhmer, R. Shear-Modulus Investigations of Monohydroxy Alcohols: Evidence for a Short-Chain-Polymer Rheological Response. *Phys. Rev. Lett.* **2014**, *112* (9), 098301.
(16) Hecksher, T.; Jakobsen, B. Communication: Supramolecular Structures in Monohydroxy Alcohols: Insights from Shear-Mechanical Studies of a Systematic Series of Octanol Structural Isomers. *J. Chem. Phys.* **2014**, *141* (10), 101104.
(17) Gainaru, C.; Kastner, S.; Mayr, F.; Lunkenheimer, P.; Schildmann, S.; Weber, H. J.; Hiller, W.; Loidl, A.; Böhmer, R. Hydrogen-Bond Equilibria and Lifetimes in a Monohydroxy Alcohol. *Phys. Rev. Lett.* **2011**, *107* (11), 118304.
(18) Schildmann, S.; Reiser, A.; Gainaru, R.; Gainaru, C.; Böhmer, R. Nuclear Magnetic Resonance and Dielectric Noise Study of Spectral Densities and Correlation Functions in the Glass Forming Monoalcohol 2-Ethyl-1-Hexanol. *J. Chem. Phys.* **2011**, *135* (17), 174511.
(19) Wang, L.-M.; Richert, R. Dynamics of Glass-Forming Liquids. IX. Structural versus Dielectric Relaxation in Monohydroxy Alcohols. *J. Chem. Phys.* **2004**, *121* (22), 11170.
(20) Brot, C.; Magat, M. Comment on "Dispersion at Millimeter Wavelengths in Methyl and Ethyl Alcohols". *J. Chem. Phys.* **1963**, *39* (3), 841−842.
(21) Kalinovskaya, O. E.; Vij, J. K. The Exponential Dielectric Relaxation Dynamics in a Secondary Alcohol's Supercooled Liquid and Glassy States. *J. Chem. Phys.* **2000**, *112* (7), 3262−3266.
(22) Levin, V. V.; Feldman, Y. D. Dipole Relaxation in Normal Aliphatic Alcohols. *Chem. Phys. Lett.* **1982**, *87* (2), 162−164.
(23) Déjardin, P.-M.; Titov, S. V.; Cornaton, Y. Linear Complex Susceptibility of Long-Range Interacting Dipoles with Thermal Agitation and Weak External Ac Fields. *Phys. Rev. B* **2019**, *99* (2), 024304.
(24) Jurkiewicz, K.; Kołodziej, S.; Hachuła, B.; Grzybowska, K.; Musiał, M.; Grelska, J.; Bielas, R.; Talik, A.; Pawlus, S.; Kamiński, K.; et al. Interplay between Structural Static and Dynamical Parameters as a Key Factor to Understand Peculiar Behaviour of Associated Liquids. *J. Mol. Liq.* **2020**, *319*, 114084.
(25) Singh, L. P.; Richert, R. Watching Hydrogen-Bonded Structures in an Alcohol Convert from Rings to Chains. *Phys. Rev. Lett.* **2012**, *109* (16), 167802.
(26) Gainaru, C.; Meier, R.; Schildmann, S.; Lederle, C.; Hiller, W.; Rössler, E. A.; Böhmer, R. Nuclear-Magnetic-Resonance Measurements Reveal the Origin of the Debye Process in Monohydroxy Alcohols. *Phys. Rev. Lett.* **2010**, *105* (25), 258303.
(27) Nowok, A.; Dulski, M.; Grelska, J.; Szeremeta, A. Z.; Jurkiewicz, K.; Grzybowska, K.; Musiał, M.; Pawlus, S. Phenyl Ring: A Steric Hindrance or a Source of Different Hydrogen Bonding Patterns in Self-Organizing Systems. *J. Phys. Chem. Lett.* **2021**, *12* (8), 2142−2147.
(28) Soszka, N.; Hachuła, B.; Tarnacka, M.; Grelska, J.; Jurkiewicz, K.; Geppert-Rybczyńska, M.; Wrzalik, R.; Grzybowska, K.; Pawlus, S.; Paluch, M.; et al. Aromaticity Effect on Supramolecular Aggregation. Aromatic vs. Cyclic Monohydroxy Alcohols. *Spectrochim. Acta Part A Mol. Biomol. Spectrosc.* **2022**, *276*, 121235.
(29) Nowok, A.; Jurkiewicz, K.; Dulski, M.; Hellwig, H.; Małecki, J. G.; Grzybowska, K.; Grelska, J.; Pawlus, S. Influence of Molecular Geometry on the Formation, Architecture and Dynamics of H-Bonded Supramolecular Associates in 1-Phenyl Alcohols. *J. Mol. Liq.* **2021**, *326*, 115349.
(30) Hachuła, B.; Grelska, J.; Soszka, N.; Jurkiewicz, K.; Nowok, A.; Szeremeta, A. Z.; Pawlus, S.; Paluch, M.; Kaminski, K. Systematic Studies on the Dynamics, Intermolecular Interactions and Local Structure in the Alkyl and Phenyl Substituted Butanol Isomers. *J. Mol. Liq.* **2022**, *346*, 117098.
(31) Abraham, M. J.; Murtola, T.; Schulz, R.; Páll, S.; Smith, J. C.; Hess, B.; Lindahl, E. GROMACS: High Performance Molecular Simulations through Multi-Level Parallelism from Laptops to Supercomputers. *SoftwareX* **2015**, *1−2*, 19−25.
(32) Páll, S.; Abraham, M. J.; Kutzner, C.; Hess, B.; Lindahl, E. *Tackling Exascale Software Challenges in Molecular Dynamics Simulations with GROMACS* **2015**, *8759*, 3−27.
(33) Pronk, S.; Páll, S.; Schulz, R.; Larsson, P.; Bjelkmar, P.; Apostolov, R.; Shirts, M. R.; Smith, J. C.; Kasson, P. M.; van der Spoel, D.; et al. GROMACS 4.5: A High-Throughput and Highly Parallel Open Source Molecular Simulation Toolkit. *Bioinformatics* **2013**, *29* (7), 845−854.
(34) Wang, J.; Wolf, R. M.; Caldwell, J. W.; Kollman, P. A.; Case, D. A. Development and Testing of a General Amber Force Field. *J. Comput. Chem.* **2004**, *25* (9), 1157−1174.
(35) Case, D. A.; Darden, T. A.; Cheatham, T. E., III; Simmerling, C. L.; Wang, J.; Duke, R. E.; Luo, R.; Al, E. *AMBER 9*; University of California: San Francisco, 2006.
(36) Brehm, M.; Thomas, M.; Gehrke, S.; Kirchner, B. TRAVIS—A Free Analyzer for Trajectories from Molecular Simulation. *J. Chem. Phys.* **2020**, *152* (16), 164105.
(37) Hollóczki, O.; Macchiagodena, M.; Weber, H.; Thomas, M.; Brehm, M.; Stark, A.; Russina, O.; Triolo, A.; Kirchner, B. Triphilic Ionic-Liquid Mixtures: Fluorinated and Non-Fluorinated Aprotic Ionic-Liquid Mixtures. *ChemPhysChem* **2015**, *16* (15), 3325−3333.
(38) Brehm, M.; Kirchner, B. TRAVIS - A Free Analyzer and Visualizer for Monte Carlo and Molecular Dynamics Trajectories. *J. Chem. Inf. Model.* **2011**, *51* (8), 2007−2023.
(39) Frisch, M. J.; Trucks, G. W.; Schlegel, H. B.; Scuseria, G. E.; Robb, M. A.; Cheeseman, J. R.; Scalmani, G.; Barone, V.; Mennucci, B.; Petersson, G. A.; Nakatsuji, H.; Caricato, M.; Li, X.; Hratchian, H. P.; Izmaylov, A. F.; Bloino, J.; Zheng, G.; Sonnenberg, J. L.; Hada, M.; Ehara, M.; Toyota, K.; Fukuda, R.; Hasegawa, J.; Ishida, M.; Nakajima, T.; Honda, Y.; Kitao, O.; Nakai, H.; Vreven, T.; Montgomery, J. A., Jr.; Peralta, J. E.; Ogliaro, F.; Bearpark, M.; Heyd, J. J.; Brothers, E.; Kudin, K. N.; Staroverov, V. N.; Kobayashi, R.; Normand, J.; Raghavachari, K.; Rendell, A.; Burant, J. C.; Iyengar, S. S.; Tomasi, J.; Cossi, M.; Rega, N.; Millam, J. M.; Klene, M.; Knox, J. E.; Cross, J. B.; Bakken, V.; Adamo, C.; Jaramillo, J.; Gomperts, R.; Stratmann, R. E.; Yazyev, O.; Austin, A. J.; Cammi, R.; Pomelli, C.;

https://doi.org/10.1021/acs.jpcb.3c02092
J. Phys. Chem. B 2023, 127, 9102−9110

Ochterski, J. W.; Martin, R. L.; Morokuma, K.; Zakrzewski, V. G.; Voth, G. A.; Salvador, P.; Dannenberg, J. J.; Dapprich, S.; Daniels, A. D.; Farkas, O.; Foresman, J. B.; Ortiz, J. V.; Cioslowski, J.; Fox, D. J. *Gaussian 09*, revision E.01; Gaussian, Inc.: Wallingford, CT, 2009.
(40) Dennington, R.; Keith, T. A.; Millam, J. M. *GaussView* 5.0.8; Semichem Inc: Shawnee Mission, KS, 2008.
(41) Bordewijk, P. On the Relationship between the Kirkwood Correlation Factor and the Dielectric Permittivity. *J. Chem. Phys.* **1980**, *73* (1), 595−597.
(42) Kirkwood, J. G. The Dielectric Polarization of Polar Liquids. *J. Chem. Phys.* **1939**, *7* (10), 911−919.
(43) Kao, K. C. *Dielectric Phenomena in Solids*; Elsevier Academic Press; London, 2004; pp 92−93.
(44) Jurkiewicz, K.; Hachuła, B.; Kamińska, E.; Grzybowska, K.; Pawlus, S.; Wrzalik, R.; Kamiński, K.; Paluch, M. Relationship between Nanoscale Supramolecular Structure, Effectiveness of Hydrogen Bonds, and Appearance of Debye Process. *J. Phys. Chem. C* **2020**, *124* (4), 2672−2679.
(45) Soszka, N.; Hachuła, B.; Tarnacka, M.; Kamińska, E.; Grelska, J.; Jurkiewicz, K.; Geppert-Rybczyńska, M.; Wrzalik, R.; Grzybowska, K.; Pawlus, S.; et al. The Impact of the Length of Alkyl Chain on the Behavior of Benzyl Alcohol Homologues − the Interplay between Dispersive and Hydrogen Bond Interactions. *Phys. Chem. Chem. Phys.* **2021**, *23* (41), 23796−23807.
(46) Požar, M.; Bolle, J.; Sternemann, C.; Perera, A. On the X-Ray Scattering Pre-Peak of Linear Mono-Ols and the Related Microstructure from Computer Simulations. *J. Phys. Chem. B* **2020**, *124* (38), 8358−8371.
(47) Perera, A. Charge Ordering and Scattering Pre-Peaks in Ionic Liquids and Alcohols. *Phys. Chem. Chem. Phys.* **2017**, *19* (2), 1062−1073.
(48) Vrhovšek, A.; Gereben, O.; Jamnik, A.; Pusztai, L. Hydrogen Bonding and Molecular Aggregates in Liquid Methanol, Ethanol, and 1-Propanol. *J. Phys. Chem. B* **2011**, *115* (46), 13473−13488.
(49) Choi, S.; Parameswaran, S.; Choi, J.-H. Effects of Molecular Shape on Alcohol Aggregation and Water Hydrogen Bond Network Behavior in Butanol Isomer Solutions. *Phys. Chem. Chem. Phys.* **2021**, *23* (23), 12976−12987.
(50) Mariani, A.; Ballirano, P.; Angiolari, F.; Caminiti, R.; Gontrani, L. Does High Pressure Induce Structural Reorganization in Linear Alcohols? A Computational Answer. *ChemPhysChem* **2016**, *17* (19), 3023−3029.

https://doi.org/10.1021/acs.jpcb.3c02092
J. Phys. Chem. B 2023, 127, 9102−9110

Supporting information

Experimental and Computational Approach to Studying Supramolecular Structures in Propanol and its Halogen Derivatives

Kinga Łucak[a]*, Anna Z. Szeremeta[a], Roman Wrzalik[a], Joanna Grelska[a], Karolina Jurkiewicz[a], Natalia Soszka[b], Barbara Hachuła[b], Daniel Kramarczyk[a], Katarzyna Grzybowska[a], Beibei Yao[a], Kamil Kamiński[a], Sebastian Pawlus[a].

[a] *Institute of Physics, Faculty of Science and Technology, University of Silesia in Katowice, 75 Pułku Piechoty 1, 41-500 Chorzów, Poland*

[b] *Institute of Chemistry, Faculty of Science and Technology, University of Silesia in Katowice, Szkolna 9, 40-006 Katowice, Poland*

*Correspondence e-mails: kinga.lucak@us.edu.pl

1.1. Dielectric data analysis

Figure S1 shows the dielectric loss spectra of nP. We can distinguish dielectric peaks, shifting with increasing temperature, which indicates the dielectric process. The peaks are broadened, so we presume a superposition of two dielectric processes: Debye and α - process.

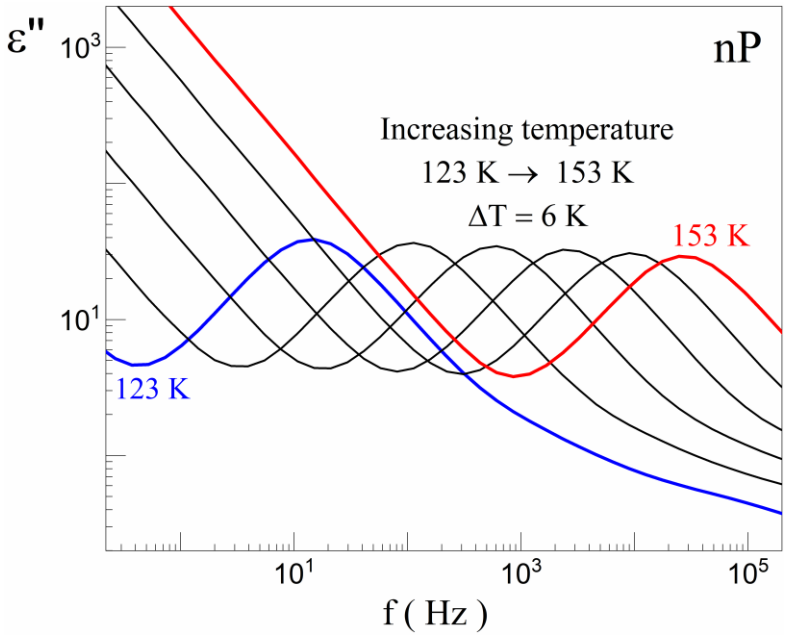

Figure S1. Dielectric loss spectra of nP for selected temperatures.

To properly analyse the observed relaxation processes for nP, the data were fitted with an equation consisting of the sum of Debye, Havriliak–Negami (HN) equation and constant-current conductivity σ_{DC}. The exponents α and β are the parameters for the symmetrical and asymmetrical broadening of the dielectric loss curve, respectively.

$$\varepsilon^*(\omega) = \varepsilon_\infty + \frac{\Delta\varepsilon}{1 + (i\omega\tau_D)} + \frac{\Delta\varepsilon}{[1 + (i\omega\tau_{HN})^\alpha]^\beta} + \frac{\sigma_{DC}}{i\omega\varepsilon_0}, \quad (1)$$

Structural relaxation can be described by the HN formula with a parameter α = 1. Which means that the HN equation reduces to the Cole-Davidson function, and finally, the data was being fit by:

$$\varepsilon^*(\omega) = \varepsilon_\infty + \frac{\Delta\varepsilon}{1 + (i\omega\tau_D)} + \frac{\Delta\varepsilon}{(1 + i\omega\tau_{CD})^\beta} + \frac{\sigma_{DC}}{i\omega\varepsilon_0}, \quad (2)$$

where ε_∞ is the high-frequency dielectric permittivity, $\Delta\varepsilon$ - the dielectric strength, ω is equal to $2\pi f$, τ_D is the Debye relaxation time and σ_{dc} is the constant-current conductivity [1, 2, 3].

The dielectric loss spectrum of halogen derivatives of propanol is affected by the contribution of the direct current (DC) conductivity σ, which partially covers the Debye process. Two equation does not sufficient to describe the relaxation phenomena at high frequencies. In this case, the data was being fit by: Debye, Cole-Davidson, Cole-Cole functions for the Debye, structural and secondary relaxation, respectively, and constant-current conductivity σ_{DC}[1].

$$\varepsilon^*(\omega) = \varepsilon_\infty + \frac{\Delta\varepsilon}{1 + (i\omega\tau_D)} + \frac{\Delta\varepsilon}{(1 + i\omega\tau_{CD})^\beta} + \frac{\Delta\varepsilon}{(1 + i\omega\tau_{CD})^\alpha} + \frac{\sigma_{DC}}{i\omega\varepsilon_0}, \quad (3)$$

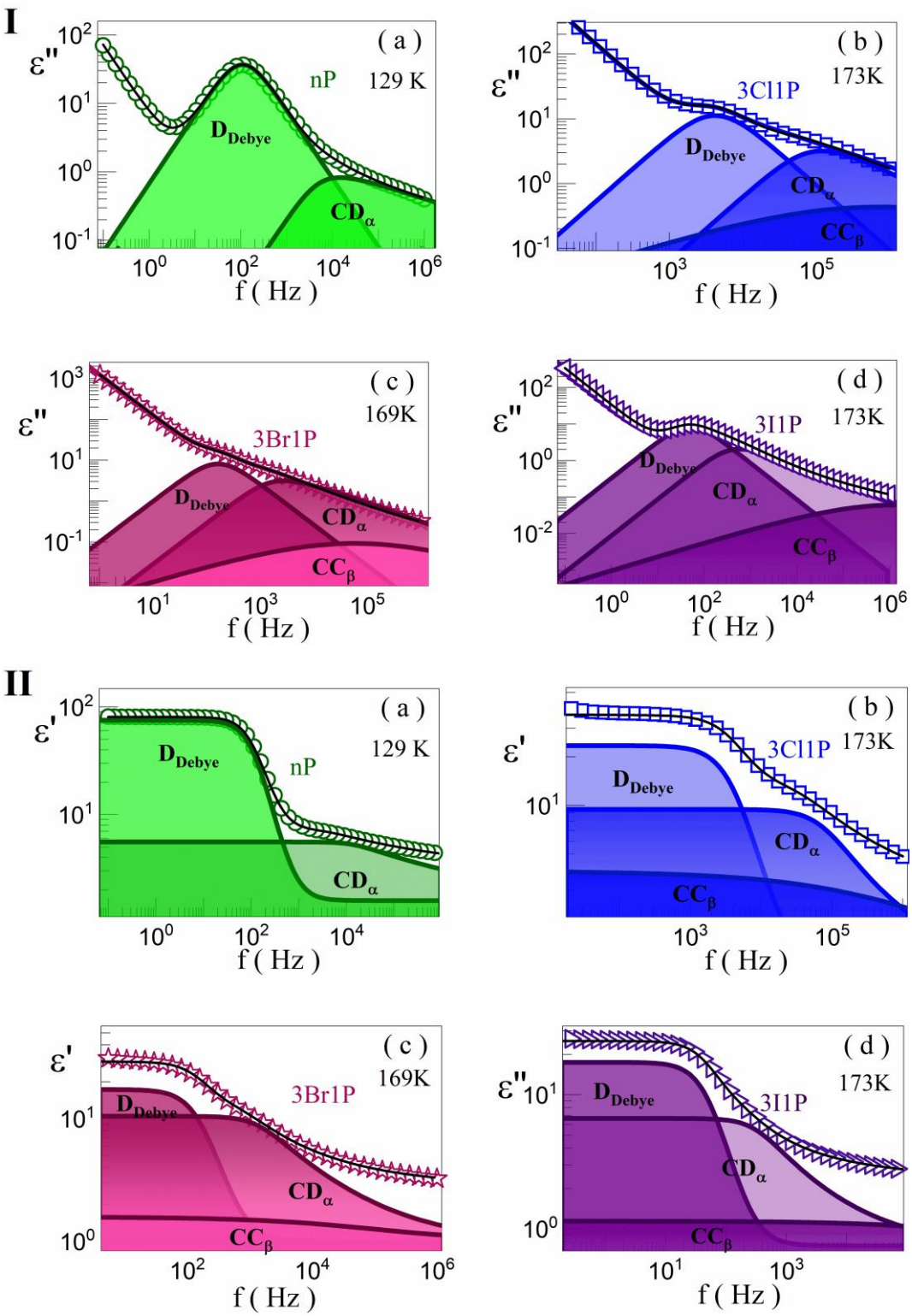

Figure S2. Imaginary (I) and real (II) parts of the dielectric permittivity, obtained for (a) nP at 129 K, (b) 3Cl1P at 173 K, (c) 3Br1P at 169 K, and (d) 3I1P at 173 K. The measurement points are marked with circles (nP), squares (3Cl1P), stars (3Br1P), and triangles (3I1P). The colorful solid lines are the results of fitting the Debye, structural and secondary relaxation

with Debye, Cole-Davidson, and Cole-Cole functions, respectively. The black solid lines show the overall fit lines of the experimental spectra.

To better show the presence of the structural process, we used the Kramers-Kronig transform of the ε' data[1].

$$\varepsilon''_{der} = -\frac{\pi}{2}\frac{\partial\, \varepsilon'(\omega)}{\partial ln\omega} \approx \varepsilon''_{rel}\ , \qquad (4)$$

Below **(Figure S3)** we show the original data at lower temperatures, where the alpha relaxation is better visible. **Figure S4** shows the data obtained after applying the Kramers-Kronig transform.

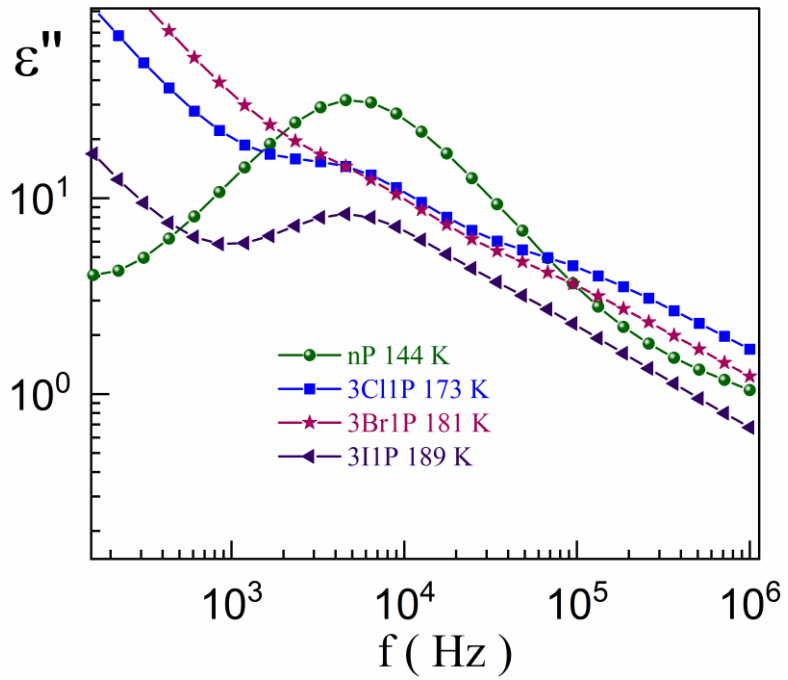

Figure S3. Original data for propanol and its halogen derivatives.

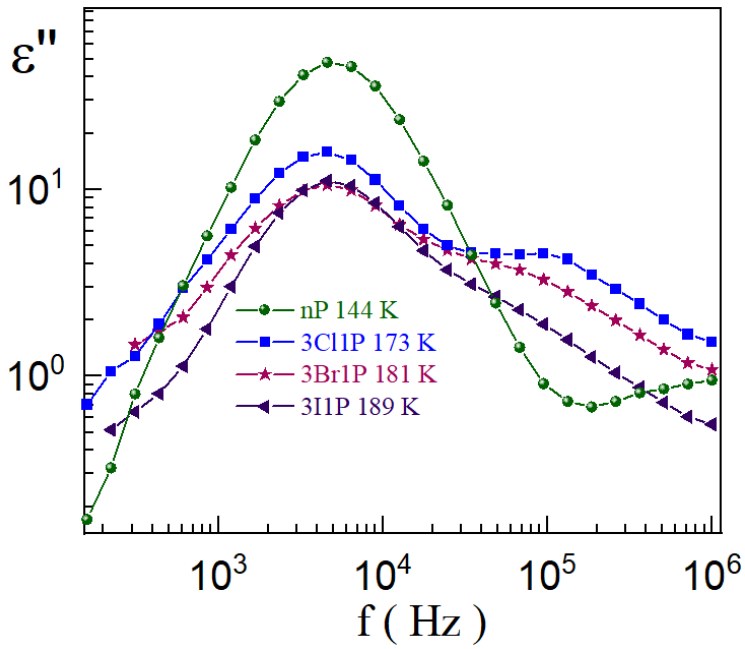

Figure S4. Data obtained using the Kramers-Kronig transform for propanol and its halogen derivatives.

1.2. Calculations of average cluster size of alcohol aggregates.

Gainaru and co-workers [4] developed a formula to estimate the average number of molecules involved in transition chain formation in monohydroxy alcohols. The Gainaru model works very well for alcohols with a hydroxyl group at the end of the carbon chain, such as butanol. In the case of monoalcohols with a halogen atom, to apply the model proposed by Gainaru, we had to take into account the dipole moment coming from the halogen atom. Using the collected data from dielectric measurements and the relation proposed by Gainaru [4], we calculated the number of molecules involved in the self-organisation into clusters via hydrogen bonds (*N*). Gainaru applied this model based on the fact that the dipole moment of A-type polymers is arranged parallel to the chain backbone [5]. This assumption leads to the following expression [4]:

$$\frac{\Delta\varepsilon_D}{\Delta\varepsilon_\alpha} = \frac{(\frac{\mu_{end-to-end}}{\mu_\perp})^2}{N} \approx 4N, \qquad (5)$$

where $\Delta\varepsilon_D$, $\Delta\varepsilon_\alpha$ are dielectric strength of the Debye and structural relaxation process, $\mu_{end\text{-}to\text{-}end}$ is of the order of $N\mu$ and $\mu_\perp$ should be $\mu/2$. nP is a simple alcohol with an OH group at the end of the chain, therefore we could implement the Gainaru model for this monoalcohol. In the case of halogen derivatives of propanol, we have to take into account atoms attached to the

3rd carbon atom: Cl, Br and J. Halogen atoms contribute to a change in the dipole moment of the molecule. In propanol μ_{OC} is according to the assumption proposed by Gainaru, while in the case of halogen derivatives of propanol these are respectively: $\mu_{\perp} \approx \mu_{OCl,}$ $\mu_{\perp} \approx \mu_{OBr,}$ $\mu_{\perp} \approx \mu_{OI.}$ (look up **Table S1**).

Table S1. Dipole moments and its components parallel and perpendicular to the cluster axis, calculated for single molecule using the B3LYP/6-311G (d, p) model.

Molecule	μ [D]	$\mu_{\perp}$ [D]	$\mu_{\parallel}$ [D]
1-propanol	1.501	0.825	1.254
3-chloro-propanol	3.269	2.122	2.486
3-bromo-propanol	3.322	2.263	2.432
3-iodo-propanol	3.175	2.142	2.343

Furthermore, the value of the perpendicular component of the molecule's dipole $\mu_{\perp}$ is comparable to the parallel component $\mu_{\parallel}$, while in the case of propanol the parallel component $\mu_{\parallel}$ is twice as large as the perpendicular component $\mu_{\perp.}$ Obtaining $\Delta_{\varepsilon D}$ and $\Delta_{\varepsilon \alpha}$ from the spectra of dielectric measurements and assuming that in $\mu_{\perp}$ we take into account a strongly electronegative atom attached at the end of the alkyl chain, we can determine the number of aggregating molecules in the supramolecular chain of halogen derivatives of propanol. The clusters has been calculated using the equation:

$$N = \left(\frac{\Delta\varepsilon_D}{\Delta\varepsilon_\alpha}\right)\left(\frac{\mu_\perp}{\mu_\parallel}\right)^2. \quad (6)$$

The *N* values for the analyzed alcohols are presented in **Table S2**.

Table S2. Temperature dependence of the number of molecules in the cluster for studied alcohols, calculated based on the Gainaru model [4].

nP

T [K]	ε_D	ε_α	$\varepsilon_D/\varepsilon_\alpha$	N
123	77.34	3.93	19.65	8.5
125	75.6	3.95	19.15	8.3
127	74.62	3.91	19.09	8.3
129	73.54	3.96	18.45	7.9
131	71.96	3.92	18.35	7.9
133	70.57	3.97	17.76	7.7
135	69.07	4.06	16.99	7.4
137	68.21	4.04	16.90	7.3
139	66.59	3.99	16.69	7.3
141	65.56	3.91	16.76	7.3

3Cl1P

T [K]	ε_D	ε_α	$\varepsilon_D/\varepsilon_\alpha$	N
149	24.48	15.55	1.57	1.1
151	27.84	11.76	2.36	1.7
153	27.42	11.72	2.33	1.7
155	26.76	11.75	2.27	1.6
157	25.96	11.69	2.22	1.6
159	25.37	11.33	2.23	1.6
161	24.97	11.57	2.15	1.6
163	24.82	11.37	2.18	1.6
165	24.49	10.75	2.27	1.7
167	24.05	10.24	2.34	1.7
169	23.26	9.887	2.35	1.7
171	23.02	9.789	2.35	1.7
173	22.83	8.401	2.71	2.0
175	22.44	8.457	2.65	2.0

3Br1P

T [K]	ε_D	ε_α	$\varepsilon_D/\varepsilon_\alpha$	N
157	18	9.61	1.87	1.6
159	16.14	11.45	1.40	1.2
161	17.35	10.39	1.66	1.4
163	16.81	10.25	1.64	1.4
165	16.09	9.75	1.64	1.4
167	16.61	9.98	1.66	1.4
169	16.29	9.46	1.72	1.5
171	16.33	8.81	1.85	1.6
173	16.27	8.5	1.91	1.7
175	15.8	7.62	2.07	1.8
177	15.8	7.62	2.07	1.8
179	15.18	8.15	1.86	1.6
181	14.75	7.46	1.97	1.7
183	14.36	7.46	1.92	1.7
185	14.08	7.96	1.76	1.5
187	14.16	7.91	1.78	1.5
189	13.76	7.89	1.74	1.5

3I1P

T [K]	ε_D	ε_α	$\varepsilon_D/\varepsilon_\alpha$	N
163	17.73	6.12	2.89	2.4
165	17.34	5.954	2.91	2.4
169	16.55	6.278	2.63	2.2
171	16.71	5.91	2.82	2.3
173	16.51	5.788	2.85	2.4
175	16.24	5.48	2.96	2.5
177	16	5.229	3.05	2.6
179	15.64	5.091	3.07	2.6
181	15.43	5.202	2.96	2.5
183	15.21	5.137	2.96	2.5
185	14.84	5.039	2.94	2.5
187	14.6	4.947	2.95	2.5
189	17.73	6.12	2.89	2.4

1.3. Fourier transform infrared and Raman spectroscopy

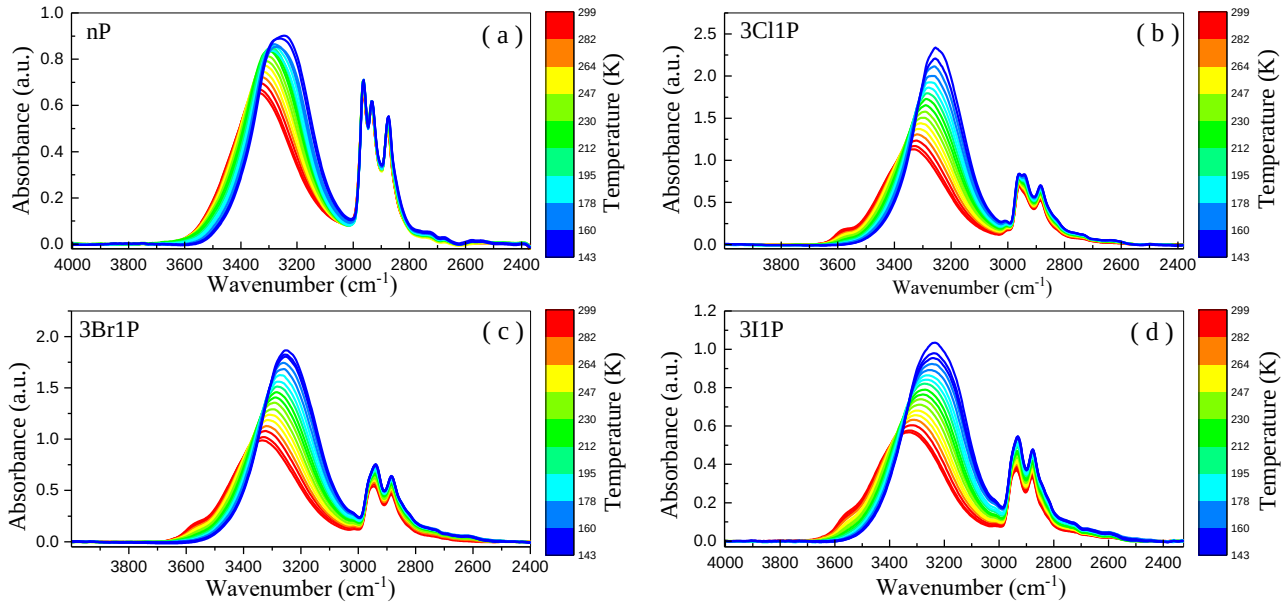

Figure S5. Temperature-dependent FTIR spectra of the analyzed alcohols: (a) nP (T = 299 - 143 K), (b) 3Cl1P (T = 299 - 143 K), (c) 3Br1P (T = 299 - 143 K), and (d) 3I1P (T = 299 - 143 K).

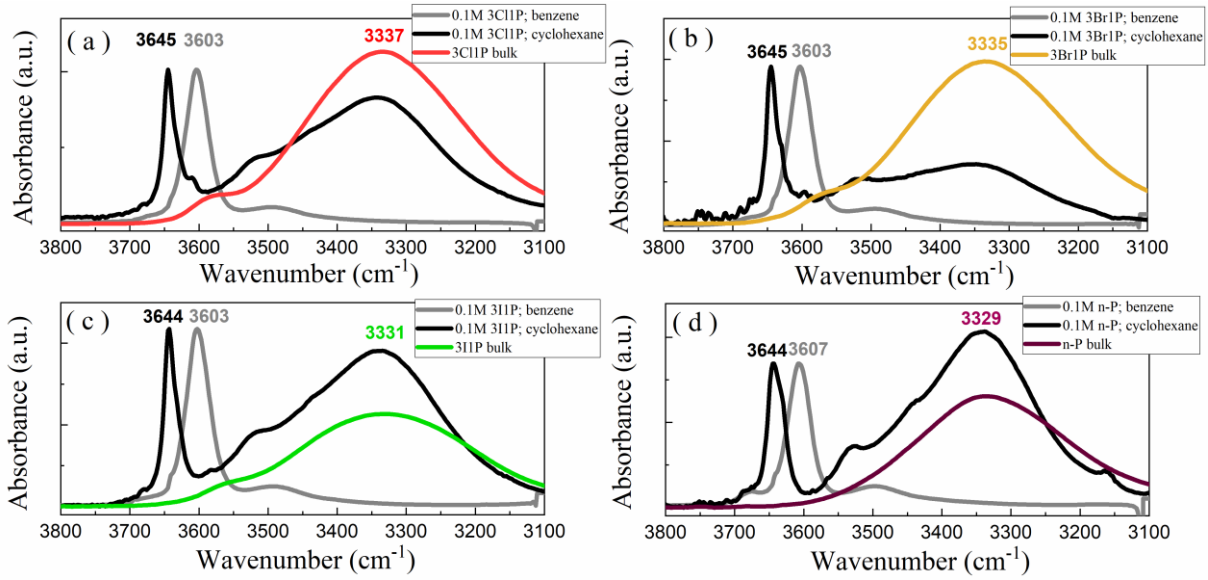

Figure S6. FTIR spectra of alcohols in bulk and dissolved in solvents (benzene, cyclohexane) in the frequency range of 3800 - 3100 cm^{-1}

Table S3. The frequency (ν) and full width at half maximum (FWHM) values of the ν_{OH}^{HB} band for measured alcohols at 299 K and T_g.

Substance	ν (cm^{-1}) at 299 K	ν (cm^{-1}) at T_g	FWHM (cm^{-1}) at 299 K	FWHM (cm^{-1}) at T_g
P	3329	--	243.87	--
3Cl1P	3337	3252	251.71	190.48
3Br1P	3335	3255	258.08	215.85
3I1P	3331	3243	282.6	249.32

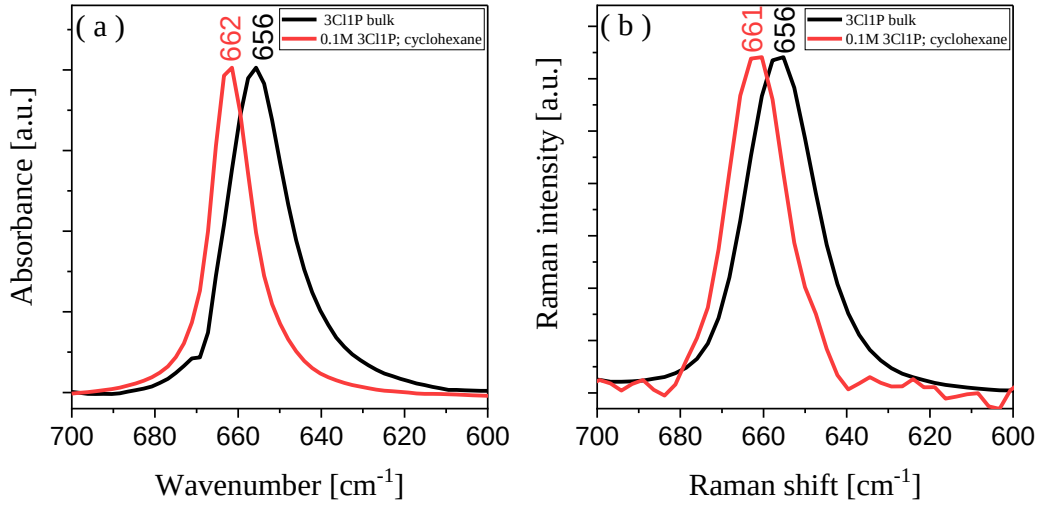

Figure S7. IR (a) and Raman (b) spectra in the frequency region 700 – 600 cm^{-1} presenting the C-Cl stretching vibration band for bulk 3Cl1P (black) and its 0.1 M solution in cyclohexane (red). The spectra were normalized to the C-Cl band intensity.

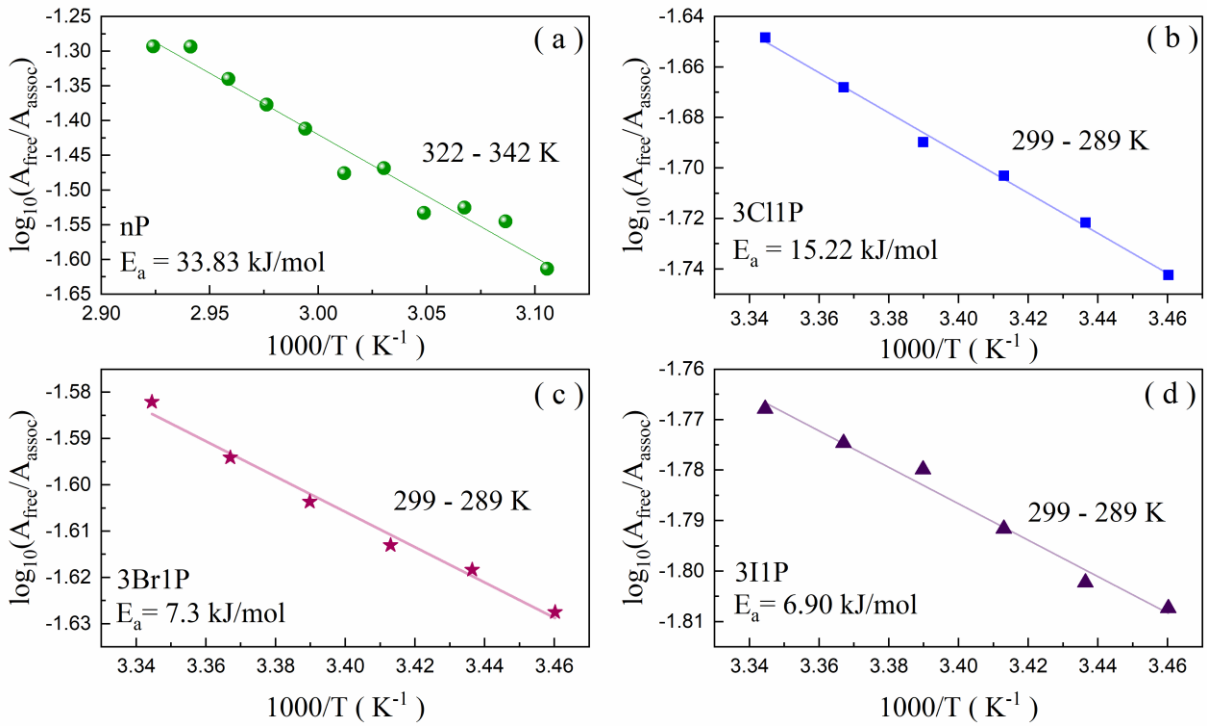

Figure S8. The van't Hoff plots for IR absorption bands of (a) nP, (b) 3Cl1P, (c) 3Br1P, and (d) 3I1P used to obtain the enthalpy of the dissociation process between the H-bonded and free OH species.

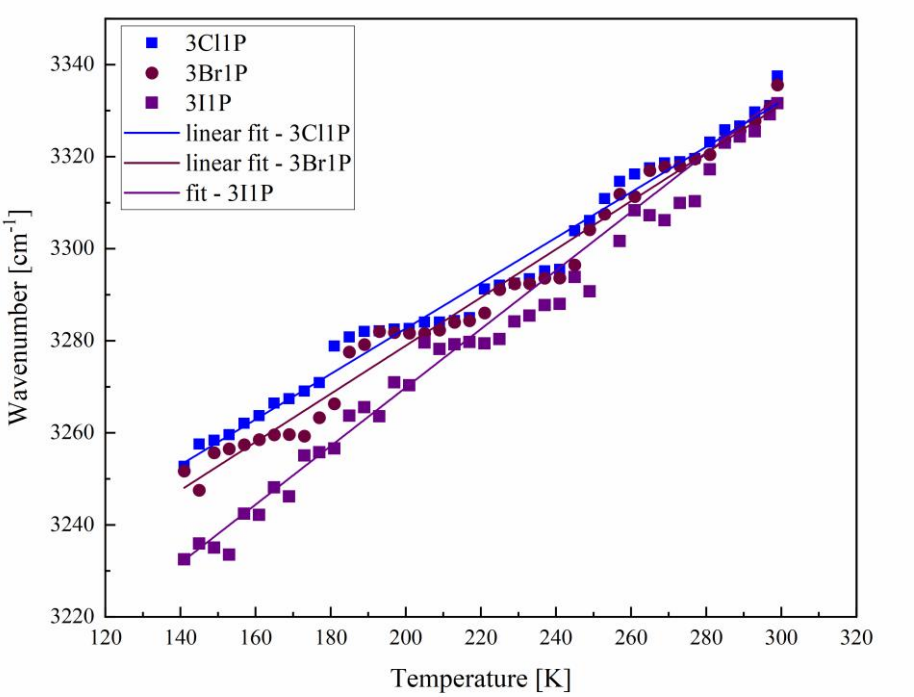

Figure S9. The temperature dependence of $\nu_{OH\ associated}$ peak position for examined halogen derivatives of propanol in the temperature range 299 – 141 K.

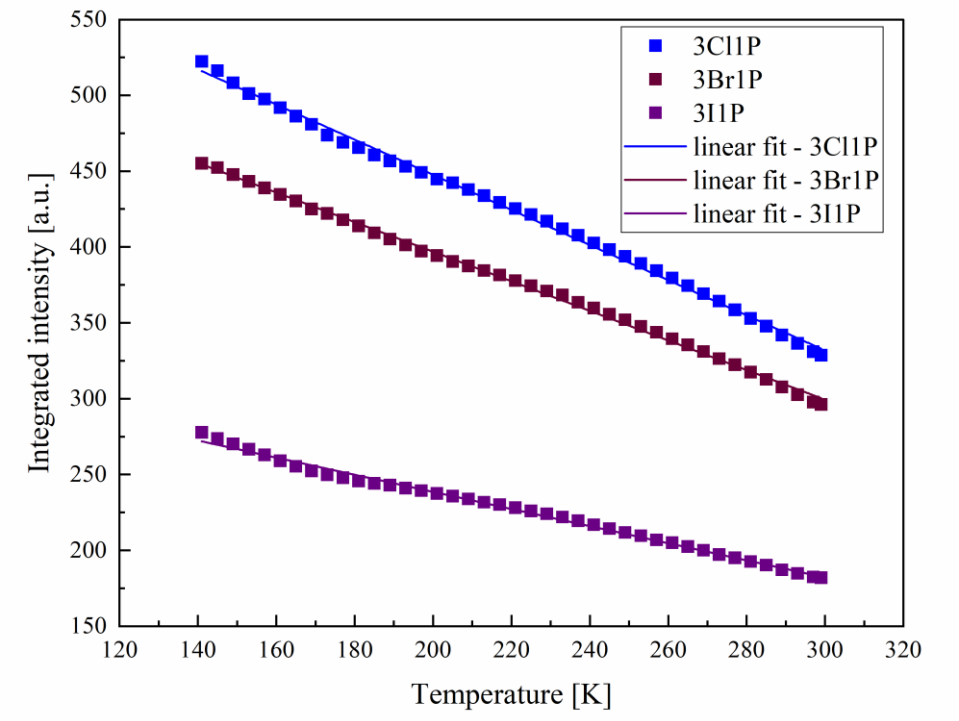

Figure S10. The temperature dependence of the integrated intensity of the ν_{OH} band for examined halogen derivatives of propanol in the temperature range 299 – 141 K.

1.4. Molecular dynamics simulations

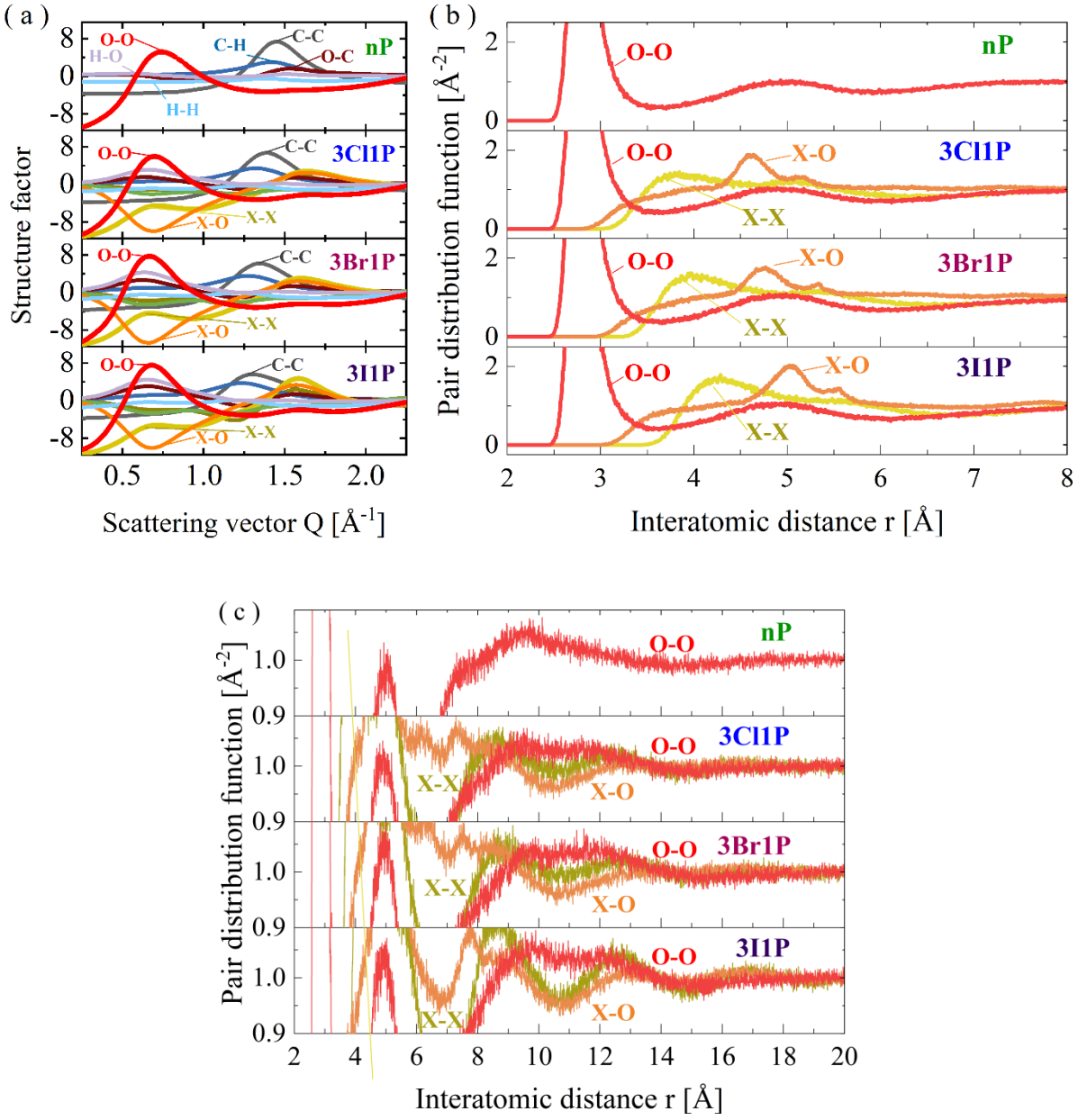

Figure S11. Results obtained from molecular dynamics simulations: all partial structure factors (a) and selected atom-atom pair distribution functions in the range 2−8 Å (b) and 2−20 Å (c). C, O, H, and X = Cl, Br or I refer to carbon, oxygen, hydrogen, and halogen elements, respectively.

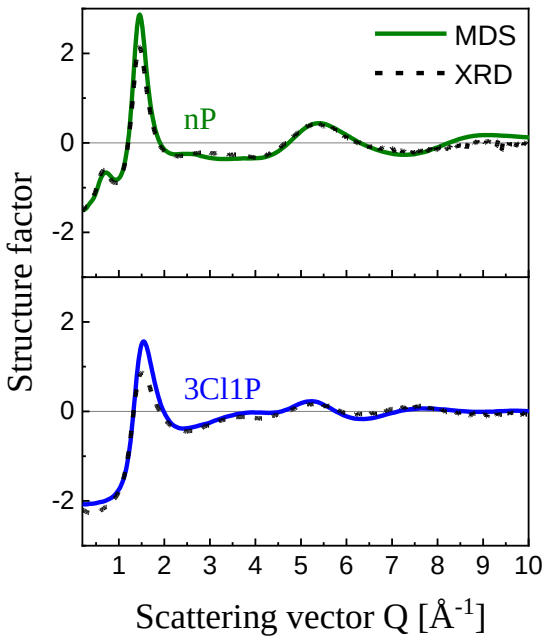

Figure S12. Comparison of experimental total structure factors for investigated nP and 3Cl1P derived from X-ray diffraction measurements (XRD) with theoretical functions derived from molecular dynamics simulations (MDS).

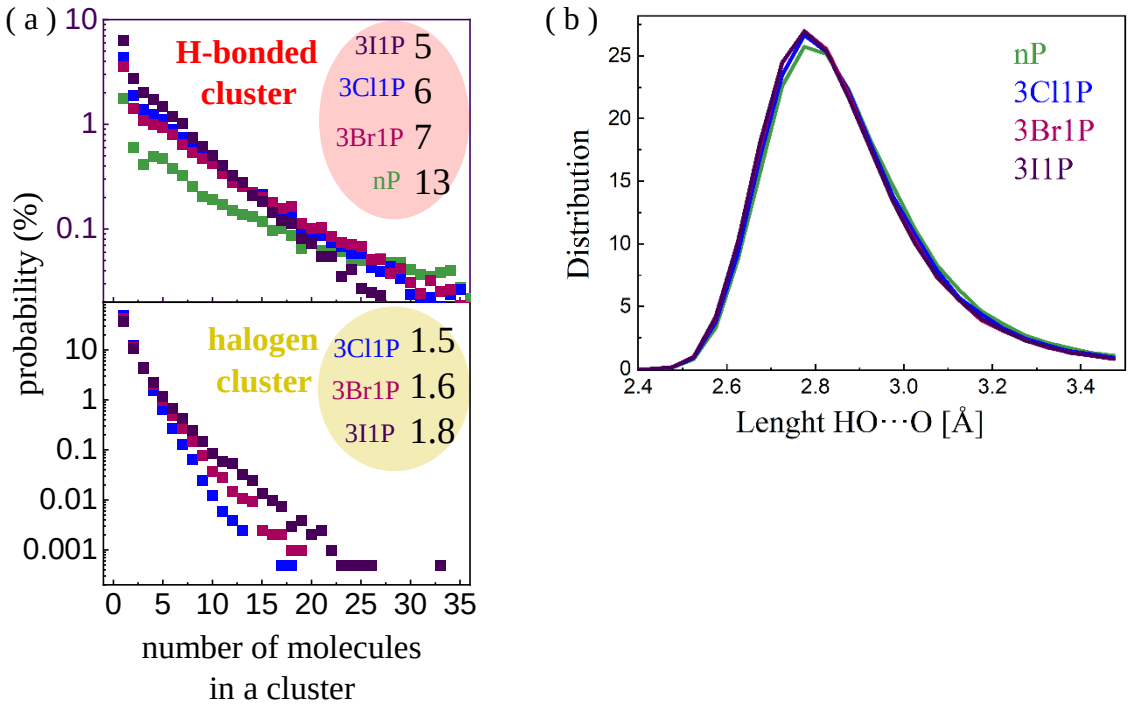

Figure S13. Histograms of probability (percent on logarithmic scale) of finding an H-bonded or halogen cluster with a given number of molecules (a). The calculated averages numbers of molecules in the clusters are displayed in the graphs. Panel (b) shows the distribution of the donor-acceptor HO···O distances of hydrogen bonds in the studied systems.

1.5. Dimer interaction energy

The analysis of intermolecular interactions was carried out on the basis of the structure parameters and interaction energies determined for three dimers: two linear (A and B) and one cyclic (C). Exemplary, optimized structures of 3Cl1P dimers are presented in **Figure S14**.

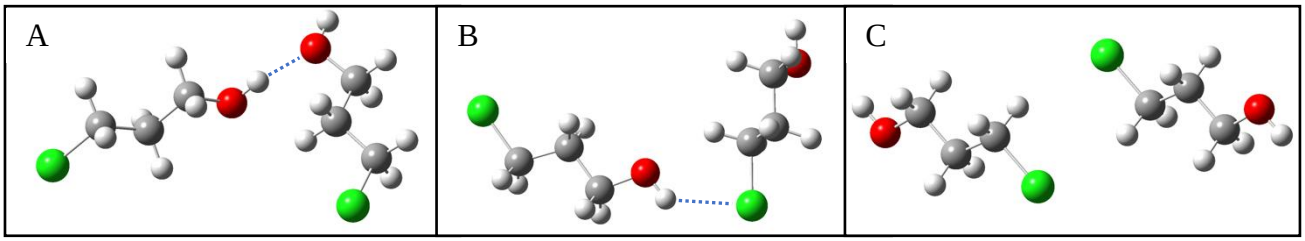

Figure S14. Structure of the optimized dimers of 3Cl1P molecules (B3LYP/6-311G (d,p) calculation model).

Table S5 presents the determined interaction energies between molecules forming dimers, and **Table S6** contains the geometry parameters of the systems. The meaning of the parameters (the distance d and D between the atoms and the angle θ between the bonds) is explained in **Figure S15.**

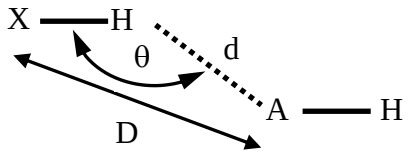

Figure S15. Definition of the geometrical parameters (d, D, θ) of a hydrogen bonded dimer.

The comparison of the determined parameters (**Table S5** – energy, **Table S6** - geometry parameters) with the criteria for classifying hydrogen interactions [6], included in **Table S4**, allows classifying the hydrogen bonds of O-H···O linear dimers of the A-type structure to strong hydrogen bonds (interaction energy E > 5 kcal mol^{-1}), while B dimer with bond between the halogen atom and the hydroxyl group (O-H···X) - to weak hydrogen bonds (E < 4 kcal mol^{-1}). Type C cyclic dimer (E ≈ 2 kcal mol^{-1}) is formed without the participation of hydrogen bonds, and the dominant contribution is made by dipole interactions (antiparallel arrangement of dipoles). Comparing the calculation results of the applied functionals, it can be seen that the correction of long-range interactions contained in the CAM-B3LYP functional significantly affects the estimated interaction energy of molecules forming the

dimers (the energy increases by 0.5 - 1.0 kcal mol^{-1}), but has a much smaller impact on the dimer geometries.

Table S4. Some properties of very strong, strong and weak hydrogen bonds [6]

Parameters	Very strong	Strong	Weak
Bond energy (kcal mol^{-1})	15-40	4-15	< 4
Bond lengths	H—A ≈ X–H	H···A > X – H	H···A>>X–H
Lengthening of δ(X–H) [Å]	0.05–0.2	0.01–0.05	<0.01
D(X···A) range [Å]	2.2–2.5	2.5–3.2	3.0–4.0
d(H···A) range [Å]	1.2–1.5	1.5–2.2	2.0–3.0
θ(X−H···A) range (°)	175–180	130–180	90–180

A – acceptor, X-H – donor

Table. S5. Dimer interaction energy in kcal mol^{-1} calculated using B3LYP and CAM-B3LYP electron density functionals with 6-311G(d,p) basis set.

Molecule	B3LYP	CAM-B3LYP
nP		
O...H-O	-5.05	-5.96
3Cl1P		
O...H-O	-5.10	-6.04
Cl…O-H	-2.72	-3.43
Cl…H-C(Cl)	-1.40	-2.03
3Br1P		
O...H-O	-5.11	-6.04
Br…O-H	-2.84	-3.52
Br…H-C(Br)	-1.39	-1.94
3I1P		
O...H-O	-5.14	-6.07
I…O-H	-2.61	-3.24
I…H-C(I)	-1.17	-1.63

Table S6. Dimer geometry parameters calculated using B3LYP and CAM-B3LYP electron density functionals with 6-311G(d,p) basis set.

O-H···O	B3LYP/6-311G(d.p)				CAM-B3LYP/6-311G(d.p)			
Parameter	nP	3Cl1P	3Br1P	3I1P	nP	3Cl1P	3Br1P	3I1P
O-H [Å]	0.969	0.969	0.969	0.969	0.968	0.968	0.968	0.960
d(H…O) [Å]	1.962	1.955	1.953	1.952	1.915	1.909	1.910	1.910
θ(O-H…O) [º]	175.56	172.45	172.56	172.45	174.67	171.40	171.48	169.39
D(O---O) [Å]	2.929	2.918	2.917	2.916	2.880	2.870	2.870	2.867
vdW criterion $d < r_O+r_H$= 2.72Å	yes	yes	yes	yes	yes	yes	yes	yes
O-H single [Å]	0.961	0.961	0.961	0.961	0.959	0.960	0.960	0.960
δ(O-H) [Å]	0.008	0.008	0.008	0.008	0.009	0.008	0.008	0.008

O-H···X	B3LYP/6-311G(d,p)			CAM-B3LYP/6-311G(d,p)		
Parameter	3Cl1P	3Br1P	3I1P	3Cl1P	3Br1P	3I1P
O-H [Å]	0.964	0.965	0.964	0.962	0.963	0.963
d(H...X) [Å]	2.636	2.726	3.007	2.591	2.699	2.692
θ(O-H...X) [º]	135.72	138.71	134.05	133.55	135.28	146.03
D(O---X) [Å]	3.393	3.509	3.742	3.328	3.450	3.537
vdW criterion $d < r_X+r_H$	yes $r_{Cl}+r_H$ =2.95	yes $r_{Br}+r_H$=3.05	yes r_I+r_H=3.18	yes $r_{Cl}+r_H$ =2.95	yes $r_{Br}+r_H$=3.05	yes r_I+r_H=3.18
O-H single [Å]	0.961	0.961	0.961	0.960	0.960	0.960
δ(O-H) [Å]	0.003	0.004	0.003	0.002	0.002	0.003

(X)C-H···X	B3LYP/6-311G(d,p)			CAM-B3LYP/6-311G(d,p)		
Parameter	3Cl1P	3Br1P	3I1P	3Cl1P	3Br1P	3I1P
C-H [Å]	1.089	1.089	1.088	1.088	1.087	1.087
d(H...X) [Å]	3.074	3.183	3.451	3.054	3.130	3.357
θ(C-H...X)	159.11	163.09	170.78	131.59	142.13	165.77
D(C---X) [Å]	4.109	4.236	4.528	3.627	4.0437	4.419
vdW criterion	no	no	no	no	no	no

$d < r_C+r_H = 2.90$Å						
(X)C-H single [Å]	1.089	1.089	1.088	1.088	1.089	1.087
δ(C-H) [Å]	0.0	0.0	0.0	0.0	0.002	0.0

X – Cl, Br, I; $r_H = 1.20$, $r_C = 1.70$, $r_O = 1.52$, $r_{Cl} = 1.75$, $r_{Br} = 1.85$, $r_I = 1.98$ Å [7]

1.6. Thermal evolution of density and RI

As shown in Figure S16a and b, the temperature dependences of ρ and RI have a linear character for each monoalcohols. Therefore, the experimental data were refined with a linear function, the extrapolation of which allowed to estimate their values at lower temperature range.

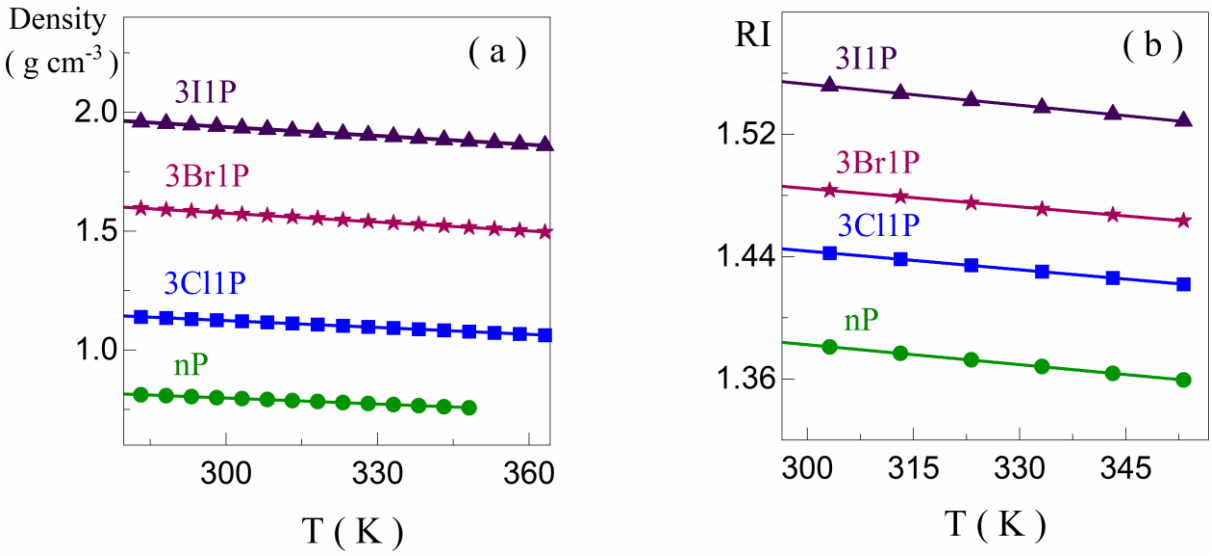

Figure S16. Thermal evolution of density of the studied alcohols (a).Thermal evolution of refractive index of the studied alcohols (b).

1.7. Differential scanning calorimetry

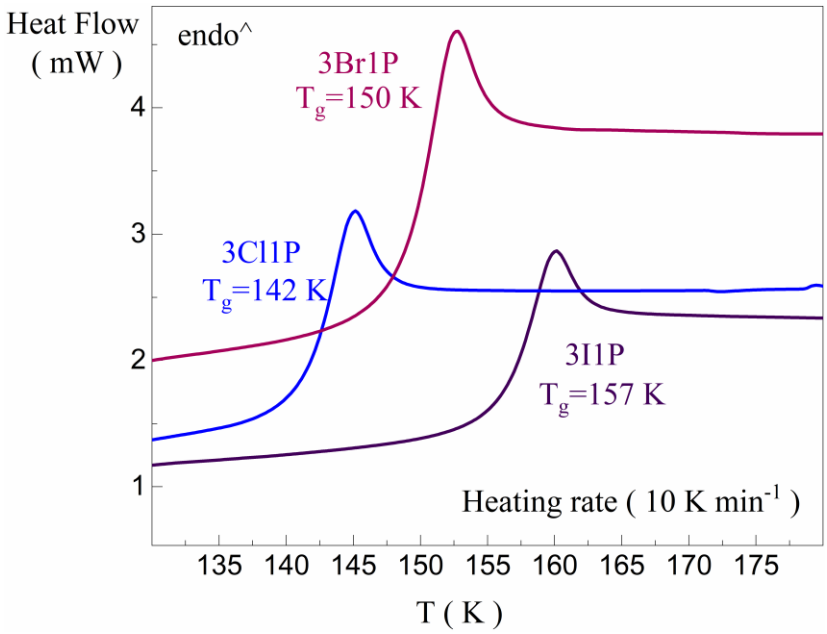

Figure S17. DSC thermograms were collected on heating with a rate of 10 K min^{-1}.

Table S7. Molar Mass (M), Glass Transition Temperature (T_g) of the studied alcohols.

Compound	nP	3Cl1P	3Br1P	3I1P
M (g mol^{-1})	60	95	139	186
T_g (K)	98[8]	142	150	157

References

(1) Kao, K. C. Dielectric Phenomena in Solidss. In *Elsevier Academic Press*; London, 2004; pp 92–95.

(2) Havriliak, S.; Negami, S. A Complex Plane Analysis of α-Dispersions in Some Polymer Systems. *J. Polym. Sci. Part C Polym. Symp.* **2007**, *14* (1), 99–117. https://doi.org/10.1002/polc.5070140111.

(3) Davidson, D. W.; Cole, R. H. Dielectric Relaxation in Glycerine. *J. Chem. Phys.* **1950**, *18* (10), 1417–1417. https://doi.org/10.1063/1.1747496.

(4) Gainaru, C.; Meier, R.; Schildmann, S.; Lederle, C.; Hiller, W.; Rössler, E. A.; Böhmer, R. Nuclear-Magnetic-Resonance Measurements Reveal the Origin of the Debye Process in Monohydroxy Alcohols. *Phys. Rev. Lett.* **2010**, *105* (25), 258303. https://doi.org/10.1103/PhysRevLett.105.258303.

(5) Strobl, G. *The Physics of Polymers*; Springer: Berlin, 1997.

(6) Desiraju, G.; Steiner, T. *The Weak Hydrogen Bond*; Oxford University Press: New York, 2001. https://doi.org/10.1093/acprof:oso/9780198509707.001.0001.

(7) Bondi, A. Van Der Waals Volumes and Radii. *J. Phys. Chem.* **1964**, *68* (3), 441–451.

(8) Ramos, M. A.; Kabtoul, B.; Hassaine, M. Calorimetric and Thermodynamic Study of Glass-Forming Monohydroxy Alcohols. *Philos. Mag.* **2011**, *91* (13–15), 1847–1856. https://doi.org/10.1080/14786435.2010.526649.

10.2 [P2] Effect of high pressure on the molecular dynamics of halogen monoalcohols

K. Łucak, A.Z. Szeremeta, J. Grelska, K. Jurkiewicz, S. Kołodziej, R. Wrzalik, K. Kamiński, S. Pawlus. *Journal of Molecular Liquids*, *423*, 127045, (2025).
DOI: 10.1016/j.molliq.2025.127045

Punkty MNiSW (2024): 100
Impact Factor (2024): 5.3

Mój wkład w publikację polegał na wykonaniu pomiarów dielektrycznych w szerokim zakresie temperatur oraz pod wysokim ciśnieniem, pomiarów kalorymetrycznych, analizie wyników i ich dyskusji oraz przygotowaniu artykułu.

Journal of Molecular Liquids 423 (2025) 127045

Contents lists available at ScienceDirect

Journal of Molecular Liquids

journal homepage: www.elsevier.com/locate/molliq

Effect of high pressure on the molecular dynamics of halogen monoalcohols

Kinga Łucak [a,*], Anna Z. Szeremeta [a], Joanna Grelska [a], Karolina Jurkiewicz [a], Sławomir Kołodziej [b], Roman Wrzalik [a], Kamil Kamiński [a], Sebastian Pawlus [a]

[a] August Chełkowski Institute of Physics, Faculty of Science and Technology, University of Silesia in Katowice, 75 Pułku Piechoty 1, 41-500 Chorzów, Poland
[b] Institute of Materials Engineering, Faculty of Science and Technology, University of Silesia in Katowice, ul. 75 Pułku Piechoty 1A, 41-500 Chorzów, Poland

ARTICLE INFO

Keywords:
Self-organization
Supramolecular clusters
Molecular dynamics
High-pressure dielectric measurements
DFT calculations

ABSTRACT

The study focuses on the effects of isomerism, the type of halogen atom (Cl, Br) as well as high pressure on the molecular dynamics and the formation of supramolecular structures in monoalcohols such as 3-chloro-1-propanol, 1-chloro-2-propanol, 3-bromo-1-propanol and 1-bromo-2-propanol. The position of the hydroxyl group and the halogen atom have been shown to affect Debye relaxation. These changes are also reflected in the values of the Kirkwood coefficient, which is greater than unity for all samples tested, suggesting that all compounds analyzed tend to organize themselves into chain aggregates. The highest value of the Kirkwood factor for 1-chloro-2-propanol indicates more intense clustering due to the specific distribution of functional groups, which affects supramolecular structures and dielectric properties. High-pressure observations show the formation of cyclic clusters in 1-bromo-2-propanol and 1-chloro-2-propanol and chain structures in 3-bromo-1-propanol. These phenomena are confirmed by molecular dynamics simulations, which further indicate an increased tendency of 3-bromo-1-propanol to form larger molecular clusters than its isomer. Notably, 3-chloro-1-propanol reveals the ability to crystallize at high pressure, which is not observed at atmospheric pressure. These data highlight the importance of understanding isomerism and the influence of the halogen atoms on the relaxation properties and the ability to form different molecular structures. Such an understanding is crucial for potential practical applications, including crystallization processes and applications in biochemical materials, where the stability and dynamics of molecular structures play a fundamental role.

1. Introduction

Monohydroxy alcohols (MAs) are model compounds for studying hydrogen bonding and supramolecular clustering phenomena across different thermodynamic conditions because of their limited ability to create complex hydrogen-bonded structures. Unlike water, MAs can be mostly easily supercooled and form glasses, which is advantageous for studying their physical properties, e.g. molecular dynamics in wide time range. What is more, it is possible to thoroughly study the impact of chemical structure, i.e. change in the position of the hydroxyl (–OH) group, the length of the backbone, the presence of side groups of various sizes on their glass-forming ability, or self-assembly processes [1–3].

The common property of many primary alcohols is the manifestation of a slow exponential relaxation, called the Debye (D) process, in the dielectric response. This unique mode is postulated to be related to the end-to-end vector motion of the whole H-bonded chains. Although Patil et al. questioned this interpretation [4]. Alternatively, it is claimed that this relaxation is associated with local movements in specific segments of the chain [4]. Also, the structural relaxation (α) associated with the reorientation motions of alkyl chains [5] is registered for MAs. This mode is characterized by a shorter relaxation time and smaller amplitude compared to the D process. Dannhauser's research indicates that the amplitude of the D process varies depending on the position of the –OH group in the alcohol backbone [6]. When the –OH group is at the terminal position, it tends to form chain-like hydrogen-bonded structures, resulting in a higher D process amplitude. Conversely, a non-terminal –OH group can favor either chain-like or more branched and ring-like structures depending on the specific molecular context, leading to variability in the amplitude of the D relaxation [6–7]. These interpretations are also supported by the analysis of the Kirkwood-Fröhlich factor (g_k), which is a useful parameter allowing us to get an insight into the long-range correlation between dipoles induced by the self-association process [8]. According to the Danhauser model applied to MAs, the value of g_k allows for distinguishing between chain and ring

* Corresponding author.
E-mail address: kinga.lucak@us.edu.pl (K. Łucak).

https://doi.org/10.1016/j.molliq.2025.127045
Received 3 October 2024; Received in revised form 26 January 2025; Accepted 28 January 2025
Available online 31 January 2025

organization of molecules in hydrogen – bonded (HB) supramolecular clusters.

Another class of MA involves systems where bulky phenyl or cyclic rings, are present. Usually, in alcohols with a cyclic ring, the population of HBs is greater, and the size of supramolecular clusters is bigger than in phenyl compounds [9]. The rigid phenyl ring plays the role of the so-called steric hindrance, reducing the tendency of molecules to self-assembly via the O-H···O scheme. In addition, the phenyl ring may be a source of intermolecular O-H···π and π···π interactions, competitive with the O–H···O bonds [9–12], which may entail the formation of other supramolecular aggregates.

The other interesting but poorly investigated so far group of MAs are systems with additional functional units in the structure. In our previous paper [13], we studied n-propanol (nP) and its halogen derivatives 3-chloro-1-propanol, 3-bromo-1-propanol, and 3-iodo-1-propanol at atmospheric pressure as a function of temperature. It was demonstrated that the introduction of X (chlorine, bromine, iodine) atoms inhibits molecular association through HBs, leading to the formation of smaller clusters bonded by H-bonds compared to pure nP. Moreover, spectroscopic studies and theoretical calculations indicated the formation of small molecular clusters through O-H···X or X···X interactions, which cause a local disorder and heterogeneity of the intermolecular structure. While high-pressure investigations have been conducted on various primary and secondary alcohols, to our knowledge, there are currently no studies focusing on the high-pressure behavior of alcohols with halogen atoms such as bromine (Br), chlorine (Cl), or iodine (I). Our study uniquely addresses, at least partially, this gap by combining experimental and computational approaches to explore the impact of isomerism, halogenation, and varying pressure and temperature conditions on these halogenated monoalcohols.

Herein, one can briefly mention that previous studies indicated that variation in the thermodynamic conditions leads to some changes in the dynamics of Debye, structural process, Kirkwood factor, steepness index, etc., which can be attributed to the change in self-assembly phenomenon in MA [14–18]. For alcohols with the hydroxyl group located in the terminal position, e.g., 2-ethyl-1-hexanol (2E1H), 2-ethyl-1-butanol (2E1B) [15–16,19] the two relaxation processes converge, and the dielectric spectra show a single peak, which is broadened on the higher frequency side at high-pressure. It is also worth to stress that the amplitude of the D process usually decreases with compression. On the other hand, in the case of alcohols with an –OH group in the middle of the alkyl chain (4-methyl-2-pentanol, 5-methyl-3-heptanol) [17–18,20], the intensity of the main process increases with pressure compared to the data obtained at $p = 0.1$ MPa at isochronal conditions. In the case of isomeric MAs with phenyl ring i.e., 1-phenyl-2-butanol (1ph2B) and 1-(4-methylphenyl)-1-propanol (1(4mph)1P) it was shown that at ambient pressure, they have almost identical temperature dependence regarding relaxation dynamics while strong differences in the steepness index (m_p) and activation volume (ΔV) became noticeable at high-pressure. In addition, an unexpected observation was made concerning 2-phenyl-1-butanol. Despite similar behavior to other isomers at ambient pressure, it showed a high tendency to crystallize when pressure was applied [21].

In the first section of our study, we examined how isomerism, specifically the position of the hydroxyl group, as well as the differences between halogen atoms (Br vs. Cl), influence molecular dynamics under atmospheric pressure and varying temperatures. These initial findings provided a foundation for understanding the basic behavior of these compounds. In the next section of the manuscript, we shift our focus to explore the effects of varying pressure and temperature conditions.

To investigate and distinguish the separate effects of hydroxyl group position and halogen substitution on molecular interactions and self-organization processes under different thermodynamic conditions. We chose two pairs of isomeric halogen derivatives of nP: 3-bromo-1-propanol (3Br1P), 1-bromo-2-propanol (1Br2P), 1-chloro-2-propanol (1Cl2P) and 3-chloro-1-propanol (3Cl1P), which differ in the type of halogen and the position of the hydroxyl group. For both halogen types (Cl, Br), it was possible to follow the impact of the OH group position between the primary and secondary alcohol. By studying these isomers, we can also investigate how different thermodynamic conditions, such as variations in pressure and temperature, influence molecular association and the formation of supramolecular structures. The study utilized broadband dielectric spectroscopy at ambient and elevated pressures, complemented by differential scanning calorimetry (DSC), X-ray diffraction (XRD), and molecular dynamics simulations (MDS) to gain insights into the interactions in these halogenated alcohols.

2. Materials and Methods

2.1. Materials

Monohydroxy alcohols: 3-chloro-1-propanol, 1-chloro-2-propanol, 3-bromo-1-propanol, under investigation, were purchased from Sigma-Aldrich and 1-bromo-2-propanol from TCI Chemicals. 3Br1P and 3Cl1P vary in the type of X alcohol, and the same is valid for 1Br2P and 1Cl1P. Furthermore, 3Br1P and 1Br2P and 3Cl1P and 1Cl2P form pairs of isomers. Before use, all alcohols were dried under a stream of liquid nitrogen. The chemical structures of the studied alcohols are presented in Fig. 1a.

2.2. Broadband dielectric spectroscopy (BDS) at ambient and elevated pressure

The dielectric studies at ambient pressure were performed using a Novocontrol BDS spectrometer equipped with an Alpha Impedance Analyzer and a Quatro Cryosystem. The capacitor used for the dielectric measurements consisted of two parallel plates of 10 mm diameter made of stainless steel, distanced with two 100 μm glass fibers, and sealed with a Teflon ring. The dielectric spectra were collected in the frequency range of 10^{-1} - 10^{6} Hz at quasi-static conditions after temperature stabilization for 3 min before each measurement using nitrogen gas, with a precision better than 0.2 K. The temperature-dependent measurements were performed with a step of $\Delta T = 2$ K. For the high-pressure experiments, the liquid specimens were poured into Teflon capsules and closed with a plug fitted with two electrodes forming a capacitor, both made from stainless steel. Electrical feedthroughs were run outside the measurement cables and then connected to the Alpha-A impedance analyzer. A special cooling/heating blanket surrounded the system from the outside. Temperature stabilization with $\Delta T = 0.5$ °C accuracy was provided by a closed-loop liquid thermostat during the measurements. The temperature was monitored using a digital thermocouple thermometer HD 2328.0.

2.3. X-ray diffraction (XRD)

The high-pressure XRD experiment was performed for 3Br1P at the ID15B beamline in the European Synchrotron Radiation Facility. The wavelength λ of the beam was 0.410984 Å and the data were collected on an EIGER2X9M CdTe flat panel detector. The sample was measured in a diamond anvil cell (DAC) with the size of the diamond culets of 300 μm. Pressure was controlled by a gas membrane and the ruby fluorescence method was used to measure the actual pressure on the sample with an accuracy of 20 MPa. All measurements were performed at room temperature (293 K). The 2D diffraction data were reduced using the DIOPTAS software and converted into intensity versus the scattering vector $Q = 4\pi\sin\theta/\lambda$, where 2θ is the scattering angle.

2.4. Molecular dynamics simulations (MDS)

The optimized simulation models for 3Br1P and 1Br2P were obtained in GROMACS package [22–24] with implemented general GAFF [25] force field. Parameters used in MDS were analogous to those used

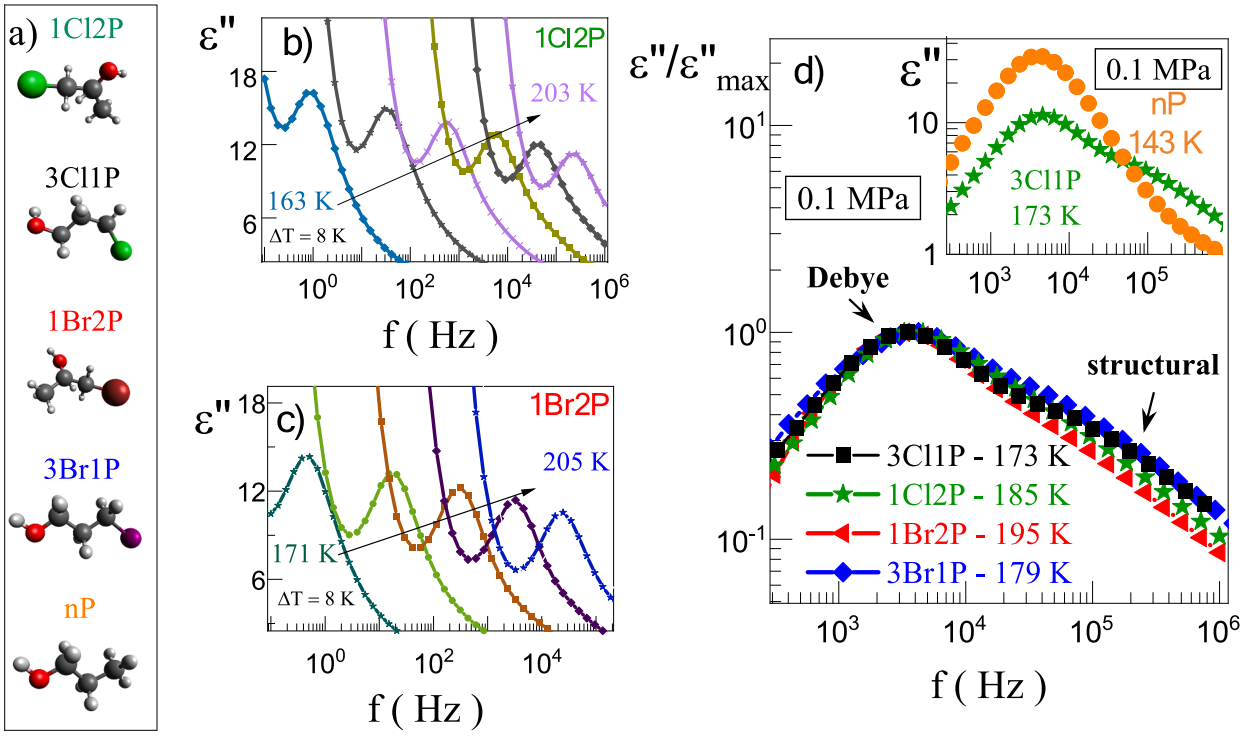

Fig. 1. Chemical structure of 1Cl2P, 3Cl1P, 1Br2P, 3Br1P (a). Dielectric loss spectra at ambient pressure for 1Cl2P (b) and 1Br2P (c). Normalized and horizontally-shifted spectra of XAs (c). The inset shows the same maximum ε"(f) peak position of 1Cl2P with reference nP.

in our previous paper [13]. The starting configuration (simulation box containing 2000 molecules) was first run at 293 K, then at 413 K and 1 bar pressure for 10 ns to get a fully disordered system. Afterward, the temperature was set at 293 K, and pressure was increased in steps from 0.1 GPa run for 40 ns, to 0.3, 0.5, 0.7, 1, 2, and 3 GPa runs for 20 ns which were sufficient to achieve equilibrated states. Total and partial structure factors, $S(Q)$ and $S_{\alpha\beta}(Q)$ respectively, according to the Faber and Ziman definition [26], were calculated from the last 10 ns at every high-pressure state using TRAVIS software [27–29], where $S(Q) = \sum_{\alpha}\sum_{\beta} S^{w}_{\alpha\beta}(Q)$, α and β indicate the atomic species, and $S^{w}_{\alpha\beta}(Q)$ is the partial structure factor $S_{\alpha\beta}(Q)$ between these species weighted by their concentrations and the atomic forms factors, as demonstrated in [30]. Cluster sizes were calculated from those configurations as well, using the GROMACS gmx clustsize program, providing conditions for the hydrogen-bonded cluster: distance O-O < 3.5 Å, and the halogen cluster: distance – Br-Br < 4 Å, which were the first minima of the partial O-O and Br-Br distribution functions. Such distances are in agreement with the literature data for O-H···O and X···X bonds [31–33]. The applied criterion for cluster formation, which is based only on the short contact distance restriction, neglecting the angular restriction was chosen for simplicity.

2.5. Density functional theory (DFT)

DFT calculations using the B3LYP hybrid functional and the aug-cc-pVDZ basis set were performed within the Gaussian 16 software package; augmented versions of the preceding basis set with added diffuse functions to describe the lone pair electrons better. Molecule geometry optimisation was performed using Opt = tight criteria, and the Polar keyword was included in the input file to calculate dipole moment and polarizability. The geometry of the rotamers was determined using the GMMX Conformer module in GaussView 6 software, and then optimisation was performed for each of them. The molecular dipole moment and polarizability (an isotropic component of the tensor) were determined by the Boltzmann weighted average.

2.6. Differential scanning calorimetry (DSC)

The studied alcohols were measured calorimetrically using a Mettler-Toledo DSC apparatus equipped with an HSS8 ceramic sensor (heat flux sensor with 120 thermocouples) and a liquid nitrogen cooling accessory. The temperature-dependent measurements were conducted on the samples previously poured into a sealed aluminum pan of 40 μl volume. The thermograms were collected on cooling and heating in the 123–298 K temperature range. The cooling and heating rates were 10 K min^{-1}, respectively. The calorimetric measurements were carried out in the nitrogen atmosphere with a flow of 60 ml min^{-1}. The glass transition temperature of each compound was determined from the heating scans as the midpoint of the glass transition step.

3. Results and discussion

3.1. Impact of isomerism and halogen type on molecular dynamics at atmospheric pressure

To investigate the effect of isomerism and type of X atom (Cl, Br) on the properties of halogen derivatives of nP, we performed dielectric measurements over a wide temperature range (Fig. 1b and c). One can add that data obtained for 3Cl1P and 3B1P were taken from Ref. [13]. Representative loss spectra ε"(f) recorded at selected temperatures revealed the presence of two relaxation processes above T_g which shift to the lower frequencies with lowering the temperature for all systems. However, it is also visible that the faster mode in some samples is less pronounced with respect to others. This effect is well illustrated in Fig. 1d, where we have shown the data normalized to the maximum of the main peak. For comparison also spectrum measured for nP was presented as inset to this graph. As can be seen the faster mode (labeled herein as α) in nP is observed as a redundant wing on the high-frequency side of the slower process (denoted as Debye or D due to its characteristic shape), whereas in the case of 3Cl1P, 1Cl2P, 3Br1P, and 1Br2P, this relaxation, although partially covered by the dominant D relaxation, is

easily detectable as a separate process. In XAs containing a chlorine atom (3Cl1P, 1Cl2P), the α relaxation process exhibits a higher relative amplitude and is more distinct compared to the Debye (D) relaxation peak than in XAs with a bromine atom (3Br1P, 1Br2P). Specifically, the α relaxation process in 3Cl1P and 1Cl2P shows a more pronounced distinction from the D process. Our fitting analysis supports this observation, showing that the α process in chlorine-containing XAs contributes more significantly to the overall dielectric response. In addition, Fig. 2a and Fig. 2b show the dielectric loss spectra ε"(f) of 1Cl2P and 1Br2P measured at 181 K together with the fits utilizing Debye, Cole-Davidson, and Cole-Cole functions, which describe respectively D, α, and β processes. Herein it should be stressed that analysis of the behavior of β process is out of the scope of this paper.

To gain further insight into how the type of X atom and the position of the –OH group affect the self-association process in the analyzed samples, we calculated the g_k according to the following formula:

$$g_k = \frac{9k_B\varepsilon_0 MT(\varepsilon_s - \varepsilon_\infty)(2\varepsilon_s + \varepsilon_\infty)}{\rho N_A \mu^2 \varepsilon_s} \quad (1)$$

where ε_s and ε_∞ are the static and high-frequency permittivity, respectively; N_A is Avogadro's number; ρ the density of the liquid at temperature T; μ_0 the dipole moment of the isolated molecule; ε_0 the absolute permittivity of vacuum; M the molecular weight, and k_B Boltzmann's constant [8]. The calculated g_k values are considerably higher than 1 for all the studied samples (see Fig. 2c). Considering the Dannhauser model, the results obtained indicate that all the analyzed compounds tend to organize into chain aggregates. Nevertheless, it should be noted that the highest g_k value determined for 2Cl1P ($g_k \approx 3.2$) suggests that this alcohol has the highest concentration of H-bonded clusters or the number of molecules in associates is the highest. More importantly, the differences between the calculated g_k in the halogen derivatives of nP suggest that the type of X atom, as well as the isomerism, play an important role in the association phenomenon. It seems that the type of halogen atom and its position in the backbone may influence the architecture of the supramolecular associates and population of ring- or chainlike clusters of the studied compounds.

3.2. High pressure effects on molecular dynamics and self-organization

3.2.1. Effect of high pressure on molecular relaxation processes: behavior of D and α processes

In the next step, we performed isothermal high-pressure experiments at around T = 208 K on the selected systems to explore the impact of strong densification on the behavior of molecular processes observed above the T_g. We observed that the difference in the time scales between the D and α relaxation processes decreases with increasing pressure, mimicking the effect of temperature lowering. Based on these observations, we chose to fit the dielectric loss spectra using a single Cole-Davidson function and constant-current conductivity. The fitting results showed that the D and α processes converge as pressure increases, leading to a single non-exponential relaxation process (labeled as Debye like (D_{like}) relaxation) in the dielectric spectra of the studied alcohols Fig. 3a. This behavior can be attributed to changes in the concentration and morphology of molecular ensembles, as well as the possibility that structural relaxation is more sensitive to compression than the Debye process. This results in reduced time scale separation or changes in the amplitude of the D and α contributions to the main peak under high pressure.

3.2.2. Structural reorganization in hydrogen-bonded clusters under pressure

Compression has been proposed to reduce the length of HB structures and the size and number of chain clusters [14]. Shorter chains relax faster, reducing the time scale separation between the D and α processes. The literature [17,19] describes that the temporal separation between the D and α relaxation processes decreases under pressure. For some monoalcohols (MAs), the morphology of HB clusters changes with pressure, as observed in 4M3H and 5M3H [14,34], where cyclic clusters transform into linear ones. In contrast, a decrease in the amplitude of the D_{like} relaxation process with increasing pressure was observed for 2E1H and 2E1B [14,19,35]. It indicates that the linear clusters in these substances may decay in favor of branched ones, which may also consist of long chains. Therefore, we attribute the reduction in D_{like} process amplitude to the shorter chains and/or their smaller population in the material. However, we acknowledge that this is just one of several possible scenarios.

Another explanation is that the D and α relaxation processes differ in sensitivity to pressure, with the α process being more pressure-sensitive, potentially reducing their separation. Studies [36–37] show that pressure affects aggregation in associating liquids, increasing the average size of hydrogen-bonded clusters while altering their architecture. Ring-shaped clusters may decrease in favor of branched or linear structures, depending on molecular structure. Thus, pressure may transform linear clusters into more complex, branched structures with larger volumes or higher molar masses, even if their length decreases [3,7,28].

3.2.3. Pressure-induced relaxation dynamics and activation volumes of halogenated alcohols: insights from steepness index, fragility, and comparative analysis

Isothermal dependence of D_{like} relaxation times, increases with compression in a non-linear manner for all analyzed alcohols, please see Fig. 3b. The relaxation times were parameterized using the pressure equivalent of the Vogel-Fulcher-Tamman-Hesse (VFTH) equation (so-called pVFTH):

$$\tau = \tau_0 exp\left(\frac{D_p P}{P_0 - P}\right) \quad (2)$$

where τ_0 is the relaxation time at ambient pressure, p_0 is the pressure of the ideal glass, and D_P is a parameter depending on the pressure

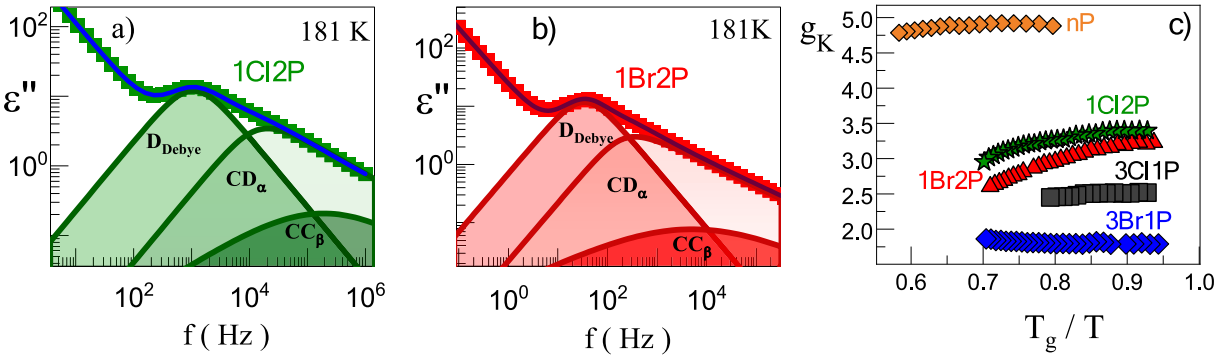

Fig. 2. Dielectric loss spectrum for 1Cl2P (a) and 1Br2P (b) at 181 K and functions: Debye, Cole-Davidson, and Cole-Cole. The g_k for the studied alcohols (c), and data obtained for nP were taken from Ref. [13].

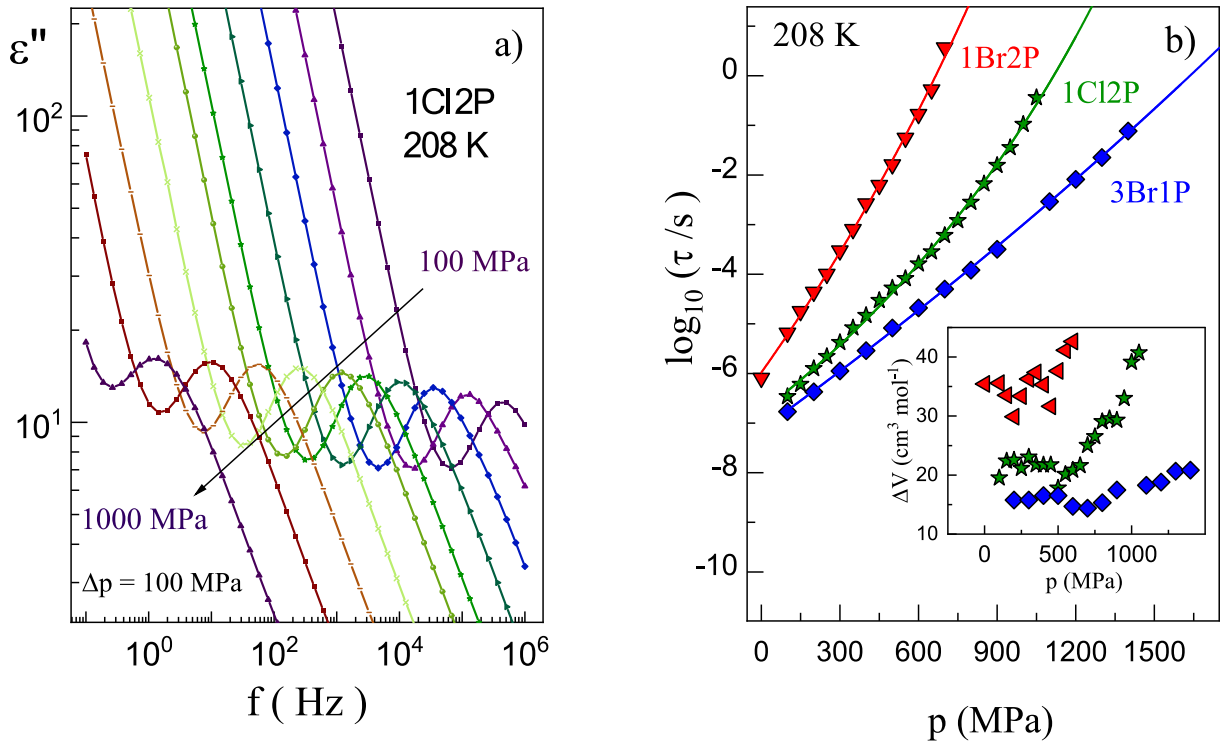

Fig. 3. Selected dielectric loss spectra ε"(f) measured in the supercooled liquid state between 100 and 1000 MPa at 208 K (a). Pressure dependence of relaxation times at 208 K for 3Br1P, 1Br2P, and 1Cl2P (b), the inset shows ΔV for individual alcohols.

sensitivity of the material [38–39]. We can observe that 1Br2P and 1Cl2P show longer relaxation times than 3Br1P for the same pressure, indicating that clusters of molecules 1Br2P and 1Cl2P need more time than 3Br1P to return to equilibrium.

The pressure sensitivity of relaxation times is quantified by ΔV, related to the local volume needed for molecular regrouping, as defined by transition state theory [39]. Under high pressure, the D_{like} process dominates the dielectric spectra, minimizing the separation between the Debye and α processes. This behavior, previously observed in poly-alcohols like glycerol and sorbitol [40], links larger van der Waals radii

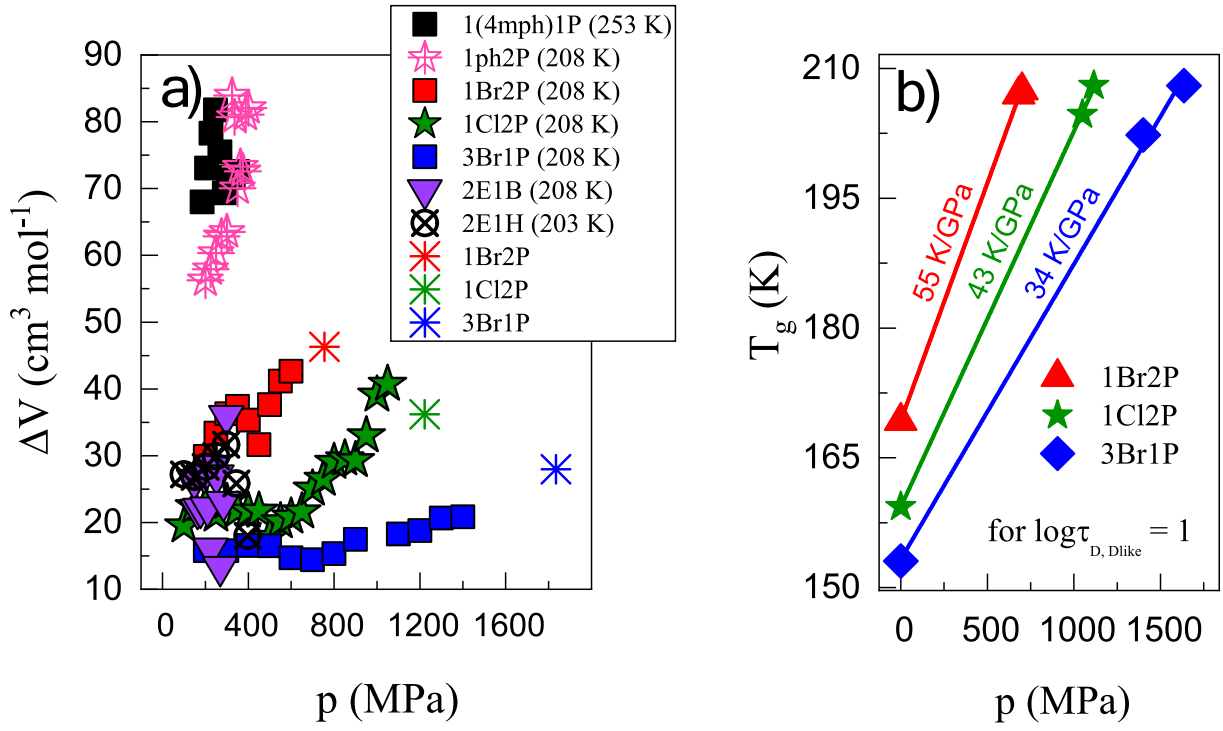

Fig. 4. Compared ΔV and $\Delta V^{\#}$ (marked with crosses) for studied halogen alcohols and alcohols with ethyl and phenyl group (a). Pressure dependence of T_g (b). The solid line indicates the linear fit function whose slope was used to determine the dT_g/dp value for each alcohol.

to greater ΔV values. Fig. 4a compares ΔV values for halogenated alcohols with monoalcohols (e.g., 2E1H, 2E1B) and phenyl-substituted alcohols (e.g., 1ph2B, 1(4mph)1P), showing that bulky substituents increase ΔV, while halogenated alcohols exhibit ΔV values closer to simpler systems due to stabilizing hydrogen-bonding networks. ΔV values calculated using Eq. (3) are shown in the inset in Fig. 3b:

$$\Delta V = RT\left(\frac{dln\tau_{D_{like}}}{dp}\right)_T \tag{3}$$

The highest ΔV value for 1Br2P, followed by 1Cl2P and 3Br1P, reflects structural and intermolecular differences. The –OH group position influences hydrogen bonding and dipole interactions, with 1Br2P and 1Cl2P forming ring-type clusters requiring larger rearrangement volumes, unlike 3Br1P with terminal –OH groups favoring chain-type aggregation. As shown in Fig. 4a, ΔV values for halogenated alcohols are comparable to simpler monoalcohols like 2-ethyl-1-hexanol (2E1H) and 2-ethyl-1-butanol (2E1B) [19], while phenyl-substituted alcohols (e.g., 1(4mph)1P, 1ph2B) exhibit significantly higher values due to rigid phenyl groups that demand greater volumes for reorientation through π-π and hydrophobic interactions. Despite halogen substituents, halogenated alcohols maintain ΔV values similar to simple monoalcohols due to effective hydrogen bonding networks [21]. This reflects analogous relaxation mechanisms under pressure, including chain mobility, bond rotation, and molecular reorientation.

3.2.4. Correlation between glass transition pressure coefficients (dT_g/dp), activation volumes, and structural relaxation in halogenated alcohols

Another important parameter that can be determined from the dielectric data collected as a function of pressure is the pressure coefficient of the glass transition temperature dT_g/dp. The T_g was defined as the temperature at which τ_{Dlike} equals 1 s [41]. While this approach deviates from the standard procedure of using the alpha process timescale, it was necessary due to the challenges in distinctly determining the alpha process under high-pressure conditions. The $T_g(p)$ relationships for all alcohols, visualized in Fig. 4b, have a linear character. In such a case, the dT_g/dp parameter, i.e., the pressure coefficient of T_g, can be estimated from the slope of the linear function [42]. The lowest value of $dT_g/dp = 33$ K/GPa was obtained for 3Br1P, for 1Cl2P $dT_g/dp = 43$ K/GPa, and the highest value of $dT_g/dp = 55$ K/GPa was estimated for 1Br2P. In the literature, a formula connecting T_g, m_p, and ΔV can be found. We determined $\Delta V^{\#}$ value using the following formula:

$$\Delta V^{\#} = 2.303RT\left(\frac{dT_r}{dp}\right)_{mD} \tag{4}$$

where R is the gas constant, dT_g/dp is the pressure coefficient of the glass transition temperature, and m_D is the steepness index for the alcohols under investigation determined from isobaric measurements (depicted in Table 1). The calculated activation volumes $\Delta V^{\#}$ at T_g for 1Br2P $\Delta V^{\#} = 46$ cm^3/mol, for 1Cl2P $\Delta V^{\#} = 36$ cm^3/mol, and for 3Br1P $\Delta V^{\#} = 28$ cm^3/mol are illustrated in Fig. 4a and marked with crosses for the studied alcohols, respectively. As seen in the figure, $\Delta V^{\#}$ values correlate well with the ΔV values. The higher dT_g/dp value for 1Br2P compared to the 3Br1P isomer suggests that 1Br2P is more sensitive to pressure changes. Further observations revealed that 1Cl2P has lower ΔV and dT_g/dp values than 1Br2P. Bromine, being heavier and larger than chlorine, disrupts molecular packing more significantly, increases polarity, and enhances van der Waals interactions due to greater polarizability. These properties make 1Br2P more sensitive to pressure changes. Bromine's higher atomic mass and polarizability compared to chlorine also influence intermolecular forces, such as hydrogen bonding and dipole–dipole interactions, which affect molecular dynamics and thermomechanical properties, including T_g. The reduced mobility of chain segments in 1Br2P further contributes to its higher ΔV and dT_g/dp values. Notably, 3Cl1P crystallizes under high pressure and could not be analyzed in this study (see Supplementary Information (SI)).

Table 1
Glass transition temperatures at ambient pressure were calculated using differential scanning calorimetry. The steepness index at ambient pressure and elevated pressure for the alcohols under investigation.

Chemical name	T_g DSC [K]	m_α	m_D	m_{Dlike}
3-bromo-1-propanol	150 ± 1	55 ± 2	43 ± 2	49 ± 2
1-bromo-2-propanol	164 ± 1	51 ± 2	44 ± 2	49 ± 2
3-chloro-1-propanol	142 ± 1	57 ± 2	43 ± 2	–
1-chloro-2-propanol	155 ± 1	62 ± 2	44 ± 2	49 ± 1

3.2.5. Steepness index (m_p): insights into molecular dynamics under pressure

The steepness index parameter (m_p) was determined using the inverse temperature dependence of relaxation times at ambient pressure (Fig. 5a). Typically, m_p is defined as the slope of the scaled temperature dependence of relaxation times. To avoid extrapolation beyond experimental data, T_g was defined as the temperature where τ_α equals 1 s (Fig. 5b). Relaxation times (τ) for both D and α processes increase nonlinearly with temperature and were fitted using the VFT equation [43–46]. The fragility parameter, defined as:

$$m_p = \left.\frac{dlog\tau}{d\left(\frac{T_g}{T}\right)}\right|_{T_{g=T_r}} \tag{5}$$

reflects the departure from pure activation behavior. At high pressure, the dynamics of the D process resemble those of α-relaxation, limiting conclusions about the structural process m_p. Dielectric loss spectra revealed a single D_{like} process (Fig. 5c) at high-pressure conditions (1.4 GPa for 3Br1P, 1050 MPa for 1Cl2P, and 700 MPa for 1Br2P). While atmospheric D relaxation showed no significant differences between alcohols (Fig. 5d), α-relaxation changes were more pronounced (Fig. 5a). Chlorine's smaller atomic radius and higher electronegativity than bromine likely enhance polarisation interactions in chloropropanols, increasing their fragility compared to bromopropanols. Variations in halogen type and position affect molecular stiffness and flexibility, influencing fragility and relaxation dynamics.

Comparing the different steepness index m_α, m_D, and m_{Dlike} provides insights into how the molecular dynamics of the studied alcohols change under varying temperature and pressure conditions. Specifically, m_α reflects the structural relaxation dynamics, m_D indicates the behavior of the hydrogen-bonded network, and m_{Dlike} shows how these dynamics adapt under high pressure. The differences in these indices help us understand the sensitivity of each relaxation process to temperature and pressure changes. The observed differences can be attributed to variations in molecular structure, intermolecular interactions, and the influence of halogen atoms [47–50].

3.2.6. Comparing pressure sensitivities across halogenated alcohols

The m_D values at atmospheric pressure for the studied monoalcohols were very similar. Under high-pressure conditions, we measured m_{Dlike} values converging to 49 ± 2 for all compounds. However, 3Br1P required 1.4 GPa, 1Cl2P – 1050 MPa, and 1Br2P only 700 MPa to reach this value. These differences reflect varying sensitivity to pressure changes, influenced by molecular structure and interactions, such as hydrogen bonds (HBs) or halogenated HBs. The halogen type affects supramolecular geometry and stability, altering intermolecular interactions and relaxation processes. Structural differences, such as dipole moments and molecular geometry, impact packing density in the glassy state and molecular dynamics under pressure. Variations in pressure required to achieve a consistent m_{Dlike} value highlight the interplay of molecular properties and relaxation behavior. This analysis provides insights into the unique behaviors of halogenated alcohols,

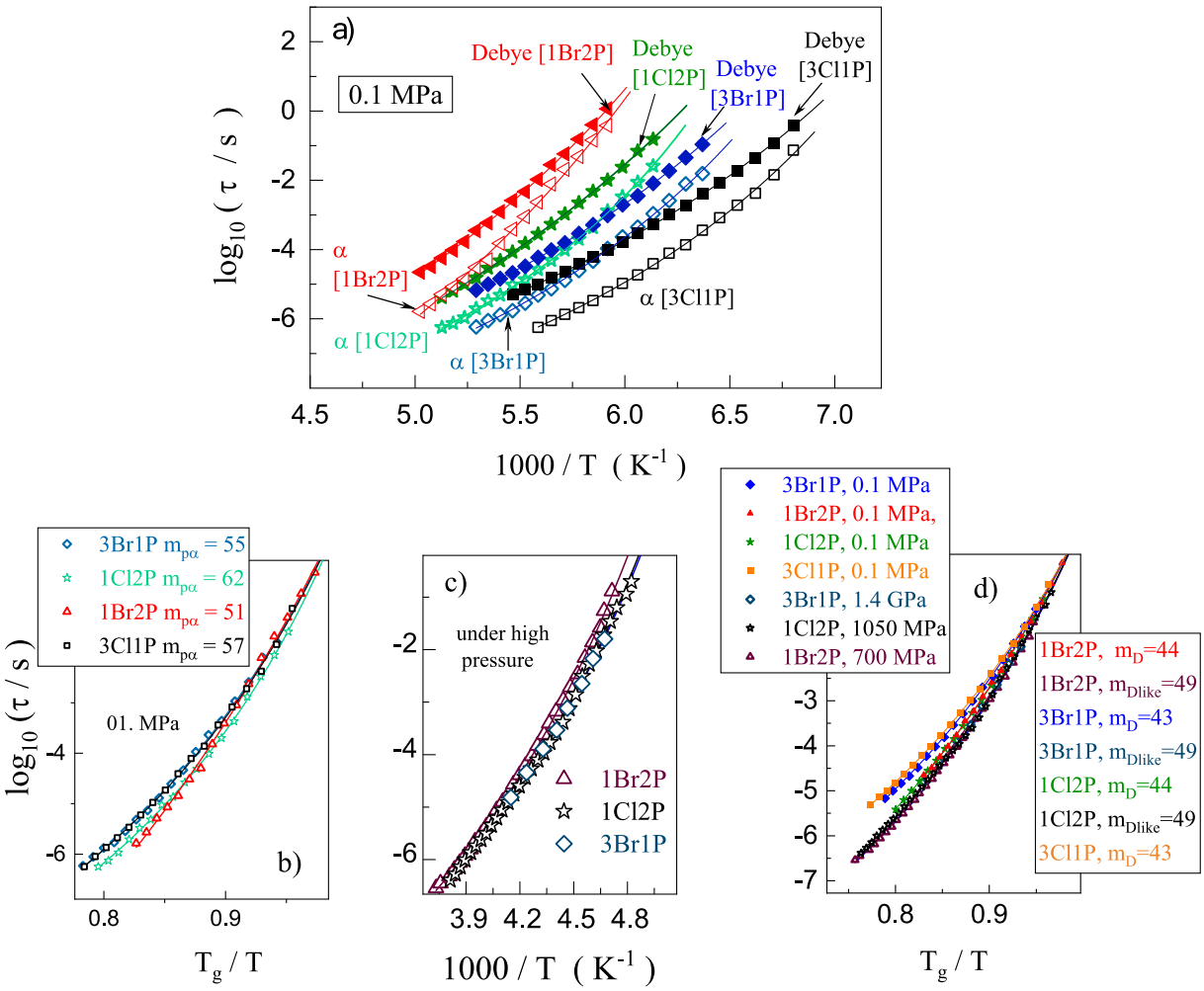

Fig. 5. The logarithm of the relaxation times (τ) vs. 1000 / T for the alpha (α) and Debye (D) processes of all studied alcohols at ambient pressure (0.1 MPa) (a). The solid lines are VFT fits to the data. Dependence of the dielectric relaxation times (τ_α) of the alpha process for 1Br2P, 3Br1P, 1Cl2P, and 3Cl1P as a function of T_g/T at ambient pressure (0.1 MPa) (b). The legend provides the fragility index m_α values for each alcohol. The logarithm of the relaxation times (τ_{Dlike}) vs. 1000/T for the D_{like} process of all studied alcohols under high-pressure conditions (specific pressures for each alcohol indicated in the legend). The solid lines are VFT fits to the data (c). Dependence of the dielectric relaxation times (τ_D and τ_{Dlike}) of the D and D_{like} processes for 1Br2P, 3Br1P, and 1Cl2P as a function of T_g/T at ambient and high-pressure. The legend provides the steepness index m_D and m_{Dlike} values for each condition. Solid lines were fitted using the VFT equation (d).

advancing the understanding of their dynamics under high-pressure conditions [51–58].

3.3. Impact of hydroxyl group position on supramolecular structures and relations dynamics under various thermodynamic conditions

3.3.1. Impact of hydroxyl group position on the amplitude of the D-process

To examine how the position of the hydroxyl group (–OH) affects supramolecular behavior under high-pressure conditions, we first analyzed the dielectric spectra of the studied compounds (Fig. 6a) as a representative example, and then compared the amplitude of the D-process for selected alcohols at the same frequency: 3Br1P (Fig. 6b), 1Br2P (Fig. 6c), and 1Cl2P (Fig. 6d). Results showed that the amplitude slightly increased for 1Br2P and 1Cl2P (with non-terminal –OH groups) under compression, while it decreased for 3Br1P (with a terminal –OH group). This suggests that the position of the –OH group significantly influences intermolecular interactions and the type of supramolecular structures formed under pressure. For 1Br2P and 1Cl2P, cyclic or branched structures appear more stable under compression, increasing the amplitude. Conversely, for 3Br1P, chain-like aggregates dominated at ambient pressure, but these structures collapsed under compression, reducing the amplitude. These results align with Dannhauser's observations [6] that non-terminal –OH groups favor ring-like hydrogen-bonded clusters, while terminal –OH groups promote chain-like structures.

3.3.2. DFT calculations

DFT calculations were conducted to further evaluate the hydrogen-bonded structures (see SI). For 1X2P (X = Cl, Br), three types of dimers were identified:

- linear dimers: O-H···O and X-H···O bonds (~5 and ~ 2 kcal/mol, respectively);
- cyclic dimers: X = H···O bonds (~2 kcal/mol).

These findings indicate that non-terminal –OH groups in 1Br2P and 1Cl2P favor stable cyclic dimers, influencing the molecular dynamics under pressure. In contrast, for 3Br1P, the terminal –OH group promotes chain-like structures that are more sensitive to compression.

Molecular dynamics simulations [37] for similar systems, such as 2E1H (terminal –OH) and 2M3H (non-terminal –OH), showed consistent trends under high pressure. For 2E1H, linear clusters decrease under compression, favoring branched structures. For 2M3H, ring clusters convert to linear structures under pressure. A similar behavior is

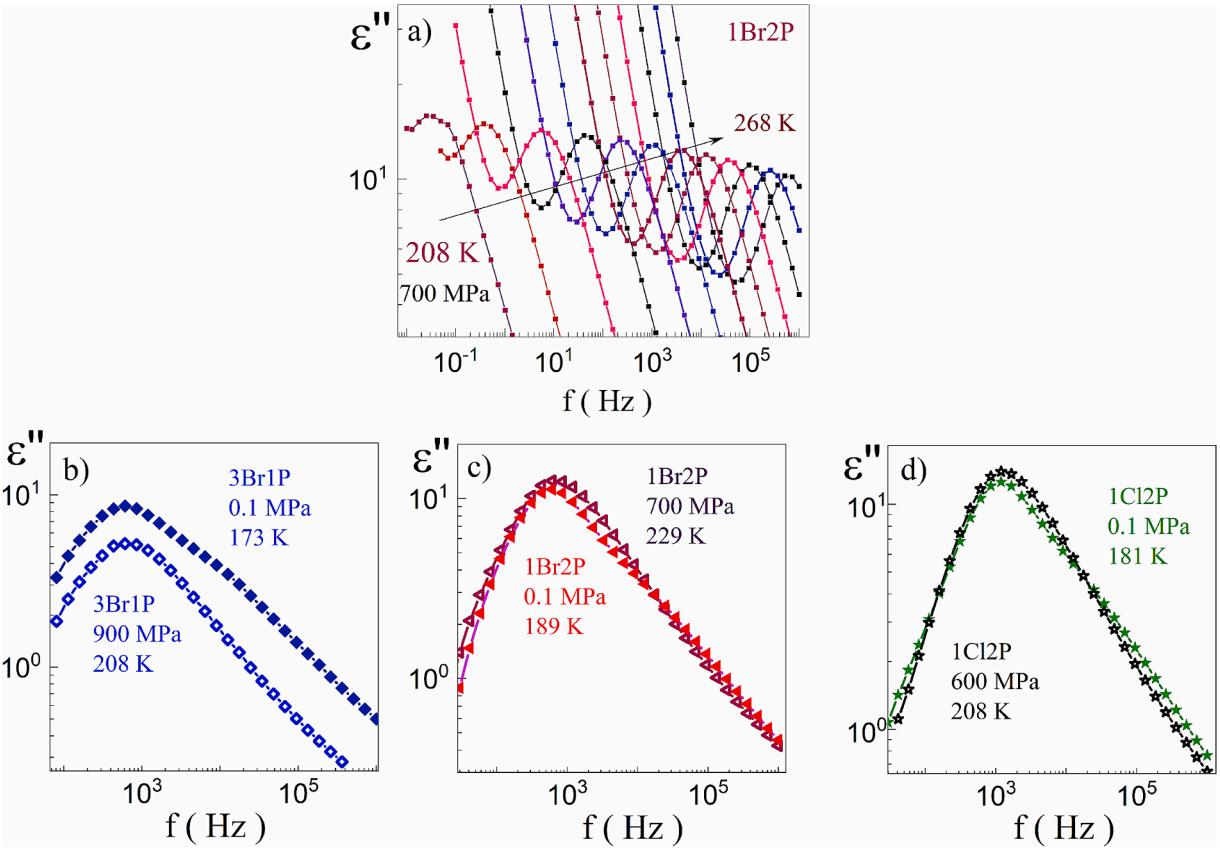

Fig. 6. Dielectric loss spectra at elevated pressure (700 MPa) for 1Br2P (a). Comparison of the main process at atmospheric and elevated pressure characterized by the same relaxation times for 3Br1P, 1Br2P, and 1Cl2P (b, c, d).

hypothesized for halogenated alcohols:

- In 3Br1P, chain structures collapse into ring or branched forms, decreasing the D-process amplitude;
- In 1Br2P and 1Cl2P, ring clusters transition into linear forms, increasing the D-process amplitude.

These results are consistent with observations for other systems like 4M3H and 5M3H [14,34], where compression led to notable changes in cluster morphology and D-process intensity.

3.3.3. *Pressure dependence of dielectric strength (Δε)*

We further compared the changes in dielectric strength (Δε) under pressure (Fig. 7). For 3Br1P, Δε decreased with increasing pressure, which can be attributed to the collapse of long chain-like hydrogen-bonded aggregates. In contrast, for 1Br2P and 1Cl2P, Δε increased, suggesting the formation of more resilient or pressure-stabilized structures, likely transitioning from cyclic to linear configurations under compression.

3.3.4. *Structural insights from experimental diffraction and molecular dynamics simulations*

3Br1P alcohol was subjected to a high-pressure diffraction experiment in diamond anvil cells at ambient temperature. The pattern of diffraction intensity versus the scattering vector (Q) (Fig. 8a) at low pressure shows one main peak at ~ 1.5 $Å^{-1}$, which moves to higher Q values and grows in intensity and width with increasing pressure. This indicates approaching intermolecular distances and increasing density, as well as an ongoing rearrangement of intermolecular structure with compression. A deeper understanding of this structural transformation was possible by analyzing partial atom–atom structure factors derived

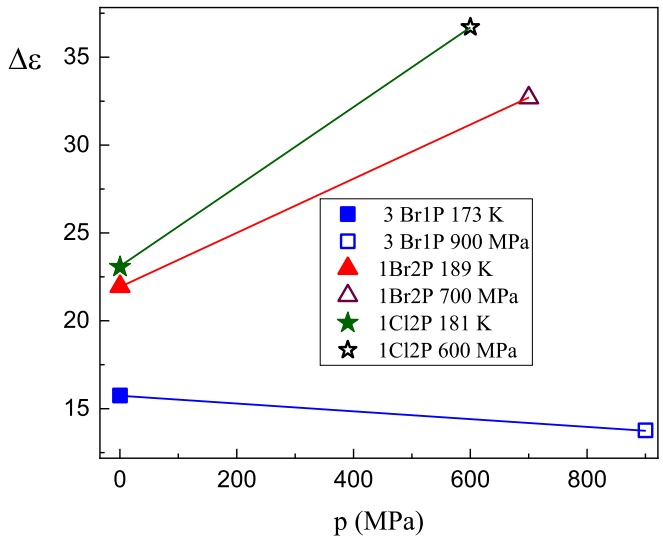

Fig. 7. Comparison of the change in Δε with pressure for the studied halogen alcohols: 3Br1P, 1Br2P, and 1Cl2P. For 3Br1P, the data were recorded at 173 K (0.1 MPa) and 208 K (900 MPa); for 1Br2P, at 189 K (0.1 MPa) and 229 K (700 MPa); and for 1Cl2P, at 181 K (0.1 MPa) and 208 K (600 MPa). Solid lines connect the points for each alcohol to enhance readability.

from the MDS. MDS provided structural models of 3Br1P at the same thermodynamic conditions as applied in the XRD experiment, and the theoretical diffraction data derived from these models in the form of total structure factors demonstrated similar behavior like the experimental data. Fig. 8a shows pressure-induced changes in the partial

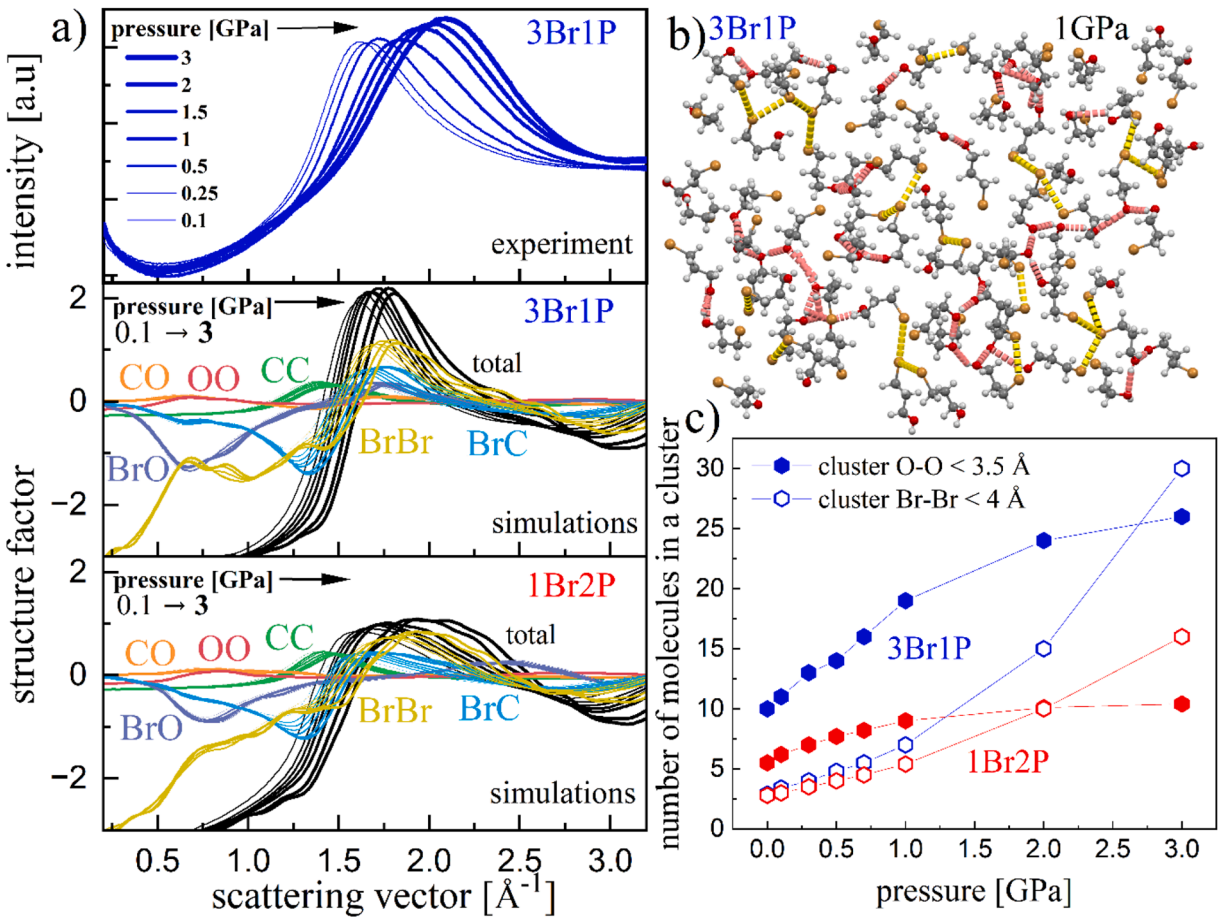

Fig. 8. Diffraction results obtained from high-pressure X-ray experiment and molecular dynamics simulations, both performed at temperature of 293 K (a). A single plane of the optimized structural model of 3Br1P with marked OO (red) and BrBr (orange) intermolecular distances (b). The evolution of the average number of molecules organized in hydrogen-bonded and halogen clusters (average cluster size) with pressure (c).

structure factors that sum up to total structure factors marked with a black line. The strongest contribution to the main diffraction peak is given by BrBr correlations. One can see that the Br-Br function has a similar course with compression as the main peak in the total structure factor. Therefore, one can assign the changes in the intermolecular local structure at high pressure to enhanced correlations between Br atoms. Besides, BrBr, BrO, and OO correlations at ~ 0.6–0.7 Å^{-1} appear due to a medium-range ordering, which usually arises when molecules organize themselves in supramolecular clusters due to intermolecular interactions. A similar behavior was observed for 1Br2P (the lowest panel in Fig. 8a). However, these peaks hardly change with pressure. In particular, the OO function, which results from a medium-range order of hydroxyl groups organized in small supramolecular clusters via O-H···O HBs, is invariant to pressure changes. Our previous paper demonstrated that halogen alcohols at ambient pressure exhibit a significant supramolecular clustering via HBs and weaker association via halogen atoms [13]. Since the studied alcohols contain one X atom per molecule, they may hypothetically form attractive intermolecular halogen interactions according to the X···X scheme, which can be detected by, among others, short XX contacts. Agglomeration of such XX contacts indicates the formation of supramolecular halogen clusters, while agglomeration of short OO contacts signifies HB clusters. Here, we checked how these two types of molecular organizations evolved with increasing pressure based on the models derived from MDS (please see a representative plane of the model for the 3Br1P at 1GPa in Fig. 8b). In Fig. 8c, one can see the evolution of the average size of the O-O and Br-Br clusters (the average number of molecules forming such clusters) with compression. Firstly, 1Br2P forms smaller clusters, both O-O and Br-Br, than its isomer 3Br1P. This behavior was explained earlier due to a bigger steric hindrance in 1Br2P arising from the hydroxyl group's position in the molecule's center. Secondly, both 3Br1P and 1Br2P have, on average, bigger O-O than Br-Br clusters up to pressure ~ 2–2.5 GPa when the halogen clusters gain greater sizes. Both types of clusters grow with compression, but the halogen aggregates rise much more rapidly.

A simple interpretation of changes in the architecture of supramolecular clusters performed based on dielectric measurements by themselves may be misleading. Their architecture cannot be fully characterized based on just dielectric data alone, because, as the XRD and MDS data revealed, with compression, halogen clusters grow. However, they may possess a zero resultant dipole moment, so cannot be fingerprinted by dielectric spectroscopy. Moreover, they may compete with clusters formed by HBs and decrease their size. The amplitude of the D process in the dielectric spectra may decrease, first of all, through some kind of rearrangement of linear clusters into more branched or ring clusters. Secondly, due to the presence of additional types of supramolecular clusters, formed by Cl-Cl/Br-Br, as well as Cl-O and Br-O interactions indicated by DFT, which may grow faster in 3Br1P than in 1Br2P under pressure and reduce the average number of supramolecular structures connected by classical hydrogen bonds. The terminal position of the OH group in 3Br1P seems to favor the formation of linear hydrogen-bonded clusters, which are less stable due to the lack of interaction with the X-H···O hydrogen bonds suggested by the DFT calculations. Simultaneously, the average number of molecules in the stable H-bonded clusters may increase with higher pressure – as presented in Fig. 8c, the average size of O-O correlations resulting from the hydrogen bonds structuring are getting bigger with higher pressure. It is

also worth noting here that the results from molecular dynamics simulations at least partially support the previous interpretations [12,19] of dielectric spectra. They say that depending on the position of the OH group in the carbon chain, in the non-terminal or terminal position, there is a decrease or increase in the amplitude of the D process. However, in general, the picture is more complicated than can be concluded from a simple interpretation of dielectric data. The results from molecular dynamics simulations reveal structural details that are difficult to deduce from the dielectric data, and without them, it would be impossible to make a correct interpretation of the architecture of supramolecular structures.

High-pressure X-ray diffraction (XRD) and molecular dynamics simulations (MDS) provided structural insights at room temperature (293 K), while dielectric spectroscopy characterized these systems at lower temperatures in the supercooled state. Despite technical limitations, we assumed the general structural trends observed at room temperature hold at lower temperatures [37]. Key observations from 2E1H and 2M3H studies [37] showed that:

- lower temperatures favor the growth of branched and ring-like clusters;
- isothermal compression reduces monomers and ring-like clusters while increases branched aggregates (2E1H) or linear clusters (2M3H).

Applying this understanding to halogenated alcohols, we hypothesize:

- 3Br1P: Pressure reduces chain structures, promoting ring and branched clusters [14,34].
- 1Br2P and 1Cl2P: Pressure induces a transition from stable ring clusters to linear structures, enhancing the amplitude of the D-process.

By analyzing the D-process amplitude, dielectric strength, and structural configurations, we conclude that the position of the –OH group plays a critical role in determining supramolecular organization and relaxation dynamics under compression. Terminal –OH groups favor chain-like structures that collapse under pressure, while non-terminal –OH groups promote cyclic and linear clusters, which transition under compression, stabilizing the dynamics of the D process.

3.3.5. *Future perspectives*

The findings from this study open avenues for further exploration, particularly in the context of halogenated monoalcohols and their potential applications. Among other things, our future work focuses on studying the molecular dynamics and supramolecular organization of halogenated monoalcohols such as 2-chloro-1-ethanol, 3-chloro-1-propanol, 2-bromo-1-ethanol, 3-bromo-1-propanol, 2-iodo-1-ethanol, and 3-iodo-1-propanol under different thermodynamic conditions. High-pressure studies have already demonstrated that the carbon chain length and halogen type significantly influence the transition between cyclic and chain-like aggregates. Expanding these investigations to other halogenated alcohols could reveal additional insights into the interplay between molecular structure and supramolecular organization.

Furthermore, the understanding of crystallization tendencies and self-assembly phenomena of these materials holds particular relevance for cryopreservation applications. For example, alcohols with shorter carbon chains, which exhibit a greater tendency to form hydrogen-bonded clusters, may act as cryoprotectants by reducing crystallization during freezing. Specifically, understanding how these compounds stabilize amorphous phases and prevent ice nucleation could contribute to the development of advanced cryopreservation protocols for biological and biochemical materials [59–60].

By extending this research to a broader range of halogenated alcohols and examining their behavior under varying conditions, we aim to deepen our understanding of the relationship between molecular dynamics, supramolecular assembly, and practical applications, including materials design and cryopreservation [3].

4. Conclusions

- The position of the –OH group (primary or secondary) and the type of halogen atom (Cl or Br) significantly affect the molecular dynamics of the studied monoalcohols:
- 3-chloro-1-propanol, 1-chloro-2-propanol, 3-bromo-1-propanol, and 1-bromo-2-propanol. The differences are particularly reflected in the behavior of the D relaxation under varying thermodynamic conditions.
- Hydroxyl group positioning influences the dominant relaxation process under high-pressure and low-temperature conditions. For example, 1-bromo-2-propanol exhibits higher pressure coefficients and activation volumes than 3-bromo-1-propanol.
- Under high pressure, 3-bromo-1-propanol shows a decrease, while 1-bromo-2-propanol and 1-chloro-2-propanol exhibit a slight increase in the amplitude of the main relaxation process compared to ambient pressure spectra. These differences are attributed to the formation of cyclic supramolecular clusters in 1-bromo-2-propanol and 1-chloro-2-propanol, and chain structures in 3-bromo-1-propanol, as confirmed by DFT calculations.
- Analysis of the steepness index for the Debye process reveals distinct responses to compression among the alcohols.
- DFT calculations demonstrate that 1X2P (X = Cl, Br) forms cyclic dimers through hydrogen bonds (O–H···O and X = H···O), whereas 3X1P does not, due to steric repulsion from methyl groups.
- Experimental spectroscopy and molecular dynamics simulations confirm that supramolecular clusters are stabilized by hydrogen bonds and weaker halogen interactions. Simulations also reveal that 3-bromo-1-propanol forms larger clusters than
- 1-bromo-2-propanol, highlighting the limitations of dielectric spectroscopy in depicting supramolecular structures.
- Under high pressure, molecular dynamics simulations show the formation of unusual clusters organized by halogen-halogen or halogen-OH interactions. These clusters compete with classical hydrogen-bonded aggregates, affecting the Debye process. Their presence, not easily detectable by dielectric measurements, likely explains differences in relaxation dynamics.
- The tendency of 3-chloro-1-propanol to crystallize under high pressure, not observed at ambient pressure, underscores the importance of high-pressure studies in understanding molecular behavior.
- The findings highlight the role of high-pressure investigations in elucidating the effects of molecular structure and intermolecular interactions on the relaxation dynamics of associating liquids.

We acknowledge the European Synchrotron Radiation Facility (ESRF), Grenoble, France, for the high-pressure XRD experiment at the ID15B beamline (proposal SC-5158). We are grateful to Michael Hanfland at the ESRF for providing assistance in using the beamline and to Andrzej Burian for his help in the diffraction data treatment and analysis. The access to ESRF was financed by the Polish Ministry of Education and Science – decision number: 2021/WK/11. The research was financed with financial support from the National Science Centre, Poland within the OPUS Project No. UMO-2019/35/B/ST3/02670, which K. Ł., J. G., K. J., K. K., and S.P. would like to acknowledge.

CRediT authorship contribution statement

Kinga Łucak: Conceptualization, Visualization, Methodology, Investigation, Formal analysis, Writing – original draft, Writing – review & editing. Data Curation. **Anna Z. Szeremeta:** Investigation, Formal analysis, Writing – review & editing. **Joanna Grelska:** Investigation, Formal analysis. **Karolina Jurkiewicz:** Investigation, Formal analysis,

Writing – original draft, Writing – review & editing. **Sławomir Kołodziej:** Writing – review & editing. **Roman Wrzalik:** Investigation, Formal analysis. **Kamil Kamiński:** Writing – review & editing. **Sebastian Pawlus:** Conceptualization, Writing – review & editing, Project administration, Data Curation, Funding acquisition.

Declaration of competing interest

The authors declare that they have no known competing financial interests or personal relationships that could have appeared to influence the work reported in this paper.

Appendix A. Supplementary data

Supplementary data to this article can be found online at https://doi.org/10.1016/j.molliq.2025.127045.

Data availability

Data will be made available on request.

References

[1] J. Grelska, K. Jurkiewicz, A. Burian, S. Pawlus, Supramolecular Structure of Phenyl Derivatives of Butanol Isomers, J. Phys. Chem. B 126 (19) (2022) 3563–3571, https://doi.org/10.1021/acs.jpcb.2c01269.

[2] S. Pothoczki, L. Pusztai, I. Bakó, Variations of the Hydrogen Bonding and Hydrogen-Bonded Network in Ethanol-Water Mixtures on Cooling, J. Phys. Chem. B 122 (26) (2018) 6790–6800, https://doi.org/10.1021/acs.jpcb.8b02493.

[3] R. Böhmer, C. Gainaru, R. Richert, Structure and Dynamics of Monohydroxy Alcohols—Milestones towards Their Microscopic Understanding, 100 years after Debye, Phys. Rep. 545 (4) (2014) 125–195, https://doi.org/10.1016/j.physrep.2014.07.005.

[4] S. Patil, R. Sun, S. Cheng, S. Cheng, Molecular Mechanism of the Debye Relaxation in Monohydroxy Alcohols Revealed from Rheo-Dielectric Spectroscopy, Phys. Rev. Lett. 130 (9) (2023), https://doi.org/10.1103/PhysRevLett.130.098201.

[5] C. Gainaru, R. Meier, S. Schildmann, C. Lederle, W. Hiller, E.A. Rössler, R. Böhmer, Nuclear-Magnetic-Resonance Measurements Reveal the Origin of the Debye Process in Monohydroxy Alcohols, Phys. Rev. Lett. 105 (25) (2010), https://doi.org/10.1103/PhysRevLett.105.258303.

[6] W. Dannhauser, Dielectric Study of Intermolecular Association Isomeric Octyl Alcohols, J. Chem. Phys. 48 (11) (1968) 1911, https://doi.org/10.1063/1.1668989.

[7] L.P. Singh, R. Richert, Watching Hydrogen-Bonded Structures in an Alcohol Convert from Rings to Chains, Phys. Rev. Lett. 109 (16) (2012), https://doi.org/10.1103/PhysRevLett.109.167802.

[8] P. Bordewijk, On the relationship between the Kirkwood correlation factor and the dielectric permittivity, J. Chem. Phys. 73 (1) (1980) 595–597, https://doi.org/10.1063/1.439841.

[9] N. Soszka, B. Hachuła, M. Tarnacka, J. Grelska, K. Jurkiewicz, M. Geppert-Rybczyńska, R. Wrzalik, K. Grzybowska, S. Pawlus, M. Paluch, Aromaticity effect on supramolecular aggregation. Aromatic vs. cyclic monohydroxy alcohols, Spectrochim. Acta A Mol. Biomol. Spectrosc. 276 (2022), https://doi.org/10.1016/j.saa.2022.121235.

[10] A. Nowok, M. Dulski, J. Grelska, A.Z. Szeremeta, K. Jurkiewicz, K. Grzybowska, M. Musiał, S. Pawlus, Phenyl Ring: A Steric Hindrance or a Source of Different Hydrogen Bonding Patterns in Self-Organizing Systems? J. Phys. Chem. Lett. 12 (8) (2021) 2142–2147, https://doi.org/10.1021/acs.jpclett.1c00186.

[11] A. Nowok, K. Jurkiewicz, M. Dulski, H. Hellwig, J.G. Małecki, K. Grzybowska, J. Grelska, S. Pawlus, Influence of molecular geometry on the formation, architecture and dynamics of H-bonded supramolecular associates in 1-phenyl alcohols, J. Mol. Liq. 326 (2021), https://doi.org/10.1016/j.molliq.2021.115349.

[12] J. Grelska, K. Jurkiewicz, A. Nowok, S. Pawlus, Computer simulations as an effective way to distinguish supramolecular nanostructure in cyclic and phenyl alcohols, Phys. Rev. E 108 (2) (2023), https://doi.org/10.1103/PhysRevE.108.024603.

[13] K. Łucak, A.Z. Szeremeta, R. Wrzalik, J. Grelska, K. Jurkiewicz, N. Soszka, B. Hachuła, D. Kramarczyk, K. Grzybowska, B. Yao, K. Kamiński, S. Pawlus, Experimental and Computational Approach to Studying Supramolecular Structures in Propanol and Its Halogen Derivatives, J. Phys. Chem. B 127 (42) (2023) 9102–9110, https://doi.org/10.1021/acs.jpcb.3c02092.

[14] D. Fragiadakis, C.M. Roland, R. Casalini, Insights on the origin of the Debye process in monoalcohols from dielectric spectroscopy under extreme pressure conditions, J. Chem. Phys. 132 (2010), https://doi.org/10.1063/1.3374820.

[15] S. Pawlus, M. Paluch, M. Dzida, Molecular Dynamics Changes Induced by Hydrostatic Pressure in a Supercooled Primary Alcohol, J. Phys. Chem. Lett. 1 (21) (2010) 3249–3253, https://doi.org/10.1021/jz101288v.

[16] E. Thomas, S. Kołodziej, M. Wikarek, S. Klotz, S. Pawlus, M. Paluch, Inflection point in the Debye relaxation time of 2-butyl-1-octanol, J. Chem. Phys. 149 (21) (2018), https://doi.org/10.1063/1.5064757.

[17] S. Pawlus, M. Wikarek, C. Gainaru, M. Paluch, R. Böhmer, How do high pressures change the Debye process of 4-methyl-3-heptanol? J. Chem. Phys. 139 (6) (2013) 06450, https://doi.org/10.1063/1.4816364.

[18] S. Pawlus, M. Paluch, M. Nagaraj, J.K. Vij, Effect of high hydrostatic pressure on the dielectric relaxation in a noncrystallizable monohydroxy alcohol in its supercooled liquid and glassy states, J. Chem. Phys. 135 (8) (2011), https://doi.org/10.1063/1.3626027.

[19] M. Wikarek, S. Pawlus, S.N. Tripathy, A. Szulc, M. Paluch, How Different Molecular Architectures Influence the Dynamics of H-bonded Structures in Glass-Forming Monohydroxy Alcohols, J. Phys. Chem. B 120 (25) (2016) 5744–5752, https://doi.org/10.1021/acs.jpcb.6b01458.

[20] Y. Guo, X. Jin, L. Wang, Unusual Debye relaxation in 4-methyl-2-pentanol evidenced by high-pressure dielectric studies, J. Phys. Condens. Matter 33 (2) (2021) 02540, https://doi.org/10.1088/1361-648X/abb742.

[21] S. Kołodziej, J. Knapik-Kowalczuk, K. Grzybowska, A. Nowok, S. Pawlus, Essential meaning of high pressure measurements in discerning the properties of monohydroxy alcohols with a single phenyl group, J. Mol. Liq. 305 (2020), https://doi.org/10.1016/j.molliq.2020.112863.

[22] M.J. Abraham, T. Murtola, R. Schulz, S. Páll, J.C. Smith, B. Hess, E. Lindahl, GROMACS: high performance molecular simulations through multi-level parallelism from laptops to supercomputers, SoftwareX 1–2 (2015) 19–25, https://doi.org/10.1016/j.softx.2015.06.001.

[23] S. Páll, M.J. Abraham, C. Kutzner, B. Hess, E. Lindahl, Tackling Exascale Software Challenges in Molecular Dynamics Simulations with GROMACS, (2015) 3–27. doi: 10.1007/978-3-319-15976-8_1.

[24] S. Pronk, S. Páll, R. Schulz, P. Larsson, P. Bjelkmar, R. Apostolov, M.R. Shirts, J.C. Smith, P.M. Kasson, D. van der Spoel, et al., GROMACS 4.5: a high-throughput and highly parallel open source molecular simulation toolkit, Bioinformatics 29 (7) (2013) 845–854. doi: 10.1093/bioinformatics/btt055.

[25] J. Wang, R.M. Wolf, J.W. Caldwell, P.A. Kollman, D.A. Case, Development and testing of a general amber force field, J. Comput. Chem. 25 (9) (2004) 1157–1174, https://doi.org/10.1002/jcc.20035.

[26] T.E. Faber, J.M. Ziman, A theory of the electrical properties of liquid metals: III. the resistivity of binary alloys, Philos. Mag. 11 (109) (1965) 153–173. doi: 10.1080/14786436508211931.

[27] M. Brehm, M. Thomas, S. Gehrke, B. Kirchner, TRAVIS—a free analyzer for trajectories from molecular simulation, J. Chem. Phys. 152 (16) (2020), https://doi.org/10.1063/5.0005078.

[28] O. Hollóczki, M. Macchiagodena, H. Weber, M. Thomas, M. Brehm, A. Stark, O. Russina, A. Triolo, B. Kirchner, Triphilic Ionic-Liquid Mixtures: Fluorinated and Non-fluorinated Aprotic Ionic-Liquid Mixtures, ChemPhysChem 16 (15) (2015) 3325–3333, https://doi.org/10.1002/cphc.201500473.

[29] M. Brehm, B. Kirchner, TRAVIS—A Free Analyzer and Visualizer for Monte Carlo and Molecular Dynamics Trajectories, J. Chem. Inf. Model. 51 (8) (2011) 2007–2023, https://doi.org/10.1021/ci200217w.

[30] F. Zhang, Y. Sun, Z. Ye, Y. Zhang, C.Z. Wang, M.I. Mendelev, K.M. Ho, Solute–solute correlations responsible for the prepeak in structure factors of undercooled Al-rich liquids: a molecular dynamics study, J. Phys. Condens. Matter 27 (20) (2015), https://doi.org/10.1088/0953-8984/27/20/205701.

[31] J.A. Padró, L. Saiz, E. Guardia, Hydrogen bonding in liquid alcohols: a computer simulation study, J. Mol. Struct. 416 (1–3) (1997) 243–248, https://doi.org/10.1016/S0022-2860(97)00162-7.

[32] Z.Y. Yi, X.Q. Yang, J.J. Duan, X. Zhou, T. Chen, D. Wang, L.J. Wan, Evolution of Br···Br contacts in enantioselective molecular recognition during chiral 2D crystallization, Nat. Commun. 13 (1) (2022) 5850, https://doi.org/10.1038/s41467-022-33575-8.

[33] Y. Xu, A. Hao, P. Xing, X···X halogen bond-induced supramolecular helices, Angew. Chem. Int. Ed. 61 (2) (2022), https://doi.org/10.1002/anie.202113786.

[34] S. Schildmann, A. Reiser, R. Gainaru, C. Gainaru, R. Böhmer, Nuclear magnetic resonance and dielectric noise study of spectral densities and correlation functions in the glass forming monoalcohol 2-ethyl-1-hexanol, J. Chem. Phys. 135 (17) (2011), https://doi.org/10.1063/1.3647954.

[35] C.M. Roland, S. Hensel-Bielowka, M. Paluch, R. Casalini, Supercooled dynamics of glass-forming liquids and polymers under hydrostatic pressure, Rep. Prog. Phys. 68 (2005) 1405–1447, https://doi.org/10.1088/0034-4885/68/6/R03.

[36] B. Hachuła, P. Włodarczyk, K. Jurkiewicz, J. Grelska, D. Scelta, S. Fanetti, M. Paluch, S. Pawlus, K. Kamiński, Pressure-Induced Aggregation of Associating Liquids as a Driving Force Enhancing Hydrogen Bond Cooperativity, J. Phys. Chem. Lett. 15 (1) (2024) 127–135, https://doi.org/10.1021/acs.jpclett.3c03037.

[37] J. Grelska, L. Temleitner, C. Park, K. Jurkiewicz, S. Pawlus, High-Pressure and Temperature eEffects on the Clustering Ability of Monohydroxy Alcohols, J. Phys. Chem. Lett. 15 (11) (2024) 3118–3126, https://doi.org/10.1021/acs.jpclett.4c00085.

[38] A. Błażytko, M. Rams-Baron, M. Paluch, The influence of molecular shape on reorientation dynamics of sizable glass-forming isomers at ambient and elevated pressure, Sci. Rep. 14 (2024) 887, https://doi.org/10.1038/s41598-023-50894-8.

[39] G. Floudas, M. Paluch, A. Grzybowski, K.L. Ngai, Molecular dynamics of glass-forming systems. Effects of pressure, Springer, 2010.

[40] M. Paluch, K. Grzybowska, A. Grzybowski, Effect of high pressure on the relaxation dynamics of glass-forming liquids, J. Phys. Condens. Matter 19 (20) (2007), https://doi.org/10.1088/0953-8984/19/20/205117.

[41] G. Adam, J. Gibbs, On the Temperature Dependence of Cooperative Relaxation Properties in Glass-Forming Liquids, J. Chem. Phys. 43 (66) (1965) 139–146. https://api.semanticscholar.org/CorpusID:38862577.
[42] K. Koperwas, A. Grzybowski, K. Grzybowska, Z. Wojnarowska, J. Pionteck, A. P. Sokolov, M. Paluch, Pressure coefficient of the glass transition temperature in the thermodynamic scaling regime, Phys. Rev. E 86 (6) (2012), https://doi.org/10.1103/PhysRevE.86.041502.
[43] M. Paluch, J. Gapinski, A. Patkowski, E.W. Fischer, Does fragility depend on pressure? A dynamic light scattering study of a fragile glass-former, J. Chem. Phys. 114 (2001) 8048–8055, https://doi.org/10.1063/1.1362293.
[44] H. Vogel, The law of the relation between the viscosity of liquids and the temperature, Phys. Z. 22 (1921) 645–646.
[45] G.S. Fulcher, Analysis of recent measurements of the viscosity of glasses, J. Am. Ceram. Soc. 8 (1925) 339–355.
[46] V.G. Tamman, W. Hesse, Die Abhängigkeit der Viscosität von der Temperatur bei unterkühlten Flüssigkeiten, Z. Anorg. Allg. Chem. 156 (1926) 245–257, https://doi.org/10.1002/zaac.19261560121.
[47] C.A. Angell, J. Non-Cryst, Solids 13 (1991) 131–133.
[48] V.N. Novikov, A.P. Sokolov, Poisson's ratio and the fragility of glass-forming liquids, Nature 431 (7010) (2003) 961–963, https://doi.org/10.1038/nature02947.
[49] R. Böhmer, K.L. Ngai, C.A. Angell, D.J. Plazek, Nonexponential relaxations in strong and fragile glass formers, J. Chem. Phys. 99 (5) (1993) 4201–4209, https://doi.org/10.1063/1.466117.
[50] E. Donth, The glass transition: relaxation dynamics in liquids and disordered materials, Springer (2001) 61–63, https://doi.org/10.1063/1.1537917.
[51] K.C. Kao, Dielectric phenomena in solids, Elsevier Academic Press, London, 2004, pp. 92–95.
[52] S. Havriliak, S. Negami, A complex plane analysis of α-dispersions in some polymer systems, J. Polym. Sci., Part C: Polym. Symp. 14 (1) (2007) 99–117, https://doi.org/10.1002/polc.5070140111.
[53] D.W. Davidson, R.H. Cole, Dielectric Relaxation in Glycerine, J. Chem. Phys. 18 (10) (1950) 1417, https://doi.org/10.1063/1.1747496.
[54] L.-M. Wang, C.A. Angell, R. Richert, Fragility and thermodynamics in nonpolymeric glass-forming liquids, J. Chem. Phys. 125 (2006), https://doi.org/10.1063/1.2244551.
[55] C. Hansen, I.R. McDonald, Theory of simple liquids, third ed., Academic Press, London, 2006, pp. 180–220.
[56] P.G. Debenedetti, Metastable Liquids: Concepts and Principles, Princeton University Press, Princeton, NJ, 1996, pp. 125–150.
[57] C.A. Angell, Formation of Glasses from Liquids and Biopolymers, Science 267 (5206) (1995) 1924–1935, https://doi.org/10.1126/science.267.5206.1924.
[58] R. Richert, C.A. Angell, Dynamics of glass-forming liquids. V. On the link between molecular dynamics and configurational entropy, J. Chem. Phys. 108 (21) (1998) 9016–9026, https://doi.org/10.1063/1.476348.
[59] H.S. Chen, D. Turnbull, J. Appl. Phys. 40 (1969) 4214–4215.
[60] D.E. Pegg, Principles of Cryopreservation, in: J.G. Day, G.N. Stacey (Eds.), Cryopreservation and Freeze-Drying Protocols, Methods Mol. Biol., vol. 368, Humana Press, 2007, pp. 39–57. doi: 10.1007/978-1-59745-362-2_3.

Supporting information

Effect of high pressure on the molecular dynamics of halogen monoalcohols

Kinga Łucak[a]*, Anna Z. Szeremeta[a], Joanna Grelska[a], Karolina Jurkiewicz[a], Sławomir Kołodziej[b], Roman Wrzalik[a], Kamil Kamiński[a], Sebastian Pawlus[a].

[a] *August Chełkowski Institute of Physics, Faculty of Science and Technology, University of Silesia in Katowice, 75 Pułku Piechoty 1, 41-500 Chorzów, Poland*

[b] *Institute of Materials Engineering, Faculty of Science and Technology, University of Silesia in Katowice, ul. 75 Pułku Piechoty 1A, 41-500 Chorzów, Poland*

*Correspondence e-mails: kinga.lucak@us.edu.pl

1.1. Dielectric data analysis under pressure

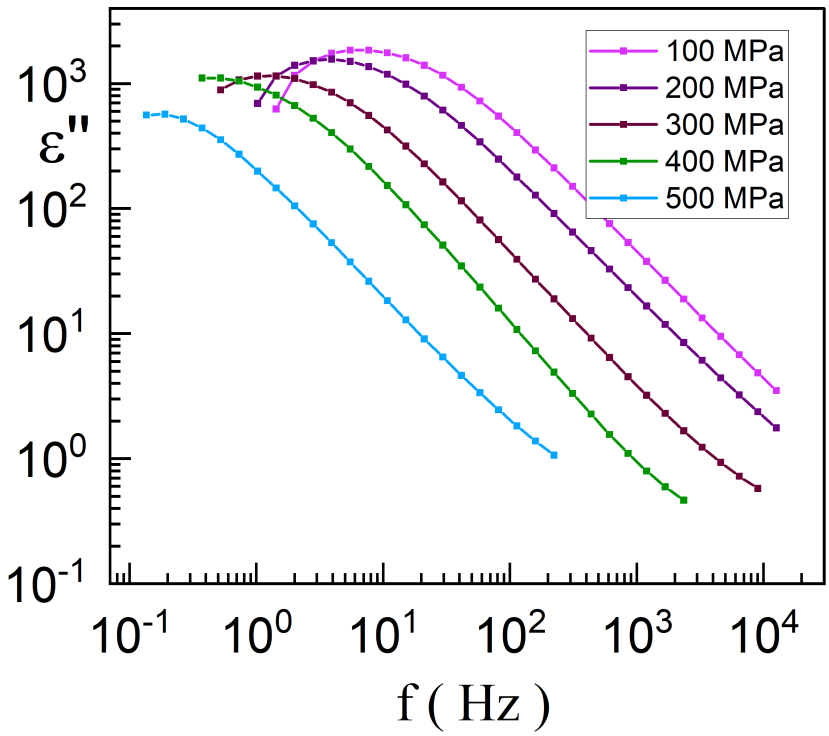

Fig. S1. Dielectric loss spectra of 3Cl1P, which crystallizes under pressure.

1.2. Dielectric data analysis at atmospheric pressure

To properly analyze the observed relaxation processes for studied alcohols, the data were fitted by: Debye, Cole-Davidson, and Cole-Cole functions for the Debye, structural and secondary relaxation, respectively, and constant-current conductivity σ_{DC} [1,2,3].

$$\varepsilon^*(\omega) = \varepsilon_\infty + \frac{\Delta\varepsilon}{1+(i\omega\tau_D)} + \frac{\Delta\varepsilon}{(1+(i\omega\tau_{CD})^{\beta})} + \frac{\Delta\varepsilon}{(1+(i\omega\tau_{CC})^{1-\alpha})} + \frac{\sigma_{DC}}{i\omega\varepsilon_0}, \quad (1)$$

In the case of the structural relaxation, the data were described using the Cole-Davidson function. The shape parameter β for the Cole-Davidson function in our samples was found to be similar across all, around 0.5. For secondary relaxation processes, if observed, they were described using the Cole-Cole function.

1.3. Dielectric data analysis at high pressure

To properly analyze the observed relaxation processes for studied alcohols, the data were fitted by the Cole-Davidson function and constant-current conductivity σ_{DC}.

$$\varepsilon^*(\omega) = \varepsilon_\infty + \frac{\Delta\varepsilon}{(1+i\omega\tau_{CD})^{\beta}} + \frac{\sigma_{DC}}{i\omega\varepsilon_0}, \quad (2)$$

where ε_∞ is the high-frequency dielectric permittivity, $\Delta\varepsilon$ - the dielectric strength, ω is equal to $2\pi f$ and σ_{dc} is the constant-current conductivity [1,2,3].

2.1 The analysis of intermolecular interactions

The hydrogen bond energy of dimers was calculated using Gaussian 16 and GaussView 6 software (4) for molecules with trans-carbon chain geometry. The B3LYP/6-31+G(d,p) DFT model was used with tight geometry optimization criteria and a counterpoise option. The structures of the dimers are shown in **Fig. S2.** and the calculated corrected complexation energies for 3-X-1-propanol and 1-X-2-propanol (X=Cl, Br) molecules are presented in the **Table S1.**

Table S1. Hydrogen bond energy, E (kcal/mol), calculated for the molecules under investigation, calculated using B3LYP/6-31+(d,p) DFT model.

Molecule	O···H-O	Cl···H-O linear	Cl···H-O cyclic
3-chloro-1-propanol	5.20	2.97	-
3-bromo-1-propanol	5.20	3.00	-
1-chloro-2-propanol	5.32	1.72	2.13
1-bromo-2-propanol	5.19	1.37	2.08

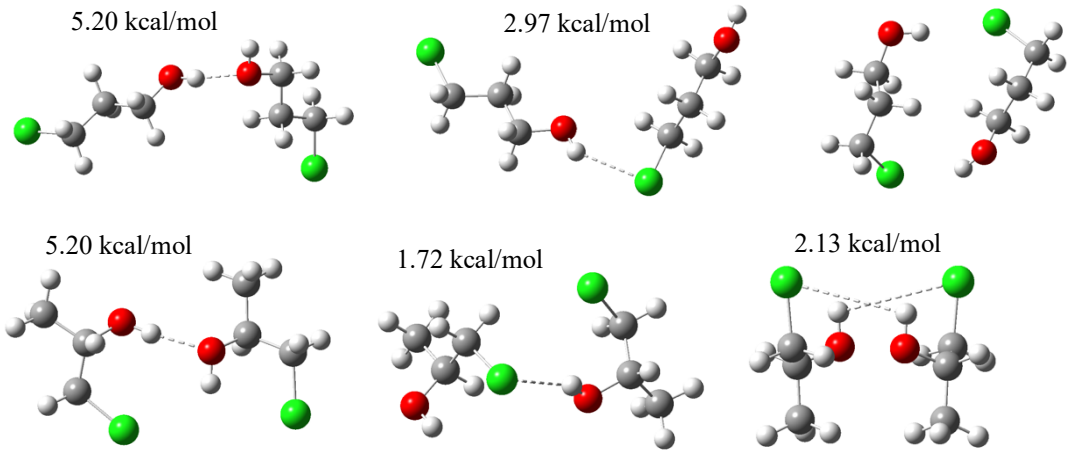

Fig. S2. HB dimer structure for 3-chloro-1-propanol and 1-chloro-2-propanol was calculated using the B3LYP/6-31+G(d,p) model (hydrogen bonds are marked with a dashed line).

The energies of O···H-O and Cl···H-O hydrogen bonds in linear dimers for the molecules 3-X-1-propanol and 1-X-2-propanol (X=Cl, Br) have similar values ($E_{O...H-O}$ ~ 5 kcal/mol and $E_{Cl...H-O}$ ~ 3 kcal/mol). In the case of 1-X-2-propanol molecules, the creation of a cyclic dimer with an X···H-O double bond with an energy of about 2 kcal/mol is possible. Meanwhile, for 3-X-1-propanol molecules, a cyclic dimer with this type of double hydrogen bond does not form due to steric obstacles and repulsive interactions between the CH_2 groups of molecules in the dimer. The possibility of the formation of cyclic dimers for 1-X-2-propanol molecules promotes the formation of more strongly bonded cyclic systems in these alcohols.

Table S2. Dipole moments calculated for single molecule using the B3LYP/6-311G (d, p) model.

Molecule	μ [D]
1-propanol	1.602
3-chloro-1-propanol	1.863
1-chloro-2-propanol	1.779
3-bromo-1-propanol	1.905
1-bromo-2-propanol	1.799

References

[1] K.C. Kao**,** Dielectric phenomena in solids, Elsevier Academic Press, London, 2004, pp. 92–95.

[2] S. Havriliak, S. Negami, A Complex Plane Analysis of α-Dispersions in Some Polymer Systems. J. Polym. Sci. Part C Polym. Symp. 14 (1) (2007) 99–117. https://doi.org/10.1002/polc.5070140111.

[3] D.W. Davidson, R.H. Cole, Dielectric relaxation in glycerine, J. Chem. Phys. 18 (10) (1950) 1417–1417. https://doi.org/10.1063/1.1747496.

[4] D.W. Frisch, G.W. Trucks, H.B. Schlegel, G.E. Scuseria, M.A. Robb, J.R. Cheeseman, G. Scalmani, V. Barone, G.A. Petersson, H. Nakatsuji, X. Li, M. Caricato, A.V. Marenich, J. Bloino, B.G. Janesko, R. Gomperts, B. Mennucci, H.P. Hratchian, J.V. Ortiz, A.F. Izmaylov, J.L. Sonnenberg, D. Williams-Young, F. Ding, F. Lipparini, F. Egidi, J. Goings, B. Peng, A. Petrone, T. Henderson, D. Ranasinghe, V.G. Zakrzewski, J. Gao, N. Rega, G. Zheng, W. Liang, M. Hada, M. Ehara, K. Toyota, R. Fukuda, J. Hasegawa, M. Ishida, T. Nakajima, Y. Honda, O. Kitao, H. Nakai, T. Vreven, K. Throssell, J.A. Montgomery Jr., J.E. Peralta, F. Ogliaro, M.J. Bearpark, J.J. Heyd, E.N. Brothers, K.N. Kudin, V.N. Staroverov, T.A. Keith, R. Kobayashi, J. Normand, K. Raghavachari, A.P. Rendell, J.C. Burant, S.S. Iyengar, J. Tomasi, M. Cossi, J.M. Millam, M. Klene, C. Adamo, R. Cammi, J.W. Ochterski, R.L. Martin, K. Morokuma, O. Farkas, J.B. Foresman, D.J. Fox, Gaussian 16, Revision C.01, Gaussian, Inc., Wallingford CT, 2016.

10.3 [P3] Influence of molecular structure and thermodynamic conditions on the dynamics, halogen bonding, and self–assembly of halogenated monoalcohols

K. Łucak, A.Z. Szeremeta, A. Janowska, K. Jurkiewicz, K. Grzybowska, K. Kamiński, S. Pawlus. *Journal of Molecular Liquids*, 433, 127787, (2025).
DOI: 10.1016/j.molliq.2025.127787

Punkty MNiSW (2024): 100
Impact Factor (2024): 5.3

Mój wkład w publikację polegał na wykonaniu pomiarów dielektrycznych w szerokim zakresie temperatur oraz pod wysokim ciśnieniem, analizie wyników i ich dyskusji oraz przygotowaniu artykułu.

Journal of Molecular Liquids 433 (2025) 127787

Contents lists available at ScienceDirect

Journal of Molecular Liquids

journal homepage: www.elsevier.com/locate/molliq

Influence of molecular structure and thermodynamic conditions on the dynamics, halogen bonding, and self-assembly of halogenated monoalcohols

Kinga Łucak *, Anna Z. Szeremeta, Anna Janowska, Karolina Jurkiewicz, Katarzyna Grzybowska, Kamil Kamiński, Sebastian Pawlus

August Chełkowski Institute of Physics, Faculty of Science and Technology, University of Silesia in Katowice, 75 Pułku Piechoty 1, 41-500 Chorzów, Poland

A B S T R A C T

The research focuses on the effects of carbon chain length, halogen atom type (Cl, Br, I), and thermodynamic conditions on the molecular dynamics and formation of supramolecular structures in halogenated monoalcohols such as 2-chloro-1-ethanol, 3-chloro-1-propanol, 2-bromo-1-ethanol, 3-bromo-1-propanol, 2-iodo-1-ethanol, and 3-iodo-1-propanol. The results showed that the carbon chain length and the type of halogen atom significantly affect the relaxation processes and the ability to organize into supramolecular aggregates. Alcohols with shorter carbon chains, such as 2-chloro-1-ethanol, 2-bromo-1-ethanol, and 2-iodo-1-ethanol, showed higher Kirkwood factor values than their longer alkyl chain counterparts, suggesting a greater abundance of H-bonded clusters and/or a greater aggregation of molecules in these structures. High-pressure dielectric data combined with molecular dynamics simulations revealed that halogen-halogen interactions contribute to enhanced local structural heterogeneity, especially in brominated systems. The results indicate a greater tendency for Br atoms to form local clusters, which promotes the formation of larger and more branched O-H···O hydrogen-bonded networks. These observations highlight the critical role of halogen type and carbon chain length in shaping molecular dynamics and driving the formation of diverse supramolecular structures.

1. Introduction

Monohydroxy alcohols (MAs) are model compounds for studying hydrogen bonding and supramolecular clustering phenomena under various thermodynamic conditions due to their diverse ability to form complex hydrogen-bonded structures. In contrast to water, MAs can be readily supercooled and vitrified, facilitating thorough investigations of their physical behavior over broad temperature, time, and pressure ranges. Additionally, their relatively simple chemical architecture makes them well-suited for systematic investigations of how molecular structure, such as the position of the hydroxyl group, carbon chain length, or presence of side groups, influences self-assembly and vitrification tendencies [1–3]. A common feature of many primary alcohols is the presence of a slower-than-structural, exponential relaxation called the Debye (D) process, which is related to the end-to-end motion of hydrogen-bonded chain-like nano-associates. The dynamics of this mode are strongly modulated by structural parameters, including the position of the hydroxyl group [4,5]. Studies have also shown that changes in the organization of supramolecular clusters can be observed by analyzing the Kirkwood factor (g_k). Values of $g_k > 1$ indicate dipolar correlations typical of chain-like structures, while $g_k < 1$ indicates dipolar anticorrelations associated with ring-like molecular associates [6–8]. In addition, the structural (α) relaxation process observed in MAs is attributed to the reorientational dynamics of alkyl segments [4]. This relaxation has a shorter timescale and a smaller amplitude compared to the D process.

Our previous studies demonstrated that substituting a hydrogen atom in n-propanol (nP) with a halogen (Cl, Br, or I) weakens the hydrogen bonding network, leading to smaller supramolecular clusters and enhanced structural heterogeneity. Studies of isomers indicate that halogen type and molecular structure influence the D process, structural relaxation, and the Kirkwood factor. Under high pressure, 3-bromo-1-propanol (3Br1P) tends to form cyclic structures, while 1-bromo-2-propanol (1Br2P) and 1-chloro-2-propanol (1Cl2P) favor chain aggregation, highlighting the effect of halogen substitution and pressure on supramolecular organization [9,10].

Although pressure effects in hydrogen-bonded liquids have been widely examined, the influence of alkyl chain length on the behavior of halogenated monoalcohols remains poorly investigated. Gaining a deeper understanding of molecular dynamics under variable thermodynamic conditions is essential for disentangling the respective contributions of temperature and pressure to supramolecular organization and

* Corresponding author.
E-mail address: kinga.lucak@us.edu.pl (K. Łucak).

https://doi.org/10.1016/j.molliq.2025.127787
Received 17 March 2025; Received in revised form 7 May 2025; Accepted 13 May 2025
Available online 14 May 2025

relaxation processes. To address this gap, the present study explores how alkyl chain length and halogen type govern molecular dynamics and self-organization over a broad range of pressures and temperatures, focusing on three key aspects:

Part 1: Examination of how variations in carbon chain length and halogen identity (Cl, Br, I) influence molecular dynamics under ambient pressure conditions. The study encompasses six halogenated derivatives of n-propanol: 3-iodo-1-propanol (3I1P), 2-iodo-1-ethanol (2I1E), 3-chloro-1-propanol (3Cl1P), 2-chloro-1-ethanol (2Cl1E), 3Br1P, and 2-bromo-1-ethanol (2Br1E). These compounds differ in both chain length and halogen type, enabling a systematic analysis of their dielectric and calorimetric behavior.

Part 2: Validation of the dielectric relaxation times obtained from broadband dielectric spectroscopy (BDS) by comparison with calorimetric relaxation times derived from stochastic temperature-modulated differential scanning calorimetry (TOPEM).

Part 3: Integration of interpretations derived from BDS and molecular dynamics simulations (MDS) to assess changes in supramolecular structure under high-pressure conditions. BDS offers experimental insight into how elevated pressure influences relaxation processes and molecular aggregation in halogenated monoalcohols, while MDS complements these results by providing detailed insights into molecular organization, hydrogen bonding, and the role of halogen substitution in cluster formation.

Using a combination of BDS, TOPEM, and MDS techniques, this work provides a comprehensive understanding of the molecular dynamics and thermodynamic behavior of halogenated monoalcohols. It fills gaps in the existing knowledge and gives practical insights into their dielectric, thermal, and structural properties.

2. Materials and Methods

2.1. Materials

Monohydroxy alcohols: 3-iodo-1-propanol, 2-iodo-1-ethanol, 3-chloro-1-propanol, 2-chloro-1-ethanol, 3-bromo-1-propanol, and 2-bromo-1-ethanol, under investigation, were purchased from Sigma-Aldrich. 3Br1P, 3Cl1P, and 3I1P differ in the type of halogen atom, X, and the same applies to 2Br1E, 2Cl1E, and 2I1E. The alcohols studied can also be divided into two groups according to the length of the carbon chain: ethyl derivatives (2Br1E, 2Cl1E, 2I1E) with a two-carbon chain and propyl derivatives (3Br1P, 3Cl1P, 3I1P) with a three-carbon chain. Before use, all alcohols were dried under a stream of liquid nitrogen. The chemical structures of the studied alcohols are presented in Fig. 1.

2.2. Broadband dielectric spectroscopy (BDS) at ambient and elevated pressure

The dielectric studies at ambient pressure (p) were performed using a Novocontrol BDS spectrometer equipped with an Alpha Impedance Analyzer and a Quatro Cryosystem. The capacitor used for the dielectric measurements consisted of two parallel plates of 10 mm diameter made of stainless steel, spaced with two 100 μm glass fibers, and sealed with a Teflon ring. The dielectric spectra were collected in the frequency (f) range of 10^{-1} - 10^{6} Hz at quasi-static conditions after temperature (T) stabilization for 3 min before each measurement using nitrogen gas, with an accuracy better than 0.2 K. The temperature-dependent measurements were performed with a step of $\Delta T = 2$ K. For the high-pressure experiments, the liquid specimens were poured into Teflon capsules and closed with a plug fitted with two electrodes forming a capacitor, both made from stainless steel. The electrical feedthroughs were led outside the high-pressure chamber and connected to the Alpha-A impedance analyzer via measurement cables. The system was surrounded by a cooling/heating blanket. Temperature stabilization with an accuracy of $\Delta T = 0.5$ °C was provided by a closed-loop liquid thermostat during the measurements. The temperature was monitored using a digital thermocouple thermometer HD 2328.0.

2.3. Measurements of temperature dependences of isobaric heat capacity (by stochastic temperature-modulated DSC – TOPEM®)

To determine the accurate temperature dependences of the isobaric heat capacity of the examined compounds near their glass transition, we exploited the stochastic temperature-modulated differential scanning calorimetry technique (TMDSC) implemented by Mettler-Toledo (TOPEM®). The quenched sample was heated at a rate of 0.5 K/min. In the experiment, a temperature amplitude of the pulses of 0.5 K was selected with a switching time range of 15–30 s. We adjusted our evaluations of the temperature dependence of the quasi-static heat capacity using a sapphire reference curve.

2.4. Molecular dynamics simulations (MDS)

Molecular dynamics simulations of the structure for two selected alcohols, 2Br1E and 3Br1P, were carried out using GROMACS package (version 2024) [11–17]. The starting simulation boxes for each compound contained 2000 randomly distributed molecules. First, the systems were equilibrated with the use of a steep algorithm, followed by 20 ns production runs at room conditions: T = 293 K and p = 0.1 MPa. Then, 20 ns simulation runs were carried out for systems cooled down to T = 208 K at p = 0.1 MPa. Finally, 20 ns simulations were performed for the alcohols under high-pressure (p = 500 MPa for 2Br1E and p = 900

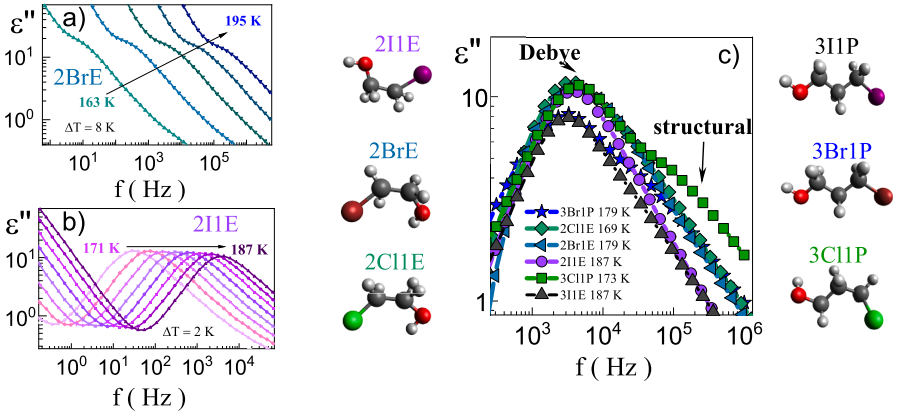

Fig. 1. Dielectric loss spectra at ambient pressure for 2Br1E (a) and 2Cl1E (b). Chemical structure of 2I1E, 2Cl1E, 2Br1E, 3I1P 3Cl1P, 3Br1P, and 3Cl1P. The same approximate maximum ε"(f) peak position of the studied XAs (c).

MPa for 3Br1P) at T = 208 K in order to replicate the thermodynamic conditions used in the BDS studies. All the production runs were carried out in the NPT ensemble with the use of v-rescale thermostat and C-rescale barostat. The topology files were created with the ACPYPE server [18,19]. The interactions between atoms were described by the general AMBER force field (GAFF) [20,21]. The trajectories of the final 100 atomic configurations recorded from the last 10 ns of each of the production runs were collected for the analysis of the systems. Total and partial structure factors S(Q) and radial distribution functions rdf(r) were computed using the TRAVIS software [22,23] in order to determine the short- and medium-range order structural correlations between atoms and reveal the nature of the changes in the structure of the studied halogen alcohols under high-pressure. The gmx_hbond and gmx_clust-size programs in the GROMACS package were used to calculate the average number of classical O-H···O hydrogen bonds (HBs) and the distributions of the molecular clusters (fraction of clusters versus the number of molecules linked in clusters) linked by such HBs.

3. Results and discussion

3.1. Effect of halogen type and molecular structure on dynamics of halogenated alcohols at atmospheric pressure

To investigate the effect of the carbon chain length and the type of X atom (Cl, Br, I) on the properties of halogenated monoalcohols, dielectric measurements were conducted for all the studied alcohols over a wide temperature range. The dielectric loss spectra, ε"(f), recorded at selected temperatures, revealed two relaxation processes, labeled D and α, that are observed above the glass transition temperature (T_g). Both processes shift to higher frequencies with increasing temperature for all analyzed systems, see Fig. 1**a** and **b**.

For alcohols with longer carbon chains (3Cl1P, 3Br1P, and 3I1P) shown in Fig. 1**c**, the α process is more distinct and well separated from the D process. In contrast, for alcohols with shorter carbon chains (2Cl1E, 2Br1E, and 2I1E), the amplitude of the α relaxation is weaker, and the existence of this process is much more challenging to identify, as it overlaps with the D relaxation. For the shorter carbon chains, the formation of more structured and tightly packed supramolecular clusters is favored, where the molecules are arranged in a more regular and ordered manner due to stronger dipolar interactions and hydrogen bonding, resulting in a higher amplitude of the D process. In contrast, for longer carbon chains, the formation of larger but less organized supramolecular clusters is promoted, where increased molecular mobility disrupts the regular packing, leading to a more disordered arrangement and, consequently, a lower intensity of the D process. Chlorinated alcohols (both short and long chain) exhibit more intense structural relaxation compared to their brominated and iodinated counterparts. This is attributed to the higher electronegativity of chlorine, which enhances dipolar interactions and facilitates supramolecular organization. The D process dominates in shorter chains (2Cl1E, 2Br1E, and 2I1E), potentially masking the α process. Longer chains allow for the separation of these processes, resulting in a more pronounced structural relaxation. In addition, Fig. 2**a** and **b** show the dielectric loss spectra ε"(f) of 3Cl1P measured at 173 K (data obtained for 3Cl1P from ref. [9]) and 2Cl1E at 167 K along with fits using the Debye, Cole-Davidson and for 3Cl1P additionally Cole-Cole functions describing the D, α and β processes, respectively. At this point, it should be noted that an analysis of the behavior of the β-process is beyond the scope of this article.

To gain further insight into how the type of X atom and different carbon chain lengths affect the self-association process in the samples analyzed, we calculated the Kirkwood correlation factor g_k according to the following formula:

$$g_k = \frac{9k_B\varepsilon_0 MT(\varepsilon_s - \varepsilon_\infty)(2\varepsilon_s + \varepsilon_\infty)}{\rho N_A \mu^2 \varepsilon_s}, \quad (1)$$

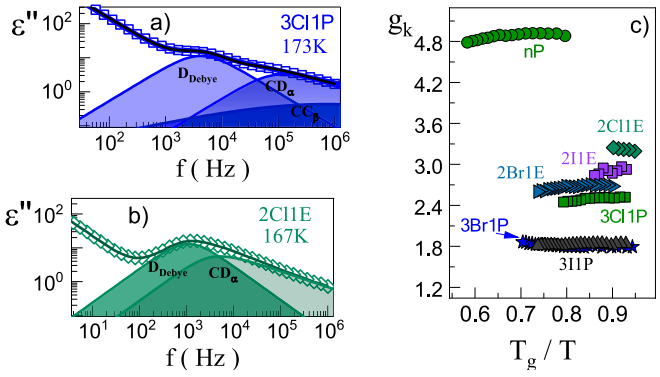

Fig. 2. Dielectric loss spectrum for 3Cl1P at 173 K was taken from ref. [9] (a) and 2Cl1E (b) at 167 K and functions: Debye, Cole-Davidson, and additionally for 3Cl1P with function Cole-Cole. The g_k for the studied alcohols (c), and data obtained for nP were taken from ref. [9].

where: ε_s and ε_∞ – the static and high-frequency permittivity, respectively; N_A – the Avogadro's number; ρ – the density of the liquid at temperature T; μ_0 – the dipole moment of the isolated molecule; ε_0 – the absolute permittivity of vacuum; M – the molecular weight, and k_B – the Boltzmann constant [7]. The calculated g_k values are significantly greater than 1 for all the investigated samples (see Fig. 2**c**). According to the Danhauser model, these results indicate that all the analyzed compounds tend to organize into chain-like aggregates. However, it is important to note that the g_k values for all halogenated alcohols are significantly lower than those observed for nP, suggesting that the presence of halogen atoms disrupts the formation of extended hydrogen-bonded chain structures. Among the halogenated alcohols, the highest ($g_k \approx 3.2$) value was observed for 2Cl1E, indicating the highest concentration of H-bonded clusters or the largest number of molecules in the aggregates. Longer carbon chains, such as those in 3-halogenated alcohols (3Cl1P, 3Br1P, and 3I1P) are associated with lower g_k values, implying less organized supramolecular structures resembling loosely bound clusters. Chlorine promotes stronger dipole alignment, which explains the high g_k value for 2Cl1E. In comparison, bromine and iodine, with their higher polarizability, result in lower g_k values and less ordered supramolecular assemblies. Higher Kirkwood factor values indicate a tendency to form densely packed, well-ordered chain-like structures, while lower values suggest loosely organized clusters. Shorter carbon chains promote more ordered supramolecular structures, which directly affect the dielectric properties and molecular dynamics of the compounds.

3.2. Dielectric and calorimetric insights into the structural relaxation process

The relaxation processes in the studied halogenated alcohols were analyzed by fitting the dielectric spectra, as mentioned in the previous section, with the Debye and Cole-Davidson functions, supplemented by a constant-current conductivity term (σ_{DC}) to account for low-frequency contributions. The Cole-Davidson function, applied to describe the α relaxation, exhibited a consistent shape parameter (β≈0.5) across all samples [24,25]. Using this approach, relaxation maps were constructed for the systems above their glass transition temperature (T_g). The temperature dependence of the relaxation times for both α and D processes, presented in Fig. 3**a-c**, exhibits nonlinear behavior that was successfully fitted using the Vogel-Fulcher-Tammann-Hesse (VFTH) equation [26–29]:

$$\tau_\alpha = \tau_\infty exp\left(\frac{B}{T - T_0}\right), \quad (2)$$

where τ_∞ – the pre-exponential factor, B – the material constant, and T_0

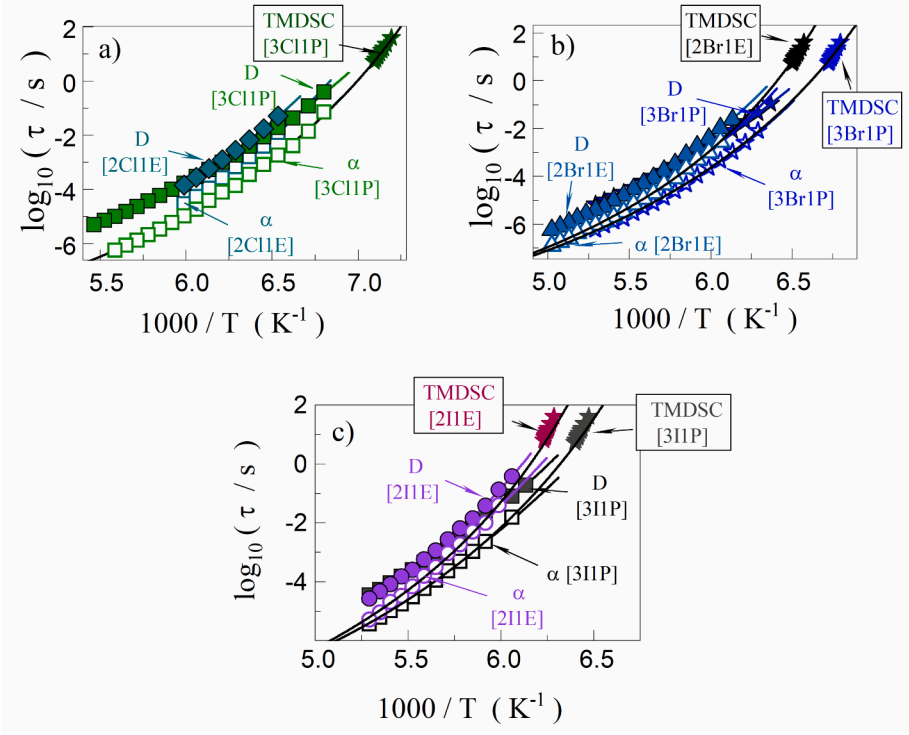

Fig. 3. Relaxation times for 3Cl1P, 2Cl1E (a), for 3Br1P, 2Br1E (b), and for 3I1P, 2I1E (c) with VFTH fits (black lines) and calorimetric relaxation times (asterisks).

– the so-called ideal glass temperature.

As mentioned earlier, the α and D relaxation processes are coupled in the dielectric loss spectra, especially strongly for alcohols with shorter carbon chains. To be sure that the dielectric structural relaxation times were correctly identified and evaluated, we compared them with the calorimetric relaxation times determined based on temperature dependencies of the quasi-static heat capacity C_{p0}. The temperature dependences of the C_{p0} have been obtained using the stochastic temperature-modulated DSC (TOPEM) for the tested alcohols and are shown in Fig. 4**a.** We excluded 2Cl1E from this analysis due to the strong evaporation of this substance and the difficulty of accurately determining heat capacity. As can be seen in Fig. 4**a**, there are sigmoidal changes in the C_{p0} (T) for each material, which are characteristics of the glass transition. Among the compounds, only 2I1E reveals cold

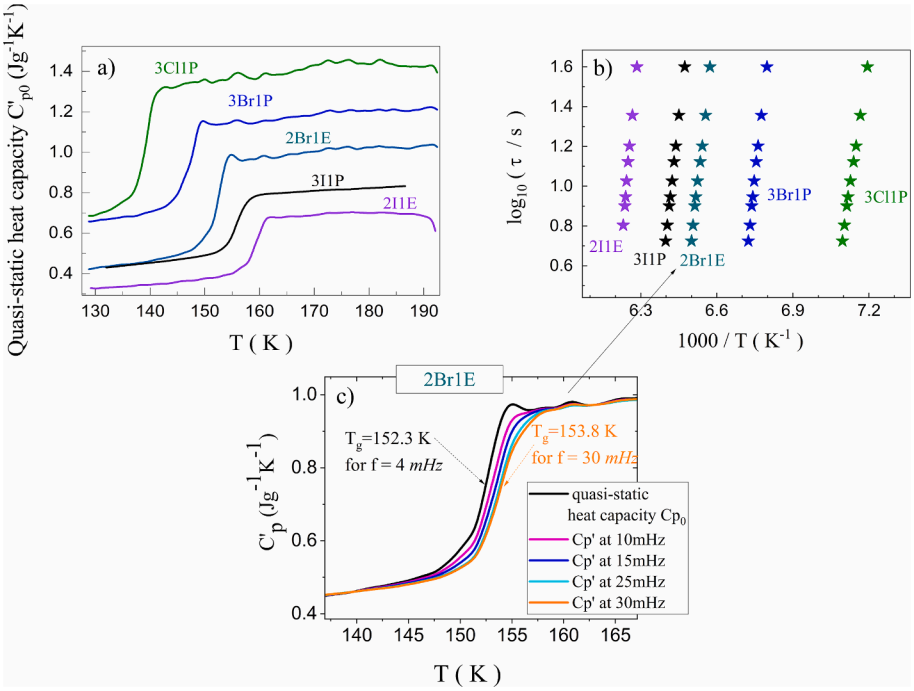

Fig. 4. Temperature dependences of quasi-static specific heat capacity C_{p0} for the examined alcohols near their T_g (a). Temperature dependences of the structural calorimetric relaxation times of the alcohols studied (b). Temperature dependencies of the real part of the complex heat capacity $C'_p(T)$ for selected frequencies, based on which the calorimetric relaxation times were determined. The dependencies are shown as an example for 2Br1E (c).

crystallization on heating above the T_g (i.e., at about 190 K), the remaining alcohols were physically stable in the tested temperature range. An interesting observation from the obtained $C_p(T)$ diagrams is that the jumps in the specific heat ΔC_p at the glass transition temperature have similar values for alcohols with the same halogen atom.

It has been observed that the temperature dependences of the real part of the complex heat capacity $C'_p(T)$ are frequency-dependent in the glass transition region for all investigated alcohols. This phenomenon is shown, for example, for 2Br1E in Fig. 4**c**. It is noted that the sigmoidal changes in the dependences $C'_p(T)$ shift towards high temperatures with increasing frequency f. Such behavior is indicative of relaxation processes. The calorimetric structural relaxation times, defined as $\tau_\alpha = 1/2\pi f$, have been determined from the dependences $C'_p(T)$ obtained at different frequencies in the glass transition range. The glass transition temperatures T_g were determined for $C'_p(T)$ at various frequencies as the temperatures corresponding to the midpoint of the step height of $C'_p(T)$. The obtained calorimetric relaxation times as a function of temperature for examined alcohols are presented in Fig. 4**b**.

To compare the obtained calorimetric relaxation times with the dielectric ones, they were placed on the dielectric relaxation maps of alcohols (see Fig. 3**a-c**). It turned out that the dielectric α-relaxation times determined at higher temperatures can be successfully extrapolated using the VFTH function to lower temperatures, where the calorimetric relaxation times (star points) are located. A particularly good agreement was obtained regarding the extrapolated VFTH fit of dielectric data for compounds containing chlorine and bromine, for which the calorimetric relaxation times lie along the VFTH fit curve. In the case of iodinated alcohols, we observe small discrepancies that may be due to the limited range of dielectric data, which may affect the accuracy of extrapolation. Nevertheless, the TOPEM analysis confirmed that the dielectric α-relaxation processes were correctly determined from the complex dielectric spectra and that they are related to the glass transition of the studied alcohols.

3.3. High-pressure dielectric spectroscopy and molecular dynamics simulations

To investigate the influence of supramolecular structures on high-pressure behavior, we performed BDS and MDS measurements on halogenated monoalcohols differing in carbon chain length and halogen type. High-pressure dielectric studies reveal how relaxation processes evolve under compression, shedding light on the influence of molecular architecture on the supramolecular organization. Complementary MDS analyses provide microscopic insights into hydrogen bonding, molecular clustering, and the role of halogen substitution in shaping aggregation patterns [30–32].

3.3.1. Pressure-dependent dielectric relaxation processes

To investigate the effect of compression on molecular dynamics above the glass transition temperature (T_g), isothermal high-pressure experiments were performed around.

T = 208 K. The BDS results showed that for 2Br1E and 3Br1P [10] it was possible to make measurements over a wide range of pressures, indicating the ability of these systems to supercool to the glassy state upon pressurization. For 2I1E and 3I1P **(**Fig. 5**a, 5b)**, crystallization was observed, which prevented analysis at higher pressures. It is worth noting that 2I1E tends to crystallize already at atmospheric pressure at T < 190 K. In the case of 2I1E and 3I1P, crystallization prevents further analysis in the supercooled state under pressure, suggesting that intermolecular interactions involving iodine promote ordered structures rather than stable supercooled molecular aggregates [33]. The dielectric loss spectra recorded at selected pressures for the studied halogen alcohols presented in Fig. 5**a, 5b, and 5c**, reveal a systematic shift of the relaxation processes towards lower frequencies with increasing pressure. The difference between the D relaxation time and the α relaxation time decreases under compression. Based on these results, we decided to model the dielectric loss spectra with a single Cole-Davidson function and include the contribution of constant-current conductivity. Analysis of the fitted curves showed that with increasing pressure, the D and α processes gradually approach each other, eventually leading to a homogeneous, non-exponential relaxation process (labeled as Debye-like (D_{like})) visible in the dielectric spectra of the studied alcohols, Fig. 5**a, 5b, and 5c.** This behavior can be explained by the greater susceptibility of the structural relaxation to compression compared to the D process. Consequently, there is a reduction in the differences in the time scales of the two processes or changes in their relative contribution to the main dielectric peak at high-pressure. The observed trend is consistent with previous findings for halogen monoalcohols, where the morphology of hydrogen-bonded clusters undergoes transformations under pressure. However, for 2Cl1E and 3Cl1P [10], the analysis was not possible due to the onset of crystallization at elevated pressures. The propensity of chlorinated alcohols to crystallize at high-pressure conditions can be attributed to the nature of the intermolecular interactions, particularly hydrogen bonds and van der Waals forces. High-pressure

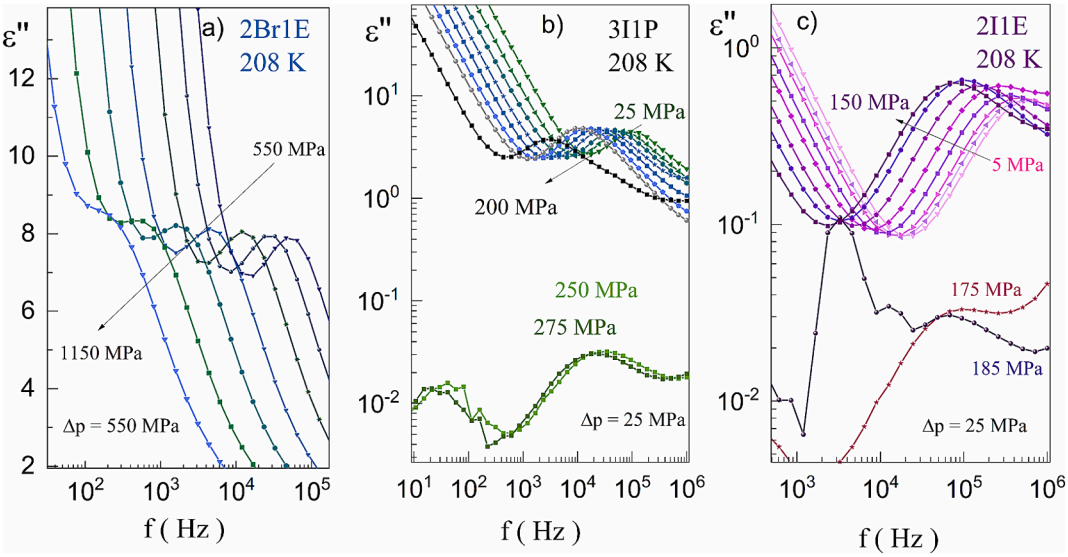

Fig. 5. Selected dielectric loss spectra ε"(f) measured at elevated pressure between 550 and 1150 MPa at 208 K for 2Br1E (a), between 25 and 275 MPa at 208 K for 3I1P (b), and between 5 and 185 MPa at 208 K for 2I1E (c).

crystallography studies have demonstrated that varying pressure influences these interactions, leading to structural transformations in organic compounds. For example, Boldyreva [33] showed that pressure-induced modifications in hydrogen bonding and van der Waals interactions can trigger crystallization, as observed in compounds such as amino acids and coordination complexes, where increased pressure led to a transition from disordered to ordered molecular packing. Therefore, the high degree of crystallization observed in chlorinated alcohols at elevated pressure is likely due to the specific way in which pressure alters intermolecular forces, favoring ordered, crystalline arrangements over amorphous structures.

3.3.2. *Effect of pressure on molecular dynamics and activation volumes in halogenated alcohols*

The isothermal dependence of the D_{like} relaxation times increases non-linearly with compression for all analyzed halogenated alcohols, as shown in Fig. 6**a**. The relaxation times were parameterized using the pressure equivalent of the Vogel-Fulcher-Tamman-Hesse equation (so-called pVFTH):

$$\tau = \tau_0 exp\left(\frac{D_p P}{P_0 - P}\right) \quad (3)$$

where τ_0 – the relaxation time at ambient pressure, p_0 – the pressure of the ideal glass, and

D_P – the parameter depending on the pressure sensitivity of the material [34,35].

A comparison of the studied alcohols shows that iodinated alcohols (2I1E, 3I1P) exhibit shorter relaxation times over the range of available pressures compared to their brominated counterparts (3Br1P, 2Br1E). However, this effect is primarily attributed to the higher glass transition temperatures (T_g) of iodinated alcohols rather than inherent differences in molecular packing or supramolecular organization. The presence of iodine, which has a larger van der Waals radius compared to bromine, may influence local molecular interactions. Still, the dominant factor controlling the observed relaxation times is the shift in the temperature scale. There are no direct comparative studies in the literature focusing specifically on the relaxation times of iodinated and brominated alcohols. Nevertheless, studies on the effect of bulky substituents on hydrogen bond networks in alcohols suggest that larger substituents can disrupt the regularity of the hydrogen bond network, which in principle could lead to less rigid structures and faster molecular reorganization [36]. However, in the case of the studied iodinated alcohols, the observed differences in relaxation times can be explained mainly by their higher glass transition temperatures.

The activation volume (ΔV) quantifies how strongly the relaxation process depends on pressure changes and is related to the spatial requirements for molecular rearrangement in the transition state. In the case of halogenated alcohols, whose dynamics are strongly governed by hydrogen-bond networks and dipolar interactions, ΔV provides crucial insights into the mechanisms of molecular reorganization under compression [35,37].

Studies have shown that it was not possible to determine the activation volume ΔV for 2Cl1E and 3Cl1P because these compounds crystallized at relatively low pressure. This indicates that their molecular structures cannot gradually reorganize under compression and instead undergo a sudden transition to the solid phase, preventing further analysis of their relaxation dynamics in the liquid state. On the other hand, 2Br1E, 3Br1P, 2I1E, and 3I1P exhibit differences in activation volume ΔV, indicating varying susceptibility of these liquids to high-pressure (please see the inset in Fig. 6**a**). The highest ΔV values were obtained for 2I1E and 3I1P, suggesting that these alcohols require a larger local volume for molecular reorganization. Their strong tendency to crystallize at low pressures indicates that their interaction network is more susceptible to destabilization under compression, leading to a limitation of dynamic changes in the liquid phase and forcing a transition to an ordered solid structure. In the case of the brominated alcohols (2Br1E and 3Br1P), the ΔV values are lower than those for their iodinated counterparts. This observation is consistent with their ability to maintain stable liquid structures over a wide range of pressures. Bromine, as a halogen with lower polarizability than iodine, provides a balance between the stability of hydrogen bond networks and structural flexibility, allowing for a more gradual reorganization of supramolecular clusters [38,39].

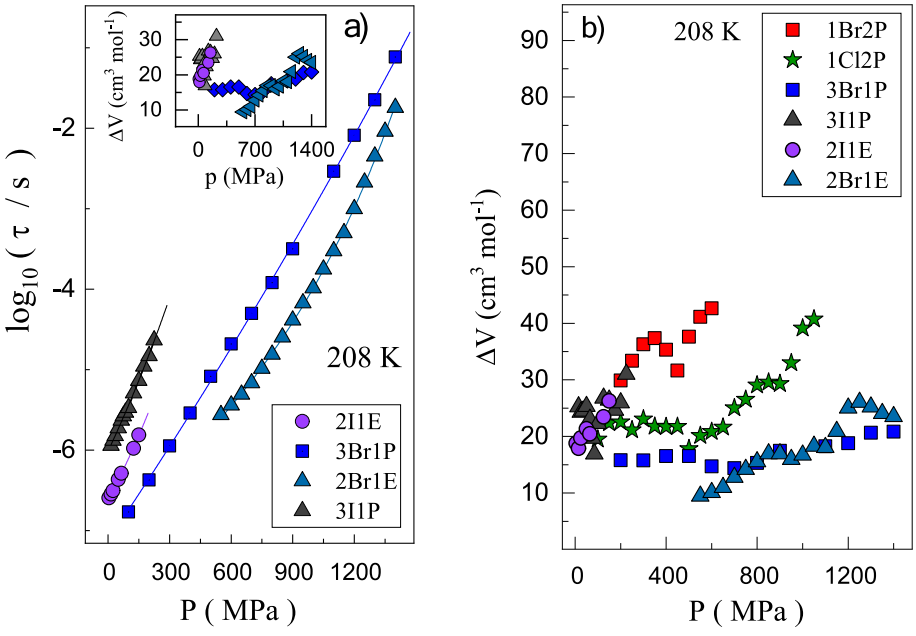

Fig. 6. Pressure dependence of the relaxation times for halogenated monoalcohols (2I1E, 3Br1P, 2Br1E, and 3I1P) at 208 K. The inset shows the pressure dependence of the activation volume (ΔV) for the same compounds (a). Pressure dependence of the ΔV for a broader set of halogenated monoalcohols at 208 K (b), data obtained for (1Br2P, 1Cl2P, 3Br1P) were taken from ref. [10].

3.3.3. Pressure-dependent activation volume in halogenated alcohols: Comparison with previously studied alcohols

Interestingly, recent findings on halogenated alcohols [10] suggest that the activation volume (ΔV) in these compounds is strongly correlated not only with the type of halogen, but also with molecular geometry, including the length of the carbon chain and the position of the hydroxyl (–OH) group within the carbon backbone. Comparison of the currently studied halogenated alcohols (2I1E, 3I1P, 2Br1E, and 3Br1P) with previously studied compounds (1Br2P, 1Cl2P) shows that alcohols with the hydroxyl group in a central position (e.g., 1Cl2P, 1Br2P) tend to exhibit higher ΔV values compared to their counterparts with the hydroxyl group in a terminal position (e.g., 3Br1P, 3I1P) as shown in Fig. 6**b**.

This observation suggests that the relative positioning of the –OH group concerning the halogen, together with the molecular structure of the alkyl chain, plays a crucial role in defining the hydrogen-bond topology and molecular rearrangement under high-pressure conditions. The differences in ΔV values indicate that alcohols with a centrally positioned hydroxyl group may experience more extensive hydrogen-bond rearrangement, requiring larger activation volumes, whereas those with terminal –OH groups may undergo a more localized, restricted molecular reorganization.

3.3.4. Correlation between molecular structure and fragility in halogenated alcohols

The steepness index (m_p) is a key parameter for understanding the temperature dependence of the relaxation dynamics in molecular systems. It provides insight into the *fragility* of a liquid by quantifying how the relaxation times change as the system approaches the glass transition temperature (T_g). The parameter was determined from the inverse temperature dependence of relaxation times at ambient pressure (Fig. 7**a**), using the standard definition:

$$m_p = \left.\frac{d\log\tau}{d\left(\frac{T_g}{T}\right)}\right|_{T_g}, \quad (4)$$

where: T_g – the glass transition temperature, defined as the temperature at which the relaxation time (τ_α) equals 1 s [40].

The structural differences between the studied halogenated alcohols significantly influence the rigidity and adaptability of their hydrogen-bonded networks, as shown in Fig. 7**a**. The ethyl-substituted alcohols (2Br1E: m_p = 58, 2I1E: m_p = 47) exhibit slightly greater *fragility* and molecular flexibility compared to their propanol counterparts (3Br1P: m_p = 55, 3I1P: m_p = 45). This trend is due to the shorter alkyl chains in ethyl-substituted alcohols, which reduce steric constraints and increase molecular mobility, leading to a more dynamic and adaptable hydrogen-bonding network. In the case of chlorinated alcohols, 1Cl2E (m_p = 54) has a slightly lower *fragility* index than 3Cl1P (m_p = 57), despite its shorter alkyl chain. This can be attributed to the higher hydrogen-bond density in 1Cl2E, which results in a more compact molecular arrangement, strengthening intermolecular interactions and stabilizing the structure. In contrast, the longer alkyl chain in 3Cl1P weakens hydrogen-bond connectivity, leading to increased molecular flexibility and slightly higher *fragility* [41]. Similarly, in brominated and iodinated alcohols, longer chains contribute to the lower *fragility* by stabilizing the supramolecular structure. The observed differences are also reflected in their *fragility* indices, with ethyl alcohols consistently having slightly higher values than their corresponding propanol derivatives. Interestingly, iodinated alcohols, despite following this trend, show overall lower *fragility* indices than their chlorinated and brominated counterparts. This is likely due to the steric hindrance and high polarizability of the iodine atom, which weakens dipolar interactions and contributes to a more rigid network [41,42].

3.3.5. Steepness index (of the Debye process) and molecular rigidity

The steepness index parameter (m_D) provides valuable insight into the dynamics of the hydrogen-bonded network, as illustrated in Fig. 7**b**.

- 2Cl1E (m_D=49), 2Br1E (m_D=52), and 2I1E (m_D=54) exhibit higher m_D values than their 3-substituted counterparts (3Cl1P, 3Br1P, and 3I1P, all m_D=43), suggesting that despite their shorter alkyl chains, these compounds exhibit greater structural flexibility in the formation and adaptation of hydrogen-bonded networks.
- this trend indicates that shorter-chain (2-substituted) alcohols can more effectively rearrange their hydrogen-bonding interactions, allowing for dynamic reorganization of supramolecular structures.

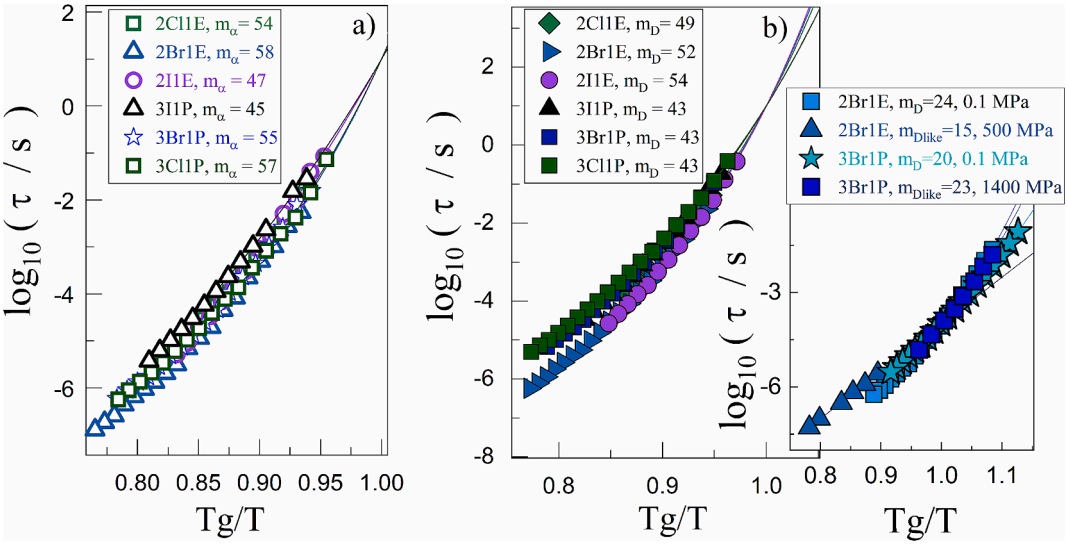

Fig. 7. The logarithm of the relaxation times (τ) as a function of the reciprocal temperature scaled by the glass transition temperature (T_g/T) for the alfa (a) and Debye (b) processes of all studied alcohols at ambient pressure (0.1 MPa). The solid lines represent fits to the VFTH equation. The legends show the values of the fragility index (m_α) and the steepness index (m_D) for each alcohol. The inset in the right panel compares the pressure dependence of m_D for 2Br1E and 3Br1P, with both indices determined at τ_{Debye} = -4 for consistency. For 2Br1E, m_D = 24 at atmospheric pressure, and m_{Dlike} = 15 at 500 MPa. For 3Br1P, m_D = 20 at atmospheric pressure, and m_{Dlike} = 23 at 1.4 GPa. Data for 3Br1P were taken from ref. [10].

- in contrast, 3-substituted analogues with lower m_D values exhibit a more rigid organization, where their hydrogen-bonding networks remain more constrained.

Interestingly, the highest m_D value is observed for 2I1E (m_D=54), followed by 2Br1E.

(m_D=52) and 2Cl1E (m_D=49), suggesting that the presence of a larger halogen atom increases the ability of molecules to rearrange under ambient conditions. This may be due to the iodine atom's steric and electronic effects, weakening dipolar interactions and allowing greater supramolecular adaptability [37–43].

Furthermore, the observed increase in m_D values with increasing halogen atomic mass (Cl < Br < I) suggests that heavier halogens enhance the ability of molecules to reorganize their hydrogen-bonded networks. A possible explanation is that with increasing halogen mass, the polarizability of the molecule increases, leading to weaker directional hydrogen bonding and more flexible molecular arrangements [39]. In addition, heavier halogens introduce stronger dispersion forces (London interactions) that can compete with and weaken hydrogen bonding, allowing greater molecular mobility and structural adaptability [37].

3.3.6. *High-pressure behavior and m_{Dlike} trends*

A more detailed analysis of pressure-dependent changes in the molecular dynamics of brominated alcohols is obtained by comparing the m_D and m_{Dlike} parameters under consistent conditions – specifically, with the same relaxation time, τ_{Debye} = -4. This approach ensures methodological consistency and minimizes potential artifacts resulting from extrapolating temperature-dependent relaxation times over wide pressure ranges.

For 2Br1E, the comparison shows that even a relatively moderate pressure increase (to ~ 500 MPa) leads to a pronounced decrease in fragility, with m_D decreasing from 24 at atmospheric pressure to m_{Dlike} = 15 at 500 MPa. This substantial decrease indicates that the hydrogen-bonded network in 2Br1E is highly sensitive to compression and undergoes significant structural reorganization at relatively low pressure. Such behavior suggests that the initial supramolecular structure at ambient conditions, characterized by relatively rigid and densely packed hydrogen-bonded chains, is destabilized under compression, favoring more compact and possibly cyclic arrangements that reduce overall fragility.

For 3Br1P, the same analysis (at τ_{Debye} = -4) shows a very different response to pressure. Despite being subjected to a much higher pressure (~1400 MPa), the change in fragility is small: m_D increases slightly from 20 at atmospheric pressure to m_{Dlike} = 23 at 1400 MPa. This limited response suggests that the hydrogen-bonded network in 3Br1P is structurally more adaptable and retains a higher degree of flexibility under compression. This behavior likely reflects the more extended carbon chain, which introduces additional conformational degrees of freedom and reduces the sensitivity of the supramolecular network to pressure-induced rearrangements.

The inset in Fig. 7**b** highlights this contrast: 2Br1E shows a sharp drop in fragility even at relatively low pressure, while 3Br1P shows only minor changes in fragility, despite the much higher pressure applied. This observation underscores the greater structural rigidity of the shorter-chain alcohol, driven by its tighter hydrogen-bonding network, and the enhanced flexibility of the longer-chain analog, where steric hindrance and the larger molecular volume weaken the cooperative hydrogen-bond network, allowing it to accommodate compression more gradually.

These results are fully consistent with previous reports on pressure effects in hydrogen-bonded systems, which showed that shorter-chain alcohols tend to form more rigid hydrogen-bonded networks, while longer-chain analogues exhibit more flexible supramolecular arrangements under elevated pressure due to increased steric effects. Furthermore, previous studies showed that the type of halogen substitution significantly modifies the balance between hydrogen bonding, dipolar forces, and dispersion interactions. This interplay becomes even more pronounced under high-pressure, where compression enhances specific halogen interactions, such as halogen-halogen and halogen-oxygen interactions, further modifying the pressure-dependent relaxation dynamics [41–48].

3.3.7. *Limitations in m_{Dlike} analysis due to crystallization*

However, due to the crystallization of chlorinated alcohols under pressure (2Cl1E and 3Cl1P) and the crystallization of iodinated alcohols (2I1E and 3I1P) at higher pressures, it was not possible to determine their m_{Dlike} values. This suggests that these compounds are less able to reorganize their hydrogen bond networks under extreme compression, leading to crystallization. The inability to measure m_{Dlike} highlights the structural limitations imposed by halogen type and molecular geometry on the adaptability of these alcohols under high pressure [41,42].

3.3.8. *Structural reorganization in hydrogen-bonded clusters under pressure*

The analysis of changes in the dielectric loss amplitude (ε") under pressure provides valuable insights into the structural reorganization of supramolecular clusters in halogenated alcohols. The amplitude of ε" is closely related to the strength of dipole fluctuations and the extent of cooperative molecular motions. A decrease in ε" under pressure indicates reduced dipole correlations, which may result from the restructuring of the hydrogen bond network, a reduction in cluster size, or a decrease in molecular mobility [30,42].

To investigate how alkyl chain length and halogen substitution affect supramolecular behavior under high pressure, we analyzed the dielectric spectra of the studied compounds (Fig. 8) as representative examples, focusing on the amplitude of the D-process for 2Br1E (Fig. 8**a**) and 3I1P (Fig. 8**b**). The observed decrease in ε" for both compounds under compression suggests that initially dominant chain-like supramolecular structures are transformed into more branched or cyclic forms. This structural reorganization likely reduces molecular mobility and dipolar fluctuations, accounting for the decrease in ε".

Applying this understanding to halogenated alcohols, we observe that pressure significantly affects their supramolecular organization and relaxation dynamics, consistent with previous findings on halogenated monoalcohols [10], where 3Br1P showed a transition from linear chain-like arrangements to more compact cyclic and branched clusters under compression, while 2Br1E and 2Cl1E, with internal –OH groups, formed stable cyclic hydrogen-bonded networks that better adapted to pressure changes. For 2Br1E, the presence of bromine may enhance specific halogen interactions, promoting cyclic supramolecular arrangements under compression. In contrast, the large iodine atom in 3I1P introduces steric hindrance, limiting the formation of extended chains and favoring branched or cyclic clusters under pressure [5,37,48,49, 50].

To further verify the dielectric spectroscopy results and to gain deeper insight into how alkyl chain length affects the architecture of supramolecular structures under high-pressure conditions, MDS were performed. The results of these simulations allow us to determine the degree of the association via HBs, the size, and type (linear, cyclic, or branched) of H-bonded supramolecular structures that are formed under ambient and high-pressure conditions and provide insight into the general structural organization of the studied MAs. Additionally, the simulations reveal other types, besides H-bonded clusters, of supramolecular associations that may result from interactions formed by halogen atoms.

3.3.9. *Insights into the structural organization from molecular dynamics simulations*

To better understand the changes generated by high pressure in the organization of the molecules between the studied halogen alcohols differing in the chain length, models of the structure for selected compounds, 2Br1E and 3Br1P, were derived from MDS. A similar procedure for obtaining three-dimensional models of halogen alcohols at room T

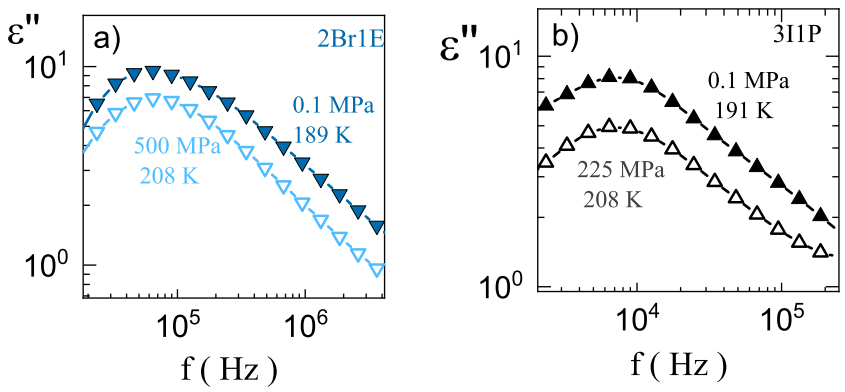

Fig. 8. Comparison of the main process at atmospheric and elevated pressure characterized by the same relaxation times for 2Br1E (a) and 3I1P (b).

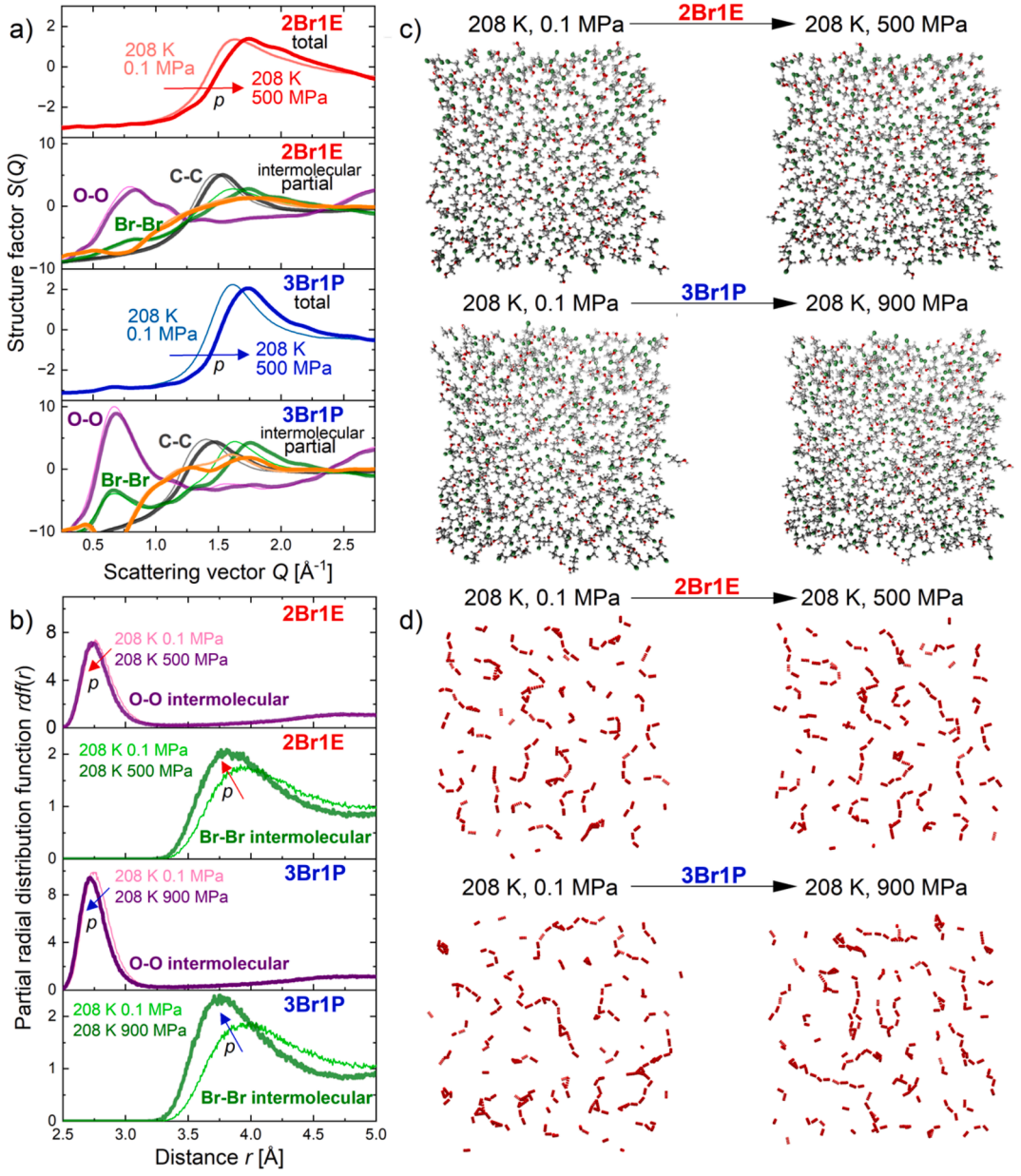

Fig. 9. Total and selected partial atom–atom (C-C, O-O, and Br-Br) intermolecular structure factors calculated based on the MD models of 2Br1E and 3Br1E alcohols at T = 208 K and p = 0.1 MPa, and at T = 208 K and p = 500 or 900 MPa, respectively (a). Partial O-O and Br-Br radial distribution functions corresponding to the nearest-neighbour intermolecular correlations between these atoms (b). Visualization of the arrangement of molecules (c) as well as solely O-H···O hydrogen bonds (d) on cross-sections of the MD models (5 Å thick planes cut from 20 Å x 20 Å boxes) for 2Br1E and 3Br1E at the ambient and high-pressure conditions at 208 K.

and various p conditions has been demonstrated in our previous papers [9,10]. It is worth adding that the structure factors representing atomic pairwise correlations in reciprocal space computed for those models were in good agreement with the experimental data measured using X-ray diffraction at corresponding thermodynamic conditions. Herein, it is worth adding that we have selected only these compounds because they did not crystallize upon high-pressure dielectric investigations. Thus, it is possible to directly compare experimental and theoretical results.

The results of the MDS performed at conditions T = 208 K and p = 0.1 MPa as well as higher p = 500 and 900 MPa for 2Br1E and 3Br1P, respectively, are presented in Fig. 9. Fig. 9**a** shows the total structure factors S(Q) as well as selected partial atom–atom S(Q), which give the strongest contribution to the total functions in the presented low scattering vector range (Q = 0.25 – 2.75 $Å^{-1}$). The diffraction peaks in such low Q-region originate mainly from the medium- and short-range intermolecular correlations. The main peak in the total S(Q) represents the short-range intermolecular arrangement and shifts towards higher Q with the rise in p for both alcohols due to the densification and decrease of the average intermolecular distances. It can also be seen that the shape of the right shoulder of the main peak evolves with the compression, and a similar behavior is observed for partial Br-Br functions, whereas C-C functions are less affected by the compression for both alcohols. It suggests that the changes in their short-range molecular organization induced by high-pressure involve a rearrangement of Br atoms. Br-Br functions reveal additional maxima at lower Q ≈ 0.6 – 0.8 $Å^{-1}$. Such peaks arise from structural correlations between Br atoms at longer distances d = 2π/Q ≈ 8 – 11 Å, and they evidence the existence of a medium-range order of Br atoms in both alcohols, whereas the amplitude of these features is slightly higher for 3Br1P than for 2Br1P. Even stronger medium-range order correlations emerge for O atoms, as one can see by the evidence of O-O maxima at nearly the same Q positions as the Br-Br bumps. They appear because of the presence of a medium-range order of O atoms linked together by HBs and forming supramolecular clusters. It is worth mentioning that in the total S(Q), the peaks related to the medium-range structural correlations are barely distinguished since they are extinguished by anti-peaks coming from mostly Br-O correlations. The Q position of the O-O maximum reflects the repeating distance between the clusters of linked OH groups. As one can see, the positions of the O-O maxima slightly shift towards higher Q with compression for both alcohols, while their amplitudes drop down. It can, therefore, be assumed that some modulation of the HBs pattern occurs under compression. That is confirmed by a subtle decrease in the amplitude of O-O peak in the rdf(r) at r ≈ 2.78 Å, which is the average distance between O donors and acceptors in HBs of various MAs [3]. Such structural features demonstrate a destructive effect of high-pressure on the HBs in the studied MAs with substituted halogen atoms. The representative arrangement of molecules as well as O-H···O hydrogen bonds for 2Br1E and 3Br1E at the ambient and high-pressure conditions at 208 K are presented in panels **(c) and (d) of** Fig. 9. They reveal the structural organization within the selected planes (5 Å thick in each case) cut from the bigger simulation models (20 x 20 Å). The characteristic feature of the structure of both studied alcohols, 2Br1E and 3Br1P, are the chains of HBs, marked schematically **in** Fig. 9**d**. At T = 208 K and p = 0.1 MPa, the chains are branched and tangled. Note that bigger associates of HBs are not displayed in these planes due to their limited thickness. Cyclic – ring-like associates of HBs are rather rare for both systems. Upon an increase in p the HBs systems slightly transform. To describe the changes quantitatively, the average number of O-H···O HBs, as well as the average sizes of H-bonded clusters (average number of molecules in H-bonded clusters) were determined and are listed in Table 1. The total number of molecules in each model was 2000. Thus, 3Br1P with the number of 1947 HBs at T = 208 K and p = 0.1 MPa can be treated as system almost completely associated via HBs. 2Br1E with 1871 HBs is a slightly less associated system – it contains more molecules not linked by HBs, compared to 3Br1P at the same conditions. Such a difference between these two compounds was

Table 1
The average number of O-H···O hydrogen bonds and molecules associated in the hydrogen-bonded clusters for 2Br1E and 3Br1P systems, calculated based on the MDS models.

Compound	Thermodynamic conditions			
	T = 208, p = 0.1 MPa		T = 208, p = 500/900 MPa	
	Number of HBs	Average number of molecules in HBs clusters	Number of HBs	Average number of molecules in HBs clusters
2Br1E	1871	19	1868	21
3Br1P	1947	17	1930	26

preserved also under high-pressure. However, simultaneously, a slight decrease in the total amount of HBs under high-pressure was reported for both systems, which was previously evidenced by the decrease in the O-O structural correlations in the S(Q) and rdf(r) functions. Nonetheless, the average size of the H-bonded clusters for both alcohols increases with compression due to the increase in the size of particularly large clusters. The changes in the distribution of the sizes of the H-bonded clusters may be better followed in histograms presented in Fig. S1 and S2 in Supporting Information.

The other characteristic feature of the transformation of the intermolecular structure of the studied halogen alcohols under high-pressure is the enhancement of intermolecular Br-Br correlations, which may be followed by the increase in the area of the first Br-Br intermolecular rdf(r) peak in Fig. 9**b**. The maximum of this peak shifts towards a smaller distance, r ≈ 3.8 Å, and gets sharper and more intense with compression for both alcohols. This behavior is directly related to the already mentioned changes in the main Br-Br peak in the S(Q) and suggests a rise in the organization of Br atoms – inversely to the structure of O atoms (visualization of the structure of Br atoms is presented in Fig. S3 in Supporting Information). The transformation of the structure of Br sites is more significant for 3Br1P than for 2Br1E, the same as in the case of O sites. Thus, the MDS data reveal that the supramolecular structure of 3Br1P is more affected by the high-pressure than 2Br1E, which forms more stable supramolecular associates. The changes in the structure of O and Br atoms support the hypothesis proposed in our previous paper [10] that under high-pressure, there is an increase in the number of intermolecular interactions involving halogen atoms and that they aggregate more rapidly with compression than O atoms via the O-H···O HBs. This, therefore, supports the competition between the different types of intermolecular interactions. As a result, the organization of molecules gets more complex and heterogeneous compared to the structure at ambient pressure conditions, where classical O-H···O HBs play a more significant role in the association and structuring of molecules.

Together with the increase in Br-Br correlations under high-pressure, the results of MDS also indicated an increase in the Br-O correlations. However, they are much weaker than Br-Br correlations, as can be compared based on Fig. S4 in the Supporting Information**.** The amplitude and area of the first intermolecular Br-O peak are much lower compared to those for the Br-Br peak for both alcohols (by about half). Therefore, in the manuscript, we focused mainly on the halogen-halogen clusters, which were more numerous. Nevertheless, we cannot exclude the possibility of the formation of heteroatomic Br-OH halogen bonds in the studied systems.

3.3.10. Linking dielectric spectroscopy and molecular dynamics simulations – A complementary picture

The combined analysis of BDS and MDS allows for a deeper understanding of the pressure-induced structural reorganization in halogenated monoalcohols. BDS reveals a gradual decrease in the amplitude of the D process (ε") under high-pressure, indicating reduced dipolar correlations and changes in the hydrogen bond network. MDS confirms that these changes are related to the transformation of supramolecular

clusters — from more extended, chain-like structures towards compact and branched aggregates. Additionally, MDS shows that pressure enhances halogen-halogen interactions, especially in brominated systems, which directly competes with classical hydrogen bonding (O-H···O). This growing competition between different types of interactions leads to a more heterogeneous molecular structure under pressure. The combination of BDS and MDS clearly shows that the observed changes in relaxation processes originate from specific structural rearrangements, which would not be fully accessible from dielectric data alone.

4. Conclusions

The molecular structure, including the carbon chain length and the type of halogen atom, significantly influences the relaxation processes and self-assembly behaviour of the studied alcohols. Shorter carbon chains favour the formation of more ordered hydrogen-bonded clusters, while longer chains promote more flexible, branched, and less cohesive supramolecular structures. Among the studied alcohols, chlorinated compounds exhibited the highest degree of dipolar correlation, as reflected in higher Kirkwood factor values. In contrast, brominated and iodinated alcohols showed weaker dipole interactions and more disordered cluster structures.

High-pressure dielectric spectroscopy and molecular dynamics simulations confirmed that pressure induces structural reorganization. Under high-pressure conditions, the supramolecular structures of the studied alcohols transform from chain-like arrangements into more compact cyclic or branched clusters. High pressure leads to a decrease in dielectric loss amplitude (ε”), indicating reduced dipolar correlations, restructuring of the hydrogen bond network, and decreased molecular mobility. Molecular dynamics simulations revealed that the supramolecular structure of 3-bromo-1-propanol is more affected by high pressure than that of 2-bromo-1-ethanol, which forms more stable molecular associations.

High-pressure alters the supramolecular organization formed at ambient pressure. The molecules in the studied alcohols exhibit a stronger tendency to organize halogen atoms in clusters under high pressure than the oxygen atoms. This indicates the increase in the significance of the halogen-halogen interactions under high-pressure compared to O-H···O interactions. Despite a slight decrease in the total number of O-H···O hydrogen bonds, the average size of supramolecular clusters increases under high pressure, despite the difference between the carbon chain length, suggesting greater stability of larger molecular assemblies. Halogen-halogen (Br-Br) associates compete with hydrogen-bonded (O-H···O) associates, leading to a more heterogeneous molecular organization under high-pressure conditions compared to systems under ambient pressure, where the structures are dominated by aggregation via the classical hydrogen bonds. The obtained results provide new insights into the impact of molecular structure and halogen substitution on the relaxation dynamics of halogenated monoalcohols and the mechanisms of their supramolecular reorganization under high-pressure conditions.

CRediT authorship contribution statement

Kinga Łucak: Writing – review & editing, Writing – original draft, Visualization, Methodology, Investigation, Formal analysis, Data curation, Conceptualization. **Anna Z. Szeremeta:** Writing – review & editing, Investigation, Formal analysis. **Anna Janowska:** Investigation, Formal analysis. **Karolina Jurkiewicz:** Writing – review & editing, Writing – original draft, Investigation, Formal analysis. **Katarzyna Grzybowska:** Writing – original draft, Investigation, Formal analysis. **Kamil Kamiński:** Writing – review & editing. **Sebastian Pawlus:** Writing – review & editing, Project administration, Funding acquisition, Data curation, Conceptualization.

Declaration of competing interest

The authors declare the following financial interests/personal relationships which may be considered as potential competing interests: Prof. dr hab. Sebastian Pawlus reports financial support was provided by National Science Centre Poland. If there are other authors, they declare that they have no known competing financial interests or personal relationships that could have appeared to influence the work reported in this paper.

Acknowledgements

We gratefully acknowledge Polish high-performance computing infrastructure PLGrid (HPC Center: ACK Cyfronet AGH) for providing computer facilities and support within computational grants no. PLG/2025/018012 and PLG/2024/016967. A. J. acknowledges the financial support within the scholarship from the Institute of Physics, University of Silesia in Katowice. The research was financed with financial support from the National Science Centre, Poland, within the OPUS Project No. UMO-2019/35/B/ST3/02670, which K. Ł., K. J., K. K., and S.P. would like to acknowledge.

Appendix A. Supplementary data

Supplementary data to this article can be found online at https://doi.org/10.1016/j.molliq.2025.127787.

Data availability

Data will be made available on request.

References

[1] R. Böhmer, C. Gainaru, R. Richert, Structure and Dynamics of Monohydroxy Alcohols—Milestones towards Their Microscopic Understanding, 100 years after Debye, Phys. Rep. 545 (4) (2014) 125–195, https://doi.org/10.1016/j.physrep.2014.07.005.
[2] S. Pothoczki, L. Pusztai, I. Bakó, Variations of the Hydrogen Bonding and Hydrogen-Bonded Network in Ethanol–Water Mixtures on Cooling, J. Phys. Chem. B 122 (26) (2018) 6790–6800, https://doi.org/10.1021/acs.jpcb.8b02493.
[3] J. Grelska, K. Jurkiewicz, A. Burian, S. Pawlus, Supramolecular Structure of Phenyl Derivatives of Butanol Isomers, J. Phys. Chem. B 126 (19) (2022) 3563–3571, https://doi.org/10.1021/acs.jpcb.2c01269.
[4] C. Gainaru, R. Meier, S. Schildmann, C. Lederle, W. Hiller, E.A. Rössler, R. Böhmer, Nuclear-Magnetic-Resonance Measurements Reveal the Origin of the Debye Process in Monohydroxy Alcohols, PhysRevLett.1 105 (25) (2010) 258303, https://doi.org/10.1103/PhysRevLett.105.258303.
[5] W. Dannhauser, Dielectric Study of Intermolecular Association Isomeric Octyl Alcohols, J. Chem. Phys. 48 (11) (1968) 1911, https://doi.org/10.1063/1.1668989.
[6] L.P. Singh, R. Richert, Watching Hydrogen-Bonded Structures in an Alcohol Convert from Rings to Chains, PhysRevLett.1 109 (16) (2012) 167802, https://doi.org/10.1103/PhysRevLett.109.167802.
[7] P. Bordewijk, On the relationship between the Kirkwood correlation factor and the dielectric permittivity, J. Chem. Phys. 73 (1) (1980) 595–597, https://doi.org/10.1063/1.439841.
[8] N. Soszka, B. Hachuła, M. Tarnacka, J. Grelska, K. Jurkiewicz, M. Geppert-Rybczyńska, R. Wrzalik, K. Grzybowska, S. Pawlus, M. Paluch, Aromaticity effect on supramolecular aggregation. Aromatic vs. cyclic monohydroxy alcohols, Spectrochim. Acta Part A Mol. Biomol. Spectrosc. 276 (2022) 121235, https://doi.org/10.1016/j.saa.2022.121235.
[9] K. Łucak, A.Z. Szeremeta, R. Wrzalik, J. Grelska, K. Jurkiewicz, N. Soszka, B. Hachuła, D. Kramarczyk, K. Grzybowska, B. Yao, K. Kamiński, S. Pawlus, Experimental and Computational Approach to Studying Supramolecular Structures in Propanol and Its Halogen Derivatives.
[10] J. Phys, Chem. B 127 (42) (2023) 9102–9110, https://doi.org/10.1021/acs.jpcb.3c02092.
[11] K. Łucak, A.Z. Szeremeta, J. Grelska, K. Jurkiewicz, S. Kołodziej, R. Wrzalik, K. Kamiński, S. Pawlus, Effect of high pressure on the molecular dynamics of halogen monoalcohols, J. Mol. Liq. 423 (2025) 127045, https://doi.org/10.1016/j.molliq.2025.127045.
[12] M.J. Abraham, T. Murtola, R. Schulz, S. Páll, J.C. Smith, B. Hess, E. Lindahl, GROMACS: high performance molecular simulations through multi-level parallelism from laptops to supercomputers, SoftwareX 1–2 (2015) 19–25, https://doi.org/10.1016/j.softx.2015.06.001.

[13] S. Páll, M.J. Abraham, C. Kutzner, B. Hess, E. Lindahl, Tackling Exascale Software Challenges in Molecular Dynamics Simulations with GROMACS (2015) 3–27, https://doi.org/10.1007/978-3-319-15976-8_1.
[14] S. Pronk, S. Páll, R. Schulz, P. Larsson, P. Bjelkmar, R. Apostolov, M.R. Shirts, J.C. Smith, P.M. Kasson, D. van der Spoel, et al., GROMACS 4.5: a high-throughput and highly parallel open source molecular simulation toolkit, Bioinformatics 29 (7) (2013) 845–854.DOI: 10.1093/bioinformatics/btt055.
[15] B. Hess, C. Kutzner, D. Van Der Spoel, E. Lindahl, GROMACS 4: algorithms for highly efficient, load-balanced, and scalable molecular simulation, J. Chem. Theory Comput. 4 (3) (2008) 435–447, https://doi.org/10.1021/ct700301q.
[16] D. Van Der Spoel, E. Lindahl, B. Hess, G. Groenhof, A.E. Mark, H.J. Berendsen, GROMACS: fast, flexible, and free, J. Comput. Chem. 26 (16) (2005) 1701–1718, https://doi.org/10.1002/jcc.20291.
[17] E. Lindahl, B. Hess, D., Van Der Spoel, GROMACS 3.0: a package for molecular simulation and trajectory analysis, Mol. Model. Annu. 7 (2001) 306–317, https://doi.org/10.1007/s008940100045.
[18] H.J. Berendsen, D. Van Der Spoel, R. Van Drunen, GROMACS: A message-passing parallel molecular dynamics implementation, Comput. Phys. Commun. 91 (1–3) (1995) 43–56, https://doi.org/10.1016/0010-4655(95)00042-E.
[19] A.W. Sousa da Silva, W.F. Vranken, ACPYPE - Antechamber Python Parser Interface, BMC Res. Notes 5 (2012) 1–8, https://doi.org/10.1186/1756-0500-5-367.
[20] L. Kagami, A. Wilter, A. Diaz, W. Vranken, The ACPYPE web server for small-molecule MD topology generation, Bioinformatics 39 (6) (2023) btad350, https://doi.org/10.1093/bioinformatics/btad350.
[21] J. Wang, R.M. Wolf, J.W. Caldwell, P.A. Kollman, D.A. Case, Development and testing of a general amber force field, J. Comput. Chem. 25 (9) (2004) 1157–1174, https://doi.org/10.1002/jcc.20035.
[22] D.A. Case, T.A. Darden, T.E. Cheatham III, C.L. Simmerling, J. Wang, R.E. Duke, R. Luo, et al., AMBER 9, University of California, San Francisco, 2006.
[23] M. Brehm, M. Thomas, S. Gehrke, B. Kirchner, TRAVIS—a free analyzer for trajectories from molecular simulation, J. Chem. Phys. 152 (16) (2020) 164105, https://doi.org/10.1063/5.0005078.
[24] O. Hollóczki, M. Macchiagodena, H. Weber, M. Thomas, M. Brehm, A. Stark, O. Russina, A. Triolo, B. Kirchner, Triphilic Ionic-Liquid Mixtures: Fluorinated and Non-fluorinated Aprotic Ionic-Liquid Mixtures, ChemPhysChem 16 (15) (2015) 3325–3333, https://doi.org/10.1002/cphc.201500473.
[25] K.C. Kao, Dielectric phenomena in solids, Elsevier Academic Press, London, 2004, pp. 92–95.
[26] S. Havriliak, S. Negami, A Complex Plane Analysis of α-Dispersions in Some Polymer Systems. J. Polym. Sci. Part C Polym. Symp. 14 (1) (2007) 99–117. DOI: 10.1002/polc.5070140111.
[27] M. Paluch, J. Gapinski, A. Patkowski, E.W. Fischer, Does fragility depend on pressure? A dynamic light scattering study of a fragile glass-former, J. Chem. Phys. 114 (2001) 8048–8055, https://doi.org/10.1063/1.1362293.
[28] H. Vogel, The law of the relation between the viscosity of liquids and the temperature, Phys. z. 22 (1921) 645–646.
[29] G.S. Fulcher, Analysis of recent measurements of the viscosity of glasses, J. Am. Ceram. Soc. 8 (1925) 339–355.
[30] V.G. Tamman, W. Hesse, Die Abhängigkeit der Viscosität von der Temperatur bei unterkühlten Flüssigkeiten, Z. Anorg. Allg. Chem. 156 (1926) 245–257, https://doi.org/10.1002/zaac.19261560121.
[31] F. Kremer, A. Schönhals, The Scaling of the Dynamics of Glasses and Supercooled Liquids, in: F. Kremer, A. Schönhals (Eds.), Broadband Dielectric Spectroscopy, Springer, Berlin, Heidelberg, 2003, pp. 99–129, https://doi.org/10.1007/978-3-642-56120-7_4.
[32] R. Buchner, G. Hefter, Interactions and dynamics in electrolyte solutions by dielectric spectroscopy, Phys. Chem. Chem. Phys. 11 (40) (2009) 8984–8999, https://doi.org/10.1039/B906555P.
[33] A. Kaiser, M. Ritter, R. Nazmutdinov, M. Probst, Hydrogen Bonding and Dielectric Spectra of Ethylene Glycol-Water Mixtures from Molecular Dynamics Simulations, J. Phys. Chem. B 120 (40) (2016) 10515–10523, https://doi.org/10.1021/acs.jpcb.6b05236.
[34] E. V. Boldyreva, Understanding Intermolecular Interactions in the Solid State: Approaches and Techniques, in: D. Chopra (Ed.), The Royal Society of Chemistry, 2018, pp. 32–97. DOI: 10.1039/9781788013086-00032.
[35] A. Błażytko, M. Rams-Baron, M. Paluch, The influence of molecular shape on reorientation dynamics of sizable glass-forming isomers at ambient and elevated pressure, Sci. Rep. 14 (2024) 887, https://doi.org/10.1038/s41598-023-50894-8.
[36] G. Floudas, M. Paluch, A. Grzybowski, K.L. Ngai, Molecular dynamics of glass-forming systems, Effects of pressure, Springer, 2010.
[37] N. Sugawara, P.-J. Hsu, A. Fujii, J.-L. Kuo, Competition between hydrogen bonds and van der Waals forces in intermolecular structure formation of protonated branched-chain alcohol clusters, Phys. Chem. Chem. Phys. 20 (2018) 25482–25494, https://doi.org/10.1039/C8CP05222K.
[38] G. Cavallo, P. Metrangolo, R. Milani, T. Pilati, A. Priimagi, G. Resnati, G. Terraneo, The Halogen Bond, Chem. Rev. 116 (4) (2016) 2478–2601, https://doi.org/10.1021/acs.chemrev.5b00484.
[39] D. Wang, X. Zhang, Z.Y. Yi, et al., Evolution of Br···Br and I···I contacts in chiral 2D crystallization, Nat. Commun. 13 (1) (2022) 5850, https://doi.org/10.1038/s41467-022-33446-y.
[40] P. Politzer, J.S. Murray, T. Clark, Halogen bonding and other σ-hole interactions: A perspective, Phys. Chem. Chem. Phys. 15 (27) (2013) 11178–11189, https://doi.org/10.1039/C3CP00054K.
[41] C.A. Angell, J. Non-Cryst, Solids 13 (1991) 131–133.
[42] J. Sun, D.A. Decato, V.S. Bryantsev, E.A. John, O.B. Berryman, The interplay between hydrogen and halogen bonding: substituent effects and their role in the hydrogen bond enhanced halogen bond, Chem. Sci. 14 (2023) 8924–8935, https://doi.org/10.1039/D3SC02348F.
[43] C.A. Angell, K.L. Ngai, G.B. McKenna, P.F. McMillan, S.W. Martin, Relaxation in glassforming liquids and amorphous solids, J. Appl. Phys. 88 (6) (2000) 3113–3157, https://doi.org/10.1063/1.1286035.
[44] R. Böhmer, K.L. Ngai, C.A. Angell, D.J. Plazek, Nonexponential relaxations in strong and fragile glass formers, J. Chem. Phys. 99 (5) (1993) 4201–4209, https://doi.org/10.1063/1.466117.
[45] L. Wilson, R. Alencastro, C. Sandorfy, Hydrogen Bonding of n-Alcohols of Different Chain Lengths, Can. J. Chem. 63 (2011) 40–45, https://doi.org/10.1139/v85-007.
[46] P. Metrangolo, G. Resnati, Halogen Bonding: Fundamentals and Applications, Springer International Publishing (2008), https://doi.org/10.1007/978-3-540-74330-9.
[47] C. Laurence, J.-F. Gal, The Strength of Hydrogen Bonds: From Isolated Hydrogen Bonds to Solvation and Proton Transfer in Molecular Interactions, John Wiley & Sons (2010), https://doi.org/10.1002/9780470661345.
[48] M.D. Ediger, Spatially Heterogeneous Dynamics in Supercooled Liquids, Annu. Rev. Phys. Chem. 51 (2000) 99–128, https://doi.org/10.1146/annurev.physchem.51.1.99.
[49] R.J. Hemley, Effects of High Pressure on Molecules, Annu. Rev. Phys. Chem. 51 (2000) 763–800, https://doi.org/10.1146/annurev.physchem.51.1.763.
[50] D. Fragiadakis, C.M. Roland, R. Casalini, Insights on the origin of the Debye process in monoalcohols from dielectric spectroscopy under extreme pressure conditions, J. Chem. Phys. 132 (2010) 144505, https://doi.org/10.1063/1.3374820.

Supporting information

Influence of molecular structure and thermodynamic conditions on the dynamics, halogen bonding, and self-assembly of halogenated monoalcohols

Kinga Łucak[a]*, Anna Z. Szeremeta[a], Anna Janowska[a], Karolina Jurkiewicz[a], Katarzyna Grzybowska[a], Kamil Kamiński[a], Sebastian Pawlus[a].

[a] *August Chełkowski Institute of Physics, Faculty of Science and Technology, University of Silesia in Katowice, 75 Pułku Piechoty 1, 41-500 Chorzów, Poland*

*Correspondence e-mails: kinga.lucak@us.edu.pl

1.1. Molecular dynamics simulations

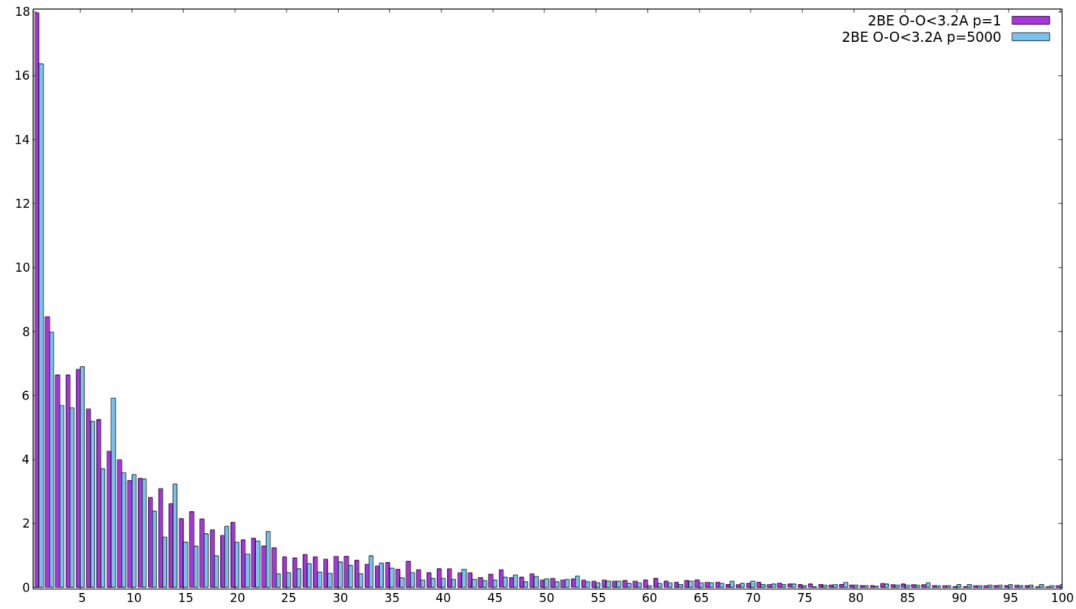

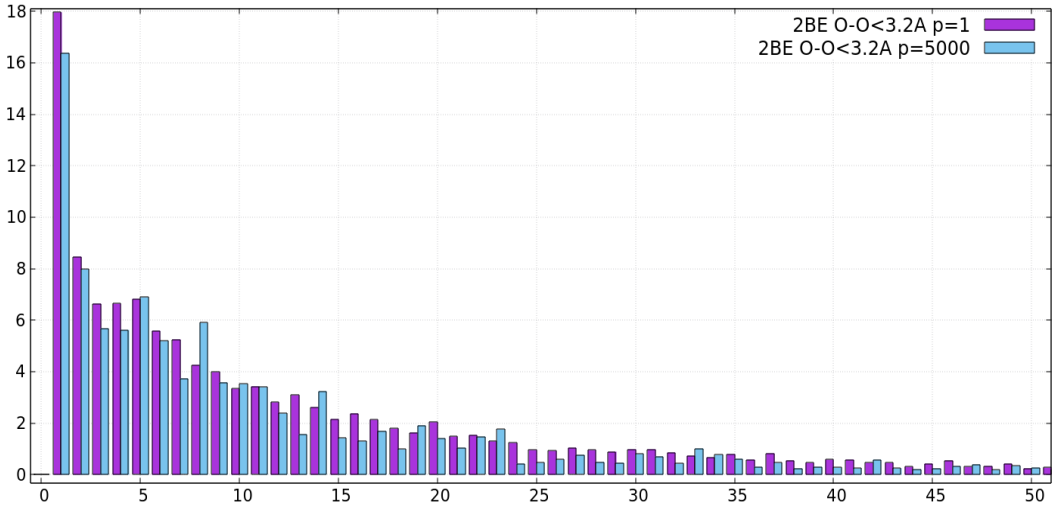

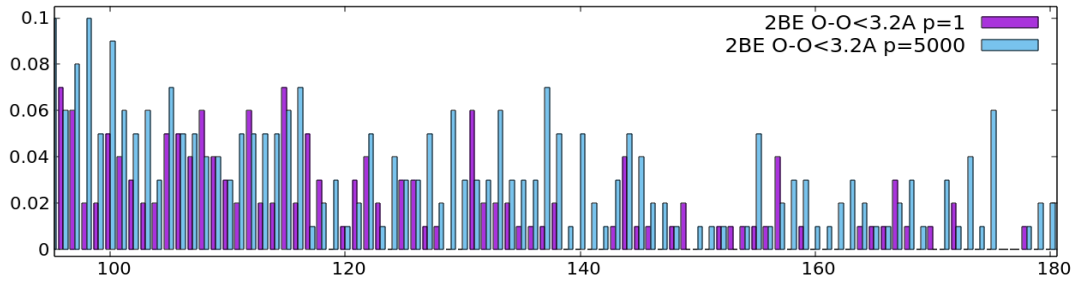

Figure S1. Comparison of distribution of the size of hydrogen-bonded molecular clusters (the number of molecules linked in clusters by hydrogen bonds) in 2Br1E for T = 208 K and p = 0.1 MPa (purple columns) and for T = 208 K and p = 500 MPa (blue columns). The O-O acceptor-donor cut-off distance for the formation of the H-bond was set as < 3.2 Å, based on the first minimum of the O-O radial distribution function.

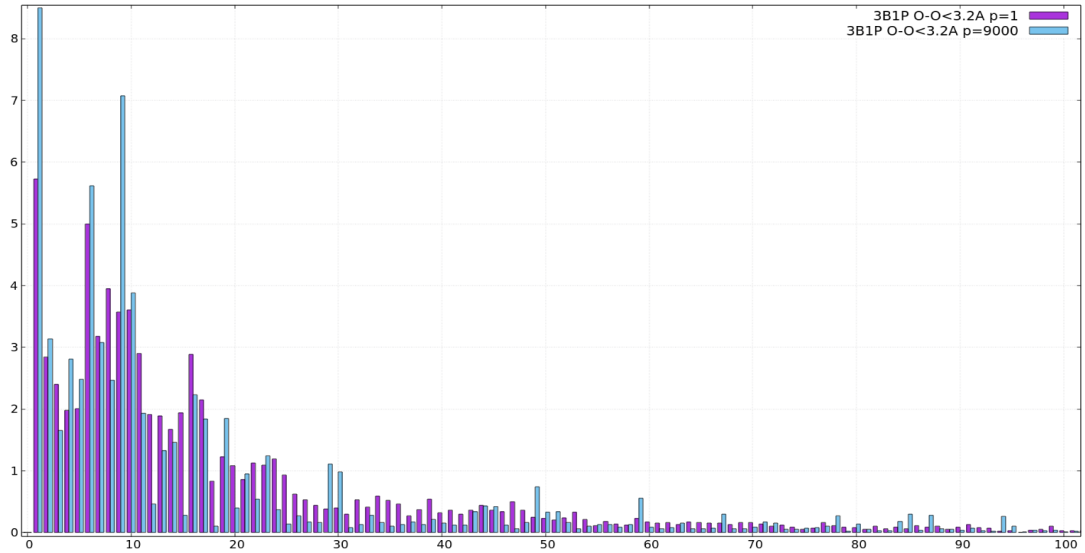

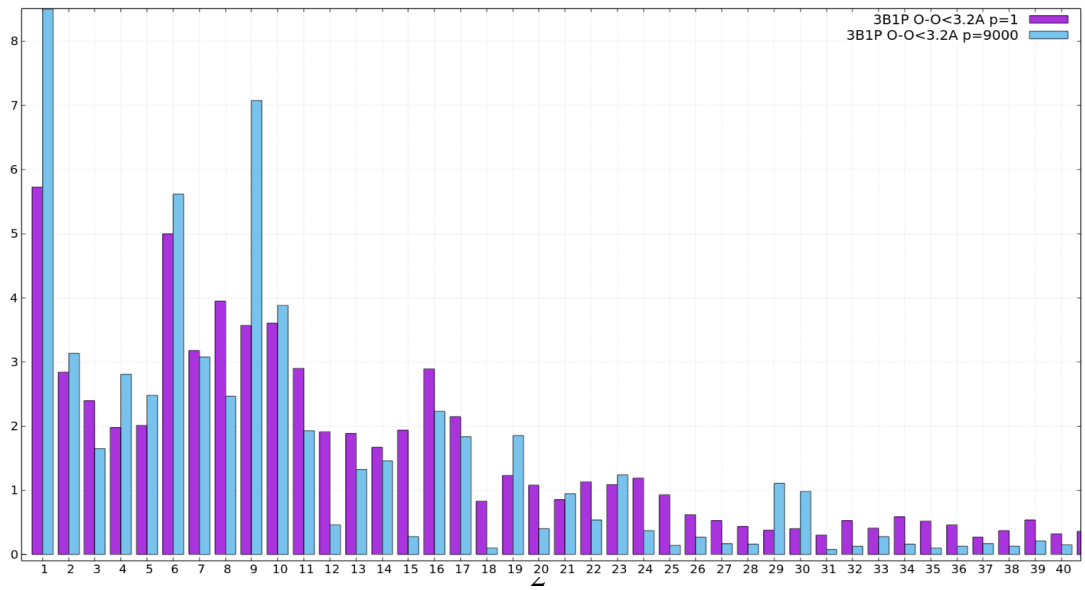

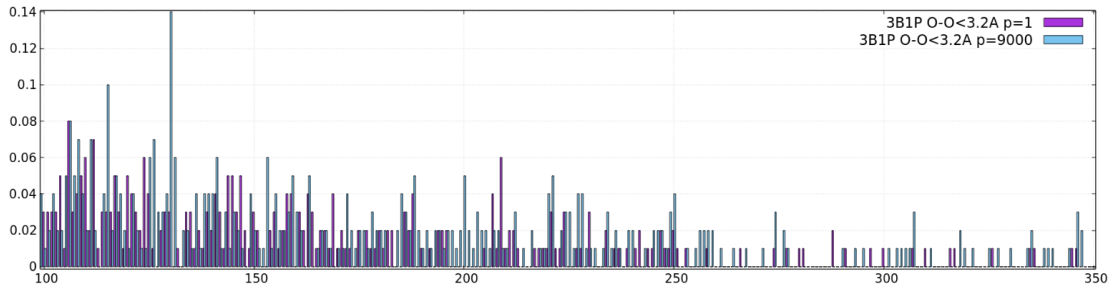

Figure S2. Comparison of distribution of the size of hydrogen-bonded molecular clusters (the number of molecules linked in clusters by hydrogen bonds) in 3Br1P for T = 208 K and p = 0.1 MPa (purple columns) and for T = 208 K and p = 900 MPa (blue columns). The O-O acceptor-donor cut-off distance for the formation of the H-bond was set as < 3.2 Å, based on the first minimum of the O-O radial distribution function.

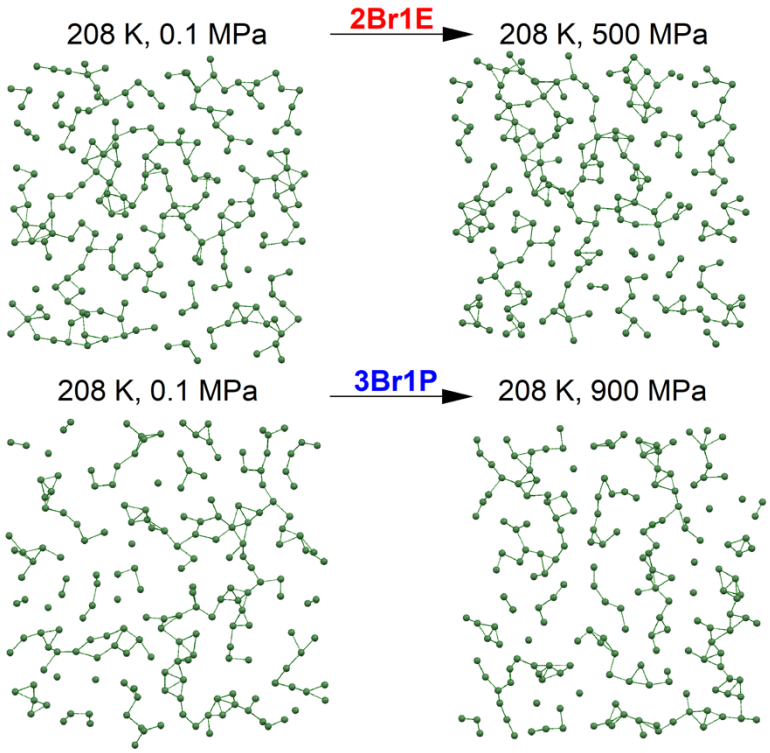

Figure S3. Visualization of the arrangement of Br atoms on cross-sections of the MD models (5 Å thick planes cut from 20 Å x 20 Å boxes) for 2Br1E and 3Br1E at the ambient and high-pressure conditions at 208 K. The lines represent short contacts between Br atoms of 4.9 Å for systems at ambient pressure and 4.8 Å for systems at higher pressure (estimated as the first minimum of the Br-Br radial distribution functions).

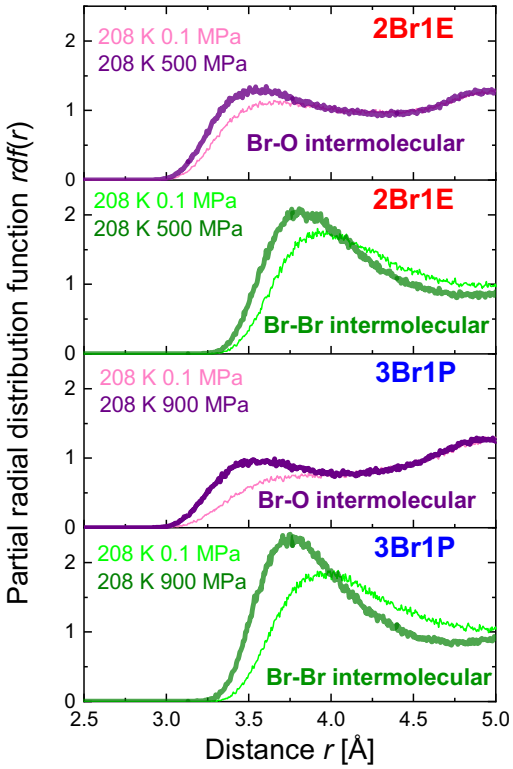

Figure S4. Partial Br-Br and Br-O radial distribution functions corresponding to the nearest-neighbour intermolecular correlations between these atoms were calculated based on the MD models of 2Br1E and 3Br1E alcohols at T = 208 K and p = 0.1 MPa, and at T = 208 K and p = 500 or 900 MPa, respectively.

1.2. Differential scanning calorimetry

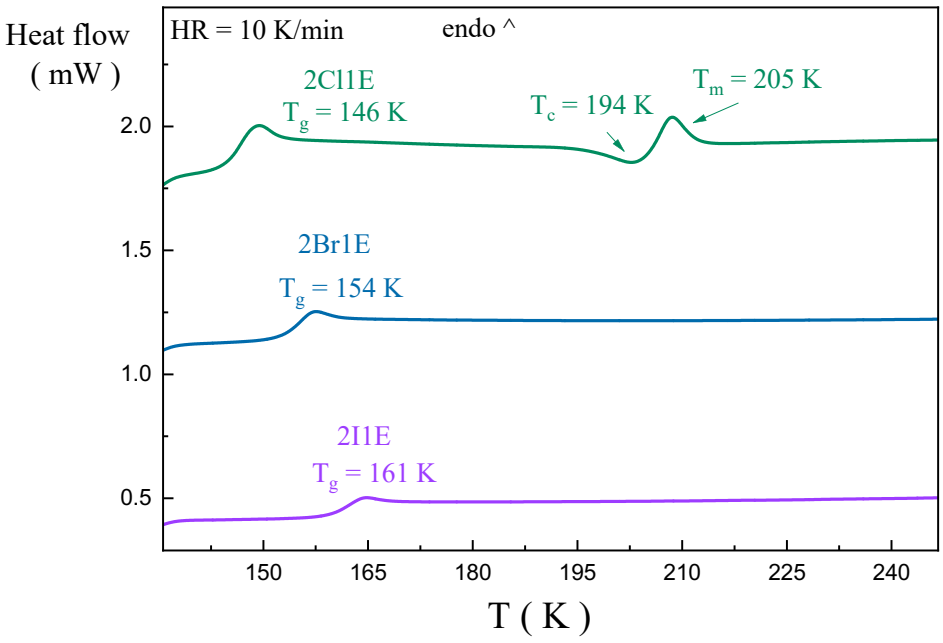

Figure S5. DSC thermograms were collected on heating with a rate of 10 K min^{-1}.

Table S1. Molar Mass (M), Glass Transition Temperature (T_g) of the studied alcohols.

Compound	2Cl1E	3Cl1P	2Br1E	3Br1P	2I1E	3I1P
M (g mol^{-1})	81	95	125	139	172	186
T_g (K)	146[1]	142	154[1]	150	161	157[1]

1.3. Thermal evolution of density and RI

As shown in Figure S5a and b, the temperature dependences of ρ and RI have a linear character for each monoalcohols. Therefore, the experimental data were refined with a linear function, the extrapolation of which allowed to estimate their values at lower temperature range.

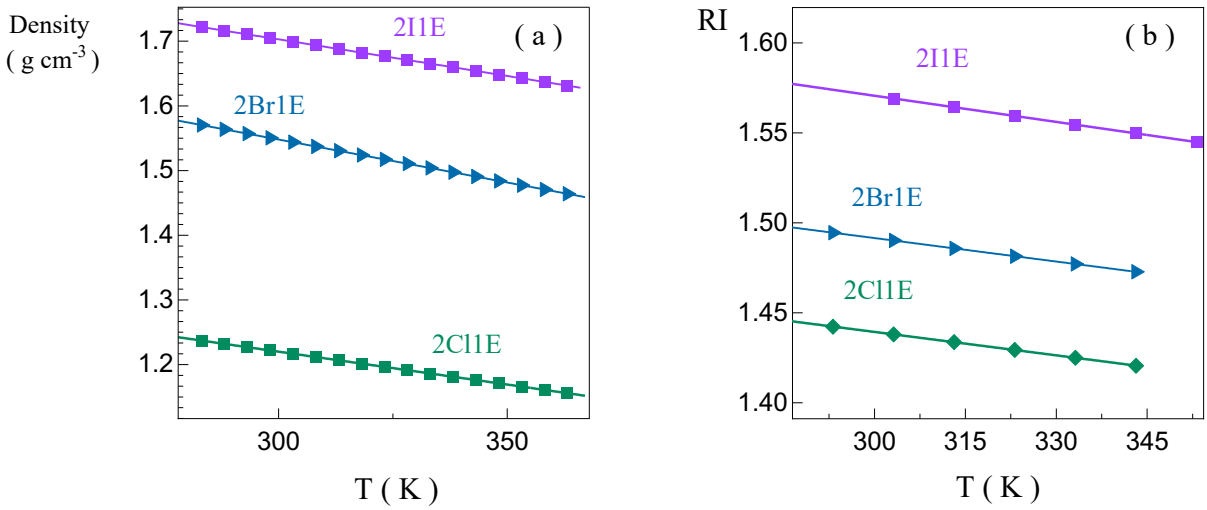

Figure S6. Thermal evolution of density of the studied alcohols (a).Thermal evolution of refractive index of the studied alcohols (b).

References

[1] K. Łucak, A.Z. Szeremeta, R. Wrzalik, J. Grelska, K. Jurkiewicz, N. Soszka, B. Hachuła, D. Kramarczyk, K. Grzybowska, B. Yao, K. Kamiński, S. Pawlus, Experimental and Computational Approach to Studying Supramolecular Structures in Propanol and Its Halogen Derivatives,
J. Phys. Chem. B 127 (42) (2023) 9102–9110.
https://doi.org/10.1021/acs.jpcb.3c02092.

11. Oświadczenia współautorów

Chorzów, 11.06.2025

Prof. dr hab. Sebastian Pawlus
Instytut Fizyki im. A. Chełkowskiego
Wydział Nauk Ścisłych i Technicznych
Uniwersytet Śląski w Katowicach
ul. 75 Pułku Piechoty 1, 41-500 Chorzów

OŚWIADCZENIE

Oświadczam, że w następujących pracach:

P1. K. Łucak, A.Z. Szeremeta, R. Wrzalik, J. Grelska, K. Jurkiewicz, N. Soszka, B. Hachuła, D. Kramarczyk, K. Grzybowska, B. Yao, K. Kamiński, S. Pawlus. Experimental and computational approach to studying supramolecular structures in propanol and its halogen derivatives. *The Journal of Physical Chemistry B*, *127*(42), 9102–9110, (2023).

P2. K. Łucak, A.Z. Szeremeta, J. Grelska, K. Jurkiewicz, S. Kołodziej, R. Wrzalik, K. Kamiński, S. Pawlus. Effect of high pressure on the molecular dynamics of halogen monoalcohols. *Journal of Molecular Liquids*, *423*, 127045, (2025).

P3. K. Łucak, A.Z. Szeremeta, A. Janowska, K. Jurkiewicz, K. Grzybowska, K. Kamiński, S. Pawlus. Influence of molecular structure and thermodynamic conditions on the dynamics, halogen bonding, and self–assembly of halogenated monoalcohols. *Journal of Molecular Liquids,* 433, 127787, (2025).

Mój wkład w każdej z powyższych publikacji obejmował udział w analizie i interpretacji wyników, oraz współtworzenie i korektę manuskryptu.

Chorzów, 11.06.2025

Dr inż. Anna Szeremeta, prof. UŚ
Instytut Fizyki im. A. Chełkowskiego
Wydział Nauk Ścisłych i Technicznych
Uniwersytet Śląski w Katowicach
ul. 75 Pułku Piechoty 1, 41-500 Chorzów

OŚWIADCZENIE

Oświadczam, że w następujących pracach:

P1. K. Łucak, A.Z. Szeremeta, R. Wrzalik, J. Grelska, K. Jurkiewicz, N. Soszka, B. Hachuła, D. Kramarczyk, K. Grzybowska, B. Yao, K. Kamiński, S. Pawlus. Experimental and computational approach to studying supramolecular structures in propanol and its halogen derivatives. *The Journal of Physical Chemistry B*, *127*(42), 9102–9110, (2023).

P2. K. Łucak, A.Z. Szeremeta, J. Grelska, K. Jurkiewicz, S. Kołodziej, R. Wrzalik, K. Kamiński, S. Pawlus. Effect of high pressure on the molecular dynamics of halogen monoalcohols. *Journal of Molecular Liquids*, *423*, 127045, (2025).

P3. K. Łucak, A.Z. Szeremeta, A. Janowska, K. Jurkiewicz, K. Grzybowska, K. Kamiński, S. Pawlus. Influence of molecular structure and thermodynamic conditions on the dynamics, halogen bonding, and self–assembly of halogenated monoalcohols. *Journal of Molecular Liquids,* 433, 127787, (2025).

Mój wkład obejmował udział w analizie otrzymanych wyników, dyskusję otrzymanych wyników oraz korektę manuskryptu każdej z powyższych publikacji.

Anna Szeremeta

Chorzów, 09.06.2025

Dr inż. Karolina Jurkiewicz
Instytut Fizyki im. A. Chełkowskiego
Wydział Nauk Ścisłych i Technicznych
Uniwersytet Śląski w Katowicach
ul. 75 Pułku Piechoty 1, 41-500 Chorzów

OŚWIADCZENIE

Oświadczam, że w następujących pracach:

P1. K. Łucak, A.Z. Szeremeta, R. Wrzalik, J. Grelska, K. Jurkiewicz, N. Soszka, B. Hachuła, D. Kramarczyk, K. Grzybowska, B. Yao, K. Kamiński, S. Pawlus. Experimental and computational approach to studying supramolecular structures in propanol and its halogen derivatives. *The Journal of Physical Chemistry B*, *127*(42), 9102–9110, (2023).

P2. K. Łucak, A.Z. Szeremeta, J. Grelska, K. Jurkiewicz, S. Kołodziej, R. Wrzalik, K. Kamiński, S. Pawlus. Effect of high pressure on the molecular dynamics of halogen monoalcohols. *Journal of Molecular Liquids*, *423*, 127045, (2025).

P3. K. Łucak, A.Z. Szeremeta, A. Janowska, K. Jurkiewicz, K. Grzybowska, K. Kamiński, S. Pawlus. Influence of molecular structure and thermodynamic conditions on the dynamics, halogen bonding, and self–assembly of halogenated monoalcohols. *Journal of Molecular Liquids,* 433, 127787, (2025).

Mój wkład polegał na nadzorowaniu przeprowadzanego eksperymentu, współpracy przy analizie wyników, dyskusji otrzymanych wyników oraz współtworzeniu manuskryptu każdej z powyższych publikacji.

Jurkiewicz

Warszawa, 10.06.2025

Dr Joanna Grelska
Wydział Chemii
Uniwersytet Warszawski
ul. Ludwika Pasteura 1, 02-093 Warszawa

OŚWIADCZENIE

Oświadczam, że w następujących pracach:

P1. K. Łucak, A.Z. Szeremeta, R. Wrzalik, J. Grelska, K. Jurkiewicz, N. Soszka, B. Hachuła, D. Kramarczyk, K. Grzybowska, B. Yao, K. Kamiński, S. Pawlus. Experimental and computational approach to studying supramolecular structures in propanol and its halogen derivatives. *The Journal of Physical Chemistry B*, *127*(42), 9102–9110, (2023).

P2. K. Łucak, A.Z. Szeremeta, J. Grelska, K. Jurkiewicz, S. Kołodziej, R. Wrzalik, K. Kamiński, S. Pawlus. Effect of high pressure on the molecular dynamics of halogen monoalcohols. *Journal of Molecular Liquids*, *423*, 127045, (2025).

Mój wkład polegał na wykonaniu pomiarów dyfrakcji rentgenowskiej, symulacji dynamiki molekularnej, analizie wyników, dyskusji otrzymanych wyników oraz współtworzeniu manuskryptu każdej z powyższych publikacji.

Joanna Grelska

Chorzów, 09.06.2025

Prof. dr hab. Roman Wrzalik
Instytut Fizyki im. A. Chełkowskiego
Wydział Nauk Ścisłych i Technicznych
Uniwersytet Śląski w Katowicach
ul. 75 Pułku Piechoty 1, 41-500 Chorzów

OŚWIADCZENIE

Oświadczam, że w następujących pracach:

P1**.** K. Łucak, A.Z. Szeremeta, R. Wrzalik, J. Grelska, K. Jurkiewicz, N. Soszka, B. Hachuła, D. Kramarczyk, K. Grzybowska, B. Yao, K. Kamiński, S. Pawlus. Experimental and computational approach to studying supramolecular structures in propanol and its halogen derivatives. *The Journal of Physical Chemistry B*, *127*(42), 9102–9110, (2023).

Mój wkład polegał na przeprowadzeniu obliczeń z wykorzystaniem teorii funkcjonału gęstości (DFT), analizie i interpretacji uzyskanych wyników, a także na współopracowaniu koncepcji zastosowania modelu łańcucha przejściowego (TCM, *transient chain model*) do opisu badanych alkoholi halogenowych.

P2. K. Łucak, A.Z. Szeremeta, J. Grelska, K. Jurkiewicz, S. Kołodziej, R. Wrzalik, K. Kamiński, S. Pawlus. Effect of high pressure on the molecular dynamics of halogen monoalcohols. *Journal of Molecular Liquids*, *423*, 127045, (2025).

Mój wkład polegał na przeprowadzeniu obliczeń z wykorzystaniem teorii funkcjonału gęstości (DFT), analizie i interpretacji uzyskanych wyników.

Chorzów, 09.06.2025

Dr hab. Barbara Hachuła, prof. UŚ
Wydział Nauk Ścisłych i Technicznych
Instytut Chemii
Uniwersytet Śląski w Katowicach
Ul. Szkolna 9
40-006 Katowice

OŚWIADCZENIE

Oświadczam, że w pracy:

P1. K. Łucak, A.Z. Szeremeta, R. Wrzalik, J. Grelska, K. Jurkiewicz, N. Soszka, B. Hachuła, D. Kramarczyk, K. Grzybowska, B. Yao, K. Kamiński, S. Pawlus. Experimental and computational approach to studying supramolecular structures in propanol and its halogen derivatives. *The Journal of Physical Chemistry B*, *127*(42), 9102–9110, (2023).

Mój wkład polegał na wykonaniu pomiarów oraz analizie wyników uzyskanych za pomocą spektroskopii w podczerwieni z transformacją Fouriera (FTIR) i spektroskopii Ramana, dyskusji wyników oraz współtworzeniu manuskryptu.

Barbara Hachuła

Chorzów, 09.06.2025

Dr Natalia Soszka
Wydział Nauk Ścisłych i Technicznych
Instytut Chemii
Uniwersytet Śląski w Katowicach
Ul. Szkolna 9
40-006 Katowice

OŚWIADCZENIE

Oświadczam, że w pracy:

P1. K. Łucak, A.Z. Szeremeta, R. Wrzalik, J. Grelska, K. Jurkiewicz, N. Soszka, B. Hachuła, D. Kramarczyk, K. Grzybowska, B. Yao, K. Kamiński, S. Pawlus. Experimental and computational approach to studying supramolecular structures in propanol and its halogen derivatives. *The Journal of Physical Chemistry B*, *127*(42), 9102–9110, (2023).

Mój wkład polegał na pomiarach oraz analizie wyników za pomocą metod spektroskopii w podczerwieni (FTIR) oraz spektroskopii Ramana, dyskusji otrzymanych wyników oraz korekcji manuskryptu.

Natalia Soszka

Chorzów, 11.06.2025

Prof. dr hab. Kamil Kamiński
Instytut Fizyki im. A. Chełkowskiego
Wydział Nauk Ścisłych i Technicznych
Uniwersytet Śląski w Katowicach
ul. 75 Pułku Piechoty 1, 41-500 Chorzów

OŚWIADCZENIE

Oświadczam, że w następujących pracach:

P1. K. Łucak, A.Z. Szeremeta, R. Wrzalik, J. Grelska, K. Jurkiewicz, N. Soszka, B. Hachuła, D. Kramarczyk, K. Grzybowska, B. Yao, K. Kamiński, S. Pawlus. Experimental and computational approach to studying supramolecular structures in propanol and its halogen derivatives. *The Journal of Physical Chemistry B*, *127*(42), 9102–9110, (2023).

P2. K. Łucak, A.Z. Szeremeta, J. Grelska, K. Jurkiewicz, S. Kołodziej, R. Wrzalik, K. Kamiński, S. Pawlus. Effect of high pressure on the molecular dynamics of halogen monoalcohols. *Journal of Molecular Liquids*, *423*, 127045, (2025).

P3. K. Łucak, A.Z. Szeremeta, A. Janowska, K. Jurkiewicz, K. Grzybowska, K. Kamiński, S. Pawlus. Influence of molecular structure and thermodynamic conditions on the dynamics, halogen bonding, and self–assembly of halogenated monoalcohols. *Journal of Molecular Liquids,* 433, 127787, (2025).

Mój wkład w każdej z powyższych publikacji polegał na dyskusji wyników.

Chorzów, 09.06.2025

Dr Katarzyna Grzybowska, prof. UŚ
Instytut Fizyki im. A. Chełkowskiego
Wydział Nauk Ścisłych i Technicznych
Uniwersytet Śląski w Katowicach
ul. 75 Pułku Piechoty 1, 41-500 Chorzów

OŚWIADCZENIE

Oświadczam, że w następujących pracach:

P1. K. Łucak, A.Z. Szeremeta, R. Wrzalik, J. Grelska, K. Jurkiewicz, N. Soszka, B. Hachuła, D. Kramarczyk, K. Grzybowska, B. Yao, K. Kamiński, S. Pawlus. Experimental and computational approach to studying supramolecular structures in propanol and its halogen derivatives. *The Journal of Physical Chemistry B*, *127*(42), 9102–9110, (2023).

Mój wkład polegał na udziale w pomiarach z wykorzystaniem różnicowej kalorymetrii skaningowej (DSC) oraz na współpracy przy analizie uzyskanych wyników.

P3. K. Łucak, A.Z. Szeremeta, A. Janowska, K. Jurkiewicz, K. Grzybowska, K. Kamiński, S. Pawlus. Influence of molecular structure and thermodynamic conditions on the dynamics, halogen bonding, and self–assembly of halogenated monoalcohols. *Journal of Molecular Liquids*, 433, 127787, (2025).

Mój wkład polegał na pomiarach za pomocą różnicowej kalorymetrii skaningowej z modulacją temperatury (TMDSC), analizie wyników, dyskusji otrzymanych wyników oraz współtworzeniu manuskryptu.

Katarzyna Grzybowska

Chorzów, 09.06.2025

Dr inż. Sławomir Kołodziej
Instytut Inżynierii Materiałowej
Wydział Nauk Ścisłych i Technicznych
Uniwersytet Śląski w Katowicach
ul. 75 Pułku Piechoty 1A, 41-500 Chorzów

OŚWIADCZENIE

Oświadczam, że w pracy:

P2. K. Łucak, A.Z. Szeremeta, J. Grelska, K. Jurkiewicz, S. Kołodziej, R. Wrzalik, K. Kamiński, S. Pawlus. Effect of high pressure on the molecular dynamics of halogen monoalcohols. *Journal of Molecular Liquids*, *423*, 127045, (2025).

Mój wkład polegał na współtworzeniu oraz korekcie manuskryptu.

Sławomir Kołodziej

Chorzów, 09.06.2025

Dr inż. Daniel Kramarczyk
Instytut Fizyki im. A. Chełkowskiego
Wydział Nauk Ścisłych i Technicznych
Uniwersytet Śląski w Katowicach
ul. 75 Pułku Piechoty 1, 41-500 Chorzów

OŚWIADCZENIE

Oświadczam, że w pracy:

P1. K. Łucak, A.Z. Szeremeta, R. Wrzalik, J. Grelska, K. Jurkiewicz, N. Soszka, B. Hachuła, D. Kramarczyk, K. Grzybowska, B. Yao, K. Kamiński, S. Pawlus. Experimental and computational approach to studying supramolecular structures in propanol and its halogen derivatives. *The Journal of Physical Chemistry B*, *127*(42), 9102–9110, (2023).

Mój wkład polegał na udziale w pomiarach z wykorzystaniem różnicowej kalorymetrii skaningowej (DSC) oraz na współpracy przy analizie uzyskanych wyników.

Kramarczyk Daniel

Oak Ridge, 10.06.2025

Dr Beibei Yao
Chemical Sciences Division
Oak Ridge National Laboratory
1 Bethel Valley Road
Oak Ridge, TN, US, 37830

STATEMENT

I hereby state that in the work

P1. K. Łucak, A.Z. Szeremeta, R. Wrzalik, J. Grelska, K. Jurkiewicz, N. Soszka, B. Hachuła, D. Kramarczyk, K. Grzybowska, B. Yao, K. Kamiński, S. Pawlus. Experimental and computational approach to studying supramolecular structures in propanol and its halogen derivatives. *The Journal of Physical Chemistry B*, *127*(42), 9102–9110, (2023).

My contribution consisted of performing density measurements for the manuscript.

Beibei Yao

Chorzów, 09.06.2025

Anna Janowska

OŚWIADCZENIE

Oświadczam, że w pracy:

P3. K. Łucak, A.Z. Szeremeta, A. Janowska, K. Jurkiewicz, K. Grzybowska, K. Kamiński, S. Pawlus. Influence of molecular structure and thermodynamic conditions on the dynamics, halogen bonding, and self–assembly of halogenated monoalcohols. *Journal of Molecular Liquids*, 433, 127787, (2025).

Mój wkład polegał na wykonaniu symulacji dynamiki molekularnej, analizie wyników i współtworzeniu manuskryptu.

Anna Janowska

12. Bibliografia

(1) Dodziuk, H. Wstęp do chemii supramolekularnej; Wydawnictwo Naukowe PWN: Warszawa, 2002.

(2) Steed, J. W.; Atwood, J. L. Supramolecular Chemistry, 3rd ed.; Wiley: Chichester, 2022.

(3) Böhmer, R.; Gainaru, C.; Richert, R. Structure and dynamics of monohydroxy alcohols–Milestones towards their microscopic understanding, 100 years after Debye. *Phys. Rep.* **2014**, *545* (4), 125–195. https://doi.org/10.1016/j.physrep.2014.07.005.

(4) Lehn, J.–M. Supramolecular Chemistry: Concepts and Perspectives; Wiley–VCH: Weinheim, 1995.

(5) Metrangolo, P.; Resnati, G. (Eds.). Halogen Bonding: Fundamentals and Applications; Springer: Berlin, 2008.

(6) Desiraju, G. R.; Steiner, T. The Weak Hydrogen Bond: In Structural Chemistry and Biology; Oxford University Press: Oxford, 1999.

(7) Pothoczki, S.; Pusztai, L.; Bakó, I. Variations of the Hydrogen Bonding and Hydrogen–Bonded Network in Ethanol–Water Mixtures on Cooling. *J. Phys. Chem. B* **2018**, *122* (26), 6790–6800. https://doi.org/10.1021/acs.jpcb.8b02493.

(8) Grelska, J.; Jurkiewicz, K.; Burian, A.; Pawlus, S. Supramolecular Structure of Phenyl Derivatives of Butanol Isomers. *J. Phys. Chem. B* **2022**, *126* (19), 3563–3571. https://doi.org/10.1021/acs.jpcb.2c01269.

(9) Prins, L. J.; Reinhoudt, D. N.; Timmerman, P. Noncovalent Synthesis Using Hydrogen Bonding. *Angew. Chem. Int. Ed.* **2001**, 40 (13), 2382–2426. https://doi.org/10.1002/1521–3773(20010702)40:13<2382::AID–ANIE2382>3.0.CO;2–G.

(10) Beer, P. D.; Barendt, T. A.; Lim, J. Y. C. Supramolecular Chemistry: Fundamentals and Applications, 2nd ed.; Oxford University Press: Oxford, 2022.

(11) Nitzan, A. Chemical Dynamics in Condensed Phases: Relaxation, Transfer, and Reactions in Condensed Molecular *Systems*; Oxford University Press: New York, 2006.

(12) Hassion, F. X.; Cole, R. H. Dielectric Properties of Liquid Ethanol and 2-Propanol. *J. Chem. Phys.* **1955**, *23* (10), 1756–1761. https://doi.org/10.1063/1.1740575.

(13) Gainaru, C.; Kastner, S.; Mayr, F.; Lunkenheimer, P.; Schildmann, S.; Weber, H. J.; Hiller, W.; Loidl, A.; Böhmer, R. Hydrogen-Bond Equilibria and Lifetimes in a Monohydroxy Alcohol. *Phys. Rev. Lett.* **2011**, *107* (11), 118304. https://doi.org/10.1103/PhysRevLett.107.118304.

(14) Gainaru, C.; Meier, R.; Schildmann, S.; Lederle, C.; Hiller, W.; Rössler, E. A.; Böhmer, R. Nuclear-Magnetic-Resonance Measurements Reveal the Origin of the Debye Process in Monohydroxy Alcohols. *Phys. Rev. Lett.* **2010**, *105* (25), 258303. https://doi.org/10.1103/PhysRevLett.105.258303.

(15) Jurkiewicz, K.; Hachuła, B.; Kamińska, E.; Grzybowska, K.; Pawlus, S.; Wrzalik, R.; Kamiński, K.; Paluch, M. Relationship between Nanoscale Supramolecular Structure, Effectiveness of Hydrogen Bonds, and Appearance of Debye Process. *J. Phys. Chem. C* **2020**, 124 (4), 2672–2679. https://doi.org/10.1021/acs.jpcc.9b09803.

(16) Hansen, C.; Stickel, F.; Berger, T.; Richert, R.; Fischer, E. W. Dynamics of Glass-Forming Liquids. III. Comparing the Dielectric α- and β-Relaxation of 1-Propanol and o-Terphenyl. *J. Chem. Phys.* **1997**, *107* (4), 1086–1093. https://doi.org/10.1063/1.474456.

(17) Bauer, S.; Burlafinger, K.; Gainaru, C.; Lunkenheimer, P.; Hiller, W.; Loidl, A.; Böhmer, R. Debye Relaxation and 250 K Anomaly in Glass Forming Monohydroxy Alcohols. *J. Chem. Phys.* **2013**, *138* (9), 094505. https://doi.org/10.1063/1.4793469.

(18) Soszka, N.; Hachuła, B.; Tarnacka, M.; Grelska, J.; Jurkiewicz, K.; Geppert–Rybczyńska, M.; Wrzalik, R.; Grzybowska, K.; Pawlus, S.; Paluch, M. Aromaticity Effect on Supramolecular Aggregation. Aromatic vs. Cyclic Monohydroxy Alcohols. *Spectrochim. Acta Part A Mol. Biomol. Spectrosc.* **2022**, 276, 121235. https://doi.org/10.1016/j.saa.2022.121235.

(19) Bolle, J.; Bierwirth, S. P.; Požar, M.; Perera, A.; Paulus, M.; Münzner, P.; Albers, C.; Dogan, S.; Elbers, M.; Sakrowski, R.; et al. Isomeric Effects in Structure Formation and Dielectric Dynamics of Different Octanols. *Phys. Chem. Chem. Phys.* **2021**, *23* (42), 24211–24221. https://doi.org/10.1039/D1CP02468J.

(20) Ngai, K. L.; Wang L. Relations between the Structural α-Relaxation and the Johari–Goldstein β-Relaxation in Two Monohydroxyl Alcohols: 1-Propanol and 5-Methyl-2-hexanol. J. Phys. Chem. B 2019, 123 (3), 714–719. https://doi.org/10.1021/acs.jpcb.8b11453.

(21) Ngai, K. L.; Pawlus, S.; Paluch, M. Explanation of the Difference in Temperature and Pressure Dependences of the Debye Relaxation and the Structural α-Relaxation near T of Monohydroxy Alcohols. *Chem. Phys.* **2020**, *530*, 110617. https://doi.org/10.1016/j.chemphys.2019.110617.

(22) Schildmann, S.; Reiser, A.; Gainaru, R.; Gainaru, C.; Böhmer, R. Nuclear Magnetic Resonance and Dielectric Noise Study of Spectral Densities and Correlation Functions in the Glass Forming Monoalcohol 2-Ethyl-1-Hexanol. *J. Chem. Phys.* **2011**, *135* (17), 174511. https://doi.org/10.1063/1.3647954.

(23) Łucak, K.; Szeremeta, A.Z.; Wrzalik, R.; Grelska, J.; Jurkiewicz, K.; Soszka, N.; Hachuła, B.; Kramarczyk, D.; Grzybowska, K.; Yao, B.; Kamiński, K.; Pawlus, S. Experimental and Computational Approach to Studying Supramolecular Structures in Propanol and Its Halogen Derivatives. *J. Phys. Chem. B* **2023**, 127 (42), 9102–9110. https://doi.org/10.1021/acs.jpcb.3c02092.

(24) Łucak, K.; Szeremeta, A.Z.; Grelska, J.; Jurkiewicz, K.; Kołodziej, S.; Wrzalik, R.; Kamiński, K.; Pawlus, S. Effect of High Pressure on the Molecular Dynamics of

Halogen Monoalcohols. *J. Mol. Liq.* **2025**, 423, 127045. https://doi.org/10.1016/j.molliq.2025.127045.

(25) Patil, S.; Sun, R.; Cheng, S.; Cheng, S. Molecular Mechanism of the Debye Relaxation in Monohydroxy Alcohols Revealed from Rheo-Dielectric Spectroscopy. *Phys. Rev. Lett.* 2023, *130* (9), 098201. https://doi.org/10.1103/PhysRevLett.130.098201.

(26) Nowok, A.; Jurkiewicz, K.; Dulski, M.; Hellwig, H.; Małecki, J. G.; Grzybowska, K.; Grelska, J.; Pawlus, S. Influence of Molecular Geometry on the Formation, Architecture and Dynamics of H–Bonded Supramolecular Associates in 1–Phenyl Alcohols. *J. Mol. Liq.* **2021**, 326, 115349. https://doi.org/10.1016/j.molliq.2021.115349.

(27) Nowok, A.; Dulski, M.; Grelska, J.; Szeremeta, A.Z.; Jurkiewicz, K.; Grzybowska, K.; Musiał, M.; Pawlus, S. Phenyl Ring: A Steric Hindrance or a Source of Different Hydrogen Bonding Patterns in Self–Organizing Systems? *J. Phys. Chem. Lett.* **2021**, 12 (8), 2142–2147. https://doi.org/10.1021/acs.jpclett.1c00186.

(28) Singh, L.P.; Richert, R. Watching Hydrogen–Bonded Structures in an Alcohol Convert from Rings to Chains. *Phys. Rev. Lett.* **2012**, 109 (16), 167802. https://doi.org/10.1103/PhysRevLett.109.167802.

(29) Jurkiewicz, K.; Kołodziej, S.; Hachuła, B.; Grzybowska, K.; Musiał, M.; Grelska, J.; Bielas, R.; Talik, A.; Pawlus, S.; Kamiński, K.; et al. Interplay between Structural Static and Dynamical Parameters as a Key Factor to Understand Peculiar Behaviour of Associated Liquids. *J. Mol. Liq.* **2020**, *319*, 114084. https://doi.org/10.1016/j.molliq.2020.114084.

(30) Hachuła, B.; Grelska, J.; Soszka, N.; Jurkiewicz, K.; Nowok, A.; Szeremeta, A. Z.; Pawlus, S.; Paluch, M.; Kaminski, K. Systematic Studies on the Dynamics, Intermolecular Interactions and Local Structure in the Alkyl and Phenyl Substituted Butanol Isomers. *J. Mol. Liq.* **2022**, *346*, 117098. https://doi.org/10.1016/j.molliq.2021.117098.

(31) Łucak, K.; Szeremeta, A. Z.; Janowska, A.; Jurkiewicz, K.; Grzybowska, K.; Kamiński, K.; Pawlus, S. Influence of molecular structure and thermodynamic conditions on the dynamics, halogen bonding, and self–assembly of halogenated monoalcohols. *J. Mol. Liq.* **2025,** 433, 127787. https://doi.org/10.1016/j.molliq.2025.127787.

(32) Fragiadakis, D.; Roland, C.M.; Casalini, R. Insights on the Origin of the Debye Process in Monoalcohols from Dielectric Spectroscopy under Extreme Pressure Conditions. *J. Chem. Phys.* **2010**, 132, 144505. https://doi.org/10.1063/1.3374820.

(33) Pawlus, S.; Paluch, M.; Dzida, M. Molecular Dynamics Changes Induced by Hydrostatic Pressure in a Supercooled Primary Alcohol. *J. Phys. Chem. Lett.* **2010**, *1* (21), 3249–3253. https://doi.org/10.1021/jz101288v.

(34) Kołodziej, S.**;** Knapik–Kowalczuk, J.; Grzybowska, K.; Nowok, A.; Pawlus, S. Essential Meaning of High Pressure Measurements in Discerning the Properties of Monohydroxy Alcohols with a Single Phenyl Group. *J. Mol. Liq.* **2020**, *305*, 112863. https://doi.org/10.1016/j.molliq.2020.112863.

(35) Grelska, J.**;** Temleitner, L.; Park, C.; Jurkiewicz, K.; Pawlus, S. High–Pressure and Temperature Effects on the Clustering Ability of Monohydroxy Alcohols. *J. Phys. Chem. Lett.* **2024**, *15* (11), 3118–3126. https://doi.org/10.1021/acs.jpclett.4c00085.

(36) Hachuła, B.**;** Włodarczyk, P.; Jurkiewicz, K.; Grelska, J.; Scelta, D.; Fanetti, S.; Paluch, M.; Pawlus, S.; Kamiński, K. Pressure–Induced Aggregation of Associating Liquids as a Driving Force Enhancing Hydrogen Bond Cooperativity. *J. Phys. Chem. Lett*. **2024**, *15* (1), 127–135. https://doi.org/10.1021/acs.jpclett.3c03037.

(37) Dannhauser, W. Dielectric Study of Intermolecular Association Isomeric Octyl Alcohols. *J. Chem. Phys.* **1968**, *48* (11), 1911.

(38) Janik, J. Fizyka Chemiczna; Polskie Wydawnictwo Naukowe: Warszawa, 1989.

(39) Chełkowski, A. Fizyka Dielektryków; Polskie Wydawnictwo Naukowe: Warszawa, 1979.

(40) Kremer, F.; Schönhals, A. Broadband Dielectric Spectroscopy; Springer: Berlin, 2003.

(41) Cole, K.S.; Cole, R.H. Dispersion and Absorption in Dielectrics I. Alternating Current Characteristics. *J. Chem. Phys.* **1941**, 9 (4), 341–351. https://doi.org/10.1063/1.1750906.

(42) Davidson, D. W.; Cole, R. H. Dielectric Relaxation in Glycerine. *J. Chem. Phys.* **1950**, 18 (10), 1417–1417. https://doi.org/10.1063/1.1747496.

(43) Davidson, D.W.; Cole, R.H. Dielectric Relaxation in Glycerol, Propylene Glycol, and n-Propanol. *J. Chem. Phys*. **1951**, 19 (12), 1484–1490. https://doi.org/10.1063/1.1748105.

(44) Havriliak, S.; Negami, S. A Complex Plane Representation of Dielectric and Mechanical Relaxation Processes in Some Polymers. *Polymer* **1967**, 8, 161–210. https://doi.org/10.1016/0032–3861(67)90021–3.

(45) Lunkenheimer, P.; Schneider, U.; Brand, R.; Loidl, A. Broadband dielectric response of glycerol and propylene carbonate: a comparison. *AIP Conf. Proc*. **1999**, 469, 433–440. https://doi.org/10.1063/1.58527.

(46) Schneider, U.; Lunkenheimer, P.; Brand, R.; Loidl, A. Broadband Dielectric Spectroscopy on Glass-Forming Propylene Carbonate. *Phys. Rev. E* **1999**, *59* (6), 6924–6936. https://pubmed.ncbi.nlm.nih.gov/11969680/.

(47) Politzer, P.; Murray, J.S.; Clark, T. Halogen Bonding and Other σ–Hole Interactions: A Perspective. *Phys. Chem. Chem. Phys*. **2013**, 15 (27), 11178–11189. https://doi.org/10.1039/C3CP00054K.

(48) Cavallo, G.; Metrangolo, P.; Milani, R.; Pilati, T.; Priimagi, A.; Resnati, G.; Terraneo, G. *The Halogen Bond*. Chem. Rev. **2016**, *116* (4), 2478–2601. https://doi.org/10.1021/acs.chemrev.5b00484.

(49) Xu, Y.; Hao, A.; Xing, P. X···X halogen bond–induced Supramolecular Helices. *Angew. Chem. Int. Ed*. **2022**, 61 (2), e202113786. https://doi.org/10.1002/anie.202113786.

(50) Sun, J.; Decato, D.A.; Bryantsev, V.S.; John, E.A.; Berryman, O.B. The Interplay between Hydrogen and Halogen Bonding: Substituent Effects and Their Role in the Hydrogen Bond Enhanced Halogen Bond. *Chem. Sci*. **2023,** 14, 8924–8935. https://doi.org/10.1039/D3SC02348F.